# DNA Damage Induced Cell Fates during Aging

**Marjolein Baar**

# DNA Damage Induced Cell Fates during Aging

Door DNA schade veroorzaakte cellulaire processen tijdens veroudering

Proefschrift

ter verkrijging van de graad van doctor aan de
Erasmus Universiteit Rotterdam
op gezag van de
rector magnificus

Prof.dr. R.C.M.E. Engels

en volgens besluit van het College voor Promoties.
De openbare verdediging zal plaatsvinden op

12 juni 2019 om 11.30

**Marjolein Petronella Baar**
geboren op 18 november 1989 te Hilversum

**Promotiecommissie:**

**Promotor:**        Prof. dr. J.H.J Hoeijmakers
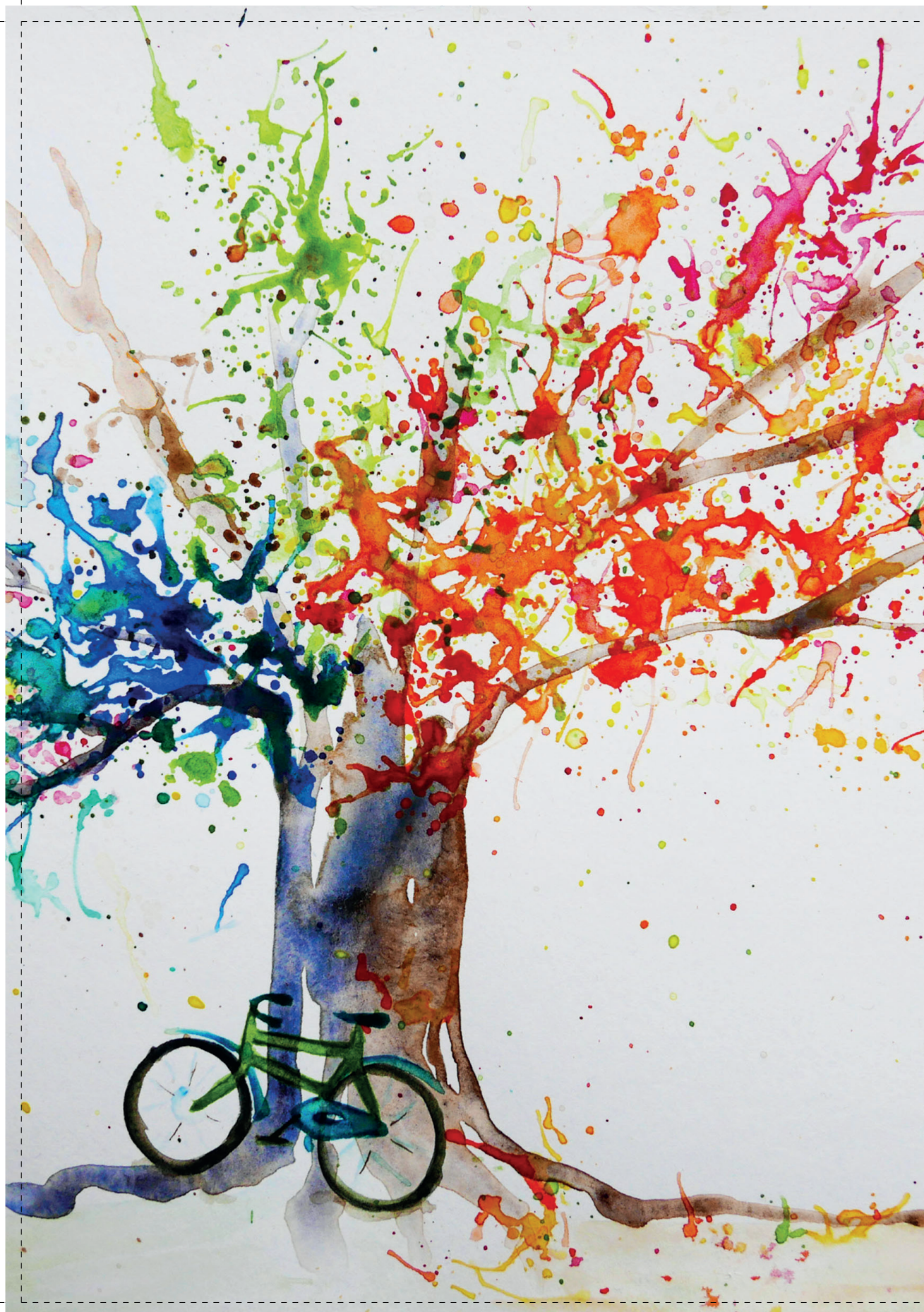
**Overige leden:**   Dr. Ing. R.W.F de Bruin
                     Prof. Dr. Ing. G.W. Jenster
                     Prof. Dr. B. Burgering

**Copromotoren:**    Dr. J. Pothof
                     Dr. P.L.J. de Keizer

## Table of Contents

# CHAPTER 1

## General introduction

## Aging is characterized by a progressive functional decline

Sooner or later, the elderly come to suffer from age-related disabilities that severely reduce the quality of life. Overall, a general progressive deterioration of function occurs during aging and thereby people are frailer and more likely to suffer accidents or catch an infection. Each individual ages at different pace. Consequently, there is great variation in the type and severity of disabilities or diseases that people develop during aging. These disabilities can include small aches and loss of strength that can affect normal daily activities, but also life-threatening diseases such as Alzheimer's disease and cancer. With this increased morbidity, people lose their independence and can suffer from various afflictions for years. With the considerable increase in average population lifespan over the last decades, the aged population has increased as well [1]. For example, while people born in the 1950's had an average life expectancy of 72 in the Netherlands, this has now changed to 82 [2]. Furthermore, in 2017 4.3% of the Dutch population is age 80 years or up and this percentage is expected to be doubled already in 2025 [1]. This elderly population suffers from a wide variety of age-related disorders. For example, a shocking amount of 1.2 million people in the Netherlands were estimated to have arthritis in 2016 [3]. Furthermore, 270000 people suffer from dementia in the Netherlands, which is expected to increase to 500000 in 2040 [4]. Ultimately, providing care and treatment for this progressively growing group of elderly will become too high of a burden on the working population [1]. In addition, the elderly rarely suffer from just one disease, but rather experience multiple chronic conditions in parallel, resulting in several disease-specific treatments at once [5]. Such multi-disease targeting approaches are an individual burden, time-consuming, expensive and increases the risk of toxicity. Furthermore, most treatments are focused on reducing symptoms, rather than the root of the problem, and are as such unable to cure or prevent the disease. Taking all of this into account, the quality of life would be improved considerably by targeting the underlying cause of all these disorders: the aging process itself. To be able to do so, it is first crucial to understand what drives aging at a molecular and cellular level in order to determine how the aging process can be postponed or reversed.

Cellular aging can be seen as the overall decline in efficiency in the maintenance of physiological processes [6]. This means that because of an age-related deterioration, cells are less able to maintain homeostasis and are thereby less stress resistant [7, 8]. Therefore, the overall cellular function decreases over time, leading to a disruption of tissue structure and an overall decline in tissue function during aging. External cues can affect aging. However, a clear cell-intrinsic component is thought to be decisive. For example, it is hypothesized that organisms will still age

even when they would live in a perfectly undamaging environment [9]. This is likely due to the imperfectness of biological processes. For example, endogenous DNA damage provokes mutations and damage accumulation, while protein synthesis is almost never error free, leading to an increase in misfolded proteins when folding chaperone function decreases with age [10-12]. In general, cellular damage will accumulate over time, leading to a functional decline.

## Chronic DNA damage results in cellular aging

There are various theories on the causes of aging at a cellular level, including cellular waste accumulation theories, the DNA damage theory and the free radical theory of aging [13]. Here, I will focus on the DNA damage theory. During life, cells are continuously damaged by extrinsic and intrinsic stressors [14]. Fortunately, cells can employ various DNA repair pathways that can efficiently repair distinct DNA damages [15]. However, repair processes are not flawless and unresolved DNA lesions accumulate in virtually all organs with time [16, 17]. An involvement of DNA damage in the aging process was proposed already in the 1950s, when it was observed that ionizing radiation reduces lifespan in animals [9]. Nowadays, we have further evidence. A clear causal link between DNA damage and aging is demonstrated by the fact that defects in DNA repair genes lead to accelerated aging syndromes such as Cockayne syndrome and Trichothiodystrophy (TTD) [14, 18]. In addition, mice that have a severe reduction in DNA repair exhibit accelerated aging as well and suffer from a multitude of age-related pathologies [19, 20]. For example, $Ercc1^{\Delta/-}$ mice have a reduced function of three repair pathways and therefore show an accelerated increase in DNA damage and a dramatic decrease in lifespan [20]. Furthermore, $Xpd^{TTD/TTD}$ mice have a nucleotide excision repair defect and show many features of aging at a relatively young age [21]. Both these mouse models show age-related pathologies in almost all organs and are therefore valuable models to study aging *in vivo*.

The accumulation of genomic mutations and damage ultimately leads to loss of cellular function through alternative transcription, gene expression and splicing [22-24]. Ultimately, processes that ensure homeostasis are affected by the DNA damage that accumulates during aging. For example, nuclear DNA damage induces nuclear to mitochondria signaling and thereby reduces mitochondrial function and mitophagy [25]. Furthermore, persistent DNA damage can cause metabolic changes, such as a downregulation of carbohydrate, amino acid, and lipid metabolism and altered AMPK signaling [26]. In addition, oncogenic mutations may occur that facilitate cancer growth [27]. In order to prevent excessively damaged cells from remaining to be present

in tissues, cells are equipped with additional fail-safe mechanisms. These include processes as apoptosis and cellular senescence. Apoptosis is a cell death program that can be induced by extrinsic or intrinsic stimuli [28]. Therefore, multiple apoptosis pathways exist, but these pathways all converge on the activation of caspases that fragment the cellular content, leading to cell shrinkage and membrane blebbing [29, 30]. Besides apoptosis, the proliferation of damaged cells can also be prevented by inducing a permanent cell cycle arrest termed senescence. Senescence can be induced by various stress signals, including telomere dysfunction, DNA damage, oxidative stress, oncogene activation and cytotoxic drugs [31]. Often these stressors induce a DNA damage response (DDR) and although multiple signaling pathways can be involved in senescence induction, these pathways ultimately lead to the activation of proteins involved in cell cycle arrest, such as p16$^{Ink4a}$ and p53 [32]. Thus, damaged cells are unable to divide and oncogenesis is prevented.

## An excessive amount of apoptosis during aging threatens tissue integrity

Apoptosis induction has a role in maintaining a normal physiology. For example, apoptosis is crucial in development [33], wound healing [34] or it can be induced in cells that are damaged or infected with pathogens [35]. However, due to deterioration of cellular components during aging, the apoptosis incidence increases in various tissues. Thus, an excessive amount of cells are lost and organ function declines.

The level of apoptotic cells observed during aging varies between tissues and between the distinct cell types in an organ. Examples of tissues that express an increased level of apoptosis during aging are brain [36, 37], heart [38], thymus [39], macula of the eye, the inner ear [40] and enhanced apoptosis levels are detected in germ cells in the prostate gland [41] and in the ovaries. In all these organs a loss of function is observed during aging due to this disproportional amount of apoptotic cells. Since DNA damage accumulates during aging, it could be expected that apoptosis often occurs in aged tissue. However, apoptotic genes are downregulated with age in various cell types [42, 43] and pro-apoptotic markers are reduced in human serum [44]. The level of key signaling proteins such as ATM and p53 are not increased during aging either when measured over a whole organ [45, 46], while more damage foci are found [47, 48]. Interestingly, research has shown that aged cells can even be remarkably resistant to apoptosis after DNA damage. In these studies, aged mice, or cells isolated from mice or humans, show a reduced p53 activation after damage and less apoptosis than young mice that were given the same dose of damage [46, 49-51]. Tissues that show a reduced apoptotic

response with age include liver, spleen and skin, while this effect was not observed in intestinal cells. It appears that a desensitization to damage occurs during aging in these organs, preventing the induction of cellular aging phenotypes. This could be beneficial during aging, since apoptotic cells are less likely to be replaced in aged tissue, compared to a young organisms where a tissue still has a high regenerative capacity. Overall, apoptosis induction in response to age-dependent cellular damage is cell type and tissue specific.

Apoptosis has a crucial role in many age-related pathologies. For example, apoptosis plays a role in relatively mild afflictions, such as age-related hearing loss [52], but an excessive amount of apoptotic cells also causes heart failure [53] or neurodegenerative diseases such as Alzheimer's disease, Parkinson's disease or a stroke [54-56]. For example, an age-related decline in cardiac function and an increased risk of a myocardial infarction is caused by the loss of cardiomyocytes [57-59]. These cells constitute the heart muscle and an increase in cardiomyocyte apoptosis is observed during aging [60]. Additionally, neurodegenerative diseases are caused by an increased number of apoptotic neurons. These neurons die due to multiple factors, including an increase in DNA damage and a decrease in mitochondrial function [61, 62]. Apoptosis inhibition may prevent age-related diseases. However, this may also lead to cancer in certain tissues, since apoptosis is an important process in oncogenesis as well [63].

## An age-related accumulation of senescent cells disrupts tissue homeostasis

A second major cellular difference in damage response during aging is that aged tissues accumulate senescent cells. Senescent cells undergo profound changes in chromatin structure and show an altered gene expression, including an increase in expression of cell cycle inhibitors [31, 64]. Therefore, these cells are genetically and morphologically different from normal healthy cells. Chromatin remodeling after senescence induction is caused by the loss of nuclear lamina protein LaminB1, leading to an alteration in the shape and stability of the nucleus [65]. The resulting cellular changes include an increase in size of the cytoplasm, nucleus and mitochondria [66-68]. In most cases the expression of β-galactosidase in lysosomes is increased in senescent cells, and detection of lysosomal β-galactosidase is widely used as a marker for senescence [69]. Furthermore, senescent cells often have persistent nuclear damage foci called DNA-SCARS (DNA segments with chromatin alterations reinforcing senescence) that contain DDR proteins such as 53BP1, γH2AX and activated p53 [70]. DNA-SCARS have been shown to fuse with PML nuclear bodies,

nuclear structures that contain a high concentration of the promyelocytic leukema (PML) protein and are formed in response to genomic damage and cellular stress [70, 71]. These foci have shown to be crucial for maintaining the permanent growth arrest [70, 72].

Senescent cells exhibit an altered secretion phenotype compared to healthy cells. This senescence-associated secretory phenotype (SASP) can contain a great variety of proteins such as growth factors, proteases and pro-inflammatory cytokines and is facilitated by the chromosomal rearrangements and the DNA-SCARS [70, 73]. In young and healthy organisms, the SASP mainly functions as a signal for the immune system to clear senescent cells [74-76]. Senescence thereby has a beneficial role in important processes such as wound healing and tissue repair. This is a programmed acute senescence induction. However, during aging there is an increase in DNA damage in combination with a decreased immune clearance of senescent cells due to an age-related decline in immune system functioning [77]. Together this leads to an accumulation of chronically present senescent cells and concomitant SASP [78]. Mainly through this higher expression of SASP factors, senescent cells are thought to play a crucial role in a great variety of age-related diseases. For example, senescent cells secrete pro-inflammatory proteins such as IL-1 and IL-6 to the microenvironment that affect gene expression and homeostasis in neighboring cells and that can stimulate proliferation of malignant cells [79-81]. Furthermore, the SASP can affect the extracellular matrix via MMPs, ultimately leading to loss of tissue structure [82, 83]. Tissue integrity is also threatened by perturbation of the stem cell niche. Chronic expression of SASP proteins such as IL-1 and IL-6 have shown to negatively influence stem cell function [84, 85]. Overall, the increased expression of SASP proteins during aging disrupts a normal tissue homeostasis and promotes age-related diseases.

An age-related increase in senescence is observed in many tissues [47, 86-88]. These cells are detected trough different markers *in vivo.* There is a great heterogeneity in the senescence phenotype and therefore no marker is expressed by all senescent cells or is exclusive for senescence. Therefore, an increase in senescence can only be detected through using multiple markers. Organs that show an increase in multiple established senescence markers include the skin [88, 89], heart [87, 90], lung [47, 86], spleen [47, 86], Kidney [91-93] and the joints [94]. In addition, senescent cells are found at the site of pathology in many different age-related diseases, including chronic kidney disease [95, 96], osteoarthritis [97, 98], idiopathic pulmonary fibrosis [99, 100], diabetes [101], atherosclerosis [102], Parkinson's disease [103] and autoimmune disorders [104]. In these age-related diseases, senescent cells contribute to disease progression due to the loss

of proliferative capacity and through the SASP. For example, senescent cells in the kidney tubules prevent regeneration of damaged tubular cells due to loss of proliferative capacity [105]. In addition, osteoarthritis is promoted by senescent chondrocytes present in aged cartilage that secrete interleukins and MMPs [106]. Hereby, these cells induce cartilage degeneration and concomitant pain and stiffness in the joints. Furthermore, senescence in spleen stromal cells accelerates aging of the immune cells present in the spleen [104]. This is possibly caused by expression of pro-inflammatory SASP proteins such as IL-1 and IL-6 [107] and contributes to a systemic decline in immune system functioning. Lastly, senescent cells in the lung produce SASP factors such as IL-6 and MMP3 that promote fibrosis and decrease lung function [99, 108]. Thus, age-related accumulation of senescent cells is expected to be causal of a multitude of age-related pathologies.

Although senescent cells and the SASP have been implicated in several diseases, a causal link with aging was established in the p16::ATTAC and p16::3MR mouse models [109-111]. Both models enable the visualization of p16$^{INK4a}$ and the genetic clearance of senescent cells. Multiple studies using these models show that senescent cell removal improves health span in both accelerated and naturally aging mice. Specifically, progeroid BubR1$^{H/H}$ mice showed a delayed onset of frailty, fat loss and cataracts after senescent cell removal, as well as a reversal of these features when senescent cells were eliminated at an advanced age [110]. Furthermore, genetic elimination of senescent cells in naturally aged mice increased median lifespan with 25% and improved healthspan in aged mice. For example, kidney and heart function was improved during aging and age-related bone loss could be attenuated [109, 111]. These findings indicate that targeting senescent cells therapeutically will improve tissue function during aging and thereby extend health span.

## Apoptosis and senescence impair tissue renewal during aging

The tissue regenerative potential is reduced during aging due to a decline in stem cell function. Adult stem cells are undifferentiated cells that are located in every organ and have the capacity to differentiate to the various cell types of a tissue [112]. In normal conditions these cells are quiescent, but upon tissue damage stem cells are stimulated to divide. This way, daughter cells are generated that either maintain the stem cell pool or differentiate to replace damaged cells and regenerate the tissue. During aging, the amount of damage increases and the pressure on stem cells to rejuvenate the tissue thereby increases. However, stem cells exhibit age-related features as well, including an increase in unrepaired DNA damage [113]. When aged and damaged stem cells are stimulated to proliferate, apoptosis, senescence

or differentiation can be induced [114-116], reducing the number of functional stem cells during aging. For example, aged muscle stem cells show an increase in p16[ink4a] expression and when induced to proliferate, these cells undergo senescence induction [117]. These senescent stem cells are not able to respond anymore to environmental stimuli in order to proliferate or differentiate. Furthermore, a decline in the number of neuronal stem cells is observed with age due to differentiation into astrocytes [118, 119]. Not all tissues show a decrease in stem cell number during aging [120-122]. For example, hematopoietic stem cell numbers increase in the bone marrow. However, the self-renewal capacity of these cells decreases and a shift in differentiation is detected from lymphoid lineage cells to myeloid lineage cells, increasing the risks of infections [123, 124]. Overall, less stem cells are able to regenerate damaged tissue during aging due to stem cell loss or senescence.

Intrinsic stem cell aging is a main contributor to the loss of regenerative potential during aging. On top of that, another important factor for stem cell functioning during aging is the stem cell niche [122, 125]. When tissue damage occurs, stem cells are induced to proliferate by stimuli from the microenvironment as a response to this damage. For example, damaged muscle cells produce IL6 and TNFa that signal to stem cells to proliferate [126, 127]. Thus, this transient expression of Il-6 by damaged myocytes activates muscle stem cells to regenerate the tissue and tissue homeostasis is retained. During aging, however, there is an increase in inflammation that disrupts normal tissue function [128]. This chronic inflammation interferes with the regenerative capacity of stem cells by altering the niche. For example, it has been shown that IL6 secreted by senescent cells can dedifferentiate muscle cells [129, 130]. This shows that senescent cells can promote the induction of reprogramming in neighboring cells. However, although reprogramming is induced, tissue regeneration capacity is reduced in aged tissue [131]. It is therefore hypothesized that persistent expression of SASP proteins in aged tissue keeps these pluripotent cells locked in a quiescent state [85]. This way, senescence prevents stem cells from differentiation and decreases their capacity to regenerate damaged tissue. Additionally, the importance of the stem cell niche is emphasized by studies that show that the function of old stem cells improves when the microenvironment is rejuvenated by exposure to young blood through parabiosis [132]. In summary, the loss of stem cell function seen during aging can be attributed to both intrinsic stem cell aging as well as the aging stem cell microenvironment. Together this leads to age-related afflictions such as anemia, sarcopenia, osteoporosis, osteoarthritis, neurodegenerative diseases [133] and a decline in immune system functioning [134].

**The SASP promotes cancer growth and migration**

Aging is the main risk factor for cancer development and therefore cancer incidence increases with age. Mutations that accumulate during aging facilitate oncogenesis [27, 135]. Specifically, oncogenic mutations may occur that provide growth advantages to cells and contribute to apoptosis resistance [136, 137]. In addition, age-related altered cellular signaling is beneficial for carcinogenesis. For example, due to an altered DDR, aged cells show an apoptotic resistance that facilitates cancer growth [138]. In general, age-related cellular changes can lead to apoptosis or senescence, but when additional mutations occur that prevent these tumor suppressor mechanisms, cancer growth is promoted.

In addition to intra-cellular alterations, an aging microenvironment facilitates tumor development as well. For example, inflammatory proteins are involved in promoting growth and genomic instability in cancer cells [139, 140], as well as processes such as angiogenesis and metastasis formation [141, 142]. This inflammation can be promoted by the age-related increase of senescent cells. Although senescence is often described as a tumor suppressive mechanism, senescent cells can escape their growth arrest or promote growth in neighboring cancer cells through the SASP [143]. For example, interleukins such as IL-6 and Il-8 secreted by senescent cells have shown to promote proliferation of premalignant epithelial cells [144]. Additionally, these interleukins contribute to various cancer hallmarks such as survival and metastasis [142]. Many other proteins of the SASP are known to promote cancer progression as well. For example, VEGF induces angiogenesis in a tumor and MMP3 facilitates invasion and metastasis [145, 146]. Thus, although senescence is seen as a tumor suppressive mechanism, it also promotes cancer during aging through the SASP. Overall, cellular aging creates cells that are geared to become cancer cells or that stimulate cancer growth in the micro-environment.

**Targeting cellular aging can delay or reverse age-related pathology**

Treatment of age-related diseases is currently based on targeting one disease at the time, while aged individuals often suffer from multiple chronic disabilities or diseases. An example is age-related frailty where multiple factors such as loss in bone and muscle strength contribute to an overall reduction in fitness. This comorbidity is difficult to treat since multiple disease-specific treatments are needed, enhancing the risk of side effects. Furthermore, treatment is often limited to the reduction of symptoms and does not eliminate the underlying cause of the disease

or disability itself. Therefore, targeting the root of age-related disabilities most likely has a greater effect on health span and probably induces less toxicity as well.

The oldest strategies to delay aging are keeping a healthy diet together with frequent exercise. These approaches improve overall fitness and prevent several afflictions, such as obesity and type 2 diabetes. Scientifically this has been proven in a multitude of model organisms [147-150]. For example, restricting food intake in an accelerated aging mouse model increases health and lifespan [149]. In addition, multiple studies show a clear benefit of exercise on health span during aging [151-154]. On a cellular level, dietary restriction has multiple beneficial effects. For example, the IGF pathway is downregulated and DNA damage is reduced during aging [155, 156]. Furthermore, dietary restriction delays senescence after damage and decreases SASP expression [157, 158]. Thus, cellular homeostasis is maintained longer and cellular aging is attenuated.

While keeping a healthy diet and exercise regime is known to improve health span in humans, it remains challenging for most to keep up this healthy life style. In addition, it is unknown which food groups to exclude or which specific diet is beneficial during aging. Therefore, strategies that require taking a drug that could achieve similar results are more likely to be effective. These drugs can either mimic dietary restriction or reverse features of aging by either removal of damaged cells and/or inducing tissue regeneration. Examples of dietary restriction mimetics are rapamycin and metformin. Rapamycin inhibits mTOR signaling and thereby extended lifespan in mice [159, 160]. Additionally, Metformin activates AMPK signaling, indirectly inhibiting the IGF pathway and mTOR as well and thereby has beneficial effects during aging [161]. For example, this drug reduced frailty and mortality in diabetes patients [162, 163]. While both these drugs could in theory benefit healthspan, Rapamycin did not show clear effects on health during aging [159] and both drugs can have severe side-effects in humans during long term treatments [161]. Another anti-aging strategy is improving mitochondrial function through, for example, increasing $NAD^+$ levels with Nicotinamide. This $NAD^+$ precursor increased mitochondrial function in mice through targeting SIRT1 [164] and has been administered to healthy adults without adverse effects [165]. Overall, these drugs show promise, but it remains unclear whether dietary restriction mimetics will delay aging when treatment is started at an older age.

Until recently, aging itself seemed inevitable and irreversible. However, promising discoveries have been made and it has been demonstrated that aging can in fact be reversed. For example, it has been proven that genetic removal of senescent cells increases health and life span in mice [109, 110]. Therapeutic anti-senescence compounds are therefore expected to restore tissue health during aging and potentially target multiple age-related diseases at once. Overall, eliminating

senescent cells targets an underlying cause of aging, explaining its significant effect on multiple pathologies. Thus, it is expected that healthspan during aging can be greatly improved when senescent cells are selectively cleared and possibly when apoptosis is prevented in cells that are not prone to oncogenesis. To achieve this, we aim to study how damaged cells decide to undergo either apoptosis or senescence, and how apoptosis resistance is regulated during aging. Furthermore, we aim to determine unique characteristics in senescent cells that can be targeted to induce apoptosis, while avoiding toxicity in non-senescent cells. Thus, new mechanisms to treat or prevent age-related diseases may be developed.

## Thesis outline

Organismal aging is defined by the loss of tissue function and homeostasis over time. Aging leads to a reduced ability to deal with stress, which consequently results in a gradual increase in tissue damage. As such, aging is a driver of a wide variety of disabilities. On a cellular level, aging is caused by the build-up of molecular damage, on the one hand by a life-long exposure to insults and on the other by the continuous functional decline in repair mechanisms. Unresolved damage to the genome is one of the main drivers of aging. It is assumed that with time, DNA repair becomes less efficient and irreparable damage inevitably accumulates. Damaged cells can undergo apoptosis or induce a permanent growth arrest termed cellular senescence. Both can prevent malignant cells from proliferating, but are a threat to tissue integrity as well. Here, we aim to study DNA damage induced cell fates in aging and age-related diseases, as well as mechanisms to treat or prevent these diseases.

A major cellular difference in damage response during aging is that aged tissues accumulate senescent cells. Senescent cells chronically secrete molecules that interfere with the local milieu in what is known as the Senescence Associated Secretory Phenotype (SASP). During aging, this means there is a build-up of local hotspots of such molecules as well. The SASP often contains an abundance of growth factors, proteases and pro-inflammatory cytokines and thereby alters the cellular microenvironment. In **Chapter 2**, we highlight how the protein FOXO4 acts as a pivot in maintaining senescent cell viability and how a FOXO4-p53 perturbation by cell penetrating peptides can force these cells into apoptosis and markedly reduce loss of tissue homeostasis in fast aging $Xpd^{TTD/TTD}$ and naturally aged mice. Furthermore, in **Chapter 3** and **Chapter 4** we discuss how compounds that target senescent cells improve healthspan during aging and how these may benefit treatment of age-related diseases. In addition, senescent cells can escape their growth arrest *in vivo* and grow out into malignant tumors. Interestingly, we observed FOXO4 upregulation

**1**

in treatment resistant melanoma cells and in **Chapter 5** we show that FOXO4-p53 inhibition induces a potent synthetic lethality in these cells

Another surprising discovery we will extrapolate on, is that although the cellular damage during aging could in theory trigger apoptosis in many cells, only relatively few apoptotic cells are detected in the majority of aged organs. Likewise, many pro-apoptotic genes are in fact downregulated. Therefore, it seems that during aging cells are somehow "preserved" from cell death. In **Chapter 6** we will highlight a micro-RNA response, in particular miR30, as the regulator of this response. We demonstrate that miR-30 is upregulated during aging and prevents DNA damage induced apoptosis through p53 inhibition. Furthermore, we show in **Chapter 7** that this DNA damage induced miRNA response can be transported to neighboring cells through extracellular vesicles, indicating that age-related DNA damage may induce systemic pro-survival cues. Lastly, in **Chapter 8** we describe the optimization of a protocol to culture adult organotypic slices *ex vivo.* This allows for molecular mechanistic experiments studying crucial age-related responses, such as apoptosis and senescence, while maintaining a natural tissue niche.

Overall, this thesis provides a reference for two major processes, apoptosis and senescence, that underlie organismal aging and provides a starting point for the development of potential therapeutic treatment of age-related functional decline.

## References

1.    CBS. *StatLine*. 2017; Available from: https://opendata.cbs.nl/statline/#/CBS/nl/.

2.    Eurostat. *Population structure and ageing*. 2017 June 2017; Available from: http://ec.europa.eu/eurostat/statistics-explained/index.php/Population_structure_and_ageing.

3.    gezondheidszorg, N.i.v.o.v.d. 2016; Available from: https://www.nivel.nl/nl/nzr/.

4.    alzheimer-nederland. 2015; Available from: https://www.alzheimer-nederland.nl/sites/default/files/directupload/factsheet-dementie-algemeen.pdf.

5.    Salive, M.E., *Multimorbidity in older adults.* Epidemiol Rev, 2013. **35**: p. 75-83.

6.    Lopez-Otin, C., et al., *The hallmarks of aging.* Cell, 2013. **153**(6): p. 1194-217.

7.    Hartl, F.U., *Cellular Homeostasis and Aging.* Annu Rev Biochem, 2016. **85**: p. 1-4.

8.    Kourtis, N. and N. Tavernarakis, *Cellular stress response pathways and ageing: intricate molecular relationships.* EMBO J, 2011. **30**(13): p. 2520-31.

9.    Strehler, B.L. and A.S. Mildvan, *General theory of mortality and aging.* Science, 1960. **132**(3418): p. 14-21.

10.   Teplyuk, N.M., *Near-to-perfect homeostasis: examples of universal aging rule which germline evades.* J Cell Biochem, 2012. **113**(2): p. 388-96.

11.   Maynard, S., et al., *DNA Damage, DNA Repair, Aging, and Neurodegeneration.* Cold Spring Harb Perspect Med, 2015. **5**(10).

12.   Drummond, D.A. and C.O. Wilke, *The evolutionary consequences of erroneous protein synthesis.* Nat Rev Genet, 2009. **10**(10): p. 715-24.

13.   Vina, J., C. Borras, and J. Miquel, *Theories of ageing.* IUBMB Life, 2007. **59**(4-5): p. 249-54.

14.   Hoeijmakers, J.H., *DNA damage, aging, and cancer.* N Engl J Med, 2009. **361**(15): p. 1475-85.

15.   Giglia-Mari, G., A. Zotter, and W. Vermeulen, *DNA damage response.* Cold Spring Harb Perspect Biol, 2011. **3**(1): p. a000745.

16.   Dolle, M.E., et al., *Distinct spectra of somatic mutations accumulated with age in mouse heart and small intestine.* Proc Natl Acad Sci U S A, 2000. **97**(15): p. 8403-8.

17.   Zahn, R.K., et al., *Age-correlated DNA damage in human muscle tissue.* Mech Ageing Dev, 1987. **41**(1-2): p. 73-114.

18.   Stefanini, M., et al., *Trichothiodystrophy: from basic mechanisms to clinical implications.* DNA Repair (Amst), 2010. **9**(1): p. 2-10.

19.   Jeppesen, D.K., V.A. Bohr, and T. Stevnsner, *DNA repair deficiency in neurodegeneration.* Prog Neurobiol, 2011. **94**(2): p. 166-200.

20.   Dolle, M.E., et al., *Broad segmental progeroid changes in short-lived Ercc1(-/Delta7) mice.* Pathobiol Aging Age Relat Dis, 2011. **1**.

**1**

21.	de Boer, J., et al., *Premature aging in mice deficient in DNA repair and transcription.* Science, 2002. **296**(5571): p. 1276-9.

22.	Gensler, H.L. and H. Bernstein, *DNA damage as the primary cause of aging.* Q Rev Biol, 1981. **56**(3): p. 279-303.

23.	Freitas, A.A. and J.P. de Magalhaes, *A review and appraisal of the DNA damage theory of ageing.* Mutat Res, 2011. **728**(1-2): p. 12-22.

24.	Schumacher, B., G.A. Garinis, and J.H. Hoeijmakers, *Age to survive: DNA damage and aging.* Trends Genet, 2008. **24**(2): p. 77-85.

25.	Fang, E.F., et al., *Nuclear DNA damage signalling to mitochondria in ageing.* Nat Rev Mol Cell Biol, 2016. **17**(5): p. 308-21.

26.	Edifizi, D., et al., *Multilayered Reprogramming in Response to Persistent DNA Damage in C. elegans.* Cell Rep, 2017. **20**(9): p. 2026-2043.

27.	Alexandrov, L.B., et al., *Clock-like mutational processes in human somatic cells.* Nat Genet, 2015. **47**(12): p. 1402-7.

28.	Elmore, S., *Apoptosis: a review of programmed cell death.* Toxicol Pathol, 2007. **35**(4): p. 495-516.

29.	Pradelli, L.A., M. Beneteau, and J.E. Ricci, *Mitochondrial control of caspase-dependent and -independent cell death.* Cell Mol Life Sci, 2010. **67**(10): p. 1589-97.

30.	Zheng, T.S., et al., *Caspase-3 controls both cytoplasmic and nuclear events associated with Fas-mediated apoptosis in vivo.* Proc Natl Acad Sci U S A, 1998. **95**(23): p. 13618-23.

31.	Campisi, J. and F. d'Adda di Fagagna, *Cellular senescence: when bad things happen to good cells.* Nat Rev Mol Cell Biol, 2007. **8**(9): p. 729-40.

32.	van Deursen, J.M., *The role of senescent cells in ageing.* Nature, 2014. **509**(7501): p. 439-46.

33.	Meier, P., A. Finch, and G. Evan, *Apoptosis in development.* Nature, 2000. **407**(6805): p. 796-801.

34.	Rai, N.K., et al., *Apoptosis: a basic physiologic process in wound healing.* Int J Low Extrem Wounds, 2005. **4**(3): p. 138-44.

35.	Roos, W.P. and B. Kaina, *DNA damage-induced cell death by apoptosis.* Trends Mol Med, 2006. **12**(9): p. 440-50.

36.	Giannaris, E.L. and D.L. Rosene, *A stereological study of the numbers of neurons and glia in the primary visual cortex across the lifespan of male and female rhesus monkeys.* J Comp Neurol, 2012. **520**(15): p. 3492-508.

37.	Andersen, B.B., H.J. Gundersen, and B. Pakkenberg, *Aging of the human cerebellum: a stereological study.* J Comp Neurol, 2003. **466**(3): p. 356-65.

38.	Kubli, D.A., et al., *Parkin protein deficiency exacerbates cardiac injury and reduces survival following myocardial infarction.* J Biol Chem, 2013. **288**(2): p. 915-26.

39. Sainz, R.M., et al., *Apoptosis in primary lymphoid organs with aging.* Microsc Res Tech, 2003. **62**(6): p. 524-39.

40. Kamogashira, T., C. Fujimoto, and T. Yamasoba, *Reactive oxygen species, apoptosis, and mitochondrial dysfunction in hearing loss.* Biomed Res Int, 2015. **2015**: p. 617207.

41. Kimura, M., et al., *Balance of apoptosis and proliferation of germ cells related to spermatogenesis in aged men.* J Androl, 2003. **24**(2): p. 185-91.

42. Alt, E.U., et al., *Aging alters tissue resident mesenchymal stem cell properties.* Stem Cell Res, 2012. **8**(2): p. 215-25.

43. Wilson, A., et al., *Age-related molecular genetic changes of murine bone marrow mesenchymal stem cells.* BMC Genomics, 2010. **11**: p. 229.

44. Kavathia, N., et al., *Serum markers of apoptosis decrease with age and cancer stage.* Aging (Albany NY), 2009. **1**(7): p. 652-63.

45. Braidy, N., et al., *Age related changes in NAD+ metabolism oxidative stress and Sirt1 activity in wistar rats.* PLoS One, 2011. **6**(4): p. e19194.

46. Feng, Z., et al., *Declining p53 function in the aging process: a possible mechanism for the increased tumor incidence in older populations.* Proc Natl Acad Sci U S A, 2007. **104**(42): p. 16633-8.

47. Wang, C., et al., *DNA damage response and cellular senescence in tissues of aging mice.* Aging Cell, 2009. **8**(3): p. 311-23.

48. Hewitt, G., et al., *Telomeres are favoured targets of a persistent DNA damage response in ageing and stress-induced senescence.* Nat Commun, 2012. **3**: p. 708.

49. Suh, Y., et al., *Aging alters the apoptotic response to genotoxic stress.* Nat Med, 2002. **8**(1): p. 3-4.

50. Polyak, K., et al., *Less death in the dying.* Cell Death Differ, 1997. **4**(3): p. 242-6.

51. Camplejohn, R.S., et al., *Apoptosis, ageing and cancer susceptibility.* Br J Cancer, 2003. **88**(4): p. 487-90.

52. Op de Beeck, K., J. Schacht, and G. Van Camp, *Apoptosis in acquired and genetic hearing impairment: the programmed death of the hair cell.* Hear Res, 2011. **281**(1-2): p. 18-27.

53. Whelan, R.S., V. Kaplinskiy, and R.N. Kitsis, *Cell death in the pathogenesis of heart disease: mechanisms and significance.* Annu Rev Physiol, 2010. **72**: p. 19-44.

54. Nikolaev, A., et al., *APP binds DR6 to trigger axon pruning and neuron death via distinct caspases.* Nature, 2009. **457**(7232): p. 981-9.

55. Barcia, C., et al., *IFN-gamma signaling, with the synergistic contribution of TNF-alpha, mediates cell specific microglial and astroglial activation in experimental models of Parkinson's disease.* Cell Death Dis, 2011. **2**: p. e142.

56. Chauvier, D., et al., *Targeting neonatal ischemic brain injury with a pentapeptide-based irreversible caspase inhibitor.* Cell Death Dis, 2011. **2**: p. e203.

**1**

57. Kwak, H.B., *Effects of aging and exercise training on apoptosis in the heart.* J Exerc Rehabil, 2013. **9**(2): p. 212-9.

58. Olivetti, G., et al., *Cardiomyopathy of the aging human heart. Myocyte loss and reactive cellular hypertrophy.* Circ Res, 1991. **68**(6): p. 1560-8.

59. Konstantinidis, K., R.S. Whelan, and R.N. Kitsis, *Mechanisms of cell death in heart disease.* Arterioscler Thromb Vasc Biol, 2012. **32**(7): p. 1552-62.

60. Kajstura, J., et al., *Necrotic and apoptotic myocyte cell death in the aging heart of Fischer 344 rats.* Am J Physiol, 1996. **271**(3 Pt 2): p. H1215-28.

61. Lu, T., et al., *Gene regulation and DNA damage in the ageing human brain.* Nature, 2004. **429**(6994): p. 883-91.

62. Lin, M.T. and M.F. Beal, *Mitochondrial dysfunction and oxidative stress in neurodegenerative diseases.* Nature, 2006. **443**(7113): p. 787-95.

63. Lowe, S.W. and A.W. Lin, *Apoptosis in cancer.* Carcinogenesis, 2000. **21**(3): p. 485-95.

64. De Cecco, M., et al., *Genomes of replicatively senescent cells undergo global epigenetic changes leading to gene silencing and activation of transposable elements.* Aging Cell, 2013. **12**(2): p. 247-56.

65. Freund, A., et al., *Lamin B1 loss is a senescence-associated biomarker.* Mol Biol Cell, 2012. **23**(11): p. 2066-75.

66. Hayflick, L., *The Limited in Vitro Lifetime of Human Diploid Cell Strains.* Exp Cell Res, 1965. **37**: p. 614-36.

67. Mitsui, Y. and E.L. Schneider, *Increased nuclear sizes in senescent human diploid fibroblast cultures.* Exp Cell Res, 1976. **100**(1): p. 147-52.

68. Kamogashira, T., et al., *Functionally and morphologically damaged mitochondria observed in auditory cells under senescence-inducing stress.* NPJ Aging Mech Dis, 2017. **3**: p. 2.

69. Dimri, G.P., et al., *A biomarker that identifies senescent human cells in culture and in aging skin in vivo.* Proc Natl Acad Sci U S A, 1995. **92**(20): p. 9363-7.

70. Rodier, F., et al., *DNA-SCARS: distinct nuclear structures that sustain damage-induced senescence growth arrest and inflammatory cytokine secretion.* J Cell Sci, 2011. **124**(Pt 1): p. 68-81.

71. White, R.R., et al., *Controlled induction of DNA double-strand breaks in the mouse liver induces features of tissue ageing.* Nat Commun, 2015. **6**: p. 6790.

72. Fumagalli, M., et al., *Stable cellular senescence is associated with persistent DDR activation.* PLoS One, 2014. **9**(10): p. e110969.

73. Rodier, F., et al., *Persistent DNA damage signalling triggers senescence-associated inflammatory cytokine secretion.* Nat Cell Biol, 2009. **11**(8): p. 973-9.

74. Demaria, M., et al., *An essential role for senescent cells in optimal wound healing through secretion of PDGF-AA.* Dev Cell, 2014. **31**(6): p. 722-33.

75. Krizhanovsky, V., et al., *Senescence of activated stellate cells limits liver fibrosis.* Cell, 2008. **134**(4): p. 657-67.

76. Jun, J.I. and L.F. Lau, *The matricellular protein CCN1 induces fibroblast senescence and restricts fibrosis in cutaneous wound healing.* Nat Cell Biol, 2010. **12**(7): p. 676-85.

77. Childs, B.G., et al., *Cellular senescence in aging and age-related disease: from mechanisms to therapy.* Nat Med, 2015. **21**(12): p. 1424-35.

78. Krishnamurthy, J., et al., *Ink4a/Arf expression is a biomarker of aging.* J Clin Invest, 2004. **114**(9): p. 1299-307.

79. Coppe, J.P., et al., *The senescence-associated secretory phenotype: the dark side of tumor suppression.* Annu Rev Pathol, 2010. **5**: p. 99-118.

80. Lewis, A.M., et al., *Interleukin-1 and cancer progression: the emerging role of interleukin-1 receptor antagonist as a novel therapeutic agent in cancer treatment.* J Transl Med, 2006. **4**: p. 48.

81. Setrerrahmane, S. and H. Xu, *Tumor-related interleukins: old validated targets for new anti-cancer drug development.* Mol Cancer, 2017. **16**(1): p. 153.

82. Liu, D. and P.J. Hornsby, *Senescent human fibroblasts increase the early growth of xenograft tumors via matrix metalloproteinase secretion.* Cancer Res, 2007. **67**(7): p. 3117-26.

83. McCulloch, K., G.J. Litherland, and T.S. Rai, *Cellular senescence in osteoarthritis pathology.* Aging Cell, 2017. **16**(2): p. 210-218.

84. Pietras, E.M., et al., *Chronic interleukin-1 exposure drives haematopoietic stem cells towards precocious myeloid differentiation at the expense of self-renewal.* Nat Cell Biol, 2016. **18**(6): p. 607-18.

85. de Keizer, P.L., *The Fountain of Youth by Targeting Senescent Cells?* Trends Mol Med, 2017. **23**(1): p. 6-17.

86. Biran, A., et al., *Quantitative identification of senescent cells in aging and disease.* Aging Cell, 2017. **16**(4): p. 661-671.

87. Chimenti, C., et al., *Senescence and death of primitive cells and myocytes lead to premature cardiac aging and heart failure.* Circ Res, 2003. **93**(7): p. 604-13.

88. Herbig, U., et al., *Cellular senescence in aging primates.* Science, 2006. **311**(5765): p. 1257.

89. Jeyapalan, J.C., et al., *Accumulation of senescent cells in mitotic tissue of aging primates.* Mech Ageing Dev, 2007. **128**(1): p. 36-44.

90. Torella, D., et al., *Cardiac stem cell and myocyte aging, heart failure, and insulin-like growth factor-1 overexpression.* Circ Res, 2004. **94**(4): p. 514-24.

91. Melk, A., et al., *Expression of p16INK4a and other cell cycle regulator and senescence associated genes in aging human kidney.* Kidney Int, 2004. **65**(2): p. 510-20.

**1**

92. Ding, G., et al., *Tubular cell senescence and expression of TGF-beta1 and p21(WAF1/CIP1) in tubulointerstitial fibrosis of aging rats.* Exp Mol Pathol, 2001. **70**(1): p. 43-53.

93. Baar, M.P., et al., *Targeted Apoptosis of Senescent Cells Restores Tissue Homeostasis in Response to Chemotoxicity and Aging.* Cell, 2017. **169**(1): p. 132-147 e16.

94. Martin, J.A. and J.A. Buckwalter, *Telomere erosion and senescence in human articular cartilage chondrocytes.* J Gerontol A Biol Sci Med Sci, 2001. **56**(4): p. B172-9.

95. Quimby, J.M., et al., *Feline chronic kidney disease is associated with shortened telomeres and increased cellular senescence.* Am J Physiol Renal Physiol, 2013. **305**(3): p. F295-303.

96. Sis, B., et al., *Accelerated expression of senescence associated cell cycle inhibitor p16INK4A in kidneys with glomerular disease.* Kidney Int, 2007. **71**(3): p. 218-26.

97. Price, J.S., et al., *The role of chondrocyte senescence in osteoarthritis.* Aging Cell, 2002. **1**(1): p. 57-65.

98. Jeon, O.H., et al., *Local clearance of senescent cells attenuates the development of post-traumatic osteoarthritis and creates a pro-regenerative environment.* Nat Med, 2017. **23**(6): p. 775-781.

99. Schafer, M.J., et al., *Cellular senescence mediates fibrotic pulmonary disease.* Nat Commun, 2017. **8**: p. 14532.

100. Yanai, H., et al., *Cellular senescence-like features of lung fibroblasts derived from idiopathic pulmonary fibrosis patients.* Aging (Albany NY), 2015. **7**(9): p. 664-72.

101. Pradhan, A.D., et al., *C-reactive protein, interleukin 6, and risk of developing type 2 diabetes mellitus.* JAMA, 2001. **286**(3): p. 327-34.

102. Uryga, A.K. and M.R. Bennett, *Ageing induced vascular smooth muscle cell senescence in atherosclerosis.* J Physiol, 2016. **594**(8): p. 2115-24.

103. Chinta, S.J., et al., *Cellular Senescence Is Induced by the Environmental Neurotoxin Paraquat and Contributes to Neuropathology Linked to Parkinson's Disease.* Cell Rep, 2018. **22**(4): p. 930-940.

104. Masters, A.R., et al., *Immune senescence: significance of the stromal microenvironment.* Clin Exp Immunol, 2017. **187**(1): p. 6-15.

105. van Willigenburg, H., P.L.J. de Keizer, and R.W.F. de Bruin, *Cellular senescence as a therapeutic target to improve renal transplantation outcome.* Pharmacol Res, 2018.

106. Portal-Nunez, S., et al., *Oxidative stress, autophagy, epigenetic changes and regulation by miRNAs as potential therapeutic targets in osteoarthritis.* Biochem Pharmacol, 2016. **108**: p. 1-10.

107. Ruhland, M.K., et al., *Stromal senescence establishes an immunosuppressive microenvironment that drives tumorigenesis.* Nat Commun, 2016. **7**: p. 11762.

108. Faner, R., et al., *Abnormal lung aging in chronic obstructive pulmonary disease and idiopathic pulmonary fibrosis.* Am J Respir Crit Care Med, 2012. **186**(4): p. 306-13.

109. Baker, D.J., et al., *Naturally occurring p16(Ink4a)-positive cells shorten healthy lifespan.* Nature, 2016. **530**(7589): p. 184-9.

110. Baker, D.J., et al., *Clearance of p16Ink4a-positive senescent cells delays ageing-associated disorders.* Nature, 2011. **479**(7372): p. 232-6.

111. Farr, J.N., et al., *Targeting cellular senescence prevents age-related bone loss in mice.* Nat Med, 2017. **23**(9): p. 1072-1079.

112. Rando, T.A., *Stem cells, ageing and the quest for immortality.* Nature, 2006. **441**(7097): p. 1080-6.

113. Choi, S.W., J.Y. Lee, and K.S. Kang, *miRNAs in stem cell aging and age-related disease.* Mech Ageing Dev, 2017. **168**: p. 20-29.

114. Walter, D., et al., *Exit from dormancy provokes DNA-damage-induced attrition in haematopoietic stem cells.* Nature, 2015. **520**(7548): p. 549-52.

115. Inomata, K., et al., *Genotoxic stress abrogates renewal of melanocyte stem cells by triggering their differentiation.* Cell, 2009. **137**(6): p. 1088-99.

116. Moehrle, B.M. and H. Geiger, *Aging of hematopoietic stem cells: DNA damage and mutations?* Exp Hematol, 2016. **44**(10): p. 895-901.

117. Sousa-Victor, P., E. Perdiguero, and P. Munoz-Canoves, *Geroconversion of aged muscle stem cells under regenerative pressure.* Cell Cycle, 2014. **13**(20): p. 3183-90.

118. Lugert, S., et al., *Quiescent and active hippocampal neural stem cells with distinct morphologies respond selectively to physiological and pathological stimuli and aging.* Cell Stem Cell, 2010. **6**(5): p. 445-56.

119. Encinas, J.M., et al., *Division-coupled astrocytic differentiation and age-related depletion of neural stem cells in the adult hippocampus.* Cell Stem Cell, 2011. **8**(5): p. 566-79.

120. Maslov, A.Y., et al., *Neural stem cell detection, characterization, and age-related changes in the subventricular zone of mice.* J Neurosci, 2004. **24**(7): p. 1726-33.

121. Molofsky, A.V., et al., *Increasing p16INK4a expression decreases forebrain progenitors and neurogenesis during ageing.* Nature, 2006. **443**(7110): p. 448-52.

122. Brack, A.S., H. Bildsoe, and S.M. Hughes, *Evidence that satellite cell decrement contributes to preferential decline in nuclear number from large fibres during murine age-related muscle atrophy.* J Cell Sci, 2005. **118**(Pt 20): p. 4813-21.

123. Chambers, S.M., et al., *Aging hematopoietic stem cells decline in function and exhibit epigenetic dysregulation.* PLoS Biol, 2007. **5**(8): p. e201.

124. Beerman, I., et al., *Functionally distinct hematopoietic stem cells modulate hematopoietic lineage potential during aging by a mechanism of clonal expansion.* Proc Natl Acad Sci U S A, 2010. **107**(12): p. 5465-70.

**1**

125. Chakkalakal, J.V., et al., *The aged niche disrupts muscle stem cell quiescence.* Nature, 2012. **490**(7420): p. 355-60.

126. Baeza-Raja, B. and P. Munoz-Canoves, *p38 MAPK-induced nuclear factor-kappaB activity is required for skeletal muscle differentiation: role of interleukin-6.* Mol Biol Cell, 2004. **15**(4): p. 2013-26.

127. Bastidas-Coral, A.P., et al., *Cytokines TNF-alpha, IL-6, IL-17F, and IL-4 Differentially Affect Osteogenic Differentiation of Human Adipose Stem Cells.* Stem Cells Int, 2016. **2016**: p. 1318256.

128. Franceschi, C., et al., *Inflamm-aging. An evolutionary perspective on immunosenescence.* Ann N Y Acad Sci, 2000. **908**: p. 244-54.

129. Chiche, A., et al., *Injury-Induced Senescence Enables In Vivo Reprogramming in Skeletal Muscle.* Cell Stem Cell, 2017. **20**(3): p. 407-414 e4.

130. Mosteiro, L., et al., *Tissue damage and senescence provide critical signals for cellular reprogramming in vivo.* Science, 2016. **354**(6315).

131. Conboy, I.M. and T.A. Rando, *Aging, stem cells and tissue regeneration: lessons from muscle.* Cell Cycle, 2005. **4**(3): p. 407-10.

132. Conboy, I.M., et al., *Rejuvenation of aged progenitor cells by exposure to a young systemic environment.* Nature, 2005. **433**(7027): p. 760-4.

133. Enwere, E., et al., *Aging results in reduced epidermal growth factor receptor signaling, diminished olfactory neurogenesis, and deficits in fine olfactory discrimination.* J Neurosci, 2004. **24**(38): p. 8354-65.

134. Warren, L.A. and D.J. Rossi, *Stem cells and aging in the hematopoietic system.* Mech Ageing Dev, 2009. **130**(1-2): p. 46-53.

135. Finkel, T., M. Serrano, and M.A. Blasco, *The common biology of cancer and ageing.* Nature, 2007. **448**(7155): p. 767-74.

136. Risques, R.A. and S.R. Kennedy, *Aging and the rise of somatic cancer-associated mutations in normal tissues.* PLoS Genet, 2018. **14**(1): p. e1007108.

137. Armitage, P., *Multistage models of carcinogenesis.* Environ Health Perspect, 1985. **63**: p. 195-201.

138. Broustas, C.G. and H.B. Lieberman, *DNA damage response genes and the development of cancer metastasis.* Radiat Res, 2014. **181**(2): p. 111-30.

139. Vakkila, J. and M.T. Lotze, *Inflammation and necrosis promote tumour growth.* Nat Rev Immunol, 2004. **4**(8): p. 641-8.

140. Lin, R., et al., *Chronic inflammation-associated genomic instability paves the way for human esophageal carcinogenesis.* Oncotarget, 2016. **7**(17): p. 24564-71.

141. Wei, L.H., et al., *Interleukin-6 promotes cervical tumor growth by VEGF-dependent angiogenesis via a STAT3 pathway.* Oncogene, 2003. **22**(10): p. 1517-27.

142. Oh, K., et al., *A mutual activation loop between breast cancer cells and myeloid-derived suppressor cells facilitates spontaneous metastasis through IL-6 trans-signaling in a murine model.* Breast Cancer Res, 2013. **15**(5): p. R79.

143. Campisi, J., *Aging, cellular senescence, and cancer.* Annu Rev Physiol, 2013. **75**: p. 685-705.

144. Krtolica, A., et al., *Senescent fibroblasts promote epithelial cell growth and tumorigenesis: a link between cancer and aging.* Proc Natl Acad Sci U S A, 2001. **98**(21): p. 12072-7.

145. Vidal-Vanaclocha, F., et al., *Interleukin-1 receptor blockade reduces the number and size of murine B16 melanoma hepatic metastases.* Cancer Res, 1994. **54**(10): p. 2667-72.

146. Radisky, D.C., et al., *Rac1b and reactive oxygen species mediate MMP-3-induced EMT and genomic instability.* Nature, 2005. **436**(7047): p. 123-7.

147. Kimura, K.D., et al., *daf-2, an insulin receptor-like gene that regulates longevity and diapause in Caenorhabditis elegans.* Science, 1997. **277**(5328): p. 942-6.

148. Kapahi, P., et al., *Regulation of lifespan in Drosophila by modulation of genes in the TOR signaling pathway.* Curr Biol, 2004. **14**(10): p. 885-90.

149. Vermeij, W.P., et al., *Restricted diet delays accelerated ageing and genomic stress in DNA-repair-deficient mice.* Nature, 2016. **537**(7620): p. 427-431.

150. Mattison, J.A., et al., *Caloric restriction improves health and survival of rhesus monkeys.* Nat Commun, 2017. **8**: p. 14063.

151. Sujkowski, A., et al., *Endurance exercise and selective breeding for longevity extend Drosophila healthspan by overlapping mechanisms.* Aging (Albany NY), 2015. **7**(8): p. 535-52.

152. Garcia-Valles, R., et al., *Life-long spontaneous exercise does not prolong lifespan but improves health span in mice.* Longev Healthspan, 2013. **2**(1): p. 14.

153. Vina, J., et al., *Exercise: the lifelong supplement for healthy ageing and slowing down the onset of frailty.* J Physiol, 2016. **594**(8): p. 1989-99.

154. Diman, A., et al., *Nuclear respiratory factor 1 and endurance exercise promote human telomere transcription.* Sci Adv, 2016. **2**(7): p. e1600031.

155. Fontana, L., L. Partridge, and V.D. Longo, *Extending healthy life span--from yeast to humans.* Science, 2010. **328**(5976): p. 321-6.

156. Rao, K.S., *Dietary calorie restriction, DNA-repair and brain aging.* Mol Cell Biochem, 2003. **253**(1-2): p. 313-8.

157. Ning, Y.C., et al., *Short-term calorie restriction protects against renal senescence of aged rats by increasing autophagic activity and reducing oxidative damage.* Mech Ageing Dev, 2013. **134**(11-12): p. 570-9.

1

158. Wang, W., G. Cai, and X. Chen, *Dietary restriction delays the secretion of senescence associated secretory phenotype by reducing DNA damage response in the process of renal aging.* Exp Gerontol, 2018. **107**: p. 4-10.

159. Neff, F., et al., *Rapamycin extends murine lifespan but has limited effects on aging.* J Clin Invest, 2013. **123**(8): p. 3272-91.

160. Li, J., S.G. Kim, and J. Blenis, *Rapamycin: one drug, many effects.* Cell Metab, 2014. **19**(3): p. 373-9.

161. Aliper, A., et al., *Towards natural mimetics of metformin and rapamycin.* Aging (Albany NY), 2017. **9**(11): p. 2245-2268.

162. Scarpello, J.H., *Improving survival with metformin: the evidence base today.* Diabetes Metab, 2003. **29**(4 Pt 2): p. 6S36-43.

163. Wang, C.P., C. Lorenzo, and S.E. Espinoza, *Frailty Attenuates the Impact of Metformin on Reducing Mortality in Older Adults with Type 2 Diabetes.* J Endocrinol Diabetes Obes, 2014. **2**(2).

164. Gomes, A.P., et al., *Declining NAD(+) induces a pseudohypoxic state disrupting nuclear-mitochondrial communication during aging.* Cell, 2013. **155**(7): p. 1624-38.

165. Dellinger, R.W., et al., *Repeat dose NRPT (nicotinamide riboside and pterostilbene) increases NAD(+) levels in humans safely and sustainably: a randomized, double-blind, placebo-controlled study.* NPJ Aging Mech Dis, 2017. **3**: p. 17.

1

# CHAPTER 2

## Targeted Apoptosis of Senescent Cells Restores Tissue Homeostasis in Response to Chemotoxicity and Aging

Marjolein P. Baar[1], Renata M.C. Brandt[1], Diana A. Putavet[1], Julian D.D. Klein[1], Kasper W.J. Derks[1], Benjamin R. M. Bourgeois[7], Sarah Stryeck[7], Yvonne Rijksen[1], Hester van Willigenburg[1], Danny A. Feijtel[1], Ingrid van der Pluijm[1,4], Jeroen Essers[1,4,5], Wiggert A. van Cappellen[2], Wilfred F.J. van IJcken[3], Adriaan B. Houtsmuller[2], Joris Pothof[1], Ron W.F. de Bruin[6], Tobias Madl[7], Jan H.J. Hoeijmakers[1], Judith Campisi[8,9], Peter L.J. de Keizer[1,8]

[1] Department of Molecular Genetics, [2] Erasmus Optical Imaging Center and Department of Pathology,

[3] Department of Cell Biology, [4] Department of Vascular Surgery, [5] Department of Radiation Oncology,

[6] Department of Surgery

Erasmus University Medical Center Rotterdam, Wytemaweg 80, 3015CN, Rotterdam, the Netherlands

[7] Institute of Molecular Biology & Biochemistry, Center of Molecular Medicine, Medical University of Graz, 8010 Graz, Austria

[8] The Buck Institute for Research on Aging, 8001 Redwood Blvd., Novato, CA 94945, USA

[9] Lawrence Berkeley National Laboratories, Berkeley, CA, USA

## **Abstract**

The accumulation of irreparable cellular damage restricts healthspan after acute stress or natural aging. Senescent cells are thought to impair tissue function and their genetic clearance can delay features of aging. Identifying how senescent cells avoid apoptosis allows for the prospective design of anti-senescence compounds to address whether homeostasis can also be restored.

Here, we identify FOXO4 as a pivot in senescent cell viability. We designed a FOXO4 peptide which perturbs the FOXO4 interaction with p53. In senescent cells, this selectively causes p53 nuclear exclusion and cell-intrinsic apoptosis. Under conditions where it was well tolerated *in vivo*, this FOXO4 peptide neutralized Doxorubicin-induced chemotoxicity. Moreover, it restored fitness, fur density and renal function in both fast aging $Xpd^{TTD/TTD}$ and naturally aged mice. Thus, therapeutic targeting of senescent cells is feasible under conditions where loss of health has already occurred and in doing so tissue homeostasis can effectively be restored.

## Introduction

Unresolved DNA damage can impair cellular function, promote disease development and accelerate aging(Lopez-Otin et al., 2013). To prevent such undesired consequences, cells are equipped with a range of DNA repair mechanisms (Hoeijmakers, 2009). However, these mechanisms are not flawless. When repair falls short, tissue integrity is still at least initially maintained by independent stress-response mechanisms as apoptosis and cellular senescence(de Keizer, 2017). Senescent cells are permanently withdrawn from the cell cycle and generally develop a persistent pro-inflammatory phenotype, called the Senescence-Associated Secretory Phenotype or SASP(Coppe et al., 2008). The SASP influences the cellular microenvironment, which can be beneficial early in life, or in an acute setting of wound healing(Demaria et al., 2014; Munoz-Espin et al., 2013). However, unlike apoptotic cells, which are permanently eliminated, senescent cells can prevail for prolonged periods of time and accumulate with age(Krishnamurthy et al., 2004). Because of their low, but chronic SASP, persistent senescent cells are thought to accelerate aging and the onset of age-related diseases(de Keizer, 2017). Indeed, senescence has been associated with a plethora of (age-related) pathologies and, conversely, genetic clearance of senescent cells can delay features of aging(Baker et al., 2016). It remains largely unclear how damaged cells avoid apoptosis in favor of senescence. We set out to address this question and to determine whether therapeutic targeting of senescent cells could not only delay, but also counteract the loss of tissue homeostasis after acute damaging medical treatments as chemotherapy, or chronic damage causer either by accelerated or natural aging.

## Results

### FOXO4 is elevated in senescent cells and maintains their viability

To identify potential pivots in senescent cell viability, we initiated this study by investigating whether apoptosis-related pathways are altered in senescent cells. We performed unbiased RNA sequencing on samples of genomically stable primary human IMR90 fibroblasts and IMR90 induced to senesce by Ionizing Radiation (Rodier et al., 2011). As senescent cells are reportedly apoptosis-resistant (Wang, 1995), we expected pro-apoptotic genes to be repressed. Surprisingly, however, senescent IMR90 showed an upregulation of prominent pro-apoptotic "initiators" PUMA and BIM while the anti-apoptotic "guardian" BCL-2 was reduced (Fig. 1A + S1A).
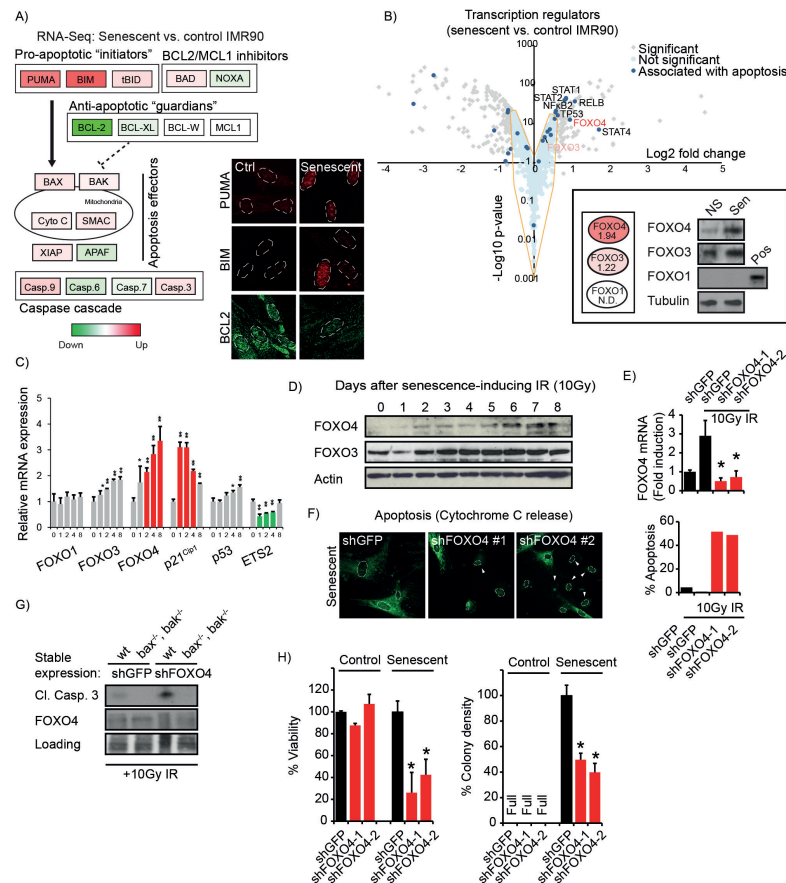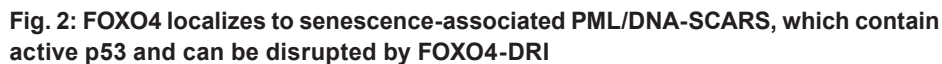
**Fig. 1: FOXO4 is elevated in senescent normal fibroblasts and ensures their viability**
A) Schematic representation of the mRNA expression changes (Fig. S1A) of the cell-intrinsic apoptosis pathway(Tait and Green, 2010) between senescent and control (proliferating) IMR90 fibroblasts. Inset: Immunofluorescence for PUMA, BIM and BCL2. B) Volcano plot comparing transcriptional regulators in senescent vs. control IMR90. (See Fig. S1B for expression and p-values). Dark blue: associated with apoptosis. Inset, left: RNA expression of the FOXO cluster. N.D. Not detectable. Right: Protein levels of the FOXO cluster. FOXO1 was ectopically expressed as positive control. C) QPCR for changes in FOXO1, 3 and 4 mRNA after senescence-induction by 10Gy IR. p21$^{Cip1}$ (biphasic increase), p53 and ETS2 (biphasic decrease) are included as controls. D) Immunoblot for changes in FOXO3 and 4 protein levels after senescence-induction by 10Gy IR. E) The senescence-induced FOXO4 mRNA expression is successfully countered by two shRNAs. F) Cytochrome-C release assay (left) as measure for apoptosis in the conditions of E), quantified in a histogram (right). G) Induction of cleaved Caspase-3 after senescence induction in (mouse-specific) FOXO4-deprived wildtype or *bax/bak*$^{-/-}$ BMK cells. H) AqueousOne viability (left) and colony density (right; see also Fig. S1C) of control and senescent IMR90 cells transduced with the short hairpins used in E).

This suggested senescent IMR90 are primed to undergo apoptosis, but that the execution of the death program is restrained. We reasoned such a brake could potentially be a transcriptional regulator and focused on transcription factors that have previously been linked to apoptosis, including STAT1, 2 and 4, RELB, NFκB, TP53 and FOXO4 (Fig. 1B + S1B). Interference with JAK-STAT signaling in known not to affect the viability of senescent cells(Xu et al., 2015) and we have previously observed similar effects for NFκB and p53 inhibition(Freund et al., 2011; Rodier et al., 2009). Our interest was therefore directed to a factor that has not yet been studied as such, FOXO4 (Fig. 1B). FOXO4 belongs to a larger mammalian family, with FOXO1 and 3 being its major siblings. FOXOs are well studied in aging and tissue homeostasis as targets of Insulin/IGF signaling and as regulators of Reactive Oxygen Species(de Keizer et al., 2011; Eijkelenboom and Burgering, 2013; Martins et al., 2016). Whereas senescence-inducing IR showed only mild effects on the expression of FOXO1 and 3, both FOXO4 mRNA and protein expression progressively increased (Fig. 1C+D). We therefore wondered whether FOXO4 could function to balance senescence and apoptosis. We stably inhibited FOXO4 expression using lentiviral shRNA (Fig. 1E). FOXO4 inhibition prior to senescence-induction resulted in a release of mitochondrial Cytochrome C (Fig. 1F) and BAX/BAK-dependent Caspase-3 cleavage (Fig. 1G). In addition, FOXO4 inhibition in cells that were already senescent, but not their control counterparts, reduced viability and cell density (Fig. 1H +S1C). Together, this shows that after acute damage FOXO4 favors senescence over apoptosis and maintains viability of senescent cells by repressing their apoptosis response.

**FOXO4-DRI disrupts PML/DNA-SCARS and releases active p53 in senescent cells**

Interference with FOXO4 signaling could be a strategy to eliminate senescent cells and thereby potentially target senescence-related diseases. However, shRNA-mediated repression of FOXO4 would be complicated to translate to the clinic. Thus, we decided to design compounds that could structurally interfere with FOXO4 function instead. Immunofluorescence experiments showed FOXO4 to be gradually recruited to euchromatin foci after senescence-induction (Fig. 2A-C+ S2A-D). As senescence develops, PML bodies fuse with 53BP1-containing DNA-SCARS to jointly regulate expression of the SASP(Rodier et al., 2011). High resolution Structured Illumination Microscopy (SIM) of nuclei of senescent cells showed FOXO4 to reside within these PML bodies, adjacent to 53BP1-containing DNA-SCARS (Fig. 2D; Mov.1+2; Fig. S2E-I).

**Fig. 2: FOXO4 localizes to senescence-associated PML/DNA-SCARS, which contain active p53 and can be disrupted by FOXO4-DRI**

A) FOXO4 foci and Senescence-Associated Heterochromatin Structures in senescent IMR90 (See also Fig. S2A-I). Bottom: Intensity plot (arbitrary units) of individual pixels measured by the indicated line. B) Quantification of cells containing ≥3 FOXO4 foci in time after senescence-inducing IR. C) FOXO4 foci in senescent cells transduced with the shRNAs against FOXO4 described in 1E. D) Structured Illumination Microscopic (SIM) image of the nucleus of a senescent IMR90 cell stained

for FOXO4, 53BP1 and PML. Yellow arrow: Area processed for 3D surface-rendering (Insets). E) FOXO4 and Ser15-phosphorylated p53, assessed as in 2A. Note that for FOXO4 a different antibody (Sigma) was used. F+G) Sequence (H indicates predicted helix) and 3D structure of FOXO4 used for the design of FOXO4-DRI. The amino acids indicated in yellow in F) are shown as yellow spheres in the displayed structure of FOXO4 (3L2C, protein databank). Green aa in F) are not visualized in this 3D structure, but are part of the FOXO4-DRI sequence. Red aa in G) change most upon p53-interaction (Wang et al., 2008). See also Fig. S2J-L. H) $^1$H,$^{15}$N HSQC NMR spectrum of 15N-labelled recombinant FOXO4$^{86-206}$ incubated with increasing stoichiometric equivalents of recombinant p53 (60, 120, 240 or 300 µM, respectively). I) Experiment as in H), but with 1x or 2x stoichiometric equivalents of FOXO4-DRI (300 or 600 µM, respectively). J) Cellular uptake of FOXO4-DRI in senescent IMR90 visualized by an antibody against the HIV-TAT sequence. K) Quantification of the number of FOXO4/PML/53BP1-DNA-SCARS in control and senescent IMR90 incubated 3d with 25µM FOXO4-DRI and the pan Caspase-inhibitor QVD-OPH. # of small 53BP1 foci shown as control. Only infrequently FOXO4 foci were visible in control cells. L) Schematic representation of the p21$^{Cip1}$ (CDKN1a) promoter in which the canonical FOXO target sequence is flanked by two p53 binding sites. M+N) Quantification of nuclear p21$^{Cip1}$ intensity of senescent IMR90 treated as in K). N) Left: Immunoblot of senescent IMR90 cells incubated for the indicated time points with FOXO4-DRI and processed for Ser15-phosphorylated and total p53. Middle: Nuclear exclusion of pSer15-p53 in cell treated as in K+M). Right: Quantification of pSer15-p53 foci per nucleus of senescent IMR90.

p53 controls both apoptosis and senescence(Kruiswijk et al., 2015) and localizes to DNA-SCARS in senescent cells(Rodier et al., 2011). Under those conditions p53 is phosphorylated by ATM on Ser15, which blocks its MDM2-mediated degradation(Rodier et al., 2009). Consistent with the observation of FOXO4 residing in PML bodies, FOXO4 localized next to phosphorylated ATM substrates (Fig. S2I) and pS15-phosphorylated p53 (Fig. 2E). This raised the question whether FOXO4 could maintain senescent cell viability by binding p53 and inhibiting p53-mediated apoptosis in favor of cell cycle arrest.

FOXOs can interact with p53, and the interaction domain has been characterized by NMR (Wang et al., 2008). To interfere with the FOXO4-p53 interaction, we therefore designed a cell-permeable peptide comprising part of the p53-interaction domain in FOXO4 (Fig. 2F+G). FOXO1 and FOXO3 are essential to numerous endogenous processes as development, differentiation and tumor suppression, roles not prominently attributed to FOXO4(Hosaka et al., 2004; Nakae et al., 2003; Paik et al., 2007; Renault et al., 2009). Another difference with FOXO1 and 3 is that FOXO4 is only marginally expressed in most tissues (Fig. S2J+K) and FOXO4 knockout mice do not show a striking phenotype (Hosaka et al., 2004; Paik et al., 2007). We therefore chose a region in FOXO4 that is conserved in both humans and mice, but differs from FOXO1 and FOXO3 (Fig. S2L).

Research on peptide chemistry has shown that protein domains containing natural L-peptides can sometimes be mimicked by using D-amino acids in a retro-reversed sequence (Guichard et al., 1994). Modification of peptides to such a D-Retro Inverso (DRI)-isoform can render peptides new chemical properties, which may

improve their potency *in vitro* and *in vivo* (Borsello et al., 2003). Several DRI-modified peptides have been shown to be well tolerated and therapeutically effective in clinical trials. These include a double blinded, randomized, placebo-controlled Phase IIb trial(Beydoun et al., 2015; Deloche et al., 2014; Suckfuell et al., 2014) and a Phase I trial for systemic treatment of solid tumors(Warso et al., 2013), together showing there is precedence for DRI peptides in clinical therapy. This provided the rationale for designing the FOXO4 peptide in a DRI conformation, henceforth named FOXO4-DRI. We performed competition experiments by NMR to investigate whether FOXO4-DRI can inhibit the interaction between p53 and FOXO4 *in vitro*. Titration of a recombinant N-terminal domain of p53 (aa1-312) to a solution containing the 1H, 15N-labelled FOXO4 Forkhead (FH) Domain (aa486-206) induced a progressive chemical shift perturbation (CSPs) of 1H, 15N HSQC cross peaks, indicating specific binding of p53 to FOXO4 (Fig. 2H). Stepwise addition of the FOXO4-DRI peptide to this complex caused the CSPs of FOXO4 to be reverted back to the unbound state, indicating FOXO4-DRI competes with FOXO4 for p53 binding in a dose-dependent manner and doing so with higher affinity (Fig. 2I).

To facilitate cellular uptake of FOXO4-DRI, it was designed as a fusion with HIV-TAT, a basic and hydrophilic sequence which allows energy-independent cellular uptake of cargo through transient pore formation (Herce and Garcia, 2007). Using an antibody against HIV-TAT, we observed FOXO4-DRI to be taken up as soon as 2-4h after administration and to remain detectable for at least 72h (Fig. 2J). Given that the affinity of antibodies is generally low, this indicates FOXO4-DRI effectively enters senescent cells at high intracellular concentrations, which remain abundant and stable over a prolonged period of time. Following its uptake, FOXO4-DRI reduced the number of senescence-induced FOXO4 foci, PML bodies and 53BP1 DNA-SCARS, while not affecting the number of small 53BP1 foci (Fig. 2K).

FOXO4 can regulate expression of the p53-target p21$^{cip1}$ in senescent cells (de Keizer et al., 2010) and through p21$^{cip1}$, p53 can induce p16$^{in4a}$-independent cell cycle arrest in senescent cells(Di et al., 1994). Moreover, p53 can induce apoptosis either through transactivating pro-apoptosis genes, but also in a transcription-independent manner by translocating to the mitochondria (Mihara et al., 2003). Examination of the promoter of Cdkn1a, the gene encoding p21$^{Cip1}$, showed a canonical FOXO target sequence to be flanked by two p53 binding sites (Fig. 2L). We therefore investigated the effect of FOXO4-DRI on p21$^{Cip1}$ and p53. FOXO4-DRI reduced senescence-associated p21$^{Cip1}$ levels (Fig. L) and promoted the accumulation and nuclear exclusion of active pSer15-p53 (Fig. 2M + S2M). Together, these results show that by competing with endogenous FOXO4 for p53 binding, FOXO4-DRI

disrupts senescence-associated FOXO4/PML/DNA-SCARS and causes nuclear exclusion of active p53.

**FOXO4-DRI can selectively and potently target senescent cells for p53-dependent apoptosis**

Given the reported pro-apoptotic role of active p53 when recruited to mitochondria, we next assessed the effects on senescent cell viability. Incubation of senescent and control IMR90 with increasing concentrations of FOXO4-DRI showed FOXO4-DRI to potently and selectively (11.73 fold difference) reduce the viability of senescent vs. control IMR90 (Fig. 3A) and other normal cells (Fig. S3A). Real-time cell density measurements revealed the effect to occur as soon as 24-36 hours after administration (Fig. 3B). Neither the same peptide in L-isoform (Fig. 3C), nor an unrelated DRI-peptide based on a distinct Forkhead protein, FOXM1 (Kruiswijk et al., 2016), affected senescent cell viability (Fig. 3D). These results show that FOXO4-DRI can target senescent cells and highlight the importance of the DRI-modification for its potency.

Two classes of anti-senescence compounds have been reported so far: Quercetin/Dasatinib, either alone or in combination(Zhu et al., 2015), and the pan-BCL inhibitors ABT-263/737(Chang et al., 2016; Yosef et al., 2016). Quercetin and Dasatinib have been reported to be non-specific(Chang et al., 2016). We found no selectivity towards senescent IMR90 (Fig. S3B), and therefore this cocktail was not explored further. ABT-263 (Chang et al., 2016) and ABT-737 (Yosef et al., 2016) target the BCL-2/W/XL family of anti-apoptotic guardians (See also Fig. 1A). Indeed, ABT-737 showed selectivity for senescent IMR90 (Fig. S3B). However, already at low doses it appeared to influence control cells as well (Fig. S3B). Also in a treatment regimen where both compounds were added in consecutive rounds of lower concentrations FOXO4-DRI proved to be selective against senescence yet safe to normal cells (Fig. 3E + S3C).

We next addressed the role of p53 in FOXO4-DRI-mediated clearance of senescent cells. Stable knock-down of p53 reduced the ability of FOXO4-DRI to target senescent IMR90 (Fig. 3F + S3D). A similar effect was observed when the senescent cells were co-incubated with the pan-caspase inhibitors QVD-OPH or ZVAD-FMK (Fig. 3G), suggesting a Caspase-dependent effect. Indeed, real-time imaging in the presence of a Caspase-3/7-activatable dye showed FOXO4-DRI to specifically induce Caspase-3/7 activation in senescent, but not control, cells (Fig. 3H + Mov. 3+4). Together, these data show that FOXO4-DRI potently and selectively reduces the viability of senescent cells by competing with FOXO4-p53 binding, thereby triggering release of active p53 to the cytosol and inducing cell-intrinsic apoptosis through Caspase-3/7. This establishes FOXO4-DRI as a genuine inducer of TASC: Targeted Apoptosis of Senescent Cells.
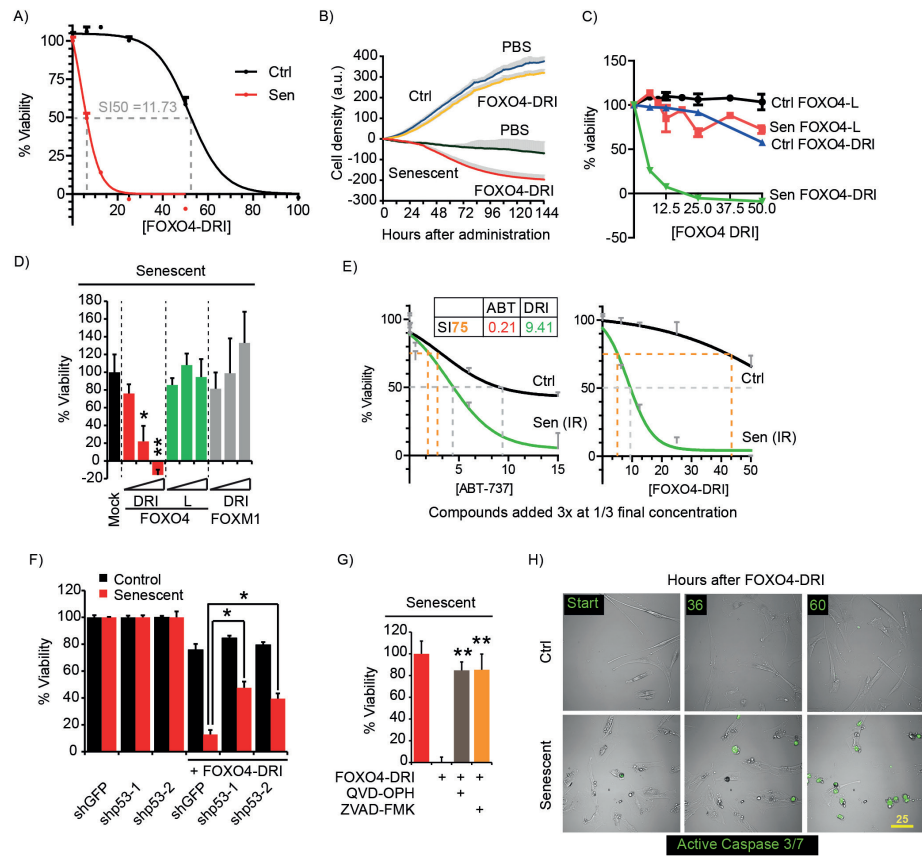
**Fig. 3: FOXO4-DRI selectively eliminates senescent cells through p53-mediated cell-intrinsic apoptosis**

A) Viability assay of senescent and control IMR90 incubated with increasing doses of FOXO4-DRI (µM). The selectivity index (SI50) reflects the differences in EC50 of a non-regression analysis for both groups. See also Fig. S3A. B) Real-time cell density measurement by xCELLigence of control and senescent IMR90 incubated with or without FOXO4-DRI (25µM). C) Viability assay comparing the effects of increasing doses of FOXO4-DRI and the same peptide in L-isoform, FOXO4-L. D) Viability assay comparing FOXO4-DRI, FOXO4-L, and an unrelated FOXM1-DRI peptide(Kruiswijk et al., 2016), at 6.25, 12.5 and 25µM, respectively. E) Viability assay comparing the pan-BCL inhibitor ABT-737 to FOXO4-DRI, when applied in three consecutive rounds at 1/3 the final concentration each (See also Fig. S3B+C). SI75 reflects differences in EC75 of a non-regression analysis for both groups. F) Viability assay comparing the effect of FOXO4-DRI on cells depleted for p53 by shRNA. See Fig. S3D for effects on p53 expression. G) Viability assay comparing the effect of FOXO4-DRI senescent cells incubated with pan-caspase inhibitors (20µM). H) Representative still images of real-time confocal-based imaging of senescent and control cells in the presence of a Caspase-3/7 activatable dye (green) and incubated with FOXO4-DRI. See also Mov. 3+4. Imaging started 8h after FOXO4-DRI addition.

**FOXO4-DRI counteracts chemotherapy-induced senescence and loss of liver function**

Given the potency of FOXO4-DRI against senescence *in vitro*, we wondered whether FOXO4-DRI could be of therapeutic use against senescence-related pathologies. We therefore employed three independent *in vivo* senescence-models, one for chemotoxicity (Fig. 4), one for accelerated aging (Fig. 5+6) and one for natural aging (Fig. 7). In all of these, we made use of the recently developed senescence-detection system: p16::3MR. In this system, the promoter of the major senescence gene p16$^{ink4a}$ drives expression of Renilla Luciferase (RLUC) to allow longitudinal visualization of senescence. In addition, it expresses a Thymidine Kinase from the Herpes Simplex virus, which induces apoptosis when cells are presented with its substrate Ganciclovir (Fig. S4A and(Demaria et al., 2014)).

Off-target toxicity limits the maximum tolerated dose of chemotherapeutic drugs and causes long term health problems in cancer survivors, including an acceleration of aging (Henderson et al., 2014). Chemotherapy can induce senescence (Ewald et al., 2010), and we therefore determined whether therapeutic removal of senescence could influence chemotoxicity. As an example, we used the common chemotherapeutic drug Doxorubicin, which can indeed induce senescence (Cahu et al., 2012; Roninson, 2003) and liver toxicity in rodents and humans(Damodar et al., 2014). In agreement with these reports, Doxorubicin induced senescence in IMR90 *in vitro*, evident by elevated SA-β-GAL activity, expression of p16$^{ink4a}$, and the early and late SASP factors IL-1α and IL-6 (Orjalo et al., 2009), respectively (Fig. 4A-C; S4B). As seen for IR-senescent cells (Fig. 2+3), Doxorubicin-induced senescent cells showed an upregulation in FOXO4 foci (Fig.4B+C) and FOXO4-DRI potently and selectively lowered the viability of Doxorubicin-senescent vs. control IMR90 (Fig. 4D). In line with the IR-senescence data, low effective doses of FOXO4-DRI were well tolerated in normal IMR90 compared to ABT-737, while being very potent against Doxorubicin-senescent cells at higher doses (Fig. 4E). Also in this setting, the potency of FOXO4-DRI was more pronounced when applied in consecutive rounds (Fig. 4F + S4C).

It could be that FOXO4-DRI merely lowers the threshold for cells to enter apoptosis after DNA damage. This would impair its potential for *in vivo* or clinical translation. Incubation of normal IMR90 with FOXO4-DRI, administered at various time-points prior to Doxorubicin-exposure, did not influence the sensitivity of cells to Doxorubicin (Fig. 4G). In contrast, Doxorubicin-senescent cells were effectively cleared. Thus, FOXO4-DRI does not predispose healthy cells to DNA-damage, but selectively targets cells that have undergone senescence as a consequence of earlier Doxorubicin-exposure. Together this prompted us to try a similar sequential treatment regimen of FOXO4-DRI in Doxorubicin-exposed mice *in vivo*.
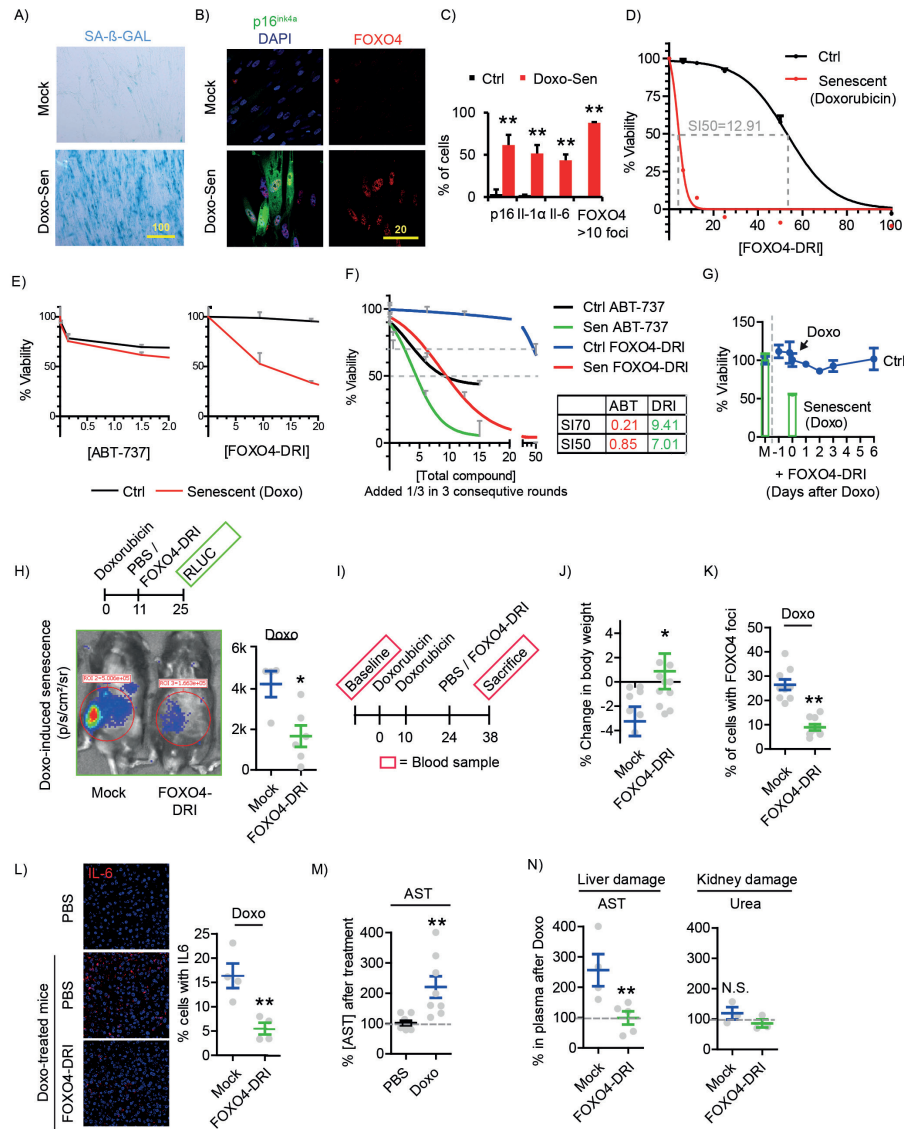
41

**Fig. 4: FOXO4-DRI counteracts Doxorubicin-induced senescence and chemotoxicity *in vivo***

A) SA-β-GAL assay to detect senescence in IMR90 7d after 2x treatment (1d in between) with 0.1μM Doxorubicin. B) Immunofluorescence for p16ink4a and FOXO4 in control or Doxo-senescent IMR90. See also Fig. S4B. C) Quantification of the % of cells positive for p16ink4a, IL1α, IL6 and FOXO4 foci after Doxorubicin-induced senescence. D) Viability assay comparing the effect of FOXO4-DRI on control and Doxo-senescent cells *in vitro*. SI determined as in Fig. 3A. E) Viability

assay comparing ABT-737 vs. FOXO4-DRI on Doxo-senescent cells. F) Same as in E, but both added 3x at 1/3 the final concentration. See also Fig. S4C. G) Viability assay comparing effects of incubation of FOXO4-DRI for various time points prior, during or after Doxorubicin exposure (blue line) vs. cells already induced to senesce by Doxorubicin (green boxes). M=Mock. H) Representative bioluminescence image and quantification of p16-driven senescence (RLUC) in p16::3MR mice (See Fig. S4A+D), treated as indicated with Doxorubicin, followed by FOXO4-DRI or Mock. I) Timeline of experiments in J-N. Doxorubicin: 2x i.p. at 10mg/kg. FOXO4-DRI: 3x i.v. at 5mg/kg, every other day (day 1, 3 and 5). J) Quantification of the % change in body weight of Doxorubicin-exposed mice treated with FOXO4-DRI or PBS, respectively. K) Quantification of the number of liver cells with ≥ 10 FOXO4 foci after Doxorubicin-exposure and treatment with PBS or FOXO4-DRI. L) Visualization and quantification of the % of liver cells from the mice in (K) expressing IL-6. M) Quantification of the Doxorubicin-induced increase in plasma AST levels as marker for liver damage. N) Quantification of the effects of PBS or FOXO4-DRI on Doxorubicin-induced plasma levels of AST and Urea as markers for liver and kidney damage, respectively. See also Fig. S4E+F.

In follow-up of the *in vitro* data, Doxorubicin progressively induced senescence *in vivo* as detected by p16[ink4a]-driven RLUC in p16::3MR mice (Fig. S4D). Furthermore, as seen in patients, Doxorubicin reduced total body weight (Fig. 4J) and induced expression of FOXO4 foci and IL-6 in the liver (Fig. 4K+L). Strikingly, these effects were neutralized after sequential treatment with FOXO4-DRI (Fig. H-L). We therefore wondered whether liver function was also affected. Doxorubicin strongly induce plasma levels of Aspartate Aminotransferase, AST, an established indicator of liver damage(Damodar et al., 2014)(Fig. 4M). Excitingly, FOXO4-DRI potently counteracted the Doxorubicin-induced increase in plasma AST (Fig. 4N). To address whether these effects are mediated through clearance of senescence, we combined treatment of FOXO4-DRI with GCV, to facilitate senescence clearance through the TK suicide gene of p16::3MR construct. GCV reduced Doxorubicin-induced p16-RLUC expression (Fig. S4E) and plasma AST levels (Fig. 4M + S4F), indicating AST reduction is indeed caused by clearance of senescent cells. In both cases, FOXO4-DRI did not further enhance these effects. Together, these data indicate that FOXO4-DRI is effective in reducing Doxorubicin-induced senescence *in vitro* and *in vivo* and in doing so neutralizes the Doxorubicin-induced loss in body weight and liver toxicity. Thus, FOXO4-DRI is effective against chemotoxicity.

**FOXO4-DRI counteracts senescence and features of frailty in fast aging *Xpd^{TTD/TTD}* mice**

We next wondered whether FOXO4-DRI could influence the healthspan of mice in which senescence and the concomitant loss of tissue homeostasis were not actively induced, but were allowed to develop spontaneously as a consequence of aging. As is the case for humans(Ferrucci et al., 2005), we expected strong biological variation in senescence and the SASP in naturally aged wildtype mice. To reduce the effects of biological noise, we therefore decided to first employ fast aging mice. We sought a model that recapitulates features of natural aging and does not suffer

from age-related pathologies caused by other processes as apoptosis(de Keizer, 2017). This we found in $Xpd^{TTD/TTD}$, a model based on the human premature aging syndrome Trichothiodystrophy (TTD)(de Boer et al., 2002; de Boer et al., 1998). Using the p16::3MR reporter system, we observed that already at young age $Xpd^{TTD/TTD}$ animals show high levels of p16-positive senescence (Fig. 5A). As also seen for Doxorubicin-induced senescence, FOXO4-DRI reduced this effect (Fig. 5B), arguing that $Xpd^{TTD/TTD}$ is a valid fast aging model for studying the effects of FOXO4-DRI on spontaneously developed senescence *in vivo*.

Underscoring their aging phenotype, $Xpd^{TTD/TTD}$ mice show accelerated loss of hair (Fig. 5D and (de Boer et al., 1998)). While not initially focused on this phenotype, we observed a robust improvement of fur density in FOXO4-DRI treated $Xpd^{TTD/TTD}$ mice (Fig. 5C+D and S5A). To address this more quantitatively, we determined the infrared-measured abdominal surface temperature of the mice. Due to the lack of fur, the abdominal temperature of $Xpd^{TTD/TTD}$ mice was several degrees higher than wildtype counterparts, an effect reduced by FOXO4-DRI (Fig. 5E). A second unexpected observation was found in the behavior of the treated mice. Whereas $Xpd^{TTD/TTD}$ mice generally show less exploratory behavior compared to wildtype littermates, FOXO4-DRI treated animals were noticeably more active (Fig. S5B). To also investigate this more quantitatively, we scored the responsiveness of the mice to gentle physical stimuli. Despite individual variation, $Xpd^{TTD/TTD}$ mice were on average considerably more responsive to such stimuli after FOXO4-DRI treatment (Fig. 5F). Finally, as a more objective measure of activity, we tracked voluntary physical activity in a set-up in which the mice were continuously housed in cages with free access to running wheels. Despite significant individual differences, $Xpd^{TTD/TTD}$ mice were found to run 1.37 ± 0.54 km/day on average, compared to 9.37 ± 1.1 km/day seen for wildtype mice, arguing they are indeed less mobile (Fig. 5G). In line with the behavioral results, exposure of the mice to FOXO4-DRI increased running wheel activity over time in the majority of these (Fig.H+I). Together, these results indicate that FOXO4-DRI can reduce cellular senescence and counteract hair loss and general frailty in fast aging $Xpd^{TTD/TTD}$ mice.
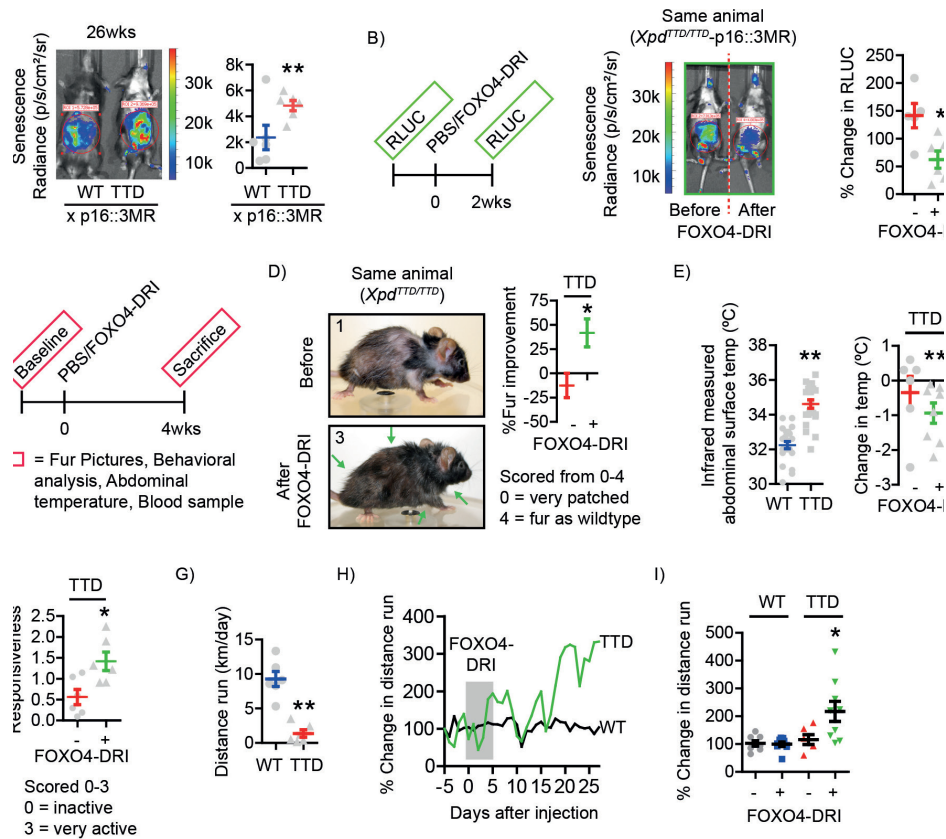
**Fig. 5: FOXO4-DRI decreases senescence and counters features of frailty in fast aging *Xpd^{TTD/TTD}* mice**

A) Representative mice and quantification of p16^{ink4a}-driven RLUC Radiance in 26wk young wildtype and *Xpd^{TTD/TTD}* mice crossed into p16::3MR. B) Left: Timeline for visualization of effects of FOXO4-DRI or PBS on p16-driven senescence by bioluminescence in *Xpd^{TTD/TTD}*. Middle: Representative visualization of p16^{ink4a}-driven senescence in the same *Xpd^{TTD/TTD}-p16::3MR* mouse before and after FOXO4-DRI. Right: Quantification of the effects of FOXO4-DRI or PBS on senescence in a larger cohort of *Xpd^{TTD/TTD}-p16::3MR* mice. C) Timeline for measuring the effects of FOXO4-DRI or PBS on hair density, behavior and running wheel activity in D-I. D) FOXO4-DRI improves fur appearance of Xpd^{TTD/TTD} mice. Left panels: Representative images of the same *Xpd^{TTD/TTD}* animal before and after treatment with FOXO4-DRI. Right panel: quantification of the average change in fur score (See also Fig. S5A). E) Quantification of abdominal temperature measured by infrared thermometer as measure for fur density of wt vs. *Xpd^{TTD/TTD}* mice (left) and the effects of FOXO4-DRI and PBS in the mice from D and Fig. S5A (right). F) Quantification of the response of the *Xpd^{TTD/TTD}* mice from D to gentle physical stimuli before and after treatment with FOXO4-DRI or PBS. Note that *Xpd^{TTD/TTD}* mice are generally relatively non-responsive. See also Fig. S5B. G) Quantification of the average distance run per day of wt. vs *Xpd^{TTD/TTD}*. H) Example of changes in running wheel behavior of a wt vs. Xpd^{TTD/TTD} mouse treated with FOXO4-DRI. Data normalized to 100% for respective running wheel activity at baseline. On day 10 a blood sample was taken, resulting in a transient decrease in activity. I) Quantification of the average change in running wheel activity in wildtype and Xpd^{TTD/TTD} mice after PBS or FOXO4-RI treatment.

**FOXO4-DRI counteracts loss of renal function in fast aging $Xpd^{TTD/TTD}$ mice**

The phenotypical and behavioral results described above are difficult to connect to a molecular mechanism. We therefore decided to focus on the role of senescence in aging-induced decline in function of specific tissues. Pilot measurements of various metabolites in plasma samples of $Xpd^{TTD/TTD}$ mice suggested they suffer from decreased renal function. As injected compounds tend to accumulate in the kidney, this together argued for investigating the potential of therapeutic removal of senescence in this organ. Urea is secreted through urine, but becomes detectable in the blood when glomerular filtration rates drop. Plasma Urea is therefore a marker of declined renal filtering capacity(Gowda et al., 2010; Lyman, 1986). In fact, it was recently established that semigenetic clearance of senescence can delay the aging-induced increase in plasma Urea, establishing senescence as a culprit for loss of renal filtering capacity during aging (Baker et al., 2016). As evident from the increase in plasma Urea levels, renal function indeed declines in wildtype mice as they age (Fig.6A; 26w vs. 130w). This was faithfully recapitulated early in life in $Xpd^{TTD/TTD}$ (Fig. 6A; 26w WT vs 26w TTD). Both naturally aged wildtype and young $Xpd^{TTD/TTD}$ kidneys showed a strong increase SA-β-GAL activity and IL-6 expression in the tubular regions (Fig. 6B+C). In addition, they also showed a significant increase in tubular cells positive for FOXO4 foci (Fig. 6D), together indicating that both modes show elevated senescence. Using an *ex vivo* system of aged kidney slices FOXO4-DRI induced strong TUNEL positivity within 3 days (Fig. 6E and S6A-D), indicating that FOXO4-DRI can also induce apoptosis in these cells. Altogether this provided rationale for investigating the potency of FOXO4-DRI on tubular senescence and renal function in *in vivo*.

A limitation to the therapeutic potential of the senolytic pan-BCL inhibitors ABT-263/ABT-737 is their tendency to cause severe thrombocytopenia(Schoenwaelder et al., 2011). This is undesirable when actually aiming to restore healthspan of aged individuals. Comparing platelet levels before and 30d after treatment showed FOXO4-DRI not to noticeably influence platelet levels (Fig. 6F) or other whole blood values (Fig. S6E). Neither did it cause deleterious effects on non-proliferative tissues as far as tested, e.g. the heart (Fig. S6F). Encouraged by the passing of at last these initial safety concerns, we progressed to measuring the effects of FOXO4-DRI on renal senescence and functional capacity. In line with the SA-β-GAL data, tubuli of $Xpd^{TTD/TTD}$ kidneys show severe loss of LMNB1 (Fig. 6G), a robust molecular marker of senescence (Freund et al., 2012). This is paralleled with elevated IL-6 (e.g. Fig. 6J), indicative of SASP, and elevated Urea levels in the blood (e.g. Fig. 6K). SASP factors as IL-6 may be the cause for the observed loss in renal function and we wondered how FOXO4-DRI would function under such high-SASP conditions. *In vitro* experiments showed FOXO4-DRI to be more potent against senescent cells in which

SASP was transiently boosted by recombinant IL1α/β or LPS, whereas an IL1 receptor antagonist or the general anti-inflammatory drug Cortisol reduced its potency (Fig. 6H+I). Thus, FOXO4-DRI actually is most effective against senescent cells expressing high levels of SASP and could as such be particularly effective against loss of renal function. Excitingly, while not substantially influencing total body nor kidney weight (Fig. S6G), FOXO4-DRI treatment normalized the percentage of tubular cells lacking LMNB1 (Fig. 6G), the tubular IL-6 elevation (Fig. 6J) and the elevations in plasma Urea levels (Fig. 6K). To address whether this is mediated by senescence-clearance, we again made use of the ability of the 3MR construct to eliminate senescent cells through GCV. As GCV is typically administered i.p, we treated a cohort of $Xpd^{TTD/TTD}$-p16::3MR mice i.p with FOXO4-DRI and GCV. GVC and FOXO4-DRI induced a comparable reduction in plasma [Urea] in both groups (Fig. 6L). Thus, FOXO4-DRI targets high SASP-expressing senescent cells that have naturally developed in the kidneys of fast aging $Xpd^{TTD/TTD}$ mice and in doing so restores kidney homeostasis.

**FOXO4-DRI counteracts frailty and loss of renal function in naturally aged mice**

Encouraged by these results, we decided to challenge whether FOXO4-DRI could also target senescence and tissue homeostasis in normal mice that were allowed to age naturally. As expected, the biological variation in p16-driven senescence was substantial in aged p16::3MR, compared to young $Xpd^{TTD/TTD}$-p16::3MR (Fig. 7A, and C). The variation in running wheel activity was too large to perform meaningful experiments (Fig. S7A). Nonetheless, while again not influencing platelet levels (Fig. 7B), FOXO4-DRI significantly reduced p16-driven RLUC (Fig 7C), and could improve fur density (Fig. 7D) and responsiveness (Fig. 7E). Furthermore, in the kidneys of these mice FOXO4-DRI increased the number of LMNB1 positive cells (Fig. 7F), reduced IL-6 expression (Fig. 7G) and restored renal filtering capacity measured by decreased plasma Urea (Fig. 7H). As an extra control, also the plasma levels of a second metabolite indicative of reduced renal function, Creatinine, was measured. Also this was reduced by FOXO4-DRI, independently confirming the beneficial effect of FOXO4-DRI on the restoration of renal filtering capacity in naturally aged mice (Fig. 7I). As seen for the $Xpd^{TTD/TTD}$-p16::3MR mice, i.p administration of FOXO4-DRI or GCV equally reduced plasma Urea and Creatinine levels (Fig. 7J). Thus, senescent cells are causal for the reduction in renal function in fast aging $Xpd^{TTD/TTD}$ and naturally aged wildtype mice and by selective targeting of high-SASP expressing senescent cells in the tubuli, FOXO4-DRI can restore kidney homeostasis. By inducing TASC, FOXO4-DRI may thus be a potent drug to restore loss of health after natural aging and is an attractive option to explore further in the battle against those age-related diseases that are at least in part driven by senescence.
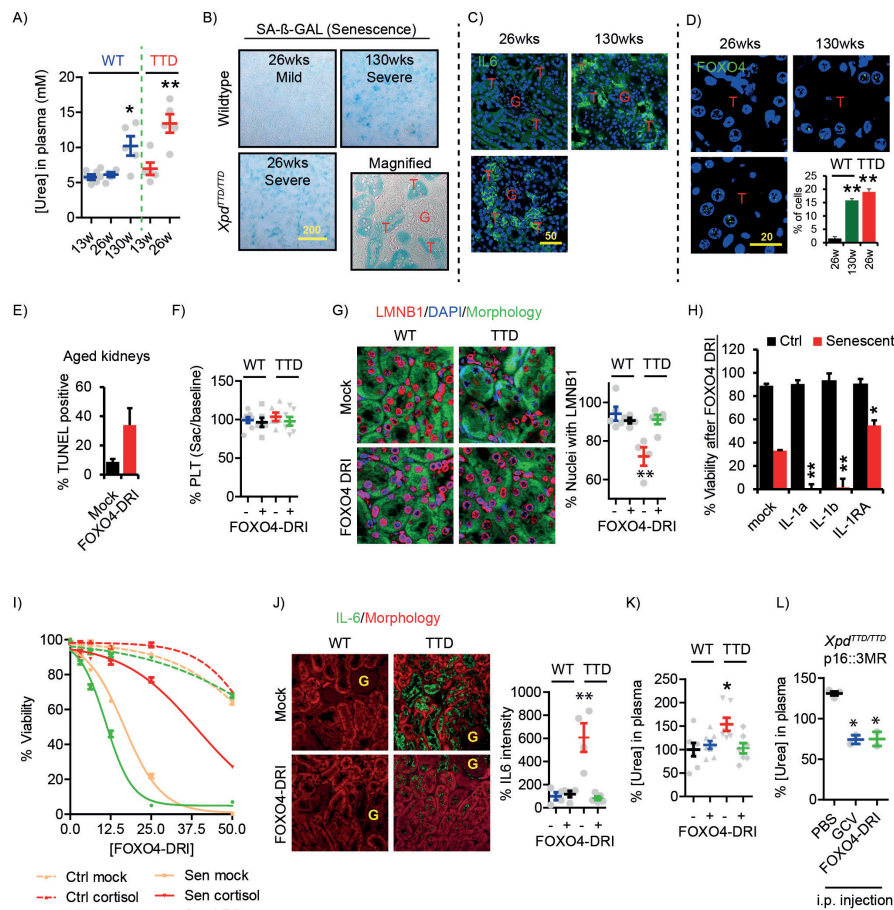
**Fig. 6: By targeting senescence, FOXO4-DRI counters loss of renal function of _Xpd^TTD/TTD_ mice**

A) Quantification of renal filtering capacity measured by plasma [Urea] in 13, 26 and 130w old wildtype mice and 13 and 26w _Xpd^TTD/TTD_ mice. B-D) Visualization of senescence (SA-β-GAL), the major SASP factor IL-6 and FOXO4 foci in 26w + 130w wildtype and 26w _Xpd^TTD/TTD_ old kidneys. Tubuli (T), Glomeruli (G). Inset C: Magnification of SA-β-GAL to reveal affected areas. Inset D) quantification of the % of renal cells expressing ≥10 FOXO4 foci. E) TUNEL assay to detect apoptosis in kidney sections of 130w old wt mice treated 3d with PBS or FOXO4-DRI. See Fig. S6A-D for pipeline and results with shFOXO4. F) Quantification of the % of platelets at time of sacrifice vs. baseline for wt and _Xpd^TTD/TTD_ mice treated with PBS or FOXO4-DRI. See also Fig. S6E. G) Representative Images of kidneys from 26w wt or _Xpd^TTD/TTD_ mice stained for LMNB1 loss. Quantified are the average number of nuclei per kidney positive for LMNB1 (at least 400nuclei per mouse). H) Viability assay on control or senescent IMR90 incubated with recombinant IL1α, IL1β or IL1 receptor antagonist (IL1-RA) 24h prior to exposure of FOXO4-DRI. I) Viability plot showing the effect of FOXO4-DRI on control and senescent IMR90 pretreated with Cortisol and LPS, prior

to FOXO4-DRI treatment. J) Staining as in G), but for the SASP marker IL-6. Quantified is the average IL-6 intensity per kidney over at least 3 frames per mouse for at least 4 mice per group. K) Quantification of the % plasma [Urea] of three pooled cohorts of wt and *Xpd^TTD/TTD* mice (n=7-8 mice/ treatment) after 30d treatment with PBS or FOXO4-DRI. Data are represented as mean +/- SEM. See also Fig. S4G. L) Experiment as in K), but using Ganciclovir (GCV) to mediate semigenetic clearance of senescent cells through the Thymidine Kinase expressed by the p16::3MR construct. As GCV is i.p. administered, also FOXO4-DRI was i.p. administered in this experiment.
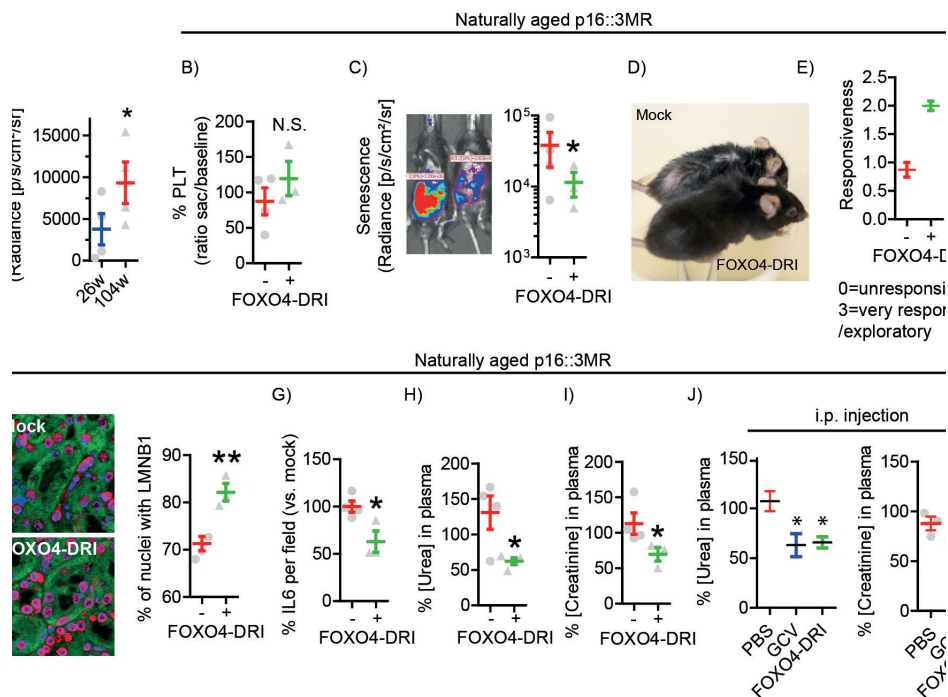


**Fig. 7: By targeting senescence, FOXO4-DRI counters frailty and loss of renal function in naturally aged p16::3MR mice**
A) Quantification of p16^ink4a-driven RLUC radiance in 104w old p13::3MR mice compared to 26w counterparts. Note there is a larger degree of spread in the signal, suggesting biological variation. B) Quantification of the % platelets at time of sacrifice/baseline of naturally aged p16::3MR mice treated with PBS or FOXO4-DRI for 30d. Procedure as in Fig. 5C. C) Representative images and quantification of p16^ink4a-driven RLUC radiance of mice the from B). D) Example of fur density in FOXO4-DRI vs. Mock-treated male p16::3MR mice. See also Fig. S7B. E) Quantification of the responsiveness of the mice in B-D treated with FOXO4-DRI or PBS. Analysis as in Fig. 5F. F-I) Quantification of the effects of FOXO4-DRI on LMNB1 loss and IL6 intensity in the kidneys and plasma [Urea] and [Creatinine] of the naturally aged p16::3MR mice from B). G) Quantification of % plasma [Urea] and [Creatinine] of naturally aged (110+wk) p16::3MR mice at 30d after i.p. injection with 3x 5mg/kg (every other day) FOXO4-DRI or 5x25mg/kg/day with GCV to clear senescent cells semigenetically.

## Discussion

With life expectancy projected to increase in the foreseeable future (Vaupel, 2010) it is important to develop strategies to extend and restore healthspan. Cell-penetrating peptides are relatively understudied in aging research. Further analysis of their use is warranted, as they serve several major advantages. Counter to broad-range inhibitors, CPPs can in theory target any surface-exposed stretch of amino acids to block specific protein-protein interactions and, in doing so, they can selectively modulate very specific downstream signaling events (Discussed in (de Keizer, 2017)). Other compounds, classified as senolytics, have been described to influence senescent cell viability. As a CPP, FOXO4-DRI differs from these by being designed around a specific amino acid sequence in a molecular target only mildly expressed in most normal tissues (see e.g. Fig. S2J+K). Though a more thorough analysis is required, as least as far as tested here FOXO4-DRI appears to be well tolerated, which is an absolutely critical milestone to pass when aiming to treat relatively healthy aged individuals(de Keizer, 2017).

FOXO4-DRI effectively disrupts the p53-FOXO4 interaction (Fig. 2H+I), but the importance of the FOXO4 protein itself is more complicated in DNA damage and senescence. As FOXO4-DRI causes nuclear exclusion of active p53, the levels of p21$^{Cip1}$ decline (Fig. 2L-N). However, the loss of p21$^{Cip1}$ alone is insufficient to induce apoptosis and was actually shown to induce a senescence-escape instead (Brown et al., 1997). Rather, the exclusion of p53 itself has been reported to induce apoptosis directly when located to mitochondria (Mihara et al., 2003), thereby explaining the FOXO4-DRI effects. FOXO4 shRNAs induce apoptosis in senescent IMR90 (Fig. 1E-H), arguing that full FOXO4 inhibition might also be of use against senescence. True as this may be, chronic FOXO4 reduction is not advisable as FOXOs play a role in DNA-damage repair and *Foxo4-/-* mice are susceptible to acute damage(Zhou et al., 2009). In contrast to loss of FOXO4, FOXO4-DRI does not sensitize healthy cells to acute DNA damage (Fig. 4G). Thus, while permanent FOXO4 inhibition is inapplicable, the fact that as a CPP it can block a specific protein-protein interaction make FOXO4-DRI selective, and thereby well-tolerated and effective.

Based on these positive effects, it is now possible to envision a point on the horizon where the disease indications are identified that could benefit most from FOXO4-DRI therapy. High SASP-secreting cells are likely to play a much larger role in disease development than more sterile senescent cells. Through SASP, senescent cells may permanently confer a state of stemness in neighboring cells and thereby impair tissue function and renewal, an effect which we recently described in the senescence-stem lock model for aging (de Keizer, 2017). FOXO4-DRI has a

strong preference for targeting high-SASP subpopulations of senescent cells, but it is unclear what causes heterogeneity in the SASP. It will be a major achievement to unravel those mechanisms and to steer these such that therapeutic targeting is most beneficial. In that sense, identification of senescence-driven pathologies that rely on SASP may help in optimizing candidates for therapy. $Xpd^{TTD/TTD}$ is pleiotropic model for aging that can be effectively used as a basis for such research. It is a well-established model for osteoarthritis, especially in cohorts of older age than we used here (52w) (Botter et al., 2011) and for the unhealthy loss in muscle (sarcopenia) and fat mass(Wijnhoven et al., 2005).

Last, it is relevant to note that independent of aging and age-related diseases, FOXO4-DRI may be of use against the progression, stemness and migration of malignant cancer. Given that SASP factors influence these(Campisi, 2013), it will be particularly interesting to determine whether FOXO4-DRI affects those p53-wt cancer cells that have adopted a more migratory and stem-like state due to reprogramming by chronic SASP exposure. In any case, the here reported beneficial effects of FOXO4-DRI provide a wide range of possibilities for studying the potential of therapeutic removal of senescence against diseases for which few options are available.

## Author contributions

## Acknowledgements

## STAR Methods

## Contact for reagent and resource sharing

Further information and requests for resources and reagents should be directed to and will be fulfilled by the Lead Contact, Peter L.J. de Keizer (p.dekeizer@erasmusmc.nl). The following materials: $Xpd^{TTD/TTD}$ mice; p16::3MR mice and the peptide FOXO4-DRI are subject to patent applications and may be shared with research organizations for research and educational purposes only under an MTA to be discussed in good faith with the recipient; such MTA may restrict recipient to make any modifications to these materials.

## Experimental model and subject details

### Mouse experiments

This study was performed in strict accordance with all applicable federal and institutional policies. The protocol was approved by the Dutch Animal Ethics Committee. All the mice used in this study were of a C57BL/6J background; either wildtype, $Xpd^{TTD/TTD}$ mutated, expressing p16::3MR, or a combination thereof. The individual strains were backcrossed at least 10 times prior to this study. For the combination $Xpd^{TTD/TTD}$ x p16::3MR the F1 generation was used. The mice were used at the ages indicated in the figures, for Doxorubicin-experiments at 10-40wks of age, for $Xpd^{TTD/TTD}$ vs. wt experiments at 26-60 wks of age and for naturally aged mice at 115-130wks of age. All mice were kept in group housing until the start of the experiment after which they were placed in individual cages containing free access to a running wheel. Both sexes were used throughout the study. Where feasible, littermates of the same sex were used. These were randomly assigned to experimental groups.

### Cell culture

The following cell lines were used in this study: IMR90 and WI-38 human fetal lung fibroblasts (female), BJ human foreskin fibroblasts (male), NIH3T3 mouse fibroblasts,

wt and *bax/bak$^{-/-}$* littermate Baby Mouse Kidney (BMK) cells, Human Embryonic Kidney (HEK) 293LTV. All cells were obtained from ATCC, except for wt and *bax/ bak$^{-/-}$* BMK cells which were a kind gift of Dr. Eileen White and have previously been described(Degenhardt et al., 2002). All cells were maintained in high glucose Dulbecco's Modified Eagle's Medium (Lonza), supplemented with 10% Fetal Calf Serum, penicillin/streptomycin and 0.05% glutamine. IMR90, BJ, WI-38 cells were kept at 5% $CO_2$, 3% $O_2$ and used between 28-45 population doublings. The BMK cells were kept at 5% $CO_2$, 3% $O_2$. The NIH3T3 and HEK293LTV cells were maintained at 5% $CO_2$, ambient $O_2$. All cell lines were regularly tested for mycoplasma contamination using MycoAlert™ Mycoplasma Detection Kit (Lonza) and by assessment of (lack of) DAPI-positive microvesicles under fluorescence microscope. For IR-induced senescence, cells were exposed to 10Gy X- or Gamma rays, and analyzed 10 days later or otherwise indicated; control (proliferating) cells were mock irradiated, meaning they were taken out of the incubator and carried to the irradiator where they were placed outside for the same period of time as the irradiated cells. Senescence was confirmed by SA-β-GAL assay(Dimri et al., 1995) and/or changes in morphology. For Doxorubicin-induced senescence, the cells were treated twice with 0.1μM Doxorubicin (Sigma) with a 2d interval and analyzed 7d later, or as otherwise indicated.

**Kidney slice culture**

For tissue slice experiments, mice were used for which approval was obtained from the Committee on the Ethics of Animal Experiments of the Erasmus MC, where possible as a left-over from other experiments. Freshly isolated kidneys were sectioned in 200μM thick slices using a Vibratome (Leica, Eindhoven, the Netherlands). The sections were cultured in Dulbecco's modified eagle medium with 10% FCS at 37°C, 5% CO2 on a shaker (60 rpm). Following incubation with shRNA-containing lentiviral particles, or FOXO4-DRI, as indicated, the slices were fixed for 30min in formalin and stored at -80. Subsequently, they were subsectioned to 10μM slices using a Cryostat, placed on a charged microscopy slide and processed for TUNEL positivity.

## Methods details

**Antibodies and reagents**

Antibodies against the following proteins were used (See also Key Resource Table): Cell Signaling: FOXO1 (2880), FOXO4 (9472), Phospho-Ser15 p53 (9286), PUMA (4976), BIM (C3C5), Cleaved Caspase-3 (9661), Sigma: FOXO4 (HPA040232), Tubulin (clone B512; no: T5168), Abcam: BCL2 (Ab7972), IL6 (ab6672), Histone H3 (Ab1791-100), BD Transduction Laboratories: p21$^{Cip1}$ (610234), BD Pharmigen:

Cytochrome C (556432), R&D systems: IL1α clone 4414, MAB200), human IL6 (AF206NA), Upstate: 53BP1 (05-726), Millipore: FOXO1 (07-702), Santa Cruz: p16$^{Ink4a}$ (JC8; sc56330), PML (N19; sc9862), LMNB1 (M-20; sc-6217), Novacastra: mouse p53 (NCL-p53-CM55).

The following reagents were used: QVD-OPH (BD biosciences), ZVAD-FMK (SelleckChem), Rotenone (Sigma-Aldrich, St. Louis, MO, USA), Doxorubicin (Santa Cruz).

**Lentivirus production and shRNAs**

Lentiviruses were produced in an MLII-certified lab area, using the 3$^{rd}$ generation production system. In brief, HEK293LTV cells were transfected (Lipofectamine2000) with the packaging/envelope plasmids pRSV-Rev, pMDLg/pRRE and pMD2.G, in combination with a lentiviral transfer plasmid of choice. The next day, the media was refreshed. After 48h, the media was collected for transduction and stored at 4ºC until needed. The following shRNA constructs were used (See also Key Resources Table): shGFP, shFOXO4-1: TRCN0000039720, Mature sequence: CCAGCTTCAGTCAGCAGTTAT, shFOXO4-2: TRCN0000039721, Mature sequence: CGTCCACGAAGCAGTTCAAAT, shFOXO4(mouse): TRCN0000071560, Mature sequence: GATCTGGATCTTGATATGTAT, shp53-1: TRCN0000003753, Mature sequence: CGGCGCACAGAGGAAGAGAAT and shp53-2: TRCN0000003754, Mature sequence: TCAGACCTATGGAAACTACTT. For transient expression of FOXO1, we transfected cells with pBabe-Puro-FOXO1(de Keizer et al., 2010). For stable transduction of HRAS$^{G12V}$, we used pLENTI-Puro (670-1)-HRAS$^{G12V}$(Freund et al., 2012). The day after transduction, the cells were refreshed and 24h later placed on selection in media containing 0.5µg/ml puromycin. Three days later, the media was refreshed with media containing 1µg/ml puromycin in which they were kept throughout the assay. After 7d of selection, the cells were used in their respective assays. The shRNA-transduced cells were subsequently exposed to senescence-inducing IR and processed for Cell viability after 6d. For assays on IMR90 cells that were already senescent, treatment occurred as indicated (Fig. S1C) and the cells were subsequently processed for cell viability or cell density.

**FOXO4 D-Retro-Inverso peptide development**

FOXO4-DRI consists of the following amino acid sequence in D-Isoform:

H-ltlrkepaseiaqsileaysqngwanrrsggkrppprrrqrrkkrg-OH. MW: 5358.2 It was manufactured by Pepscan (Lelystad, the Netherlands) at >95% purity and stored at -20°C in 1mg powder aliquots until used to avoid freeze-thawing artefacts. For *in vitro* experiments FOXO4-DRI was dissolved in PBS to generate a 2mM stock. For

*in vivo* use, FOXO4-DRI was dissolved in PBS to generate a 5mg/ml stock solution, which was kept on ice until injection. Before injection the solution was brought to room temperature.

## Total RNA isolation and mRNA sequencing sample preparation

The total RNA isolation and sequencing library preparation from IR-induced senescent and proliferating IMR90 cells was performed as follows: total RNA was isolated using Qiazol Lysis Reagent (Qiagen) and purified with the miRNeasy kit (Qiagen). The integrity (scores >9.0) of the RNA was determined on the Agilent 2100 Bioanalyzer (Agilent). Total RNA enrichment for sequencing poly(A) RNAs was performed with the TruSeq mRNA sample preparation kit (Illumina). 1µg of total RNA for each sample was used for poly(A) RNA selection using magnetic beads coated with poly-dT, followed by thermal fragmentation. The fragmented poly(A) RNA enriched samples were subjected to cDNA synthesis using Illumina TruSeq preparation kit. cDNA was synthesized by reverse transcriptase (Super-Script II) using poly-dT and random hexamer primers. The cDNA fragments were then blunt-ended through an end-repair reaction, followed by dA-tailing. Subsequently, specific double-stranded bar-coded adapters were ligated and library amplification for 15 cycles was performed. The pooled cDNA library consisted of equal concentration bar-coded samples. The pooled library was sequenced in one lane, 36 bp single read on the HiSeq2500 (Illumina). The analysis of the sequencing dataset was performed by Total RNA analysis pipeline (TRAP).

## Total RNA analysis pipeline (TRAP)

Reads were aligned to the human hg19 reference genome using the NARWHAL automation software. Exonic reads were summed per transcript. A specific transcript was considered expressed, when a minimum number of reads, i.e. 5 reads per million, could be aligned to a transcript. Pathway analysis was performed with Ingenuity Pathway Analysis Software (IPA; Version build 242990).

## Production and purification of recombinant proteins

The constructs corresponding to human FOXO4 (residues 86 – 206) and human p53 (residues 1 – 312), were purchased from Genscript in a pUC cloning vector. The DNA sequence was codon optimized for protein production in bacterial cells and flanked by NcoI and BamHI restriction sites. The coding region was cloned into a modified pETM-11 bacterial expression vector (EMBL Heidelberg) which was derived from a pET-24d(+) vector (Novagen) by insertion of a tobacco etch virus (TEV) protease cleavage site following a N terminal hexa-histidine and protein A tag. The

genes were amplified by PCR using T4 primers (New England Biolabs). The resulting PCR products and pETM-11 were double digested with NcoI and BamHI enzymes (New England Biolabs) before ligation. The construct was verified by sequencing.

The human p53$^{1-312}$, and FOXO4$^{86-206}$ DNA sequences were codon optimized for protein production in bacterial cells and flanked by NcoI and BamHI restriction sites. The coding region was cloned into a modified pETM-11 bacterial expression vector which was derived from a pET-24d(+) vector (Novagen) by insertion of a tobacco etch virus (TEV) protease cleavage site following an N terminal hexa-histidine and protein A tag.

Unlabeled and uniformly (15N) labelled protein was produced in freshly transformed E. coli BL-21 (DE3) cells. A single colony was inoculated in Luria-Bertani medium (20 ml) with kanamycin (25 mg l-1) and cultured at 37 °C overnight. From this, an aliquot (1 ml) was added to either 1 l unlabeled Luria-Bertani medium or 1 l 15N labelled M9 minimal medium (100 mM $KH_2PO_4$, 50 mM $K_2HPO_4$, 60 mM $Na_2HPO_4$, 14 mM $K_2SO_4$, 5 mM $MgCl_2$; pH 7.2 adjusted with HCl and NaOH with 0.1 dilution of trace element solution (41 mM $CaCl_2$, 22 mM $FeSO_4$, 6 mM $MnCl_2$, 3 mM $CoCl_2$, 1 mM $ZnSO_4$, 0.1 mM $CuCl_2$, 0.2 mM $(NH_4)_6Mo_7O_{24}$, 17 mM EDTA) with kanamycin (25 mg l-1) in which $^{15}N$-$NH_4Cl$ (2 g l-1) was the only source of nitrogen for NMR isotope labelling purposes, respectively (Cambridge Isotope Laboratories, Inc). The culture was incubated at 37 °C and shaken at 200 rpm until the OD600 reached 0.8. Protein expression was induced with 1 mM β-D-1-thiogalactopyranoside (IPTG) at 18 °C. The cells were pelleted after 20 hours by centrifugation using a Fiberlite F9-6x1000 rotor in a Sorvall LYNX 6000 Superspeed centrifuge at 2,000 g for 20 minutes, re-suspended in 40 ml lysis buffer containing 50 mM Tris, pH 7.5, 150 mM NaCl, 20 mM imidazole, 20 % glycerol, 2 mM TCEP, 250 units of Benzonase® Nuclease and bacterial Protease Inhibitor Cocktail (Amresco; AEBSF, E-64, Bestatin, EDTA and Pepstatin) and were subsequently lysed by sonication. Lysates were cleared by centrifugation for 45 min at 4 °C (12 000 r.p.m.; Sorvall Lynx 6 000) and filtration (0.45 μm cellulose acetate syringe filters). Proteins were purified using Ni-NTA resins for immobilized metal affinity chromatography. Lysate was applied on the column and contaminants were removed using Wash buffer 1 (50 mM Tris, pH 7.5, 150 mM NaCl, 20 mM imidazole and 2 mM TCEP) and Wash buffer 2 (50 mM Tris, pH 7.5, 1 M NaCl, 20 mM imidazole and 2 mM TCEP). Protein was eluted (50 mM Tris, pH 7.5, 1 M NaCl, 500 mM imidazole and 2 mM TCEP) and the His6-Protein A tag was cleaved overnight at 4 °C using 2 (w/w) % of 1 mg/ml recombinant His-tagged TEV protease. The protein solution was buffer exchanged to Wash buffer 1 using HiPrep 26/10 Desalting column on an ÄKTA Pure system (GE Healthcare) at room temperature. Cleaved protein was repurified from the cleaved fusion tag and TEV

protease by loading on a Ni-NTA resin column and 5 ml of the flow through was applied to a size-exclusion column (HiLoad Sepharose 16/600 75 pg, GE Healthcare) on an ÄKTA Pure system (GE Healthcare) at RT. The corresponding running buffer was composed of 50 mM sodium phosphate, pH 6.5, 150 mM NaCl and 1 mM DTT.

### NMR spectroscopy

Samples for NMR measurements contained 300 µM 15N labeled FOXO4[86-206] protein in 50 mM sodium phosphate, pH 6.5, 150 mM NaCl and 1 mM DTT with 10% $2H_2O$ added for the lock signal. For NMR titrations, 0.2, 0.4, 0.8 and 1.0 stochiometric equivalents of p53[1-312] (corresponding to 60, 120, 240 or 300 µM, respectively) and 1.0 and 2.0 stochiometric equivalents of FOXO4-DRI (corresponding to 300 or 600 µM, respectively) were added. $^1$H-$^{15}$N HSQC NMR spectra were recorded at 298 K on a 700 MHz Bruker NMR spectrometer. All spectra were recorded with an interscan delay of 1.0 s, spectral widths of 15.9/30 ppm, centered at 4.7/118.0 ppm in $^1$H/$^{15}$N, with 1,024 and 256 points, respectively, and 16 scans per increment. NMR chemical shift assignments of FOXO4[86-206] were obtained from HNCACB and HNCA spectra using 500 µM of uniformly $^{15}$N,$^{13}$C labeled protein in the aforementioned buffer at 298K on a 900 MHz Bruker Avance III NMR spectrometer equipped with a TCI cryoprobe.

### Immunofluorescence and Structured Illumination Microscopy

Cells (typically 20,000) were grown on coverslips and after the indicated treatment fixed with formalin. Subsequently, cells were washed in Tris Buffered Saline (TBS) and permeabilized for 2-5 min in 2% Triton X-100 in TBS, depending on the antibody. Especially, the FOXO4 antibody (Cell Signaling) seemed to work better with shorter permeabilization times. To reduce background staining, the cells were quenched for 10min with 50nM glycine in TBS and blocked for 30min with 5% Normal Horse Serum (NHS) or Normal Goat Serum (NGS) in 0,2% gelatin-TBS solution, depending on the isotype of the secondary antibody. Subsequently, 30µl droplets containing primary antibody dilutions were placed on parafilm in a dark moisture chamber. The coverslips were placed facing the droplets and incubated overnight at 4°C. The next day, the coverslips were lifted by adding a small volume (~200µl) of TBS-Gelatine under the coverslip and transferred back to the 24-well plate. After washing 3x 20min with 1ml 0,2% gelatin-TBS secondary antibody incubation occurred as described for the primary antibody and the coverslips were incubated for one hour at room temperature. Following 3x 10min washes with 1ml 0,2% TBS-Gelatin and 1 wash with regular TBS the slides were mounted using soft set mounting medium with DAPI (Vectashield) and sealed with nail polish. Structured Illumination Microscopy

was performed using a Zeiss Elyra PS1 microscope using a 63x 1.4 (n.a.) plan apo chromate oil immersion lens and 5 phases and 5 rotations of the illumination pattern. Intensity plots of individual pixels taken from a straight line in indicated immunofluorescence images were generated by twin slicer analysis using Huygens Professional 4.0 software (SVI, The Netherlands). Images were cropped and processed in Adobe Photoshop. When comparisons were made between images of the same experiment, all levels were adjusted equally and the ratio between the levels was not altered.

### Quantitative real-time PCR

mRNA was extracted using the Cells-to-Ct kit (Ambion). QPCR was performed using the Universal Probe Library system (Roche) with the following primer/probe combinations (5'-3'), also listed in Table S1:

FOXO1 (NM_002015.3): Fwd: tggttttagaaacccaagttcc, Rev: ttggcaccaagttcagttaca. UPL75

FOXO3 (NM_001455.3): Fwd: cagtagggcctgtgatttcc, Rev: cagcagaccaacactgttcac. UPL73

FOXO4 (NM_005938.2): Fwd: acgagtggatggtccgtact, Rev: gtggcggatcgagttcttc. UPL18

P21Cip1 (CDKN1A; NM_000389.3): Fwd: cgaagtcagttccttgtggag, Rev: catgggttctgacggacat. UPL82

ETS2 (NM_005239.4): Fwd: cagcgtcacctactgctctg, Rev: agtcgtggtctttgggagtc. UPL27

Tubulin (NM_006009.2): Fwd: cttcgtctccgccatcag, Rev: ttgccaatctggacacca. UPL58

### Immunoblotting

The dishes were washed 2x with ice-cold PBS, lysed in 1x Laemli sample buffer, and subjected to standard SDS-PAGE using separate 4%-12% Bis-Tris gels, after which the proteins were overnight transferred at 4°C to polyvinylidene fluoride membranes. The membranes were blocked using 2% BSA in Tris-buffered saline, 0.05% TWEEN (TBS-T) for 60min and incubated overnight at 4°C with the indicated primary antibodies. Following at least two 20min washing steps with TBS-T, the membranes were incubated with secondary antibodies for 60min. Following at least two 15min washing steps the membranes were developed with Enhanced Chemical Luminescence (Perkin Elmer). Images were cropped and equally processed in Adobe Photoshop.

### Cell viability assays

The cells were plated in triplicate in 96-well plates (typically 7000 senescent and 2000 non-senescent cells). Unless otherwise indicated, cell viability was assessed 6d after plating, using the AQueousOne Solution Cell Proliferation Assay (Promega).

10 ul of CellTiter AQueousOne Solution in 100ul fresh culture medium was added to the wells before a 1-3 hour incubation at 37˚C. Absorbance was measured at 490nm at a GloMax 96 well plate reader (Promega). A Mock-treated and a Puromycin (10µg/ml)-treated condition were used to set the maximal and minimal viability values, respectively, to which the experimental values were normalized.

### Cell density assays

Stably transduced and Puromycin-selected IMR90 cells were plated in 24-well plates in triplicate. After 3d, cells were fixed in methanol and stained with 0.5% crystal violet in 25% methanol. The plates were dried, and cell density was quantified by destaining in 10% acetic acid and measuring absorbance of the solution at 560 nm.

### Apoptosis assays

To assess apoptosis, two separate assays were used.
TUNEL staining was performed by permeabilizing cells fixed on coverslips for 2min with 0.1% Triton X-100 in 0.1% sodium citrate, followed by labeling with 10% TUNEL enzyme vs. label solution for 45min (Roche). Objective analysis of the percentage of TUNEL-positive cells was performed using CellProfiler software v2.3 by scoring the # of TUNEL positive objects filtered over DAPI-positive objects (Nuclei). Only TUNEL positive objects were considered that were also DAPI positive.
For the Cytochrome-C release assay, cells were seeded on coverslips in a 24-well plate and incubated for 5d total with the pan-caspase-inhibitor QVD-OPH (20µM in 500µl). The media was refreshed on day 3. Subsequently, the cells were processed for Cytochrome-C positivity by immunofluorescence. We measured the percentage of cells that showed a mitochondrial release of mitochondrial Cytochrome-C, identified either as diffuse staining, or complete absence.

### Real-time cell density assay

Real-time cell density was measured using an xCELLigence detection system (ACEA Biosciences). Prior to the measurement, 50 µL DMEM 10% FCS was added to each well of an E-plate view 16 (Roche) to establish background signal. Non-senescent (2000 cells per well) and senescent (5000 cells/well) IMR90 fibroblasts were then plated in 150 µl medium. 16h later the E-plate was placed in the xCELLigence reader and the cell density was recorded every 30min. The cells were treated with 25uM FOXO4 peptide 8h after starting the measurements. Measurements continued for the indicated intervals.

**Real-time imaging of Caspase-3/7 activation**

Cells were plated in 4-well Poly-L-Lysine coated glass bottom 35mm dishes (D141410; Matsumi, Japan) and incubated with NucView488 Caspase-3 (4440; Essen Bioscience). FOXO4-DRI or PBS was added and the cells were transferred to a Heat and $CO_2$-controlled incubator, attached to a LSM510 confocal microscope (Zeiss). 8h after addition, real-time imaging was initiated and every 30min a grid of 3x3 pictures was recorded. The imaging continued for another 6 days and the images were concatenated using Zen imaging software (Zeiss; See Mov3+4).

**Genotyping of mice**

For PCR genotyping the following primers were used (See also Table S1):
For p16::3MR-1: p16::3MR1: 5'-AACGCAAACGCATGATCACTG-3' and p16::3MR-2: 5'-TCAGGGATGATGCATCTAGC-3'. Positive animals show a band at 202bp.
For XpdTTD/TTD: p145: CCCGGCTAGAGTATCTGC, p184: GCCGGAATACGGGGCCA and pβrev :TCTATGGTTAAGTTCATGTCATAGGAAGGGGAGAA.

**Design of mouse experiments**

For the calculation of the estimated sample size a power analysis was performed according to the formula: n= $2(Z_{\alpha/2}+Z_{\beta})^2 * \sigma^2/\Delta^2$, with a power (1-β) of 80% and a significance (α) of 0.05. Prior to the study, pilot experiments were performed to determine the differences in plasma [Urea] of 26wk old wt vs. $Xpd^{TTD/TTD}$ mice. This led to a Δ and σ such that a sample size of 7 mice per group were estimated to be required to see differences in such experiments. This is shown in Fig. 6K. Later, is was found that sample sizes could be reduced when using mice of older age. This was applied in Fig. 6L and Fig. 7. For other assays, no information on Δ and σ was available and similar, or less stringent, sample sizes were deemed necessary. We only mice included mice that were of sufficient body weight at the start of the experiment, typically at least 80% of the average littermate weight of the same sex and genotype.

**Assessment of running wheel activity**

For assessment of running wheel behavior, we only included mice which at baseline ran at least 0.1km/day. Running wheel activity was continuously measured and plotted in km/day. The mice were placed in running wheel cages with ample time to adjust and get trained in using the wheel. After withdrawal of a blood sample, the mice were allowed to recover for at least 1 day and the average running wheel activity over the next two days was taken as baseline value. The mice were subsequently treated with FOXO4-DRI, or PBS (Mock) and at t=21d after baseline (t=18d after 1st treatment) the average running wheel activity over 4 days was scored. The ratio of

mice of both sexes from four independent experiments was calculated and the % activity plotted in Fig. 5I. Note that in some cases blood samples were taken at t=9 after treatment causing a temporary dip in activity.

**Fur density analysis**

$Xpd^{TTD/TTD}$ mice show reduced fur density (de Boer et al., 2002; de Boer et al., 1998). To score any changes that might occur over time, the phenotype was ranged from 0-4 where 0 was very patched and 4 was wildtype. Each mouse was scored before and after the experiment as indicated in Fig. 5C and Fig. S5A. The final score was determined as the ratio (final-baseline)/baseline and the % change was subsequently plotted. Following several initial pilot observations, the experiment shown in Fig. 5C contains mice from two independent cohorts. For naturally aged mice (Fig. 7D), only males were included, since we did not observe significant hair loss in females. In these cohorts, 80% showed (varying degrees of) loss of hair at the beginning (115+wks), or developed it over the course of the experiment.

**Infrared-measurements of abdominal temperature**

From handling wt vs. $Xpd^{TTD/TTD}$ mice, there appeared to be a difference in surface temperature. This we reasoned to be caused by changes in fur density. To further quantify such changes, the abdominal temperature was subsequently measured using an infrared thermometer. Even though the variation in individual measurements per animal was relatively large, $Xpd^{TTD/TTD}$ mice showed a significantly higher average infrared-measured abdominal temperature in general (See also Fig. 5E). There were also mice with a relatively normal temperature. To assess the effect of FOXO4-DRI vs. PBS therefore only mice with a baseline temperature >34 degrees were included as the window of visualizing any changes would otherwise be too small.

**Immunohistochemistry**

For immunohistochemistry, paraffin sections of liver and intestine specimens were deparaffinized, rehydrated in decreasing concentrations of ethanol, treated for 10 minutes with 3% $H_2O_2$ to quench endogenous peroxidase activity and heated to 100°C for 1 h in 10 mM sodium citrate buffer, pH 6, for antigen retrieval. Subsequently the tissues were processed as for immunofluorescence. Paraffin embedded heart tissue was serially sectioned into 5 μm slices, deparaffinized and rehydrated before Hematoxylin-Eosin (HE) staining or Picro Sirius Red staining was performed. For the HE staining, the sections were stained in Gills Hematoxylin (Sigma) for 4 minutes and 30 seconds in Eosin-Y solution. To stain for collagen, sections were incubated for 60 minutes in Picro Sirius Red solution (1g/L in picric acid) and briefly rinsed twice in 0.05% acetic acid.

**Bioluminescence**

For *in vivo* luminescence, mice were injected i.p. with 15 mg of Xenolight RediJect Coelentarazine (Caliper). 20 min later, the mice were anesthetized (2–4 % isoflurane) and placed in a dorsal position during imaging. Bioluminescence was measured with a Xenogen IVIS-200 Optical *in vivo* imaging System (Caliper Life Sciences; 5 min exposure). Photon flux was quantified within a circular region of interest (ROI) encompassing the site of substrate injection and the total radiance was corrected for time and surface area measured.

**Plasma values as measure for tissue function**

On the indicated time points, whole blood samples were collected in a Microvette with Lithium Heparin (Sarstedt) for plasma separation and spun for 10min at 4.6 x g. The (clear) supernatant was transferred into regular 1.5ml tubes and spun again for 5min at 4.6 x g. The supernatants were transferred again into 1.5ml tubes, snap frozen in liquid $N_2$ and stored at -80°C. [AST] was measured using an AST Activity Assay Kit (Sigma). The samples were incubated with 100µl reaction mix in a 96 well plate and placed at 37°C. The absorbance at 450nm was determined after 2 minutes for baseline analysis and after 40 minutes for a final analysis. [Urea] was measured using a QuantiChrom Urea Assay Kit (Gentaur). The samples were incubated in 200µl reaction mix for 10 minutes at room temperature before absorbance was measured at 520nm. [Creatinine] was measured using Creatinine Assay Kit (Sigma). Samples were incubated with 50µl reaction mix at 37°C for 60 minutes and the absorbance was measured at 570nm. Ratios comparing plasma values after treatment compared to baseline were determined and plotted as % over baseline in scatter plots.

**Post mortem SA-β-GAL assay**

All tissues were flash frozen in Optimal Cutting Temperature (OCT) Tissue Tek and stored until ready for processing. Subsequently, 10µm slices were cryosectioned and placed on charged microscopy slides. These were washed with ice-cold PBS for 5min and fixed in formalin for 15min on ice. Immediately after fixation the samples were washed once briefly with MilliQ and stained overnight at 37°C with fresh SA-β-GAL solution (pH 6.0), containing 2,5 mM Na2HPO4, 7,4 mM Citric Acid, 0.15M NaCl, 2mM MgCl2, 5 mM Potassium Ferricyanide, 5 mM Potassium Ferrocyanide and 25ul/ml 4% X-gal in DMF. Samples were mounted using soft set mounting medium with DAPI (Vectashield) and sealed with nail polish. Cultured cells were treated similarly.

**QUANTIFICATION AND STATISTICAL ANALYSIS**

Unpaired Student's t-tests were used to calculate the p value for pairwise comparisons. For multiple comparisons p-values were calculated using one-way ANOVA with Bonferroni post-test correction (Graph-Pad Prism). For comparisons of fold change differences an unpaired one-tailed t-test on the 2Log fold differences was applied. For the comparison of RLUC expression in naturally aged p16::3MR mice (Fig. 7A) and the change in abdominal temperature (Fig. 5E, right panel) a N-1 binary comparison test was performed. When averaging quantifications of single analyses, the "sum of squares"-rule was applied. The following indications of significance were used throughout the manuscript: * p<0.05, ** p<0.01.

**DATA AND SOFTWARE AVAILABILITY**

The RNA-Seq data obtained in this study has been uploaded to NCBI GEO datasets, under accession number GSE94395 (https://www.ncbi.nlm.nih.gov/geo/query/acc.cgi?acc=GSE94395).
The software to analyze the data is available at http://rna-ome.erasmusmc.nl/.

2

## Supplemental figures

A)

| Name | Ctrl | Sen | F.C. | p-value |
|---|---|---|---|---|
| TP53INP1 | | | 2.83 | 1.06E-80 |
| TP53 | | | 1.55 | 4.78E-17 |
| | | | | |
| PUMA | | | 2.59 | 5.06E-26 |
| BIM | | | 3.56 | 4.55E-12 |
| tBID | | | 1.31 | 5.19E-08 |
| BAD | | | 1.17 | 8.71E-04 |
| NOXA | | | -1.20 | 6.98E-03 |
| | | | | |
| Survivin | | | -12.95 | 0.00E+00 |
| BCL2 | | | -5.00 | 4.25E-19 |
| BCL-XL | | | -1.13 | 8.80E-03 |
| MCL1 | | | 1.03 | 4.35E-01 |
| BCL-W | | | 1.20 | 8.64E-05 |
| | | | | |
| BAK | | | 1.01 | 8.83E-01 |
| BAX | | | 1.17 | 1.91E-03 |
| | | | | |
| Cytochrome C | | | 1.04 | 3.53E-01 |
| SMAC | | | 1.11 | 2.53E-02 |
| | | | | |
| XIAP | | | 1.16 | 7.07E-03 |
| APAF1 | | | -1.46 | 6.57E-10 |
| | | | | |
| Caspase-9 | | | 1.48 | 2.45E-05 |
| Caspase-3 | | | 1.22 | 7.22E-05 |
| Caspase-6 | | | -1.42 | 6.23E-06 |
| Caspase-7 | | | -1.03 | 9.33E-01 |
| | | | | |
| FADD | | | -1.22 | 1.30E-04 |
| TRADD | | | 1.16 | 1.77E-02 |
| Caspase-8 | | | 1.42 | 2.37E-05 |

Difference in mRNA expression
vs. average between groups

Low  HIgh

C)



Senescent

shGFP
shFOXO4-1
shFOXO4-2

B)

| | Name | Full name | Fold change | p-value |
|---|---|---|---|---|
| Significantly down | E2F2 | E2F transcription factor 2 | 0.11 | 9.32E-33 |
| | E2F1 | E2F transcription factor 1 | 0.16 | 9.83E-173 |
| | FOS | FBJ murine osteosarcoma viral oncogene homolog | 0.48 | 2.07E-07 |
| | IRF6 | interferon regulatory factor 6 | 0.59 | 7.93E-02 |
| | E2F3 | E2F transcription factor 3 | 0.61 | 4.69E-20 |
| | FOSB | FBJ murine osteosarcoma viral oncogene homolog B | 0.62 | 1.84E-02 |
| | STAT5B | signal transducer and activator of transcription 5B | 0.62 | 6.86E-23 |
| | MSX1 | msh homeobox 1 | 0.65 | 5.60E-03 |
| | STAT5A | signal transducer and activator of transcription 5A | 0.74 | 2.33E-06 |
| | E2F4 | E2F transcription factor 4, p107/p130-binding | 0.87 | 2.95E-03 |
| | RELA | v-rel reticuloendotheliosis viral oncogene homolog A (avian) | 0.89 | 4.65E-03 |
| | JUNB | jun B proto-oncogene | 0.99 | 9.44E-01 |
| | MYC | v-myc myelocytomatosis viral oncogene homolog (avian) | 1.09 | 8.34E-02 |
| | NFKB1 | nuclear factor of kappa light polypeptide gene enhancer in B-cells 1 | 1.17 | 2.22E-04 |
| | FOXO3 | forkhead box O3 | 1.22 | 3.01E-05 |
| | MAX | MYC associated factor X | 1.28 | 5.99E-07 |
| | IRF9 | interferon regulatory factor 9 | 1.34 | 7.00E-08 |
| | TRPS1 | trichorhinophalangeal syndrome I | 1.36 | 7.50E-06 |
| | JUND | jun D proto-oncogene | 1.47 | 4.65E-14 |
| | STAT3 | signal transducer and activator of transcription 3 (acute-phase response factor) | 1.49 | 5.23E-20 |
| | STAT6 | signal transducer and activator of transcription 6, interleukin-4 induced | 1.50 | 6.90E-22 |
| | TP53 | tumor protein p53 | 1.55 | 4.78E-17 |
| Significantly up | STAT1 | signal transducer and activator of transcription 1, 91kDa | 1.76 | 1.51E-40 |
| | STAT2 | signal transducer and activator of transcription 2, 113kDa | 1.80 | 9.54E-46 |
| | NFKB2 | nuclear factor of kappa light polypeptide gene enhancer in B-cells 2 (p49/p100) | 1.81 | 9.62E-44 |
| | FOXO4 | forkhead box O4 | 1.94 | 2.52E-13 |
| | RELB | v-rel reticuloendotheliosis viral oncogene homolog B | 2.12 | 1.07E-37 |
| | STAT4 | signal transducer and activator of transcription 4 | 3.32 | 9.35E-08 |

## Supplementary figure 1

Figure S1. Related to Figure 1. A) Table showing color-coded changes in mRNA expression, fold change (F.C.) and p-values of the indicated apoptosis-associated genes in senescent vs. control IMR90. This figure is complementary to Fig. 1A showing the cell-intrinsic apoptosis pathway. B) Table showing the fold change and p-values of apoptosis-associated transcriptional regulators with FOXO4 highlighted in green. This figure complements Fig. 1B, which show a volcano plot of all transcriptional regulators. C) Treatment plan and visualization of cell density of senescent cells transduced with shRNAs against FOXO4. This figure is complementary to Fig. 1H).
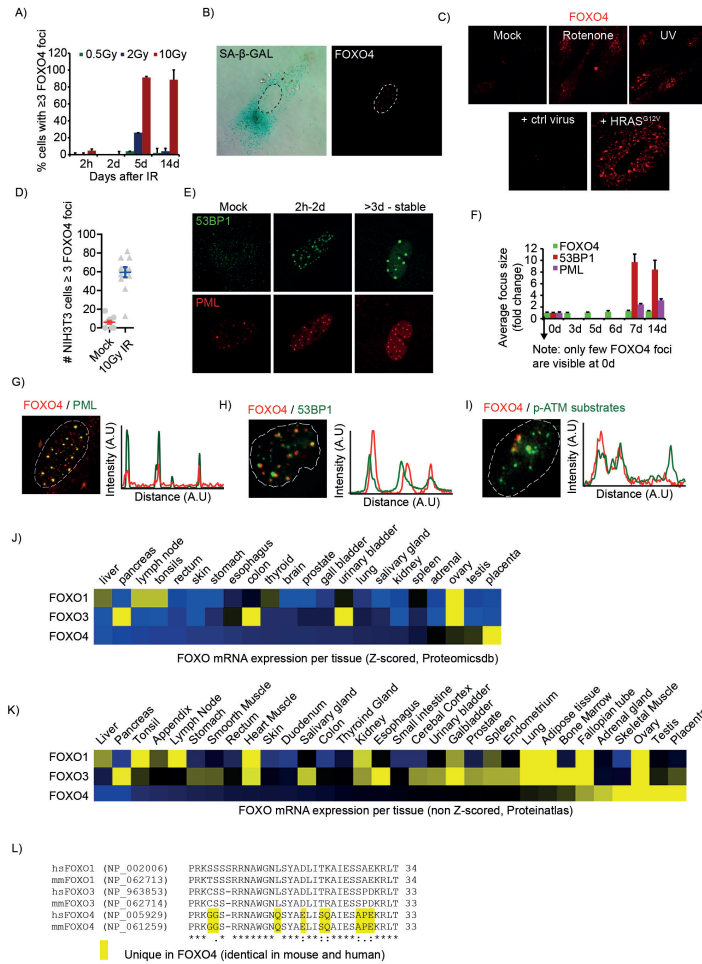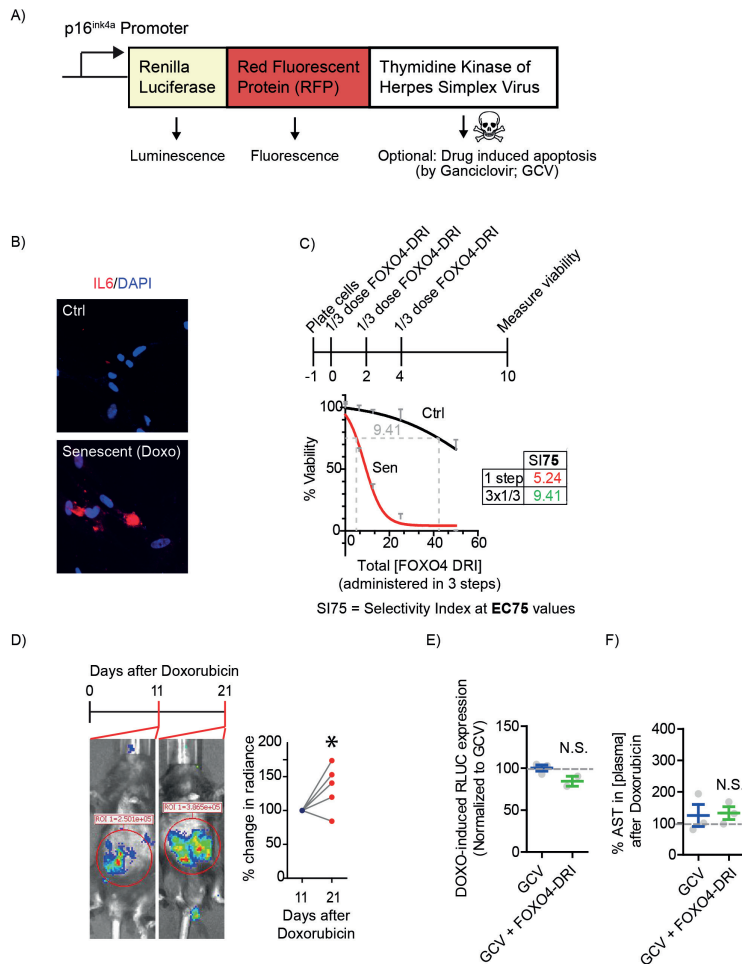
**Supplementary figure 2**

Figure S2. Related to Figure 2. A) Quantification of the % of cells containing 3 or more FOXO4 foci after non-senescence inducing levels of gamma irradiation (0.5Gy and 2Gy) or senescence-inducing levels (10Gy) in time. B) Immunofluorescence of FOXO4 foci in and SA-β-GAL positive senescent cell. C) Immunofluorescence showing formation of foci, after 200nM Rotenone, 8J/m2 UVC and Oncogene-induced senescence by stable ectopic expression of HRASG12V. D) Quantification of mouse NIH3T3 cells expressing 3 or more FOXO4 foci 7d after 10Gy IR, showing cross-species conservation of Foci formation. E+F) Visualization and quantification of the size of 53BP1, PML and FOXO4 foci in time after senescence induction, showing that 53BP1 foci and PML bodies expand, but FOXO4 foci remain the same in size. G-I) High magnification and pixel quantification of costainings between FOXO4 and PML (G), 53BP1 (H) and phosphorylated ATM-substrates (I) in nuclei of senescent IMR90. J+K) Heat-maps from two independent databases and independently scored (z-scored vs. non-z-scored), comparing FOXO1, 3 and 4 expression difference in various tissues. J) Z-scored mRNA expression profiles from Proteomicsdb(Wilhelm et al., 2014). K) Non-z-scored mRNA expression profiles from Proteinatlas(Uhlen et al., 2015). L) Sequence comparison of the sequence used for FOXO4-DRI revealing it to be identical in human and mouse FOXO4, but differs in 9 and 8 amino acids from FOXO1 and FOXO3a, respectively.

A)



B)



C)



D)
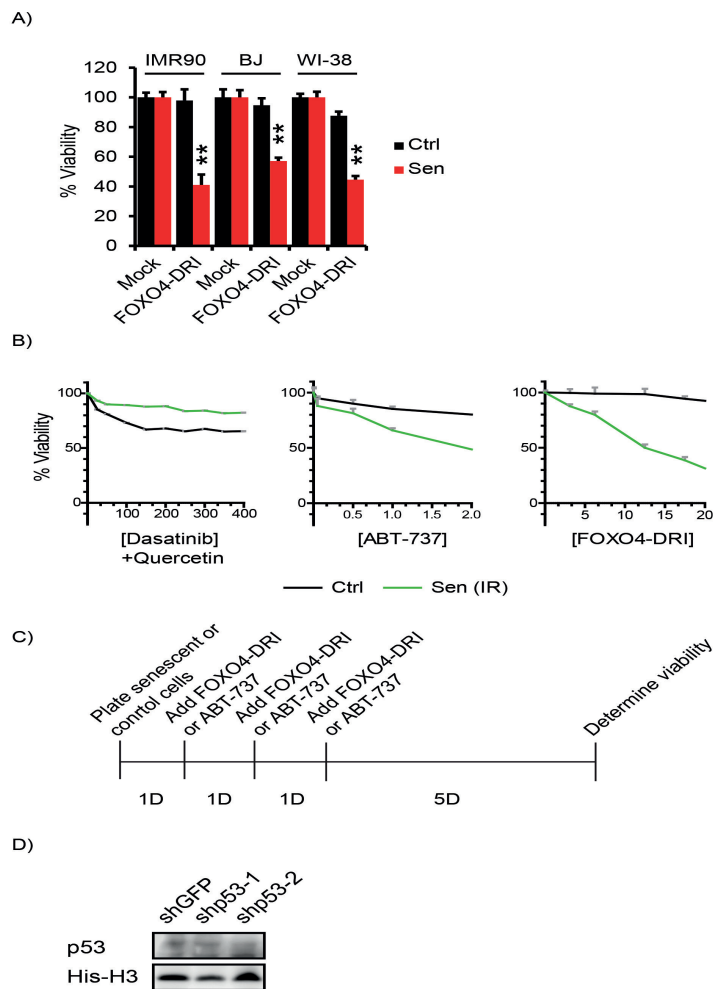


**Supplementary figure 3**

Figure S3. Related to Figure 3. A) Viability assay on control IMR90, BJ and WI-38 and counterparts induced to senesce by 10Gy IR, and incubated with FOXO4-DRI or PBS. B) Viability assays comparing the effects of the cocktail of Quercetin (20µM) with increasing doses of Dasatinib, ABT-737 or FOXO4-DRI when applied once on control or senescent IMR90. C) Treatment schedule for Fig. 3E. D) Immunoblot determining the effect of two independent short hairpins against p53 on p53 expression. NIH3T3 cells were transiently transfected with the indicated shRNAs used in Fig. 3F in combination with pBABE-Puro. After 2d Puromycin selection the samples were processed for immunoblotting.
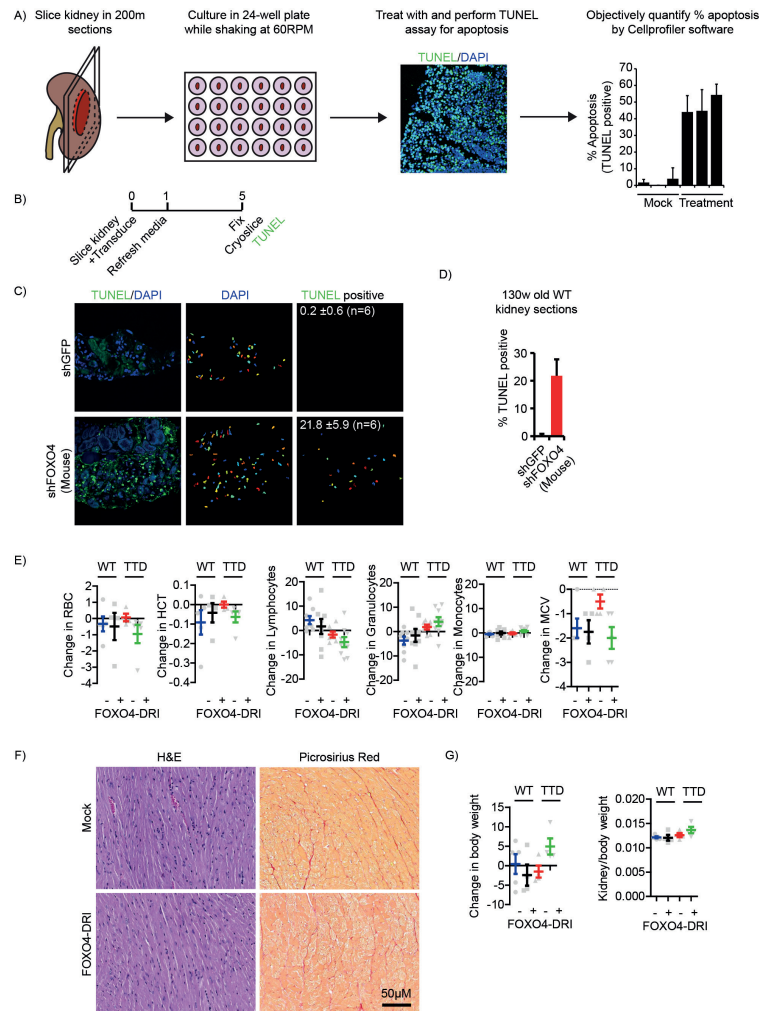
**Supplementary figure 4**

Figure S4. Related to Figure 4. A) Schematic overview of the p16::3MR construct, which comprises the promoter of p16ink4a that drives expression of a Trimodality reporter (3MR) consisting of Renilla Luciferase (RLUC) for bioluminescence detection, RFP for fluorescence detection and TK-HSV which can be used to induce selective clearance using Ganciclovir (GCV). B) Reduced, but subsequent doses of FOXO4-DRI, show to be more efficient in targeting Doxorubicin-senescent IMR90, than 1x high dose treatment. Senescent or Doxo-senescent IMR90 cells were exposed 1x to the final concentration of FOXO4-DRI, or 3x 1/3 that dose. The SI75 was compared between both treatment regimes. C) Immunofluorescence for IL6 in control or Doxo-senescent cells. D) Representative mice and quantification of p16-driven RLUC radiance in 5 mice i.p. injected with 10mg/kg Doxorubicin and analyzed on the indicated time-points. E) Visualization of change in Doxorubicin-induced p16-mediated senescence through bioluminescence in mice treated as in Fig. 4I, but with 5x 25mg/kg i.p GCV (day 1,2,3,4,5) for semigenetic clearance of senescence, or the same regimen in addition to 3x i.v. 5mg/kg FOXO4-DRI (day 1,3,5). F) Quantification of the % AST in plasma of mice from Fig. S4E after treatment vs. baseline.
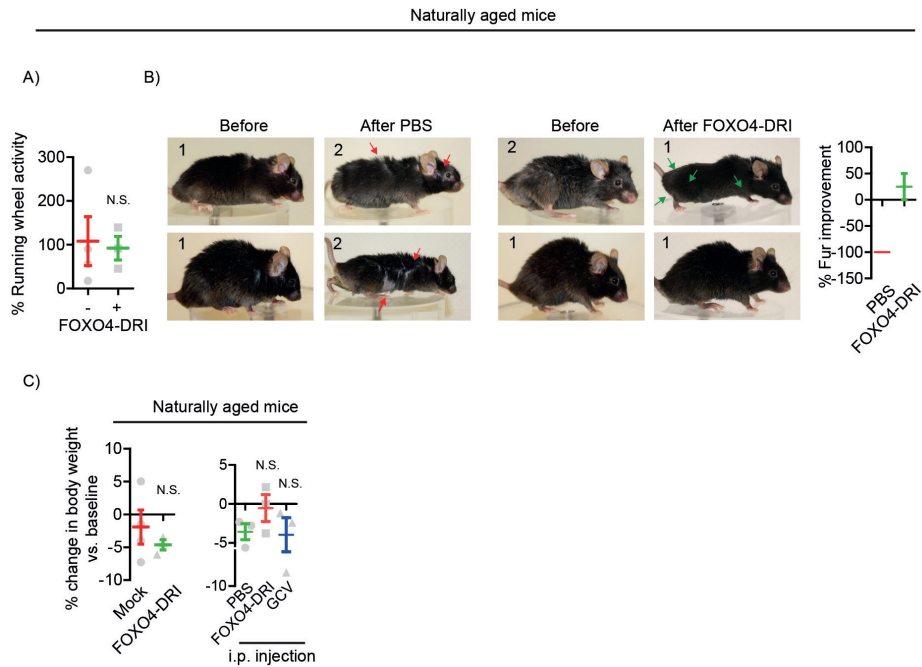
**A)**



**B)**



## Supplementary figure 5

Figure S5. Related to Figure 5. A) Overview of the fur status of the indicated XpdTTD/TTD mice before or after treatment with PBS (Left columns) or FOXO4-DRI (Right columns), respectively. The mice were scored 0-4 where 4 is fur as seen in wildtype mice and 0 is most reduced. The % change was calculated for each mouse and plotted in Fig. 5D. Red arrows indicate deterioration of the indicated area over time, whereas green arrows indicate improvement. B) Example of difference in behavior of XpdTTD/TTD mice treated with PBS, or FOXO4-DRI. To address this more quantitatively, the responsiveness to gentle stimuli was measured as described in Fig. 5F.

## Supplementary figure 6

Figure S6. Related to Figure 6. A) Schematic overview of kidney slice culture experiment and subsequent analysis. Fresh kidneys were isolated and sectioned in 200µM slices. These were placed in 24-well plate wells in tissue culture medium while rotating at 60rpm (See also(Kruiswijk et al., 2016)). Following treatment with shRNAs the slices were processed for TUNEL staining and the percentage positive cells is objectively scored. B) Treatment plan for kidney slice experiments in Fig. 6E and Fig. S6C-D. C) Example of shGFP and shFOXO4 (mouse) transduced 130w WT kidney slices stained for TUNEL (left), segmented for DAPI (middle) and scored for percentage TUNEL positive (right) using Cellprofiler V2.3. D) Quantification of n=6 kidney slices processed as in C). E) Whole blood analysis of the mice in Fig. 6F. F) Heart sections of PBS, or FOXO4-DRI treated wt mice (26w), stained by H&E for general pathology, and Picro Sirius Red to visualize collagen deposition. N>4. No apparent abnormalities were observed. G) FOXO4-DRI does not significantly alter total body weight, nor kidney weight (normalized to total body weight) of WT or XpdTTD/TTD mice. This figure complements Fig. 6G, J, K and L, by showing that while FOXO4-DRI does not influence total kidney mass it does improve renal function.

**Supplementary figure 7**

Figure S7. Related to Figure 7. A) Quantitative representation of the % p16-driven senescence (RLUC) in naturally aged mice treated with FOXO4-DRI or PBS. Note the large biological spread in signal. B) Overview of the fur status of the indicated naturally aged mice before or after treatment with PBS (Left columns) or FOXO4-DRI (Right columns), respectively. Right panel: quantification of the % change as also described in Fig. 5D. C) Quantification of the % change in body weight of naturally aged mice treated as in Fig. 7B-I (Left panel), or Fig. 7J (Right panel).

Mov. 1. Related to Fig. 2D. Structured Illumination Microscopic (SIM) image of the nucleus of a senescent IMR90 cell.

Senescent IMR90 cells were stained for FOXO4 (Alexa488; Green), 53BP1 (Alexa594; Red) and PML (Alexa647; Purple) and DAPI (Blue). A SIM image was taken and this movie shows the combinations of the respective colors of a representative image. See also Mov. 2.

Mov. 2. Related to Fig. 2D. 3D reconstruction of a representative FOXO4/53BP1/ PML cluster in the nucleus of a senescent IMR90 cell.

Senescent IMR90 cells were stained for FOXO4 (Alexa488; Green), 53BP1 (Alexa594; Red) and PML (Alexa647; Purple) and DAPI (Blue). A SIM image was taken and the focal structure indicated by the yellow line in Fig. 2D was processed for 3D reconstruction, using Amira software. See also Mov. 1.

Mov. 3. Related to Fig. 3H. Lack of Caspase-3 activity in control IMR90 cells incubated with FOXO4-DRI.

Control IMR90 cells were incubated with a dye that turns green upon activation of Caspase-3 (NucView488 Caspase-3) and 25µM FOXO4-DRI. After 8h the cells were processed for real-time imaging for 6 days in total. See also Mov. 4

Mov. 4. Related to Fig. 3H. Induction of Caspase-3 activity in senescent IMR90 cells incubated with FOXO4-DRI.

IR-senescent IMR90 cells were incubated with a dye that turns green upon activation of Caspase-3 (NucView488 Caspase-3) and 25µM FOXO4-DRI. After 8h the cells were processed for real-time imaging for 6 days in total. See also Mov. 3.

2

## References

Baker, D.J., Childs, B.G., Durik, M., Wijers, M.E., Sieben, C.J., Zhong, J., Saltness, R.A., Jeganathan, K.B., Verzosa, G.C., Pezeshki, A.*, et al.* (2016). Naturally occurring p16(Ink4a)-positive cells shorten healthy lifespan. Nature *530*, 184-189.

Beydoun, T., Deloche, C., Perino, J., Kirwan, B.A., Combette, J.M., and Behar-Cohen, F. (2015). Subconjunctival injection of XG-102, a JNK inhibitor peptide, in patients with intraocular inflammation: a safety and tolerability study. J Ocul Pharmacol Ther *31*, 93-99.

Borsello, T., Clarke, P.G., Hirt, L., Vercelli, A., Repici, M., Schorderet, D.F., Bogousslavsky, J., and Bonny, C. (2003). A peptide inhibitor of c-Jun N-terminal kinase protects against excitotoxicity and cerebral ischemia. Nat Med *9*, 1180-1186.

Botter, S.M., Zar, M., van Osch, G.J., van Steeg, H., Dolle, M.E., Hoeijmakers, J.H., Weinans, H., and van Leeuwen, J.P. (2011). Analysis of osteoarthritis in a mouse model of the progeroid human DNA repair syndrome trichothiodystrophy. Age (Dordr) *33*, 247-260.

Brown, J.P., Wei, W., and Sedivy, J.M. (1997). Bypass of senescence after disruption of p21CIP1/WAF1 gene in normal diploid human fibroblasts. Science *277*, 831-834.

Cahu, J., Bustany, S., and Sola, B. (2012). Senescence-associated secretory phenotype favors the emergence of cancer stem-like cells. Cell Death Dis *3*, e446.

Campisi, J. (2013). Aging, cellular senescence, and cancer. Annu Rev Physiol *75*, 685-705.

Chang, J., Wang, Y., Shao, L., Laberge, R.M., Demaria, M., Campisi, J., Janakiraman, K., Sharpless, N.E., Ding, S., Feng, W.*, et al.* (2016). Clearance of senescent cells by ABT263 rejuvenates aged hematopoietic stem cells in mice. Nature medicine *22*, 78-83.

Coppe, J.P., Patil, C.K., Rodier, F., Sun, Y., Munoz, D.P., Goldstein, J., Nelson, P.S., Desprez, P.Y., and Campisi, J. (2008). Senescence-associated secretory phenotypes reveal cell-nonautonomous functions of oncogenic RAS and the p53 tumor suppressor. PLoS Biol *6*, 2853-2868.

Damodar, G., Smitha, T., Gopinath, S., Vijayakumar, S., and Rao, Y. (2014). An evaluation of hepatotoxicity in breast cancer patients receiving injection Doxorubicin. Ann Med Health Sci Res *4*, 74-79.

de Boer, J., Andressoo, J.O., de Wit, J., Huijmans, J., Beems, R.B., van Steeg, H., Weeda, G., van der Horst, G.T., van Leeuwen, W., Themmen, A.P.*, et al.* (2002). Premature aging in mice deficient in DNA repair and transcription. Science *296*, 1276-1279.

de Boer, J., de Wit, J., van Steeg, H., Berg, R.J., Morreau, H., Visser, P., Lehmann, A.R., Duran, M., Hoeijmakers, J.H., and Weeda, G. (1998). A mouse model for the basal transcription/DNA repair syndrome trichothiodystrophy. Mol Cell *1*, 981-990.

de Keizer, P.L. (2017). The Fountain of Youth by Targeting Senescent Cells? Trends Mol Med *23*, 6-17.

de Keizer, P.L., Burgering, B.M., and Dansen, T.B. (2011). Forkhead box o as a sensor, mediator, and regulator of redox signaling. Antioxidants & redox signaling *14*, 1093-1106.

de Keizer, P.L., Packer, L.M., Szypowska, A.A., Riedl-Polderman, P.E., van den Broek, N.J., de Bruin, A., Dansen, T.B., Marais, R., Brenkman, A.B., and Burgering, B.M. (2010). Activation of forkhead box O transcription factors by oncogenic BRAF promotes p21cip1-dependent senescence. Cancer research *70*, 8526-8536.

Degenhardt, K., Sundararajan, R., Lindsten, T., Thompson, C., and White, E. (2002). Bax and Bak independently promote cytochrome C release from mitochondria. The Journal of biological chemistry *277*, 14127-14134.

Deloche, C., Lopez-Lazaro, L., Mouz, S., Perino, J., Abadie, C., and Combette, J.M. (2014). XG-102 administered to healthy male volunteers as a single intravenous infusion: a randomized, double-blind, placebo-controlled, dose-escalating study. Pharmacol Res Perspect *2*, e00020.

Demaria, M., Ohtani, N., Youssef, S.A., Rodier, F., Toussaint, W., Mitchell, J.R., Laberge, R.M., Vijg, J., Van Steeg, H., Dolle, M.E.*, et al.* (2014). An essential role for senescent cells in optimal wound healing through secretion of PDGF-AA. Dev Cell *31*, 722-733.

Di, L.A., Linke, S.P., Clarkin, K., and Wahl, G.M. (1994). DNA damage triggers a prolonged p53-dependent G1 arrest and long-term induction of Cip1 in normal human fibroblasts. Genes Dev *8*, 2540-2551.

Dimri, G.P., Lee, X., Basile, G., Acosta, M., Scott, G., Roskelley, C., Medrano, E.E., Linskens, M., Rubelj, I., and Pereira-Smith, O. (1995). A biomarker that identifies senescent human cells in culture and in aging skin in vivo. ProcNatlAcadSciUSA *92*, 9363-9367.

Eijkelenboom, A., and Burgering, B.M. (2013). FOXOs: signalling integrators for homeostasis maintenance. Nat Rev Mol Cell Biol *14*, 83-97.

Ewald, J.A., Desotelle, J.A., Wilding, G., and Jarrard, D.F. (2010). Therapy-induced senescence in cancer. J Natl Cancer Inst *102*, 1536-1546.

Ferrucci, L., Corsi, A., Lauretani, F., Bandinelli, S., Bartali, B., Taub, D.D., Guralnik, J.M., and Longo, D.L. (2005). The origins of age-related proinflammatory state. Blood *105*, 2294-2299.

Freund, A., Laberge, R.M., Demaria, M., and Campisi, J. (2012). Lamin B1 loss is a senescence-associated biomarker. Mol Biol Cell *23*, 2066-2075.

Freund, A., Patil, C.K., and Campisi, J. (2011). p38MAPK is a novel DNA damage response-independent regulator of the senescence-associated secretory phenotype. EMBO J *30*, 1536-1548.

2

Gowda, S., Desai, P.B., Kulkarni, S.S., Hull, V.V., Math, A.A., and Vernekar, S.N. (2010). Markers of renal function tests. N Am J Med Sci *2*, 170-173.

Guichard, G., Benkirane, N., Zeder-Lutz, G., van Regenmortel, M.H., Briand, J.P., and Muller, S. (1994). Antigenic mimicry of natural L-peptides with retro-inverso-peptidomimetics. Proceedings of the National Academy of Sciences of the United States of America *91*, 9765-9769.

Henderson, T.O., Ness, K.K., and Cohen, H.J. (2014). Accelerated aging among cancer survivors: from pediatrics to geriatrics. Am Soc Clin Oncol Educ Book, e423-430.

Herce, H.D., and Garcia, A.E. (2007). Molecular dynamics simulations suggest a mechanism for translocation of the HIV-1 TAT peptide across lipid membranes. Proceedings of the National Academy of Sciences of the United States of America *104*, 20805-20810.

Hoeijmakers, J.H. (2009). DNA damage, aging, and cancer. N Engl J Med *361*, 1475-1485.

Hosaka, T., Biggs, W.H., 3rd, Tieu, D., Boyer, A.D., Varki, N.M., Cavenee, W.K., and Arden, K.C. (2004). Disruption of forkhead transcription factor (FOXO) family members in mice reveals their functional diversification. Proc Natl Acad Sci U S A *101*, 2975-2980.

Krishnamurthy, J., Torrice, C., Ramsey, M.R., Kovalev, G.I., Al-Regaiey, K., Su, L., and Sharpless, N.E. (2004). Ink4a/Arf expression is a biomarker of aging. J Clin Invest *114*, 1299-1307.

Kruiswijk, F., Hasenfuss, S.C., Sivapatham, R., Baar, M.P., Putavet, D., Naipal, K.A., van den Broek, N.J., Kruit, W., van der Spek, P.J., van Gent, D.C.*, et al.* (2016). Targeted inhibition of metastatic melanoma through interference with Pin1-FOXM1 signaling. Oncogene *35*, 2166-2177.

Kruiswijk, F., Labuschagne, C.F., and Vousden, K.H. (2015). p53 in survival, death and metabolic health: a lifeguard with a licence to kill. Nat Rev Mol Cell Biol *16*, 393-405.

Lopez-Otin, C., Blasco, M.A., Partridge, L., Serrano, M., and Kroemer, G. (2013). The hallmarks of aging. Cell *153*, 1194-1217.

Lyman, J.L. (1986). Blood urea nitrogen and creatinine. Emerg Med Clin North Am *4*, 223-233.

Martins, R., Lithgow, G.J., and Link, W. (2016). Long live FOXO: unraveling the role of FOXO proteins in aging and longevity. Aging Cell *15*, 196-207.

Mihara, M., Erster, S., Zaika, A., Petrenko, O., Chittenden, T., Pancoska, P., and Moll, U.M. (2003). p53 has a direct apoptogenic role at the mitochondria. Molecular cell *11*, 577-590.

Munoz-Espin, D., Canamero, M., Maraver, A., Gomez-Lopez, G., Contreras, J., Murillo-Cuesta, S., Rodriguez-Baeza, A., Varela-Nieto, I., Ruberte, J., Collado, M.*, et al.* (2013). Programmed cell senescence during mammalian embryonic development. Cell *155*, 1104-1118.

Nakae, J., Kitamura, T., Kitamura, Y., Biggs, W.H., 3rd, Arden, K.C., and Accili, D. (2003). The forkhead transcription factor Foxo1 regulates adipocyte differentiation. Dev Cell *4*, 119-129.

Orjalo, A.V., Bhaumik, D., Gengler, B.K., Scott, G.K., and Campisi, J. (2009). Cell surface-bound IL-1alpha is an upstream regulator of the senescence-associated IL-6/IL-8 cytokine network. Proceedings of the National Academy of Sciences of the United States of America *106*, 17031-17036.

Paik, J.H., Kollipara, R., Chu, G., Ji, H., Xiao, Y., Ding, Z., Miao, L., Tothova, Z., Horner, J.W., Carrasco, D.R.*, et al.* (2007). FoxOs are lineage-restricted redundant tumor suppressors and regulate endothelial cell homeostasis. Cell *128*, 309-323.

Renault, V.M., Rafalski, V.A., Morgan, A.A., Salih, D.A., Brett, J.O., Webb, A.E., Villeda, S.A., Thekkat, P.U., Guillerey, C., Denko, N.C.*, et al.* (2009). FoxO3 regulates neural stem cell homeostasis. Cell Stem Cell *5*, 527-539.

Rodier, F., Coppe, J.P., Patil, C.K., Hoeijmakers, W.A., Munoz, D.P., Raza, S.R., Freund, A., Campeau, E., Davalos, A.R., and Campisi, J. (2009). Persistent DNA damage signalling triggers senescence-associated inflammatory cytokine secretion. Nat Cell Biol *11*, 973-979.

Rodier, F., Munoz, D.P., Teachenor, R., Chu, V., Le, O., Bhaumik, D., Coppe, J.P., Campeau, E., Beausejour, C.M., Kim, S.H.*, et al.* (2011). DNA-SCARS: distinct nuclear structures that sustain damage-induced senescence growth arrest and inflammatory cytokine secretion. J Cell Sci *124*, 68-81.

Roninson, I.B. (2003). Tumor cell senescence in cancer treatment. Cancer research *63*, 2705-2715.

Schoenwaelder, S.M., Jarman, K.E., Gardiner, E.E., Hua, M., Qiao, J., White, M.J., Josefsson, E.C., Alwis, I., Ono, A., Willcox, A.*, et al.* (2011). Bcl-xL-inhibitory BH3 mimetics can induce a transient thrombocytopathy that undermines the hemostatic function of platelets. Blood *118*, 1663-1674.

Suckfuell, M., Lisowska, G., Domka, W., Kabacinska, A., Morawski, K., Bodlaj, R., Klimak, P., Kostrica, R., and Meyer, T. (2014). Efficacy and safety of AM-111 in the treatment of acute sensorineural hearing loss: a double-blind, randomized, placebo-controlled phase II study. Otol Neurotol *35*, 1317-1326.

Tait, S.W., and Green, D.R. (2010). Mitochondria and cell death: outer membrane permeabilization and beyond. Nat Rev Mol Cell Biol *11*, 621-632.

Vaupel, J.W. (2010). Biodemography of human ageing. Nature *464*, 536-542.

Wang, E. (1995). Senescent human fibroblasts resist programmed cell death, and failure to suppress bcl2 is involved. Cancer research *55*, 2284-2292.

2

Wang, F., Marshall, C.B., Yamamoto, K., Li, G.Y., Plevin, M.J., You, H., Mak, T.W., and Ikura, M. (2008). Biochemical and structural characterization of an intramolecular interaction in FOXO3a and its binding with p53. J Mol Biol *384*, 590-603.

Warso, M.A., Richards, J.M., Mehta, D., Christov, K., Schaeffer, C., Rae Bressler, L., Yamada, T., Majumdar, D., Kennedy, S.A., Beattie, C.W.*, et al.* (2013). A first-in-class, first-in-human, phase I trial of p28, a non-HDM2-mediated peptide inhibitor of p53 ubiquitination in patients with advanced solid tumours. British journal of cancer *108*, 1061-1070.

Wijnhoven, S.W., Beems, R.B., Roodbergen, M., van den Berg, J., Lohman, P.H., Diderich, K., van der Horst, G.T., Vijg, J., Hoeijmakers, J.H., and van Steeg, H. (2005). Accelerated aging pathology in ad libitum fed Xpd(TTD) mice is accompanied by features suggestive of caloric restriction. DNA repair *4*, 1314-1324.

Xu, M., Tchkonia, T., Ding, H., Ogrodnik, M., Lubbers, E.R., Pirtskhalava, T., White, T.A., Johnson, K.O., Stout, M.B., Mezera, V.*, et al.* (2015). JAK inhibition alleviates the cellular senescence-associated secretory phenotype and frailty in old age. Proceedings of the National Academy of Sciences of the United States of America *112*, E6301-6310.

Yosef, R., Pilpel, N., Tokarsky-Amiel, R., Biran, A., Ovadya, Y., Cohen, S., Vadai, E., Dassa, L., Shahar, E., Condiotti, R.*, et al.* (2016). Directed elimination of senescent cells by inhibition of BCL-W and BCL-XL. Nat Commun *7*, 11190.

Zhou, W., Cao, Q., Peng, Y., Zhang, Q.J., Castrillon, D.H., DePinho, R.A., and Liu, Z.P. (2009). FoxO4 inhibits NF-kappaB and protects mice against colonic injury and inflammation. Gastroenterology *137*, 1403-1414.

Zhu, Y., Tchkonia, T., Pirtskhalava, T., Gower, A.C., Ding, H., Giorgadze, N., Palmer, A.K., Ikeno, Y., Hubbard, G.B., Lenburg, M.*, et al.* (2015). The Achilles' heel of senescent cells: from transcriptome to senolytic drugs. Aging Cell *14*, 644-658.

2

# CHAPTER 3

## Musculoskeletal senescence: A moving target ready to be eliminated

**Marjolein P. Baar[1,2], Eusebio Perdiguero[3], Pura Muñoz-Cánoves[3,4] and Peter L.J. de Keizer[1]**

[1] Department of Molecular Cancer Research, Center for Molecular Medicine, Division of Biomedical Genetics, University Medical Center Utrecht, Utrecht University, Universiteitsweg 100, 3584CG Utrecht, the Netherlands

[2] Department of Molecular Genetics, Erasmus University Medical Center, Rotterdam, the Netherlands

[3] Department of Experimental and Health Sciences, Pompeu Fabra University (UPF), CIBERNED, Barcelona, Spain.

[4] ICREA and Spanish National Center on Cardiovascular Research (CNIC), Madrid, Spain.

**Aging is the prime risk factor for the broad-based development of diseases. Frailty is a phenotypical hallmark of aging and is often used to assess whether the predicted benefits of a therapy outweigh the risks for older patients. Senescent cells form as a consequence of unresolved molecular damage and persistently secrete molecules that can impair tissue function. Recent evidence shows senescent cells can chronically interfere with stem cell function and drive aging of the musculoskeletal system. In addition, targeted apoptosis of senescent cells can restore tissue homeostasis in aged animals. Thus, targeting cellular senescence provides new therapeutic opportunities for intervention in frailty-associated pathologies and could have pleiotropic health benefits.**

**Loss of cell-intrinsic and -extrinsic integrity perturbs musculoskeletal rejuvenation during aging**

Aged individuals can deteriorate exceptionally fast after the onset of complications affecting the musculoskeletal system. Tissue erosion due to life-long mechanical and biological stress can ultimately result in pathologies such as osteoporosis, sarcopenia, and osteoarthritis, and contribute to frailty [1]. While not all elderly people develop the same age-related diseases, virtually everyone will experience musculoskeletal complications sooner or later. To extend, and possibly even restore, healthy life expectancy in old age, it is essential to understand the cellular changes underlying musculoskeletal decline. Tissue regeneration by stem-cell differentiation is critical in overcoming the relentless day-by-day damage to the musculoskeletal system. In young tissues, differentiation proceeds without much hindrance unless one exercises excessively or suffers undue levels of stress. However, during aging, the number and function of adult stem cells declines [2, 3]. For example, Pax7-expressing satellite stem cells can replace damaged muscle fibers [4]. Removing Pax7-positive cells from mice impairs muscle regeneration after injury [5], whereas increased availability of these cells enhances muscle repair [6].

In addition to cell-intrinsic regulation, muscle stem cell regenerative capacity also depends intimately on the microenvironment. During aging, the levels of inflammation chronically increase, an affect known as inflammaging [7]. Evidence for this is provided by studies showing that muscle stem cells (satellite cells) from aged mice become more fibrogenic, a conversion mediated by factors from the aged systemic environment [8]. In contrast, frailty is reduced by the JAK/STAT inhibitor Ruxolitinib, which reduces inflammation in naturally aged mice [9]. Stem-cell impairing cues do not necessarily have to come from local sources but can travel over a distance. Heterochronic parabiosis experiments showed that transfusion of old blood impairs stem cell function in young recipient mice [10], while the transfer of young blood factors restoring muscle regeneration and muscle stem-cell activation in aged animals [11]. Therefore, there is a great interest in developing methods to interfere with the age-associated pro-inflammatory signaling profile. The question is how? To address this question, cellular senescence has recently gained attention as a potential candidate for intervention.

**Signaling noise by senescent cells impedes tissue homeostasis during aging**

As we age, each cell in our body accumulates damage. Earlier in life, this damage is usually faithfully repaired [12], but over time more and more damage gets left behind. This can trigger a molecular chain of events, resulting in chromatin remodeling and the entry of cells into a permanent state of growth-factor insensitive

cell-cycle arrest, called cellular senescence. Senescence can be invoked in healthy cells that experience a chronic damage response, either involving direct DNA damage or events that mimic the molecular response, such as telomere shortening or oncogenic mutations [13]. As a consequence, these cells undergo an irreversible cell cycle arrest, effectively limiting the damage. So far, so good, except that senescent cells secrete a broad range of growth factors, pro-inflammatory proteins, and matrix proteinases that alter the microenvironment: The Senescence-Associated Secretory Phenotype (SASP) [14].

Senescent cells persist for prolonged periods of time and eventually accumulate during aging [15]. This also means there is a gradual and, importantly, ever-present build-up of deleterious molecules. Thus, senescence can have continuous detrimental effects on tissue homeostasis during aging. That senescent cells are a direct cause of aging was proven beyond a doubt in studies in which senescent cells were genetically or pharmacologically removed. In these studies, both rapidly and naturally aged mice maintained healthspan for much longer, or even showed signs of aging reversal [16-19]. Factors secreted by senescent cells can induce pluripotency *in vivo*[20]. As such, these can impair normal stem cell function by forcing a constant state of reprogramming, something we dubbed a "senescence – stem lock"[13]. This is supported by observations that factors secreted by senescent cells induce pluripotency *in vivo* [20]. Age-associated inflammation may thus deregulate normal stem cell function at different levels, for instance by preventing stem cells from producing differentiated daughter cells. Due to the constant secretion of SASP factors, senescent cells could thus impair local and distant stem cell function and differentiation in times of need. Here, we will highlight the interplay between senescence, the SASP and stemness in the individual musculoskeletal compartments: Muscle, Bone and Cartilage.
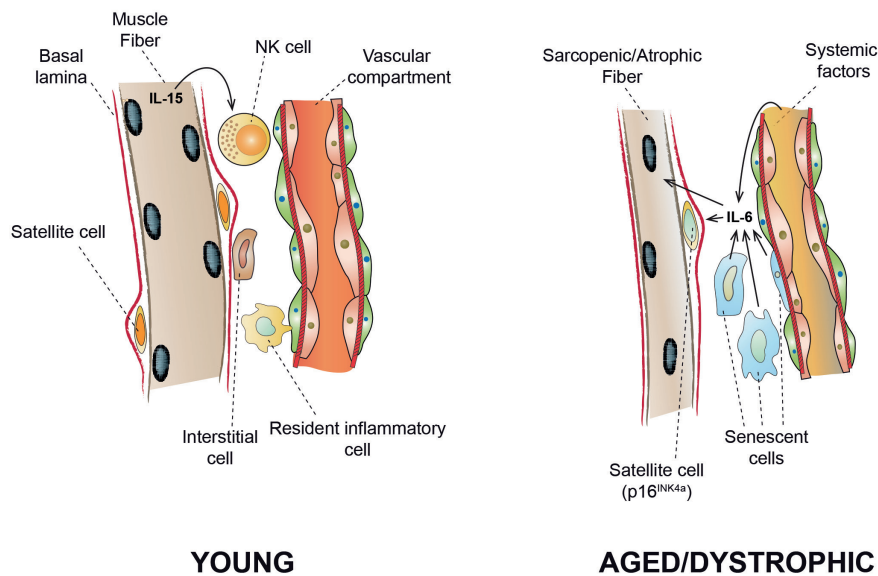
**Skeletal muscle: an intrinsic interplay between senescence and stemness**

Several reports link senescence to muscle aging and muscle stem cell dysfunction. For example, expression of the major senescence marker p16$^{INK4A}$ prevents tissue regeneration by satellite cells after damage [21]. Fast-aging *BubR1$^{H/H}$* mice develop sarcopenia, and after genetic removal of senescent cells, they showed a reduction in kyphosis and an increase in muscle fiber diameter, findings suggestive of reduced sarcopenia [16]. Likewise, senescence of muscle stem cells occurs in muscles of mice with distinct dystrophinopathies, such as Duchenne muscular dystrophy or Steinert's diseases [22-25].

The skeletal muscle stem cell niche is a candidate through which senescent cells may exert their deleterious effects. Interleukin 6 (IL-6) is a pleiotropic cytokine that

can be released by inflammatory cells and by muscle fibers (acting as a myokine). IL6 is also a major component of the SASP[14], and has been shown to regulate the transition of satellite cells from a quiescent to an activated state [26]. This is beneficial upon acute tissue stress, where IL-6 is transiently released by growing myofibers to activate satellite cells and thereby stimulate myogenesis [26]. However, the chronic IL-6 signaling caused by senescence during aging would have very detrimental effects on muscle function. Indeed, muscle atrophy is linked to high IL-6 levels in patients with inflammatory diseases such as cancer [27]. In addition, persistent IL-6 expression was shown to increase muscle degradation in combination with other circulating factors in mice [28, 29]. Interestingly, when IL-6 receptors were blocked in mice with ectopic IL-6 expression, atrophy could be attenuated, indicating a direct regulation of muscle wasting by IL-6 [30]. Chronic IL-6 signaling causes protein degradation in muscle, explaining age-related muscle wasting [31]. Additionally, IL-6 dependent muscle degradation may be linked to stem cell function. For example, senescence induction after muscle injury can promote Pax7 positive unipotent cells to undergo reprogramming and regain pluripotency [32]. This process is dependent on IL-6 secreted by the senescent cells. Further underscoring the role between the senescent niche and stemness in the muscle is provided by elegant work employing a system in which the four Yamanaka stem cell factors, Oct4, Sox2, Klf4 and c-Myc (OSKM) were transiently expressed *in vivo.* This resulted in a marked reduction in senescence, SASP factors such as IL6 and improved recovery in muscle injury experiments[33]. Together, this supports a model we postulated previously that because senescence increases locally during aging hotspots are formed of high IL6 concentrations. This can cause neighboring cells to become pluripotent. However, due to the chronic nature of the SASP, senescent cells provide a continuous source of IL6 causing these cells remain permanently locked in a pluripotent state and rendering them unable to rejuvenate the tissue after injury[13].

Although satellite dysfunction has been linked to sarcopenia, this relationship is controversial. Recent studies suggest that the decline in satellite cell function during aging is not the cause of sarcopenia [34, 35]. When satellite cells were genetically removed over a prolonged period, no difference in muscle mass was observed compared with mice that maintained their satellite cells. However, there was a clear increase in fibrosis, indicating that satellite cells are indeed crucial for muscle homeostasis. Furthermore, several studies show that sarcopenic muscle has a reduced ability to recover after injury, which is dependent on satellite cell function [5, 21, 35, 36]. Overall, while the role of satellite cells in sarcopenia is still debated, there is consensus that Pax7 positive cells are required for regeneration after muscle injury and that reduced function of these stem cells leads to age-related frailty.

Muscle Fiber, Basal lamina, NK cell, Vascular compartment, IL-15, Satellite cell, Interstitial cell, Resident inflammatory cell

Sarcopenic/Atrophic Fiber, Systemic factors, IL-6, Senescent cells, Satellite cell (p16$^{INK4a}$)

**YOUNG**          **AGED/DYSTROPHIC**

Aged muscle fibers show atrophy that is linked to an age-related increase in cellular senescence. Satellite cells lose proliferation capacity through senescence induction or the chronic presence of SASP factors such as Il-6. Thus, regeneration of damaged tissue is prevented. Additionally, IL-15 secreted by muscle tissue facilitates NK cell survival in young organisms, while IL-6 represses these immune cells during aging and thereby reduces the natural ablation of senescent cells, aggravating loss of muscle mass observed during aging.

The myokines released by muscle cells not only signal to stem cells, but also attract immune cells that can facilitate tissue repair and regulate immune cell function. IL-15 is released by muscle cells in response to exercise and promotes survival of NK cells [37, 38]; in contrast, NK cells are inhibited by IL-6 and TNFα [39]. An age-related decrease in muscle mass could therefore lead to a decrease in IL-15 and thereby a decrease in the number of NK cells, an effect aggravated by an increase in systemic IL-6 levels (Reviewed in [40]). Importantly, NK cells are natural eliminators of senescent cells [41]. Muscle atrophy during aging thus adds to the build-up of senescence by reducing the ability of the immune system to clear senescent cells. This, in turn, further accelerates muscle loss and age-related frailty. Studies are underway to determine whether anti-senescence treatment can overcome muscle loss.

Aging is the greatest risk factor for most chronic diseases, and mechanistic links between aging and disease are starting to emerge. Several studies show an involvement of cellular senescence, and in particular, muscle stem cell senescence, in distinct types of muscular dystrophies. In Myotonic dystrophy type 1 (DM1 or Steinert's disease), entry into senescence of human satellite cell-derived myoblasts

correlates with a lower proliferative rate than age-matched controls and has been causally implicated in the progressive atrophy and degeneration of DM1 muscles [22, 23]. Similarly, cellular senescence traits have been described in mdx mice, a widely used model of Duchenne muscular dystrophy (DMD), correlating with poor regenerative capacity [24, 25, 42]. Premature cellular senescence also underlies myopathy in a mouse model of limb-girdle muscular dystrophy [43]. Whether interference in cellular senescence can provide a therapeutic approach for these muscle diseases is unknown.

**Bone: senescence distorts the balance between resorption and formation**

During aging, there is an increase in senescence in the bone. This, in turn, can lead to changes in bone density. Bone consists of multiple cell types, including osteoblasts that form bone, osteoclasts that break down bone tissue, and osteocytes that make up the majority of bone cells (reviewed in [44]). Out of the various cell types that are affected, the main SASP producing cells are senescent osteocytes [45]. Osteocytes are known to influence osteoblast and osteoclast function [46], and SASP factors secreted by osteocytes, such as IL-1 and MMP13, increase osteoclast differentiation and thereby increase bone resorption to cause the age-related bone loss associated with osteoporosis [47-49]. The conditioned medium of senescent cells can decrease osteoblast function *in vitro* and promote osteoclast activity [50]. Furthermore, inhibition of senescence induction stimulates osteogenesis and prevents osteoporosis [51]. These observations indicate a causal role of senescence in disrupting the balance between bone formation and resorption, leading to osteoporosis.

There are several mouse models that show accelerated aging and are known to have an increased number of senescent cells, such as mice with DNA repair or telomerase deficiency; such mice often show osteoporosis and other musculoskeletal afflictions [60, 61]. They are therefore ideal model organisms for studying the effect of senescence in these disorders. For example, Klotho-deficient mice show accelerated senescence and a wide variety of age-related diseases, including osteoporosis. When these mice were crossed with p16[ink4a] knockout mice, osteoporosis was attenuated [61], indicating that senescent cell ablation can potentially prevent this deterioration. Indeed, osteoporosis was delayed in naturally aged INK-ATTAC mice when senescent cells, which continuously develop, were ablated twice a week. Moreover, these mice had an improved microarchitecture and strength [62]. The reduction of senescent cells likely leads to a lower level of inflammation in the bone. This then reduces the formation of osteoclasts and prevents bone degradation. Indeed, in INK-ATTAC mice, bone resorption was lowered and bone formation improved. In conclusion, senescent cell removal prevents age-related bone loss in mice.
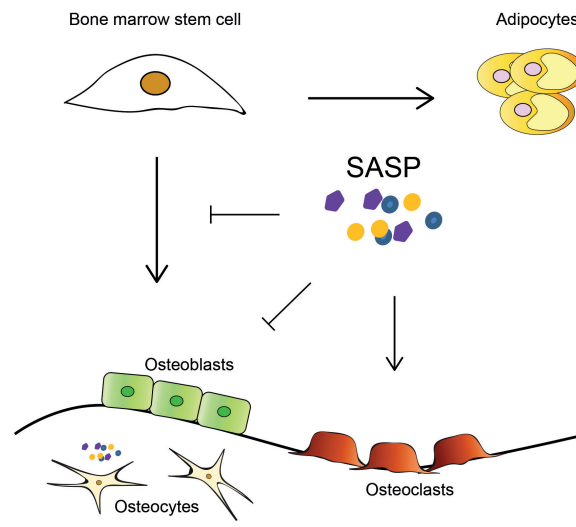
In aged bone, the balance between bone formation by osteoblasts and bone resorption by osteoclasts is distorted. An accumulation of senescent cells is observed that promote an increased osteoclast activation through the SASP. Bone loss is also worsened by the inhibition of osteoblast formation by pro-inflammatory factors. For example, known SASP factors cause mesenchymal stem cells to favor adipogenesis over osteoblast production.

Bone stem cell function during aging is likely influenced by secreted SASP factors. Osteoblasts have a relatively short lifespan and are derived from mesenchymal stem cells in the bone marrow (BMSCs), periosteum and elsewhere [52]. BMSCs can give rise to both osteoblasts and adipocytes [53]. This balance is heavily influenced by the microenvironment [54], and during osteoporosis oxidative stress and inflammatory cytokines influence BMSCs to favor adipogenesis over osteogenesis [55, 56]. Therefore adipose tissue accumulation is a hallmark of osteoporosis and is linked to senescence in the microenvironment. Furthermore, BMSCs show a reduced differentiation capacity during aging. For example, serum from aged individuals inhibits differentiation of BMSCs into osteoblasts [57]. Additionally, BMSCs can become senescent during aging, secreting SASP proteins and promoting osteoclast activity [58, 59]. Overall, these observations indicate that targeting senescent cells in bone would likely improve bone stem cell function.

**Cartilage: senescence-associated chronic inflammation perturbs cartilage regeneration**

Articular cartilage – a flexible connective tissue that protects the ends of bones within a joint – affords smooth surfaces with low friction for movement, and

facilitates transmission of loads to the underlying bone. This tissue mainly consists of extracellular matrix produced by chondrocytes, the cell type present in cartilage. The regenerative potential of cartilage after damage is limited, possibly because the tissue contains a low number of mesenchymal stem cells [63]. Furthermore, like muscle stem cells, these stem cells are less able to regenerate damaged tissue with age. This is in part due to intrinsic MSC aging and senescence induction [64, 65], but is also due to the altered tissue microenvironment and chronic inflammation [66]. Additionally, chondrocytes can express stemness markers in osteoarthritis [67, 68]. Again, inflammatory factors promote a chronic dedifferentiated state and thereby prevent tissue repair during aging [69]. Altogether, this leads to thinning of cartilage during aging, resulting in stiffness and pain in the joints that are characteristic of osteoarthritis [70]. Figuur 3 ergens hier

A causal role of senescence in osteoarthritis was shown by transplanting senescent cells into mouse joints, resulting in pain and morphological changes indicative of osteoarthritis [71].

## Young          Old
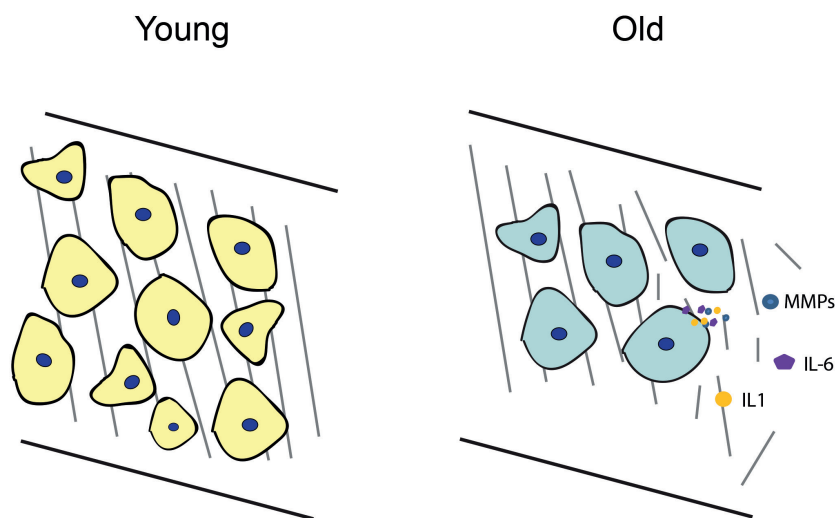


Age-related cartilage degeneration leads to osteoarthritis. Senescent chondrocytes present in aged cartilage cannot proliferate to regenerate damaged cartilage and induce extracellular matrix degeneration through the SASP. Furthermore, cartilage regeneration is inhibited during aging due to senescent mesenchymal stem cells.

Furthermore, chondrocytes show an age-related increase in senescence, and during osteoarthritis pro-inflammatory cytokines such as the prominent SASP factor IL-1 induce excess expression of matrix metalloproteinases (MMPs), leading to cartilage loss [72]. Increased levels of circulating SASP factors such

as IL-6 are linked to frailty and risk of osteoarthritis [73]. Additionally, in a mouse model of osteoarthritis, overexpression of SIRT6 prevents senescence induction and concurrent inflammation, thereby reducing cartilage degeneration [74]. This finding indicates that eliminating senescent cells from cartilage would attenuate osteoarthritis and improve joint function, especially since chondrocyte death does not seem to drive cartilage damage in response to injury [75]. Several studies have examined the effect of senescent cell removal on osteoarthritis development. For example, osteoarthritis was surgically induced in mice through anterior cruciate ligament transection (ACLT) in the knee joint. In this model, genetic removal of senescent cells delayed the development of osteoarthritis, evidenced by reduced inflammation in the knee joint and an increase in cartilage development, indicating better joint function [76]. The mice had less pain after the senescent cells were removed. Furthermore, osteoarthritis occurs naturally in aged INK-ATTAC mice, and cartilage degeneration was attenuated after removal of senescent cells in this model.

**Targeting senescence to counteract age-related frailty**

The encouraging results obtained upon genetic elimination of senescent cells have important implications for the treatment of musculoskeletal deterioration. Since senescence is thought to play a significant role in the progression of age-related frailty, anti-senescence drugs can be predicted to benefit patients with musculoskeletal disorders.

| Tissue | Model system | Senescence cleared/delayed by: | Improvements musculoskeletal system | Ref |
|---|---|---|---|---|
| | Fast aging $BubR1^{H/H}$ mice | INK-ATTAC | Kyphosis reduction, increase in muscle fibre diameter | [23] |
| | Naturally aged mice | Navitoclax | Improved muscle stem cell function | [102] |
| | Klotho deficient mice | $p16^{inkta}$ knockout | Delay in osteoporosis | [77] |
| | Naturally aged mice | INK-ATTAC | Improved bone structure and strength, improved bone formation, reduction in bone resorption | [78] |
| | ACLT in the mouse knee joint | p16::3MR | Reduced inflammation, pain reduction, increase in cartilage development | [98] |
| | Naturally aged mice | INK-ATTAC | Reduced cartilage degeneration | [98] |
| | Fast aging $Xpd^{TTD/TTD}$ mice | FOXO4-DRI | Improved running wheel performance | [104] |

Effects of senescent cell removal on the musculoskeletal system

Currently, drugs that target inflammatory cytokines are tested in patients with musculoskeletal diseases. For example, several strategies for IL1 inhibition in osteoarthritis have been explored. These therapies include IL1 receptor antagonist proteins (IRAP), monoclonal antibodies targeting free IL1 or the IL1-receptor, and an inhibitor of IL1β production called Diacerein (reviewed in [77]). Most of these therapies show a trend of pain reduction versus placebo. However, these results were often not statistically significant, possibly due to the short half-life of the antagonist proteins or blocking antibodies. Only Diacerein treatment has shown significant anti-inflammatory effects and pain reduction in most studies [77]. Treatment of mdx dystrophic mice with the NAD+ precursor nicotinamide riboside (NR) prevented senescence of muscle stem cells, and this rejuvenated their regenerative capacity [24]. The Notch pathway

is chronically activated in severely dystrophic muscles of mdx mice double mutant for dystrophin and utrophin, and blocking this pathway with the γ-Secretase inhibitor DAPT reduced stem cell senescence and the histopathological features of DMD [42]. Importantly, abolition of p16$^{INK4a}$, which accumulates abnormally in satellite cells of DM1 muscles, partially restores early growth arrest and reduces senescence in vitro [22], reinforcing the idea that this mechanism might participate in the impaired regeneration of DM1 muscles. Notably, the regenerative deficit of satellite cells from dystrophic muscles resembles that of geriatric mice, which also show p16I$^{INK4a}$-induced senescence and can be rejuvenated by silencing of the gene encoding p16$^{INK4a}$ [21]. Overall, these studies show limited effects, and the long-term safety of these drugs and/or genetic approaches has yet to be assessed. However, it is unlikely that essential molecules and pathways such as Notch or p16$^{INK4a}$ can be targeted systemically without severe secondary effects. In addition, these strategies are aimed at reducing symptoms and do not treat the underlying causes of disease progression. Removal of senescent cells is expected to reduce these inflammatory proteins while preserving stem cell function and is therefore expected to be safer and have more long-lasting effects.

The results obtained after genetic removal of senescent cells prompted a search for therapeutically applicable anti-senescence compounds. A small number of these compounds have been discovered, with varying degrees of success. One example is Navitoclax, a BCL2 family inhibitor. In the musculoskeletal system, Navitoclax was found to decrease the expression of cytokines that promote osteoclast activity *in vitro*, such as IL–1α and MMP–13 [58]. Furthermore, muscle stem cells isolated from naturally aged, Navitoclax-treated mice showed improved clonogenicity [78].

A major challenge when developing anti-senescence therapies is to avoid toxicity to healthy non-senescent cells. It is therefore important to identify the unique characteristics of senescent cells that can be targeted by a therapeutic compound. Senescent cells often express persistent nuclear damage foci called DNA-SCARS (DNA Segments with Chromatin Alterations Reinforcing Senescence) that contain DDR proteins such as 53BP1, γH2AX and activated p53[79]. These DNA-SCARS play a role in maintaining permanent growth arrest and are critical for SASP expression. In addition, we recently showed that the transcription factor FOXO4 resides within PML bodies fused to these persistent damage foci[19]. Here, FOXO4 binds p53 and prevents p53-dependent apoptosis. In order to disrupt this interaction and to induce apoptosis, we prospectively generated a D-Retro-Inverso peptide mimicking the FOXO4 p53-binding domain. This peptide, FOXO4-DRI, causes the release of p53 to the cytoplasm, where p53 indeed induces apoptosis in a transcription independent manner. Indeed, *in vivo* use of FOXO4-DRI shows promising results. For these experiments we made use of *Xpd$^{TTD/TTD}$* mice that show accelerated aging and age-related ailments such

as osteoporosis and are therefore an ideal model for musculoskeletal diseases [60]. FOXO4-DRI treatment improved overall fitness and renal function in these mice, including an improved running wheel performance[19], an especially promising result for the treatment of musculoskeletal diseases. FOXO4-DRI showed around 10 fold selectivity for eliminating senescent vs. control cells. While enough for experiments in rodents, translation to the clinic requires further improvement to eliminate toxicity, which would be intolerable in this setting. Such efforts are now underway in our laboratory.

**Unanswered questions**

As we highlighted here, the tissues of the musculoskeletal system are damaged by inflammation during aging. Cellular senescence, by driving a persistent inflammatory response, is a major contributor to these effects. However, it remains unclear which senescent cell types are the main producers of these pro-inflammatory factors. Aging of the musculoskeletal system is due to both local and systemic factors. For example, senescent cells transplanted into cartilage can independently cause osteoarthritis [71]. On the other hand, systemically increased IL-6 levels are linked to muscle wasting, and the immune system also seems to be crucial in this process [28, 29]. This systemic inflammation can be caused by many cell types. For example, adipose tissue significantly contributes to systemic inflammation [80]. Fat present in joints can produce factors that promote osteoarthritis [81]. In turn, cells of the musculoskeletal system also secrete systemic factors and influence overall tissue integrity. For example, muscle cells affect NK cells during aging and, as NK cells are responsible for clearance of senescent cells[41], these would also influence the systemic senescence burden. Since various anti-senescence compounds potentially kill distinct subsets of senescent cells, it is vital to know which cell type to target; knowledge about which senescent cells contribute most to musculoskeletal degeneration will ultimately guide the development of effective treatment. Anti-senescence therapy may also be beneficial for several incurable muscular dystrophies and for wasting, by reducing inflammaging and hence boosting the satellite cell regenerative functions. Interestingly, cellular senescence has been shown to mediate fibrotic pulmonary disease, and senescent cell ablation improves pulmonary function in this setting [82]. Most dystrophinopathies also feature increased muscle fibrosis [83], which aggravates disease progression by substituting muscle with scar tissue, and it is plausible that anti-senescence cocktails will also halt fibrosis and improve patient health status. Thus, elimination of senescent cells may have benefits for tissue repair by reversing several detrimental processes; however, it remains to be determined whether senescence should be blocked partially or totally or eliminated only once early potential stemness-related functions have been completed. The answers to these questions may not be easy to obtain, yet we are rapidly obtaining tools that allow manipulation of the senescence process (for removing senescent

cells, neutralizing the SASP, or both processes). The final goal is to preserve stem cell benefits while minimizing the deleterious consequences of senescence.

It also remains unclear how tissues rejuvenate after senescent cell ablation and whether side effects or unexpected challenges will occur. For example, in addition to its potential to eliminate senescent cells, tissue engineering is being explored as a treatment for musculoskeletal diseases. In this scenario, stem cells are isolated and healthy tissue is generated *ex vivo* to replace damaged tissues such as cartilage and bone. For example, mesenchymal stem cells can be isolated and cultured on a biodegradable scaffold where they are stimulated with TGFβ to induce differentiation into chondrocytes [84]. This newly formed cartilage could then be used for surgical reconstruction of joints. However, a major challenge in tissue engineering is to prevent stem cell senescence[85]. It remains unclear whether similar issues will arise after senescence clearance. So far, tissue regeneration seems efficient after these cells are removed. For example, although cartilage has a weak regenerative potential, it is rejuvenated after senescent cells are removed. Tissue-specific stem cells are likely key to this regeneration. It is possible that the reduction of SASP proteins in the tissue microenvironment releases these cells from their 'stem cell lock', resulting in a restored regenerative potential. In addition, cells that are dedifferentiated due to senescence, such as chondrocytes, could help rejuvenate musculoskeletal tissue. In general, multiple factors likely contribute to this rejuvenation. Both local and systemic inflammation are expected to decline, affecting immune system functioning, natural senescent cell clearance, stem cell function, and tissue regeneration.

In conclusion, targeting senescence has the potential to prevent or reverse multiple age-related diseases and to reduce frailty. Furthermore, it seems likely that therapeutically applicable anti-senescence compounds will be available in the future. However, the toxicity of these drugs remains a major concern. Periodic treatments will likely be necessary to maintain possible beneficial effects and it is still largely unknown what the effect of multiple treatment rounds will be. Therefore, the timing and frequency of these treatments should be studied, as well as the long-term effect of senescence clearance on biological processes such as stem cell function.

## Acknowledgements:

3

# References

1.  Walston, J.D., *Sarcopenia in older adults.* Curr Opin Rheumatol, 2012. **24**(6): p. 623-7.
2.  Chakkalakal, J.V., et al., *The aged niche disrupts muscle stem cell quiescence.* Nature, 2012. **490**(7420): p. 355-60.
3.  Renault, V., et al., *Regenerative potential of human skeletal muscle during aging.* Aging Cell, 2002. **1**(2): p. 132-9.
4.  von Maltzahn, J., et al., *Pax7 is critical for the normal function of satellite cells in adult skeletal muscle.* Proc Natl Acad Sci U S A, 2013. **110**(41): p. 16474-9.
5.  Sambasivan, R., et al., *Pax7-expressing satellite cells are indispensable for adult skeletal muscle regeneration.* Development, 2011. **138**(17): p. 3647-56.
6.  Cerletti, M., et al., *Short-term calorie restriction enhances skeletal muscle stem cell function.* Cell Stem Cell, 2012. **10**(5): p. 515-9.
7.  Franceschi, C., et al., *Inflamm-aging. An evolutionary perspective on immunosenescence.* Ann N Y Acad Sci, 2000. **908**: p. 244-54.
8.  Brack, A.S., et al., *Increased Wnt signaling during aging alters muscle stem cell fate and increases fibrosis.* Science, 2007. **317**(5839): p. 807-10.
9.  Xu, M., et al., *JAK inhibition alleviates the cellular senescence-associated secretory phenotype and frailty in old age.* Proc Natl Acad Sci U S A, 2015. **112**(46): p. E6301-10.
10. Villeda, S.A., et al., *The ageing systemic milieu negatively regulates neurogenesis and cognitive function.* Nature, 2011. **477**(7362): p. 90-4.
11. Conboy, I.M., et al., *Rejuvenation of aged progenitor cells by exposure to a young systemic environment.* Nature, 2005. **433**(7027): p. 760-4.
12. Hoeijmakers, J.H., *DNA damage, aging, and cancer.* N Engl J Med, 2009. **361**(15): p. 1475-85.
13. de Keizer, P.L., *The Fountain of Youth by Targeting Senescent Cells?* Trends Mol Med, 2017. **23**(1): p. 6-17.
    **(*) This paper describes the senescence-stem lock model explaining how permanent SASP secretion by senescent cells can impair tissue rejuvenation by forcing a permanent state of pluripotency in neighboring cells.**
14. Coppe, J.P., et al., *Senescence-associated secretory phenotypes reveal cell-nonautonomous functions of oncogenic RAS and the p53 tumor suppressor.* PLoS Biol, 2008. **6**(12): p. 2853-68.
15. Wang, C., et al., *DNA damage response and cellular senescence in tissues of aging mice.* Aging Cell, 2009. **8**(3): p. 311-23.
16. Baker, D.J., et al., *Clearance of p16Ink4a-positive senescent cells delays ageing-associated disorders.* Nature, 2011. **479**(7372): p. 232-6.
17. Baker, D.J., et al., *Naturally occurring p16(Ink4a)-positive cells shorten healthy lifespan.* Nature, 2016. **530**(7589): p. 184-9.
    **(*)The genetic removal of senescent cells extends health- and lifespan in natrually aging mice.**
18. Zhu, Y., et al., *The Achilles' heel of senescent cells: from transcriptome to senolytic drugs.* Aging Cell, 2015. **14**(4): p. 644-58.
19. Baar, M.P., et al., *Targeted Apoptosis of Senescent Cells Restores Tissue Homeostasis in Response to Chemotoxicity and Aging.* Cell, 2017. **169**(1): p. 132-147 e16.

**(\*) The targeted apoptosis of senescent cells by a FOXO4-p53 interfering peptide restores fur density, energy and kidney function in fast and naturally aged mice.**

20.  Mosteiro, L., et al., *Tissue damage and senescence provide critical signals for cellular reprogramming in vivo.* Science, 2016. **354**(6315).
     **(\*) The prolonged expression of the four Yamanaka (OSKM) stem cell factors leads to pluripotency in neighboring cells in vivo.**

21.  Sousa-Victor, P., et al., *Geriatric muscle stem cells switch reversible quiescence into senescence.* Nature, 2014. **506**(7488): p. 316-21.
     **(\*\*) The inhibition of senescence induction in aged satellite cells restores their muscle regenerative capacity.**

22.  Bigot, A., et al., *Large CTG repeats trigger p16-dependent premature senescence in myotonic dystrophy type 1 muscle precursor cells.* Am J Pathol, 2009. **174**(4): p. 1435-42.

23.  Thornell, L.E., et al., *Satellite cell dysfunction contributes to the progressive muscle atrophy in myotonic dystrophy type 1.* Neuropathol Appl Neurobiol, 2009. **35**(6): p. 603-13.

24.  Zhang, H., et al., *NAD(+) repletion improves mitochondrial and stem cell function and enhances life span in mice.* Science, 2016. **352**(6292): p. 1436-43.

25.  Le Roux, I., et al., *Numb is required to prevent p53-dependent senescence following skeletal muscle injury.* Nat Commun, 2015. **6**: p. 8528.

26.  Serrano, A.L., et al., *Interleukin-6 is an essential regulator of satellite cell-mediated skeletal muscle hypertrophy.* Cell Metab, 2008. **7**(1): p. 33-44.

27.  Carson, J.A. and K.A. Baltgalvis, *Interleukin 6 as a key regulator of muscle mass during cachexia.* Exerc Sport Sci Rev, 2010. **38**(4): p. 168-76.

28.  Goodman, M.N., *Interleukin-6 induces skeletal muscle protein breakdown in rats.* Proc Soc Exp Biol Med, 1994. **205**(2): p. 182-5.

29.  Tsujinaka, T., et al., *Muscle undergoes atrophy in association with increase of lysosomal cathepsin activity in interleukin-6 transgenic mouse.* Biochem Biophys Res Commun, 1995. **207**(1): p. 168-74.

30.  Tsujinaka, T., et al., *Interleukin 6 receptor antibody inhibits muscle atrophy and modulates proteolytic systems in interleukin 6 transgenic mice.* J Clin Invest, 1996. **97**(1): p. 244-9.

31.  Belizario, J.E., et al., *Skeletal muscle wasting and renewal: a pivotal role of myokine IL-6.* Springerplus, 2016. **5**: p. 619.

32.  Chiche, A., et al., *Injury-Induced Senescence Enables In Vivo Reprogramming in Skeletal Muscle.* Cell Stem Cell, 2017. **20**(3): p. 407-414 e4.
     **(\*\*) Senescence promotes reprogramming in muscle after injury, which is dependent on IL-6.**

33.  Ocampo, A., et al., *In Vivo Amelioration of Age-Associated Hallmarks by Partial Reprogramming.* Cell, 2016. **167**(7): p. 1719-1733 e12.
     **(\*) The transient expression of the four Yamanaka (OSKM) stem cell factors reduces senescence, SASP and alleviates muscle injury in aged mice.**

34.  Fry, C.S., et al., *Inducible depletion of satellite cells in adult, sedentary mice impairs muscle regenerative capacity without affecting sarcopenia.* Nat Med, 2015. **21**(1): p. 76-80.

3

35. Keefe, A.C., et al., *Muscle stem cells contribute to myofibres in sedentary adult mice.* Nat Commun, 2015. **6**: p. 7087.

36. Lepper, C., T.A. Partridge, and C.M. Fan, *An absolute requirement for Pax7-positive satellite cells in acute injury-induced skeletal muscle regeneration.* Development, 2011. **138**(17): p. 3639-46.

37. Nielsen, A.R., et al., *Expression of interleukin-15 in human skeletal muscle effect of exercise and muscle fibre type composition.* J Physiol, 2007. **584**(Pt 1): p. 305-12.

38. Prlic, M., et al., *In vivo survival and homeostatic proliferation of natural killer cells.* J Exp Med, 2003. **197**(8): p. 967-76.

39. Kang, Y.J., et al., *An increased level of IL-6 suppresses NK cell activity in peritoneal fluid of patients with endometriosis via regulation of SHP-2 expression.* Hum Reprod, 2014. **29**(10): p. 2176-89.

40. Lutz, C.T. and L.S. Quinn, *Sarcopenia, obesity, and natural killer cell immune senescence in aging: altered cytokine levels as a common mechanism.* Aging (Albany NY), 2012. **4**(8): p. 535-46.

41. Sagiv, A., et al., *NKG2D ligands mediate immunosurveillance of senescent cells.* Aging (Albany NY), 2016. **8**(2): p. 328-44.

42. Mu, X., et al., *The role of Notch signaling in muscle progenitor cell depletion and the rapid onset of histopathology in muscular dystrophy.* Hum Mol Genet, 2015. **24**(10): p. 2923-37.

43. Kudryashova, E., I. Kramerova, and M.J. Spencer, *Satellite cell senescence underlies myopathy in a mouse model of limb-girdle muscular dystrophy 2H.* J Clin Invest, 2012. **122**(5): p. 1764-76.

44. Feng, X. and S.L. Teitelbaum, *Osteoclasts: New Insights.* Bone Res, 2013. **1**(1): p. 11-26.

45. Farr, J.N., et al., *Identification of Senescent Cells in the Bone Microenvironment.* J Bone Miner Res, 2016. **31**(11): p. 1920-1929.

46. Ikeda, K., *Osteocytes in the pathogenesis of osteoporosis.* Geriatr Gerontol Int, 2008. **8**(4): p. 213-7.

47. Kim, J.H., et al., *The mechanism of osteoclast differentiation induced by IL-1.* J Immunol, 2009. **183**(3): p. 1862-70.

48. Piemontese, M., et al., *Old age causes de novo intracortical bone remodeling and porosity in mice.* JCI Insight, 2017. **2**(17).

49. Fu, J., et al., *Multiple myeloma-derived MMP-13 mediates osteoclast fusogenesis and osteolytic disease.* J Clin Invest, 2016. **126**(5): p. 1759-72.

50. Khosla, S., J.N. Farr, and J.L. Kirkland, *Inhibiting Cellular Senescence: A New Therapeutic Paradigm for Age-Related Osteoporosis.* J Clin Endocrinol Metab, 2018.

51. Wu, G., et al., *Estrogen regulates stemness and senescence of bone marrow stromal cells to prevent osteoporosis via ERbeta-SATB2 pathway.* J Cell Physiol, 2018. **233**(5): p. 4194-4204.

52. Park, D., et al., *Endogenous bone marrow MSCs are dynamic, fate-restricted participants in bone maintenance and regeneration.* Cell Stem Cell, 2012. **10**(3): p. 259-72.

53. Petecchia, L., et al., *A biophysical approach to quantify skeletal stem cells trans-differentiation as a model for the study of osteoporosis.* Biophys Chem, 2017. **229**: p. 84-92.

54. Li, J., et al., *The Role of Bone Marrow Microenvironment in Governing the Balance between Osteoblastogenesis and Adipogenesis.* Aging Dis, 2016. **7**(4): p. 514-25.

55. Kim, M., et al., *Age-related alterations in mesenchymal stem cells related to shift in differentiation from osteogenic to adipogenic potential: implication to age-associated bone diseases and defects.* Mech Ageing Dev, 2012. **133**(5): p. 215-25.

56. Sui, B., et al., *Mesenchymal progenitors in osteopenias of diverse pathologies: differential characteristics in the common shift from osteoblastogenesis to adipogenesis.* Sci Rep, 2016. **6**: p. 30186.

57. Abdallah, B.M., et al., *Inhibition of osteoblast differentiation but not adipocyte differentiation of mesenchymal stem cells by sera obtained from aged females.* Bone, 2006. **39**(1): p. 181-8.

58. Kim, H.N., et al., *DNA damage and senescence in osteoprogenitors expressing Osx1 may cause their decrease with age.* Aging Cell, 2017. **16**(4): p. 693-703.

59. Xu, R., et al., *Transplantation of osteoporotic bone marrow stromal cells rejuvenated by the overexpression of SATB2 prevents alveolar bone loss in ovariectomized rats.* Exp Gerontol, 2016. **84**: p. 71-79.

60. de Boer, J., et al., *Premature aging in mice deficient in DNA repair and transcription.* Science, 2002. **296**(5571): p. 1276-9.

61. Sato, S., et al., *Ablation of the p16(INK4a) tumour suppressor reverses ageing phenotypes of klotho mice.* Nat Commun, 2015. **6**: p. 7035.

62. Farr, J.N., et al., *Targeting cellular senescence prevents age-related bone loss in mice.* Nat Med, 2017. **23**(9): p. 1072-1079.
**(\*\*) Senescent cell removal improves bone mass and strength in aged mice by reducing bone resorption.**

63. Candela, M.E., et al., *Resident mesenchymal progenitors of articular cartilage.* Matrix Biol, 2014. **39**: p. 44-9.

64. Szychlinska, M.A., et al., *Mesenchymal Stem Cell-Based Cartilage Regeneration Approach and Cell Senescence: Can We Manipulate Cell Aging and Function?* Tissue Eng Part B Rev, 2017. **23**(6): p. 529-539.

65. Taniguchi, N., et al., *Aging-related loss of the chromatin protein HMGB2 in articular cartilage is linked to reduced cellularity and osteoarthritis.* Proc Natl Acad Sci U S A, 2009. **106**(4): p. 1181-6.

66. Ando, W., et al., *Ovine synovial membrane-derived mesenchymal progenitor cells retain the phenotype of the original tissue that was exposed to in-vivo inflammation: evidence for a suppressed chondrogenic differentiation potential of the cells.* Inflamm Res, 2012. **61**(6): p. 599-608.

67. Li, L., et al., *Superficial cells are self-renewing chondrocyte progenitors, which form the articular cartilage in juvenile mice.* FASEB J, 2017. **31**(3): p. 1067-1084.

68. Jiang, Y., et al., *Human Cartilage-Derived Progenitor Cells From Committed Chondrocytes for Efficient Cartilage Repair and Regeneration.* Stem Cells Transl Med, 2016. **5**(6): p. 733-44.

69. Varela-Eirin, M., et al., *Cartilage regeneration and ageing: Targeting cellular plasticity in osteoarthritis.* Ageing Res Rev, 2017. **42**: p. 56-71.

70. Martel-Pelletier, J., et al., *Osteoarthritis.* Nat Rev Dis Primers, 2016. **2**: p. 16072.

71. Xu, M., et al., *Transplanted Senescent Cells Induce an Osteoarthritis-Like Condition in Mice.* J Gerontol A Biol Sci Med Sci, 2017. **72**(6): p. 780-785.

3

**(\*) The injection of senescent cells into the knee joint induces osteoarthritis symptoms, showing a causal link between senescence and osteoarthritis.**

72. Portal-Nunez, S., et al., *Oxidative stress, autophagy, epigenetic changes and regulation by miRNAs as potential therapeutic targets in osteoarthritis.* Biochem Pharmacol, 2016. **108**: p. 1-10.

73. Livshits, G., et al., *Interleukin-6 is a significant predictor of radiographic knee osteoarthritis: The Chingford Study.* Arthritis Rheum, 2009. **60**(7): p. 2037-45.

74. Wu, Y., et al., *Overexpression of Sirtuin 6 suppresses cellular senescence and NF-kappaB mediated inflammatory responses in osteoarthritis development.* Sci Rep, 2015. **5**: p. 17602.

75. Zhang, M., et al., *Induced superficial chondrocyte death reduces catabolic cartilage damage in murine posttraumatic osteoarthritis.* J Clin Invest, 2016. **126**(8): p. 2893-902.

76. Jeon, O.H., et al., *Local clearance of senescent cells attenuates the development of post-traumatic osteoarthritis and creates a pro-regenerative environment.* Nat Med, 2017. **23**(6): p. 775-781.
**(\*) The ablation of senescent cells prevents post-traumatic osteoarthritis in mice, reduces pain and increases cartilage regeneration.**

77. Jotanovic, Z., et al., *Role of interleukin-1 inhibitors in osteoarthritis: an evidence-based review.* Drugs Aging, 2012. **29**(5): p. 343-58.

78. Chang, J., et al., *Clearance of senescent cells by ABT263 rejuvenates aged hematopoietic stem cells in mice.* Nat Med, 2016. **22**(1): p. 78-83.

79. Rodier, F., et al., *Persistent DNA damage signalling triggers senescence-associated inflammatory cytokine secretion.* Nat Cell Biol, 2009. **11**(8): p. 973-9.

80. Messier, S.P., et al., *Effects of intensive diet and exercise on knee joint loads, inflammation, and clinical outcomes among overweight and obese adults with knee osteoarthritis: the IDEA randomized clinical trial.* JAMA, 2013. **310**(12): p. 1263-73.

81. Distel, E., et al., *The infrapatellar fat pad in knee osteoarthritis: an important source of interleukin-6 and its soluble receptor.* Arthritis Rheum, 2009. **60**(11): p. 3374-7.

82. LeBrasseur, N.K., *Physical Resilience: Opportunities and Challenges in Translation.* J Gerontol A Biol Sci Med Sci, 2017. **72**(7): p. 978-979.

83. Mann, C.J., et al., *Aberrant repair and fibrosis development in skeletal muscle.* Skelet Muscle, 2011. **1**(1): p. 21.

84. Li, W.J., et al., *A three-dimensional nanofibrous scaffold for cartilage tissue engineering using human mesenchymal stem cells.* Biomaterials, 2005. **26**(6): p. 599-609.

85. Wagner, W., et al., *Replicative senescence of mesenchymal stem cells: a continuous and organized process.* PLoS One, 2008. **3**(5): p. e2213

3

# CHAPTER 4

## Maintenance and Repair of an Aging Life Cycle

**Marjolein P. Baar[1], Hester van Willigenburg[1] and Peter L.J. de Keizer[1]**

[1] Department of Molecular Genetics, Erasmus University Medical Center

Wytemaweg 80, 3015CN, Rotterdam, the Netherlands

**"Targeting signs of aging". It sounds more like a punch-line of a TV commercial, than a consequence of fundamental science. But as we observed recently, it might actually be possible to achieve just that, using a prospectively designed FOXO4-p53 interfering peptide that targets so-called "senescent" cells[1]. More research is needed to fully assess its true translational potential and whether it is even safe to remove such cells. However, these findings pose a very attractive starting point to develop ways to live out our final years in better health.**

Aging has often been considered as an integral part of life; a form of "noise" that cannot be targeted or tampered with. This is in part because for long the underlying causes of organismal aging were simply too elusive to comprehend, let alone modify. The chronic build-up of DNA damage has now evidently been established as a major cause for aging, but to counteract the genomic damage that has occurred over a lifetime is an entirely different challenge altogether[2]. One approach to overcome this issue, is to eliminate those cells that are too damaged to faithfully perform their duty and to replace them by fresh and healthy counterparts. Senescent cells are exciting candidates for such an approach. Comparable to formation of rust on old equipment, like a bicycle (Fig. 1), they accumulate during aging and especially at sites of pathology. They develop a chronic secretory profile that is thought to impair tissue renewal and contribute to disease development, for instance by keeping neighboring cells "locked" in a permanent state of stemness[2]. Senescence can be beneficial in a transient setting, but the genetic removal of senescent cells over a prolonged period of time was found to be safe and to potently extended health- and lifespan of naturally aging mice[3]. Thus, senescence is an irrefutable cause for aging and targeting them is warranted. But can they also be eliminated therapeutically? And are such methods then safe on their own? And last, but not least, would such methods be applicable to not merely delay, but also to reverse aging?

**Le tour de FOXO. A demanding journey, but one with great rewards.**

A first surprise when trying to address these questions was that senescent cells recruit a factor called FOXO4 to sites of persistent DNA damage, structures absent in normal healthy cells[1]. This is intriguing as FOXO4 is considered to be the ugly little sister of FOXO1 and FOXO3, which do play major roles in processes ranging from stem cell function, differentiation, tumor suppression, and, aging[4]. In senescence, however, FOXO4 appears to act as a brake on the apoptosis response by sequestering p53. Prospective design of a D-Retro-Inversed Cell Penetrating Peptide that perturbs this interaction, named FOXO4-DRI, allowed for nuclear

release of active p53, followed by cell-intrinsic apoptosis and selective elimination of the senescent cells.

Recent work elegantly proved that senescent cells are a major cause for the toxic side effects caused by multiple independent forms of chemotherapy[5]. Excitingly, FOXO4-DRI counteracted senescence caused by Doxorubicin and reversed liver toxicity providing evidence that therapeutic removal of senescent cells by FOXO4-DRI can counteract at least some aspects of chemotoxicity. Proceeding from this acute senescence-induction model, we then focused on fast aging $Xpd^{TTD/TTD}$ mice, which spontaneously develop senescence in an accelerated fashion, in parallel with organism-wide deterioration. FOXO4-DRI proved to significantly restore their health on multiple levels. Though not purposefully investigated, it was strikingly apparent that FOXO4-DRI treated mice regained fur and improved their voluntary exploratory behavior compared to PBS treated counterparts. In addition, kidney function markedly restored. Naturally aged mice showed more biological noise than the fast aging mice, making these features more difficult to address. But at least the effects on renal function were clearly prevalent in naturally aged mice. Thus, using FOXO4-DRI it indeed appears possible to not just delay aging but also reverse at least certain signs of it. So, what's next?
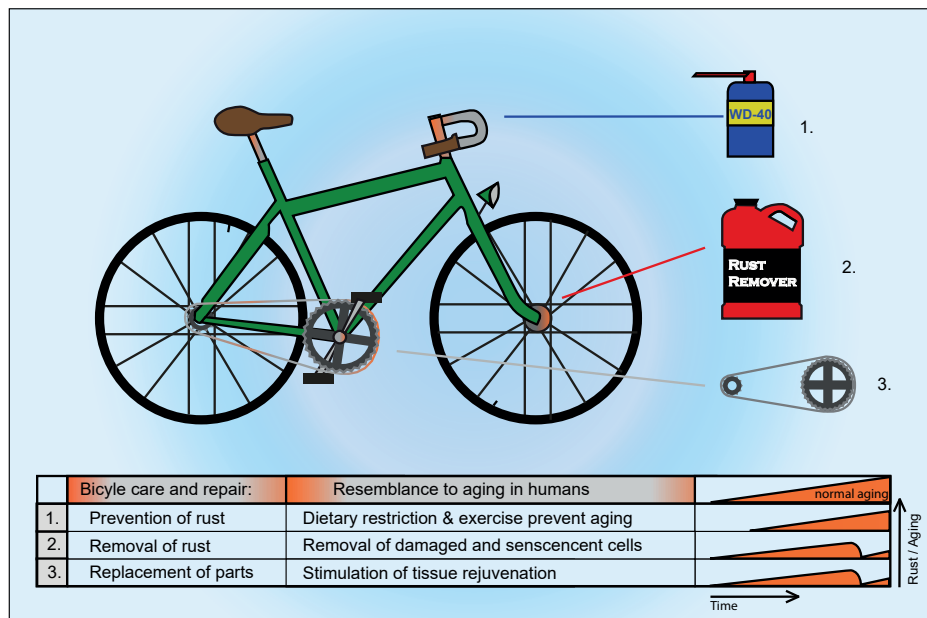
**A combination of efforts to best the mountains ahead**

Aging is ultimately still inevitable. But perhaps it can be strongly postponed, or even reversed, when independent anti-aging therapies are combined? It remains to be determined whether extension of lifespan is possible in humans[6], let alone whether this is desirable and then to what age? After all, life could at some point not simply "complete"? While this might be true for some, nobody likes being sick and frail. Imagine the possibilities if we would be able to enjoy our time with loved ones, exercise and travel more and simply just enjoy life in good health, instead of spending it in a retirement home.

Extending the healthy years of life is now closer than ever, but we are still not there yet. While mechanics can remove defective parts from an old bicycle, it is far more challenging to remove damaged parts from an old body (Fig. 1). Anti-aging strategies have therefore necessarily focused thus far on stalling the inevitable for as long as possible by eating less and exercising more. A multitude of new diets make it to the mainstream public each year, but ironically, people tend to exercise less and gain more and more weight. This argues that instead of focusing so much on dietary interventions, independent approaches deserve to be investigated. Here, we underscored the potential of therapeutic elimination of senescent cells, for instance

by FOXO4-DRI. In addition, exciting developments were recently reported in the field of stem cell biology, where it was shown that transient expression of the Yamanaka stem cell factors can promote tissue rejuvenation[7]. This is not yet therapeutically applicable, but this will most likely only be a matter of time.

It is no longer merely science-fiction to restore healthspan with rationally designed approaches. To fully achieve the best possible outcome, it will therefore deserve special consideration to combine existing methods to delay aging with the recently developed therapies that counter senescence and promote tissue rejuvenation. With these, we finally have exciting tools to maintain and repair the aging cycle of life (Fig. 1). Time to gear up and head for the finish!



| | Bicycle care and repair: | Resemblance to aging in humans | |
|---|---|---|---|
| 1. | Prevention of rust | Dietary restriction & exercise prevent aging | |
| 2. | Removal of rust | Removal of damaged and senscencent cells | |
| 3. | Replacement of parts | Stimulation of tissue rejuvenation | |

The aging cycle of life. The analogy compares senescent cells in an aged body to rust on a racing bicycle. Different strategies can be used to prevent, treat and remove rust and aging. WD-40, a corrosion inhibitor, resembles dietary restriction and regular exercise to delay rust or aging. When rust and aging have already settled, the FOXO4-DRI peptide can act as a rust remover by inducing cell death in senescent cells. Last, the stimulation of tissue rejuvenation can promote a healthy, revitalized tissue that can be compared with the replacement of bicycle parts. The combination of these strategies may be complimentary in fighting aging and age-related defects.

## References

1    Baar, M. P. *et al.* Targeted Apoptosis of Senescent Cells Restores Tissue Homeostasis in Response to Chemotoxicity and Aging. *Cell* **169**, 132-147 e116, doi:10.1016/j. cell.2017.02.031 (2017).

2    de Keizer, P. L. The Fountain of Youth by Targeting Senescent Cells? *Trends Mol Med* **23**, 6-17, doi:10.1016/j.molmed.2016.11.006 (2017).

3    Baker, D. J. *et al.* Naturally occurring p16(Ink4a)-positive cells shorten healthy lifespan. *Nature* **530**, 184-189, doi:10.1038/nature16932 (2016).

4    Eijkelenboom, A. & Burgering, B. M. FOXOs: signalling integrators for homeostasis maintenance. *Nat Rev Mol Cell Biol* **14**, 83-97, doi:10.1038/nrm3507 (2013).

5    Demaria, M. *et al.* Cellular Senescence Promotes Adverse Effects of Chemotherapy and Cancer Relapse. *Cancer Discov* **7**, 165-176, doi:10.1158/2159-8290.CD-16-0241 (2017).

6    Dong, X., Milholland, B. & Vijg, J. Evidence for a limit to human lifespan. *Nature* **538**, 257-259, doi:10.1038/nature19793 (2016).

7    Ocampo, A. *et al.* In Vivo Amelioration of Age-Associated Hallmarks by Partial Reprogramming. *Cell* **167**, 1719-1733 e1712, doi:10.1016/j.cell.2016.11.052 (2016).

4

# CHAPTER 5

## Targeting senescence properties in malignant melanoma to enhance sensitivity to targeted therapies

**Marjolein P. Baar[1,6], Diana A. Putavet[1,6], Shirley Braspenning[1], Joris Pothof[1], Judith Campisi[2], Wim Kruijt[3], Jan H.J. Hoeijmakers[1,4,5], Peter L.J. de Keizer[1, 2, 6]**

[1] Department of Molecular Genetics, Erasmus Medical Center, Rotterdam.

[2] The Buck institute for Research on Aging, Novato, CA 94945, USA

[3] Department of Medical Oncology, Erasmus Medical Center, Rotterdam.

[4] Princess Máxima Centre for Pediatric Oncology, PO Box 113, 3720 AC Bilthoven, the Netherlands

[5] CECAD, University of Cologne, Germany

[6] Department of Molecular Cancer research, Center for Molecular Medicine, University Medical Center Utrecht, the Netherlands

## Abstract

Oncogene-induced senescence is an irreversible cell cycle arrest that prevents cells with cancerous mutations from proliferating. Unfortunately, senescent cells can escape their growth arrest and give rise to malignant tumors. Metastatic melanoma is the most lethal form of skin cancer and can arise from senescent melanocytic nevi. Oncogenic mutations in BRAF are the most common driver of melanoma and treatment of BRAF-mutated melanomas with BRAF/MEK inhibitors results in strong initial tumor regression. However, therapy resistance has thus far impaired a complete treatment response both by new genetic mutations and non-genetic adjustments of treatment surviving cells. Here, we show that BRAFi-resistant melanoma cells can accumulate senescence markers associated with damage, SASP and stemness and that interference with these properties can re-instate drug sensitivity. In line with our previous work showing that FOXO4-p53 signaling is required for maintaining the viability of senescent cells, we observed FOXO4 upregulation in melanoma cells exposed to BRAFi. Strikingly, interference with FOXO4-p53 signaling either by inhibition of FOXO4 expression, or by FOXO4-p53 perturbing peptides induced strong synthetic lethality in BRAFi-resistant melanoma cells. This effect was reduced by anti-oxidants, indicating oxidative stress is required. Thus, BRAFi resistance in metastatic melanoma cells is accompanied by FOXO4-p53 signaling, interference of which can reinstate sensitivity. Since these effects hold true in *ex vivo* cultured human metastatic melanoma tissue, they open the route to translation.

## Introduction

Malignant melanoma is the most lethal form of skin cancer, with 22,200 deaths per year in Europe alone [1]. The majority of end-stage melanomas are driven by mutations in the RAS/RAF/MEK pathway, with BRAF affected in around 50% of cases and NRAS in around 20% [2, 3]. These mutations impair negative feedback signaling to these proteins, resulting in uninhibited MAPK signaling and thereby constitutive proliferative and anti-apoptotic cues.

Melanoma arises from mutated melanocytes, but oncogenic BRAF or NRAS alone are insufficient for full-blown melanoma to arise. Following such driver mutations, the affected cells indeed undergo an initial burst in proliferation. However, malignancy is prevented by the self-induced Oncogene-Induced Senescence (OIS) [4-7]. At least in part, this is caused by incessant activation of the MAPK pathway resulting in excessive ROS production and activation of the DNA damage response (DDR) [8-10]. In addition, pro-proliferative cues as FOXM1 signaling are mitigated [11]. This results in the formation of clusters of pigment producing melanocytes known as melanocytic nevi, or moles. Indeed, almost all nevi already carry either a BRAF or NRAS mutation [12-14], although most will never form a tumor.

Senescence is a permanent state of cell cycle arrest that prevents damaged cells from proliferating and undergoing malignant transformation. When senescence is induced, cells upregulate expression of cell cycle inhibitors such as $p16^{Ink4a}$ and $p21^{Cip1}$ and subsequently undergo profound chromatin changes that distinguish them from healthy cells. In addition, senescent cells often show persistent DNA damage foci known as DNA segments with chromatin alterations reinforcing senescence (DNA-SCARS) [15], that contain proteins such as γH2Ax and 53BP1. Furthermore, these cells secrete an overabundance of proteases, growth factors and pro-inflammatory factors, collectively known as the senescence associated secretory phenotype (SASP) [15, 16]. These senescence markers are found in melanocytic nevi as well [17-19], showing that these nevi are an *in vivo* example of OIS. Mutations in proteins required for oncogene-induced senescence, such as p16 are often deleted in melanoma, as are proteins that provide a negative feedback loop to proliferation, such as PTEN [20]. Thus, senescent cells can resume proliferation and grow into a malignant tumor.

Melanoma development has different stages and survival rates go down with each stage. In stage IV melanoma metastases arise at distant sites, resulting in a poor prognosis with a 5 year survival rate of around 20% [21]. As metastasized melanomas are difficult to excise, treatment has long been challenging due to the lack of targeted therapies. Recent developments have resulted in a marked

improvement in stage IV melanoma treatment compared to traditional chemotherapy. For example, melanoma patients are treated with small molecule inhibitors that specifically target mutated pathways in melanoma. The first of these drugs that gained FDA approval is Vemurafenib. This inhibitor specifically targets melanoma cells with a V600 mutation in BRAF and shows an initial tumor shrinkage in more than 50% of melanoma patients with a BRAF mutation [22]. These targeted drugs are more effective and have fewer side effects than traditional chemotherapy, since they target cancer cells with a specific mutation. However, the median overall survival is only increased by 4 months compared to traditional chemotherapy, due to rapidly occurring therapy resistance [23]. Therefore, improvements are imperative to target both intrinsic and required resistance and thereby enhance the number of patients responding to Vemurafenib and increase the overall survival.

Treatment resistance may arise through both acquired genetic mutations and non-genetic mechanisms. For example, Vemurafenib resistance occurs through reactivation of the MAPK pathway by NRAS or MEK mutations or through activation of alternative pathways such as the PI3K pathway [24]. Additionally, cancer cells can adapt by changing their phenotype without genetic mutations [25]. For example, melanoma cells can acquire more stem-like features, such as stress resistance, an increased drug efflux and increased DNA damage repair that contribute to drug resistance [26-29]. Furthermore, increased senescence markers are observed in melanoma cells after various treatments, including heterochromatin formation, DNA damage markers and expression of pro-inflammatory factors [30-32]. These non-genetic alterations are known to be reversible and highlight the plasticity of cancer cells. Overall, there are a multitude of drug resistance mechanisms, making therapy resistance a major challenge in the treatment of stage IV melanoma.

Since melanoma cells exhibit features of senescence after treatment and senescent cells are known to be extremely apoptotic resistant [33], we hypothesize that senescence markers in melanoma cells contribute to therapy resistance. Therefore, we set out to investigate the potential of anti-senescence strategies in preventing BRAFi resistance in malignant melanoma.

## Methods

### Antibodies and inhibitors

The following antibodies were used in the described immunofluorescence experiments: FOXO4 (9472S) , pSer46-p53 (2521S) and p-JNK (4668) from Cell Signaling, IL1α clone 4414 (MAB200) and IL6 (AF206NA) from R&D systems, P21$^{cip1}$ (610234) from BD Transduction Laboratories, Cytochrome C (556432) from BD

Pharmingen, Catalase (sc-50508) from Santa Cruz, Alexa Fluor donkey anti-rabbit 488 and Alexa Fluor donkey anti-mouse 594 from Life Technologies.

The following antibodies were used to block signaling of the following target proteins to their respective reporters: IL1α (MAB200) IL6 (AF206NA) from R&D systems, IL6 (ab6672) and IL1β (ab9722) from abcam. Furthermore, Cortisol was obtained from sigma, Vemurafenib from Chemie-Tech, Trametinib and JNK inhibitor IX from Seleck Biochem and and FOXO4-DRI was produced by Pepscan at >95 % purity. FOXO4-DRI consists of amino acids in the D-isofrom in the following sequence: H-ltlrkepaseiaqsileaysqngwanrrsggkrppprrrqrrkkrg-OH. This peptide was dissolved in PBS to generate a 2mM stock.

**Cell culture**

A375, LOX-IMVI, RPMI7951 and HEK293LTV and cells were cultured at 37°C and 5% CO2 and ambient oxygen in Dulbecco's Modified Eagle Medium (DMEM) culture medium supplemented with 10% FCS and 1% pen/strep.

**Lentivirus production and transduction**

HEK293LTV cells were transfected with 3µg lentiviral plasmid and similar concentrations of the packaging plasmids PDM2.G, pRRE and pRSV-REV (Addgene) using lipofectamine2000 (Life technologies) according to the manufacturer's instructions. The medium was refreshed the next day. Viruses were collected at day 3. Subsequently, the medium was centrifuged at 4000rpm for 15 minutes and filtered using a 0.45µM filter. The following shRNA sequences were used:

shFOXO4-1 CCAGCTTCAGTCAGCAGTTAT
shFOXO4-2 CGTCCACGAAGCAGTTCAAAT

A375 or LOX-IMVI cells were grown in a 10cm dish and treated with 8µg/ml polybrene before transduction with active virus particles. One day after transduction, the medium was refreshed and three days later 1 µg/ml puromycin was added to the cells. These cells were kept on puromycin selection for the entire duration of subsequently performed experiments.

**Viability assays**

To determine melanoma cell viability after treatment, cells were grown in 96 well plate at a starting concentration of 2000 cells per well. The cells were treated the day after with either small molecule inhibitors or FOXO4-DRI by adding these drugs to the medium. 6 days after treatment the medium was refreshed before 10ul

5

AQueousOne Solution Cell Proliferation assay (Promega) was added to the wells. The plate was then incubated for 0.5 to 2 hrs at 37˚C, after which the absorbance was measured at 490nm in a GloMax 96 well plate reader (Promega).

**Immunofluorescence**

To perform immunofluorescence stainings, cells were plated on 13mm microwave-sterilized coverslips in a 24-well plate before treatment. Cells were fixed at various time points after treatment in formalin, containing 3.8% PFA for 30 minutes on ice. Subsequently, cells were washed twice with Tris Buffered Saline (TBS) and permeabilized at room temperature with 0.1% TritonX-100 in TBS for 3 minutes. After permeabilization, the cells were washed again and quenched 10 minutes in TBS containing 50mM glycine. To further reduce background staining, cells were subsequently blocked with 5% normal horse serum (NHS) in 0.2% gelatin-TBS solution for at least 30 minutes. The coverslips were then put upside down on 30µl droplets of 0.2% gelatin-TBS, containing antibodies against the indicated proteins. The cells were incubated overnight with primary antibodies at 4°C in a humid environment. The next day, the coverslips were washed 3 times in 0.2% gelatin-TBS, followed by a one hour incubation with secondary antibodies at room temperature. After washing the cells twice in 0.2% gelatin-TBS, once with TBS and once briefly in $H_2O$, the coverslips were mounted with soft set mounting medium with DAPI (Vectashield). A LSM700 Zeiss Microscope was used to obtain images.

**Cytochrome C release assay**

Cells were grown on 13mm microwave-sterilized coverslips in a 24 plate and treated with 20uM QVD-OPH to inhibit caspase activity on the day of treatment and 3 days after. To assess apoptosis, cells were fixed 5 days after treatment and an immunofluorescence staining against cytochrome C was performed. Cells showing release of Cytochrome C from mitochondria were scored as apoptotic.

**Real-time cell density assay**

The xCELLigence detection system (ACEA Biosciences) was used to measure live cell density in an E-plate view 16 (Roche). To determine the background signal, 50 µL DMEM 10% FCS was added to each well. Next, 2000 LOX-IMVI cells were plated per well in 150 µl medium and placed in the xCELLigence detection system. The recording was started 16h later when the cells were properly attached and cell density was measured every 30min. 8 hours later 2µM Vemurafenib and 25 µM FOXO4-DRI were added to the wells and measurements continued for 3 days.

**Ex vivo culture of organotypic tissue slices**

Human stage IV melanoma tissue was excised and kept in DMEM culture medium on ice before being sliced. The tissue was embedded into 5% low melting agarose in PBS and adhered to the specimen holder of a Leica VT1200 S vibrating blade microtome (Leica Biosystems) using histoacryl superglue (Bison). 300 µm sections were obtained using a blade amplitude of 3 mm and a speed of 0.6 mm/s. The tissue was sliced in ice-cold PBS in a buffer tray surrounded by ice. Slices were transferred to 6 well plates containing DMEM culture medium supplemented with 10% FCS and 1% pen/strep using a brush and kept at 5% CO2 on a shaker (60RPM). The same day, the slices were either treated with 25 µM FOXO4-DRI, 2µM Vemurafenib or a combination, or transduced with lentiviral particles containing short hairpins against FOXO4 or GFP. 1 day after transduction the medium was refreshed and the slices were treated with Vemurafenib. These slices were processed for a TUNEL assay 5 days later.

**TUNEL assay**

To determine apoptosis in stage IV melanoma tissue slices, these sections were fixed in formalin containing 3.8% PFA, 5 days after treatment. The fixed organotypic slices were further processed to generate 10µm cryosections using the Cryostat HM 560 with the blade at -15°C (Thermo Scientific). The sections were washed in PBS for 30 minutes before permeabilization in 0.1% Triton X-100 in 0.1% sodium citrate on ice. Subsequently, the slices were washed in PBS before incubation in 10% TUNEL enzyme in labeling solution (ROCHE) for 1 hour at 37 °C. The tissue was then washed again in PBS and nuclei were labeled with Hoechst 33342 (ThermoFisher). Slides were mounted with soft set mounting medium (Vectashield) and a LSM510 confocal microscope (Zeiss) was used to image the TUNEL staining. The percentage of TUNEL positive cells was analyzed using CellProfiler software v2.3.

**Melanoid culture**

Patient derived melanoma organoids (melanoids) were obtained as previously described [11]. In short, an untreated stage III melanoma lymph node metastasis was sliced into 300 µm sections as described. The resulting sections were placed into matrigel (Corning) in a 24 well plate. After 5 minutes at 37°C, DMEM culture medium containing 10% FCS and 1% pen/strep was added to the wells. Following outgrowth of the melanoma cells, the melanoma slices were removed and the residual cells were passaged by resuspension, mild centrifugation and reseeding in Matrigel. After several passages these melanoma organoids showed a BRAF[V600E]-mutation and a CDKN2A mutation in >96% of the cells, as determined by whole-gene mutation

5

analysis, hotspot analysis and single-nucleotide polymorphisms analysis. At this time, melanoids were plated in triplicate in 96-well plates in order to determine viability after treatment with Vemurafenib and FOXO4-DRI. Viability was determined 3 days after treatment using the AqueousOne Celltiter assay (Promega).

**Quantitative real-time PCR**

LOX-IMVI cells were cultured in 6 cm plates (100000 cells per plate) and treated 2 days with Vemurafenib and FOXO4-DRI. Subsequently, the plates were washed with ice-cold PBS and the cells scraped in 1 ml TRI reagent (Qiagen). 200 mL chloroform per 1 ml TRI reagent was added to the samples in a 1.5 ml Eppendorf tube. The samples were shaken for 15 seconds, incubated for 5 minutes at room temperature and then centrifuged at 12000 g for 15 minutes at 4 °C. Subsequently, the upper aqueous layer was transferred to a fresh Eppendorf tube to which 500 mL isopropanol was added. The samples were centrifuged again at 12000g for 15 minutes at 4 °C after 15 seconds of shaking and 10 minutes of incubation at room temperature. After centrifugation, the supernatant was removed and the pellet was washed in 1 ml of 75% ethanol before another centrifugation step at 12000g for 15 minutes at 4 °C. The supernatant was removed again and the pellet was air dried for 15 minutes. The pellet was resuspended in 30 mL RNAse free $H_2O$ and the RNA concentration was measured using a Nanodrop 2000 (ThermoFisher). The miScript II RT Kit (Qiagen) was used according to manufacturer's instructions to reverse transcribe mRNA into cDNA. Subsequently, the cDNA was diluted 10 times in $H_2O$ and mixed with primers and SYBR Green Master Mix (Bio-Rad) for qPCR analysis. For this reaction, qPCR plates and the CFX96 Touchä Real-Time PCR Detection System were used from Bio-Rad. Relative gene expression was calculated using the DD Cq method.

**Primers used for the described experiments were:**

FOXO4: Fwd: 5'-acgagtggatggtccgtact-3' Rev: 5'-gtggcggatcgagttcttc-3'

p21[Cip1]: Fwd: 5'-cgaagtcagttccttgtggag-3' Rev: 5'-catgggttctgacggacat-3'

## Results

To study the mechanisms leading to BRAFi-therapy resistance in malignant melanoma, we employed two cell lines that show an opposite response to the targeted inhibition by Vemurafenib: A375, which are sensitive, and LOX-IMVI, which are resistant (Figure 1a). To address what non-genetic causes may lead to BRAFi-resistance, we determined to what extent Vemurafenib-surviving LOXIMVI cells would develop a senescence-like

response. As such, we stained these cells for senescence markers: p21$^{Cip1}$ as a marker for senescence-associated growth arrest, IL1α as the first protein upregulated during SASP development and FOXO4 as a marker of the senescence-associated damage response and a crucial factor in senescent cell viability [34]. Two days post Vemurafenib treatment, there was a marked increase of FOXO4, p21 and IL-1α in LOX-IMVI cells (Figure 1b).
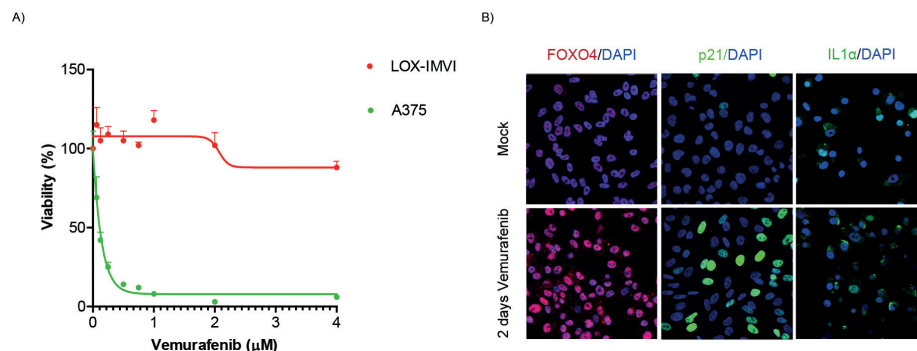


**Figure 1: Vemurafenib induces senescence properties in therapy resistant melanoma cells.**
A) A375 and LOX-IMVI cells were treated with increasing concentrations of Vemurafenib. Cell viability was determined after 6 days by a CellTiter 96 AQueous One Solution cell proliferation assay. B) LOX-IMVI cells were treated with 2μM Vemurafenib 2 days before fixation. Subsequently, an immunofluorescence staining was performed for the indicated proteins.

To determine whether these senescence properties are essential for melanoma survival after treatment, we stably repressed FOXO4 expression through lentiviral shRNAs in both A375 and LOXIMVI cells before Vemurafenib treatment. In A375, FOXO4 knockdown significantly decreased viability when these cells were treated twice with the BRAF inhibitor (Figure 2a). To address what could cause this reduction in viability, we performed a Cytochrome C release assay (Figure 2b). This revealed 70% of FOXO4 depleted A375 cells to be apoptotic after 3 days of Vemurafenib treatment, compared to 30% of control transduced cells. Furthermore, we wondered whether therapy resistant LOX-IMVI cells would exhibit a similar response after FOXO4 knockdown. Indeed, a reduction in cell viability was observed in FOXO4 depleted LOX-IMVI cells as well after Vemurafenib treatment (Figure 2c). In conclusion, FOXO4 repression is not only lethal in senescent cells, but is able to reduce viability of Vemurafenib-surviving melanoma cells as well.
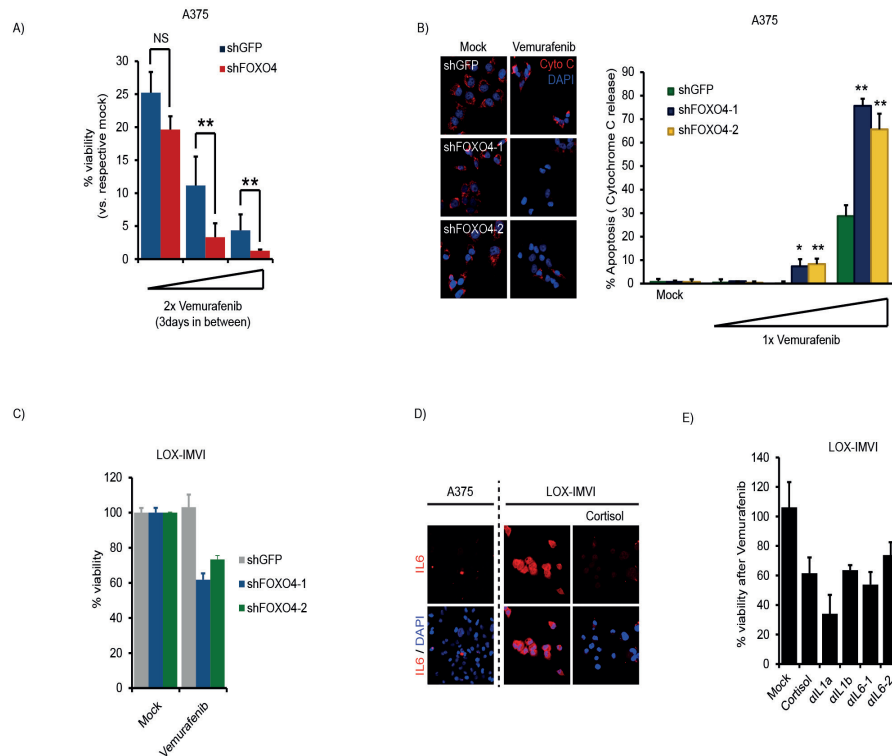
**Figure 2: Melanoma cells show sensitivity to Vemurafenib after inhibition of senescence features.**

A) A375 cells were transduced with short hairpins against FOXO4 or non-targeting control (shGFP) and treated twice with increasing concentrations of Vemurafenib. The viability at day 11 was determined by a CellTiter 96 AQueous One Solution cell proliferation assay. B) A375 cells were treated as in (A) and stained for Cytochrome C. The percentage of Cytochrome C release was quantified using the CellProfiler software. C) LOX-IMVI cells were transduced as above and treated with 2µM Vemurafenib. The viability was measured at day 6. D) A375 and LOX-IMVI cells were treated twice with 50 nM Cortisol 2 and 1 day before fixation and were stained for IL-6. E) LOX-IMVI cells were treated twice with cortisol or IL-1 and IL-6 blocking antibodies. The viability was measured 3 days after.

Since the secretion of pro-inflammatory proteins is a part of the senescence phenotype and we observed a high baseline IL-1α level in LOX-IMVI cells, we wondered whether interleukins are involved in Vemurafenib resistance. To this end, we treated these cells with anti-inflammatory drug cortisol and blocking antibodies against IL-1α, IL-1β and IL6. First, we confirmed that cortisol lowered inflammation in LOX-IMVI cells (Figure 2d). Indeed, IL-6 levels were decidedly reduced by this drug. Untreated A375 cells showed low interleukin levels and therefore, cortisol did not

have an effect in these cells. Next, we compared the viability of Vemurafenib treated LOX-IMVI cells to untreated cells after various interleukin inhibitors. Interestingly, we observed a significant decrease in viability after both treatment with cortisol and the interleukin inhibitors when these were combined with Vemurafenib (Figure 2e). This illustrates that pro-inflammatory proteins indeed are involved in apoptosis resistance in melanoma cells after MAPK-pathway inhibition.

We have previously shown that FOXO4 is crucial for senescent cell viability and described the development of a synthetic D-Retro Inverso peptide named FOXO4-DRI that potently kills senescent cells [34]. FOXO4-DRI mimics the part of FOXO4 that binds to p53 and thereby stably inhibits the interaction between these proteins. This results in the release of active p53 to the cytoplasm and induction of apoptosis. Since we observed senescence features in our melanoma cells and FOXO4 inhibition proved to sensitize treatment resistant cells, we treated Vemurafenib-resistant LOXIMVI melanoma cells with FOXO4-DRI. Indeed, we observed a decrease in viability in LOX-IMVI cells after treatment with both Vemurafenib and FOXO4-DRI (Figure 3a). In addition, the combination of FOXO4-DRI with MEK inhibitor Trametinib induced same effect. To assess whether the reduction in MTT signal is caused by cytotoxic cues, we next performed an xCELLigence real-time density measurement. After FOXO4-DRI administration the cell density sharply declined, indicating that FOXO4-DRI not merely stalls proliferation in melanoma cells, but is effective in their elimination (Figure 3b). Indeed, apoptosis was increased from 18% after Vemurafenib to 87% after the combination treatment, indicating synthetic lethality (Figure 3c).

Following experiments in intrinsically resistant melanoma cells, we generated BRAFi resistant A375 cells, by continuous culture on Vemurafenib for three weeks. Vemurafenib resistance increased every week and after 3 weeks these A375 cells acquired a similar Vemurafenib resistance to intrinsically resistant LOXIMVI cells (Figure 3d). Furthermore, whereas parental A375 cells exhibit sensitivity to FOXO4-DRI, this effect was lost in A375 cells that acquired Vemurafenib resistance (Figure 3e). However, while Vemurafenib and FOXO4-DRI alone failed to reduce viability on their own, their combination proved lethal to chronically resistant A375 or LOXIMVI.
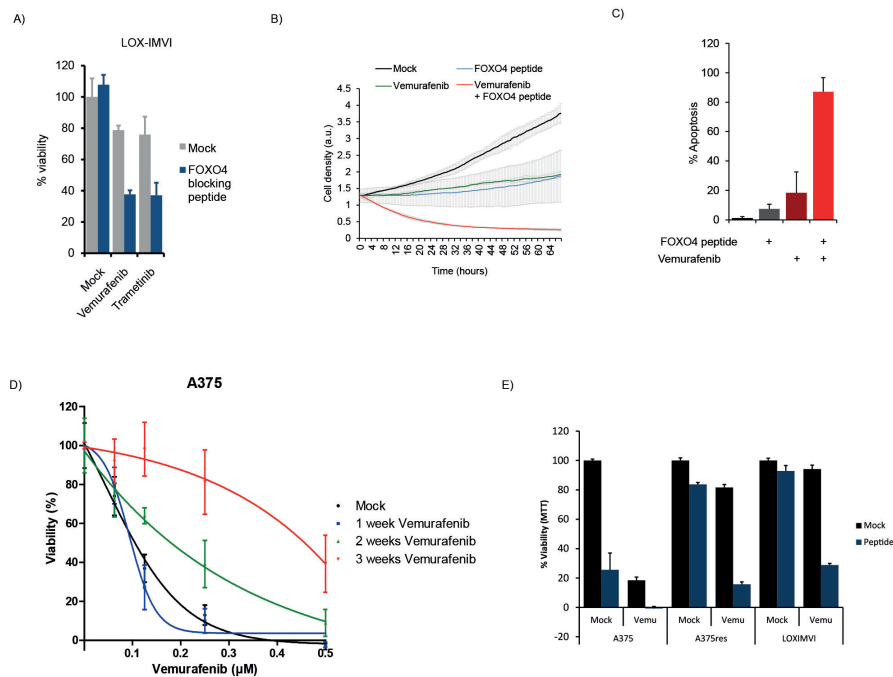
5

**Figure 3: FOXO4-DRI sensitizes resistant melanoma cells to Vemurafenib.**
A) LOX-IMVI cells were treated with 25 µM FOXO4-DRI and either 2µM Vemurafenib or 10 nM Trametinib. The viability of these cells was measured at day 6 by a CellTiter 96 AQueous One Solution cell proliferation assay. B) LOX-IMVI cells were treated as above and real-time cell density was measured using the XCELLigence machine. C) LOX-IMVI cells were treated as above and stained for Cytochrome C after 3 days. The percentage of Cytochrome C release was quantified using the CellProfiler software. D) A375 cells were incubated with Vemurafenib for 1, 2 or 3 weeks and were subsequently treated with increasing concentrations of this drug to assess resistance. Viability was measured 6 days after the second dose of Vemurafenib. E) A375 cells were made resistant by 3 week incubation with Vemurafenib. Subsequently, cell viability was compared to sensitive A375 and LOX-IMVI cells 6 days after treatment with 25 µM FOXO4-DRI and 2µM Vemurafenib.

Although FOXO4-DRI proved to reduce Vemurafenib resistance in melanoma cell lines, the mechanism of apoptosis induction remained unclear. Both melanocytes and melanoma cells have shown to be sensitive to ROS signaling and heavily rely on anti-oxidants [35]. Furthermore, FOXO4 is known to activate transcription of antioxidants [36]. Therefore, we wondered whether ROS could be involved in the mechanism of cell death after Vemurafenib and FOXO4-DRI treatment. First, we stained LOX-IMVI cells for anti-oxidants that are upregulated in response to ROS: Catalase decomposes $H_2O_2$ and JNK can activate FOXO proteins to reduce ROS levels [37, 38]. We observed an upregulation of both these proteins after Vemurafenib and FOXO4-DRI

(Figure 4a). In addition, JNK inhibition showed to induce a decrease in LOX-IMVI viability when combined with Vemurafenib (Figure 4b). Thus, JNK is required for maintaining viability of melanoma cells after Vemurafenib treatment, possibly though an anti-oxidant response. To address the importance of ROS in BRAFi resistance, we incubated our cells with either $H_2O_2$ or anti-oxidant N-Acetyl Cysteine (NAC) (Figure 4c). Whereas FOXO4-DRI did not considerably decrease viability of LOXIMVI cells on its own, this effect was observed upon co-administration with $H_2O_2$. In contrast, the viability-reducing effects of FOXO4-DRI on parental A375 cells was abrogated by NAC. Together, these results indicate that Vemurafenib-surviving cells experience an oxidative stress response, which, in turn, predisposes melanoma cells to FOXO4-DRI.
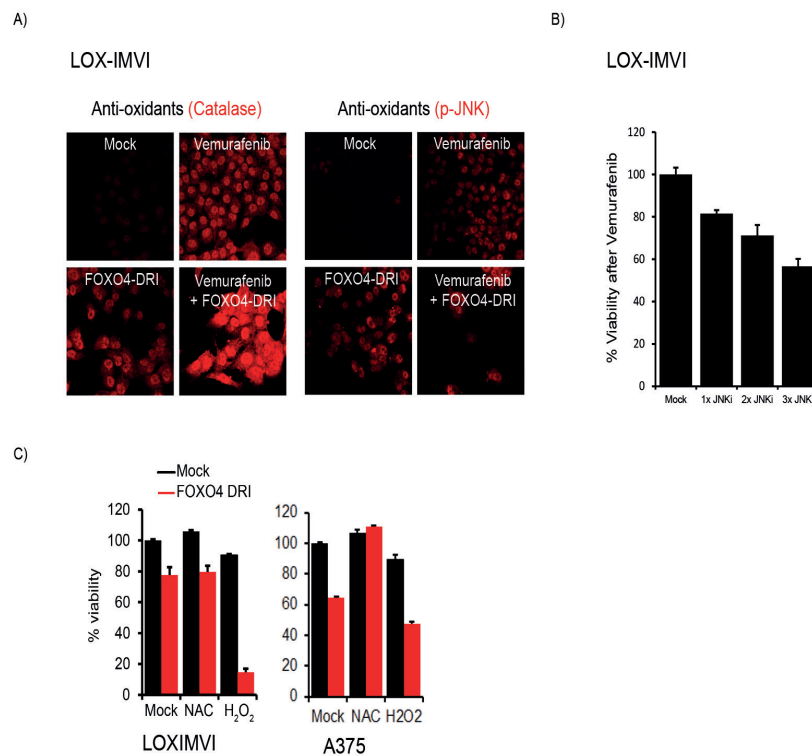


**Figure 4: Oxidative stress predisposes melanoma cells to FOXO4-DRI**
A) Vemurafenib and FOXO4-DRI induce antioxidants in resistant melanoma cells. LOX-IMVI cells were treated with 25 µM FOXO4-DRI and 2µM Vemurafenib 2 days before being stained for Catalase and p-JNK. B) JNK inhibition sensitizes melanoma cells to Vemurafenib. LOX-IMVI cells were treated once with 2µM Vemurafenib and daily with 10nM JNK-IX inhibitor. The first treatment of this inhibitor was added together with Vemurafenib and cell viability was determined after 6 days by a CellTiter 96 AQueous One Solution cell proliferation assay. C) Oxidative stress sensitizes melanoma cells to FOXO4-DRI. A375 and LOX-IMVI cells were treated with 25 µM FOXO4-DRI and either with 4µM NAC or 75µM H2O2. Viability was measured 6 days later.

Since FOXO4 interference enhanced chemosensitivity in melanoma cell lines, we next explored its effect on fresh patient material in culture. We generated melanoma organoids (melanoids) [11] and treated these with Vemurafenib and FOXO4-DRI. Again, we observed a minimal decrease in viability after Vemurafenib, but resistance was reduced in combination with FOXO4-DRI treatment (Figure 5a). In addition, we sliced 300µm sections of stage IV melanoma metastases and cultured these *ex vivo*. We incubated these slices with MAPK pathway inhibitors in combination with either FOXO4-DRI or lentiviral shRNAs against FOXO4. A TUNEL staining revealed the tissue to be resistant to both Vemurafenib and MEK inhibitor Trametinib. However, apoptosis was induced when Trametinib was combined with FOXO4-DRI (Figure 5b). Furthermore, Vemurafenib treatment in combination with reduced FOXO4 expression increased apoptosis with 30% compared to control transduced slices. The same effect was observed when FOXO4 depleted slices were treated with Trametinib. Here, an increase of more than 20% was observed. Hence, as observed for the established cell lines, FOXO4 inhibition strongly synergizes with Vemurafenib to induce apoptosis (Figure 5c). Together, this demonstrates that chemosensitivity in human melanoma tissue can be enhanced by interfering with FOXO4 function.
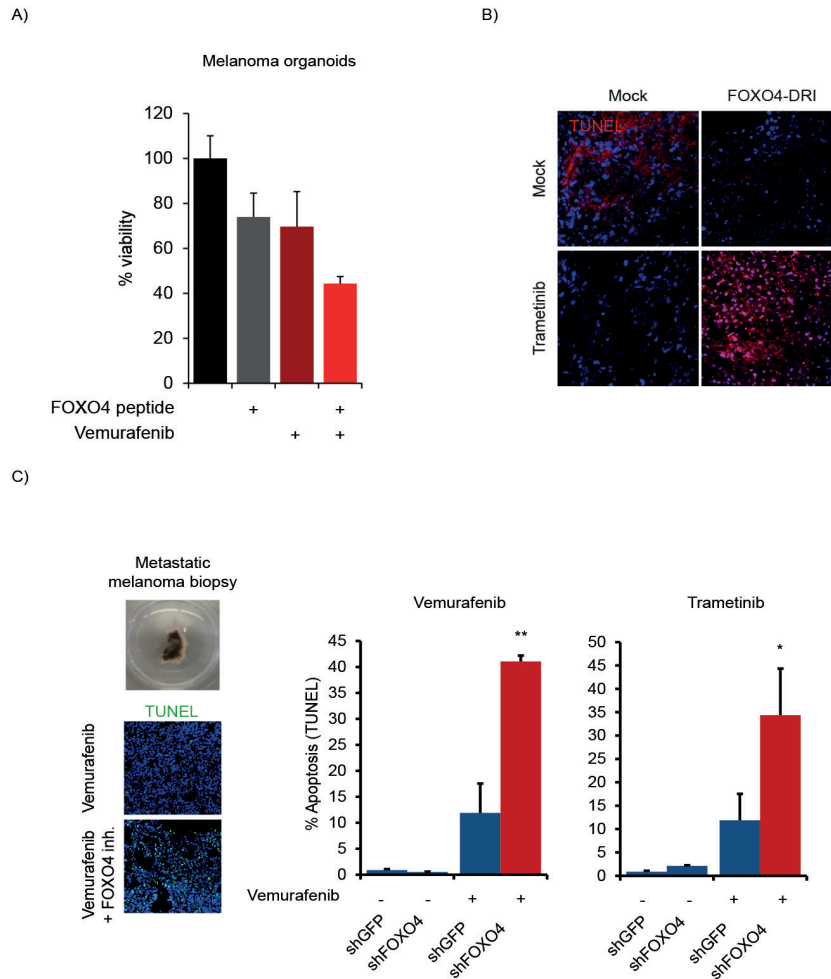
A)

Melanoma organoids



| FOXO4 peptide | | + | | + |
| Vemurafenib | | | + | + |

B)



C)



**Figure 5: FOXO4 interference sensitizes metastatic melanoma tissue to MAPK pathway inhibition.**
A) A stage III melanoma lymph node metastasis was sliced in to 300 μm sections using a Leica vibrating blade microtome and placed into matrigel. Melanoma cells that grew out were passaged and resulting organoids were treated with 12.5 μM FOXO4-DR and 2μM Vemurafenib. Viability was measured by a CellTiter 96 AQueous One Solution cell proliferation assay after 6 days. B) Melanoma slices were obtained as above and cultured in a 6-well plate on a shaker. These sections were treated the same day with 25 μM FOXO4-DRI and 10 nM Trametinib. Apoptosis was determined with a TUNEL assay. C) A stage IV melanoma metastasis was sliced and cultured as above and the obtained sections were transduced with short hairpins against FOXO4 or GFP. The day after, the slices were treated with either 2μM Vemurafenib or 10 nM Trametinib and were processed for a TUNEL assay 3 days later to assess apoptosis. Cell profiler software was used to quantify the percentage of TUNEL positive cells.

## Discussion

Therapy resistance is a complication in the treatment of inoperable cancers. In stage IV melanoma, resistance to MAPK pathway inhibition rapidly develops, reducing long term survival rate. Here, we aimed to investigate the underlying mechanism of BRAFi resistance in melanoma cells. We detected a Vemurafenib induced upregulation of established senescence markers FOXO4, p21 and IL-1α in treatment resistant cells, indicating that resistant cells seem to favor senescence induction over apoptosis. Importantly, all observed senescence properties are linked to therapy resistance. We showed that FOXO4 is crucial in preventing apoptosis after Vemurafenib treatment and that known SASP proteins IL-1 and IL-6 are involved in maintaining viability in resistant melanoma cells as well. Furthermore, IL-1α expression has been linked to therapy resistance in other cancers [39, 40] and it is known that inflammation and interleukin expression promotes plasticity and Vemurafenib resistance in melanoma cells [41-43]. In addition, cell cycle inhibitor p21$^{Cip1}$ is known to have a pro-survival role in cancer cells. For example, P21$^{Cip1}$ promotes survival in colon carcinoma after DNA damage and inhibits apoptosis in melanoma cells [44, 45]. Lastly, other senescence markers have been linked to apoptosis resistance in cancer as well. For example, proliferating oncogene expressing cells have shown to induce senescence markers such as senescence associated heterochromatin foci (SAHF) and to be hereby able to repress apoptosis [46]. In conclusion, it is likely that melanoma cells activate senescence properties to resist apoptosis after therapy.

The observed senescence features after BRAFi are possibly part of a cancer stem-like state. It has been demonstrated that melanoma cells can switch from an epithelial to a mesenchymal state that is associated with stemness, stress resistance and a reduced response to chemotherapy [47-50]. This is characterized in melanoma by a switch from E-cadherin to N-cadherin and MITF downregulation [51, 52]. Furthermore, an altered β-catenin signaling is observed in stem-like melanoma cells [49, 53, 54] and β-catenin knockdown sensitizes melanoma cells to Vemurafenib, indicating the importance of this protein in therapy resistance [55]. This stem-like state of treatment resistant melanoma cells can be linked to senescence, since chemotherapy induced senescence is thought to induce resistant and stem-like cells [56]. For example, these senescent cells have shown to express stemness markers and have a high tumor initiation potential after senescence-escape in b-cell lymphoma [57]. Interestingly, especially the senescence-escaped cancer cells showed high β-catenin signaling. Additionally, treatment surviving breast cancer cells show stemness markers and elevated anti-oxidants after senescence escape [56].

Furthermore, lung cancer cells still show an upregulation of senescence associated genes after senescence escape and these genes were linked to a more stem-like state [58]. Lastly, interruption of FOXO4-p53 binding likely induces the interaction of FOXO4 with β-catenin, which in turn represses stemness signaling [59]. Accordingly, inhibition of senescence markers possibly reduces stemness in melanoma cells and induces a more drug sensitive state.

We showed that therapy resistance in melanoma cells can be targeted with anti-senescence drug FOXO4-DRI. However, it remains unclear how FOXO4-p53 interference targets resistance in melanoma. FOXO4-DRI can eliminate senescent cells by causing active p53 to translocate from the nucleus to the cytoplasm. It remains to be determined whether the same apoptosis mechanism is induced in Vemurafenib treated cells as well, although p53 indeed appears to be required for FOXO4-DRI to be effective and p53 is only infrequently mutated in melanoma cells [60]. In addition to p53 function, we have shown oxidative stress to be crucial for the pro-apoptotic effect of FOXO4-DRI in Vemurafenib resistant melanoma cells. Vemurafenib is known to induce ROS production and it was demonstrated that this is involved in the induction of apoptosis in melanoma cells [61, 62]. However, melanoma cells also upregulate anti-oxidants such as Catalase as a reaction to increased ROS levels after Vemurafenib to prevent apoptosis [61]. These antioxidants not only protect healthy cells from oncogenesis, but also maintain homeostasis in cancer cells [63-65]. For example, it was shown that JNK signaling can have a pro-survival effect in cancer cells [66-68]. In addition, it was demonstrated that RAF and JNK inhibitors synergize in melanoma cell killing [69]. Notably, a JNK inhibiting DRI peptide has been tested in a clinical trial [70, 71] and effects of this peptide on Vemurafenib resistance in melanoma cells could be evaluated. Furthermore, increasing ROS levels by pro-oxidant treatment was shown to sensitize melanoma cells to Vemurafenib treatment [61, 62] and increasing ROS in melanoma cells is seen as a potential option to sensitize melanoma cells for apoptosis [72, 73]. Together, this highlights the crucial role of ROS and antioxidants in Vemurafenib resistance. Likely, the combination of FOXO4-DRI and Vemurafenib produces enough oxidative stress to induce apoptosis in resistant melanoma cells.

Reducing Vemurafenib resistance could expand the number of patients benefiting from this treatment and prolong progression free survival. We showed here that we can target both intrinsic and acquired resistance with FOXO4-DRI *in vitro,* highlighting the promise of targeting senescence features in malignant melanoma cells. Furthermore, FOXO4-DRI could have beneficial effects on resistance to other treatments as well. For example, 42% of melanoma patients does not respond to immune check point inhibitors and resistance is acquired as well [74, 75]. Interestingly,

it was shown that melanoma cells expressing high levels of β-catenin are resistant to immune clearance [76, 77]. Therefore, it can be determined whether FOXO4-DRI targets these stem-like β-catenin expressing cells. In addition, various cancers show therapy-induced senescence features that contribute to treatment resistance. Therefore, FOXO4-DRI could potentially target therapy resistance in multiple cancer types. Future research will be aimed at characterizing hallmarks in cancer cells that predict susceptibility to FOXO4-DRI treatment, including FOXO4 foci, p53 status, stemness markers and interleukin expression. Furthermore, the efficacy of FOXO4-DRI will be evaluated in *in vivo* cancer models.

## References

1.  Cancer Research UK. *http://www.cancerresearchuk.org/health-professional/cancer-statistics/statistics-by-cancer-type/skin-cancer/mortality#heading-Five*. 2012.

2.  Baiter, M., et al., *Pathogenetic Implications of BRAF Mutation Distribution in Stage IV Melanoma Patients.* Dermatology, 2015. **231**(2): p. 127-33.

3.  Boespflug, A., et al., *Treatment of NRAS-mutated advanced or metastatic melanoma: rationale, current trials and evidence to date.* Ther Adv Med Oncol, 2017. **9**(7): p. 481-492.

4.  Serrano, M., et al., *Oncogenic ras provokes premature cell senescence associated with accumulation of p53 and p16INK4a.* Cell, 1997. **88**(5): p. 593-602.

5.  de Keizer, P.L., et al., *Activation of forkhead box O transcription factors by oncogenic BRAF promotes p21cip1-dependent senescence.* Cancer Res, 2010. **70**(21): p. 8526-36.

6.  Dhomen, N., et al., *Oncogenic Braf induces melanocyte senescence and melanoma in mice.* Cancer Cell, 2009. **15**(4): p. 294-303.

7.  Leikam, C., et al., *Oncogene activation in melanocytes links reactive oxygen to multinucleated phenotype and senescence.* Oncogene, 2008. **27**(56): p. 7070-82.

8.  Ogrunc, M., et al., *Oncogene-induced reactive oxygen species fuel hyperproliferation and DNA damage response activation.* Cell Death Differ, 2014. **21**(6): p. 998-1012.

9.  Di Micco, R., et al., *Oncogene-induced senescence is a DNA damage response triggered by DNA hyper-replication.* Nature, 2006. **444**(7119): p. 638-42.

10. Passos, J.F., et al., *Feedback between p21 and reactive oxygen production is necessary for cell senescence.* Mol Syst Biol, 2010. **6**: p. 347.

11. Kruiswijk, F., et al., *Targeted inhibition of metastatic melanoma through interference with Pin1-FOXM1 signaling.* Oncogene, 2016. **35**(17): p. 2166-77.

12. Pollock, P.M., et al., *High frequency of BRAF mutations in nevi.* Nat Genet, 2003. **33**(1): p. 19-20.

13. Bauer, J., et al., *Congenital melanocytic nevi frequently harbor NRAS mutations but no BRAF mutations.* J Invest Dermatol, 2007. **127**(1): p. 179-82.

14. Charbel, C., et al., *NRAS mutation is the sole recurrent somatic mutation in large congenital melanocytic nevi.* J Invest Dermatol, 2014. **134**(4): p. 1067-1074.

15. Rodier, F., et al., *DNA-SCARS: distinct nuclear structures that sustain damage-induced senescence growth arrest and inflammatory cytokine secretion.* J Cell Sci, 2011. **124**(Pt 1): p. 68-81.

16. Coppe, J.P., et al., *Senescence-associated secretory phenotypes reveal cell-nonautonomous functions of oncogenic RAS and the p53 tumor suppressor.* PLoS Biol, 2008. **6**(12): p. 2853-68.

5

17. Stefanaki, C., et al., *G1 cell cycle regulators in congenital melanocytic nevi. Comparison with acquired nevi and melanomas.* J Cutan Pathol, 2008. **35**(9): p. 799-808.

18. Wasco, M.J., et al., *Expression of gamma-H2AX in melanocytic lesions.* Hum Pathol, 2008. **39**(11): p. 1614-20.

19. Michaloglou, C., et al., *BRAFE600-associated senescence-like cell cycle arrest of human naevi.* Nature, 2005. **436**(7051): p. 720-4.

20. Liu, W. and N.E. Sharpless, *Senescence-escape in melanoma.* Pigment Cell Melanoma Res, 2012. **25**(4): p. 408-9.

21. Society, A.C. *https://www.cancer.org/content/dam/cancer-org/research/cancer-facts-and-statistics/annual-cancer-facts-and-figures/2018/cancer-facts-and-figures-2018.pdf.* 2018.

22. Chapman, P.B., et al., *Improved survival with vemurafenib in melanoma with BRAF V600E mutation.* N Engl J Med, 2011. **364**(26): p. 2507-16.

23. McArthur, G.A., et al., *Safety and efficacy of vemurafenib in BRAF(V600E) and BRAF(V600K) mutation-positive melanoma (BRIM-3): extended follow-up of a phase 3, randomised, open-label study.* Lancet Oncol, 2014. **15**(3): p. 323-32.

24. Welsh, S.J., et al., *Resistance to combination BRAF and MEK inhibition in metastatic melanoma: Where to next?* Eur J Cancer, 2016. **62**: p. 76-85.

25. Pisco, A.O. and S. Huang, *Non-genetic cancer cell plasticity and therapy-induced stemness in tumour relapse: 'What does not kill me strengthens me'.* Br J Cancer, 2015. **112**(11): p. 1725-32.

26. Roesch, A., et al., *Overcoming intrinsic multidrug resistance in melanoma by blocking the mitochondrial respiratory chain of slow-cycling JARID1B(high) cells.* Cancer Cell, 2013. **23**(6): p. 811-25.

27. Redmer, T., et al., *The role of the cancer stem cell marker CD271 in DNA damage response and drug resistance of melanoma cells.* Oncogenesis, 2017. **6**(1): p. e291.

28. Luo, Y., et al., *Side population cells from human melanoma tumors reveal diverse mechanisms for chemoresistance.* J Invest Dermatol, 2012. **132**(10): p. 2440-2450.

29. Zubrilov, I., et al., *Vemurafenib resistance selects for highly malignant brain and lung-metastasizing melanoma cells.* Cancer Lett, 2015. **361**(1): p. 86-96.

30. Ohanna, M., et al., *Senescent cells develop a PARP-1 and nuclear factor-{kappa}B-associated secretome (PNAS).* Genes Dev, 2011. **25**(12): p. 1245-61.

31. Ohanna, M., et al., *Secretome from senescent melanoma engages the STAT3 pathway to favor reprogramming of naive melanoma towards a tumor-initiating cell phenotype.* Oncotarget, 2013. **4**(12): p. 2212-24.

32. Haferkamp, S., et al., *Vemurafenib induces senescence features in melanoma cells.* J Invest Dermatol, 2013. **133**(6): p. 1601-9.

33.   Wang, E., *Senescent human fibroblasts resist programmed cell death, and failure to suppress bcl2 is involved.* Cancer Res, 1995. **55**(11): p. 2284-92.

34.   Baar, M.P., et al., *Targeted Apoptosis of Senescent Cells Restores Tissue Homeostasis in Response to Chemotoxicity and Aging.* Cell, 2017. **169**(1): p. 132-147 e16.

35.   Meierjohann, S., *Oxidative stress in melanocyte senescence and melanoma transformation.* Eur J Cell Biol, 2014. **93**(1-2): p. 36-41.

36.   Szypowska, A.A., et al., *Oxidative stress-dependent regulation of Forkhead box O4 activity by nemo-like kinase.* Antioxid Redox Signal, 2011. **14**(4): p. 563-78.

37.   Adams, D.H. and F.J. Roe, *The action of some chemical substances on mouse liver catalase activity in vivo.* Br J Cancer, 1953. **7**(4): p. 509-18.

38.   Essers, M.A., et al., *FOXO transcription factor activation by oxidative stress mediated by the small GTPase Ral and JNK.* EMBO J, 2004. **23**(24): p. 4802-12.

39.   Jain, A., S. Kaczanowska, and E. Davila, *IL-1 Receptor-Associated Kinase Signaling and Its Role in Inflammation, Cancer Progression, and Therapy Resistance.* Front Immunol, 2014. **5**: p. 553.

40.   Stender, J.D., et al., *Structural and Molecular Mechanisms of Cytokine-Mediated Endocrine Resistance in Human Breast Cancer Cells.* Mol Cell, 2017. **65**(6): p. 1122-1135 e5.

41.   Holzel, M. and T. Tuting, *Inflammation-Induced Plasticity in Melanoma Therapy and Metastasis.* Trends Immunol, 2016. **37**(6): p. 364-74.

42.   Sos, M.L., et al., *Oncogene mimicry as a mechanism of primary resistance to BRAF inhibitors.* Cell Rep, 2014. **8**(4): p. 1037-48.

43.   Noguchi, K., et al., *Interleukin-like EMT inducer regulates partial phenotype switching in MITF-low melanoma cell lines.* PLoS One, 2017. **12**(5): p. e0177830.

44.   Bunz, F., et al., *Requirement for p53 and p21 to sustain G2 arrest after DNA damage.* Science, 1998. **282**(5393): p. 1497-501.

45.   Gorospe, M., et al., *p21(Waf1/Cip1) protects against p53-mediated apoptosis of human melanoma cells.* Oncogene, 1997. **14**(8): p. 929-35.

46.   Di Micco, R., et al., *Interplay between oncogene-induced DNA damage response and heterochromatin in senescence and cancer.* Nat Cell Biol, 2011. **13**(3): p. 292-302.

47.   Hoek, K.S. and C.R. Goding, *Cancer stem cells versus phenotype-switching in melanoma.* Pigment Cell Melanoma Res, 2010. **23**(6): p. 746-59.

48.   Sharma, S.V., et al., *A chromatin-mediated reversible drug-tolerant state in cancer cell subpopulations.* Cell, 2010. **141**(1): p. 69-80.

49.   Ramsdale, R., et al., *The transcription cofactor c-JUN mediates phenotype switching and BRAF inhibitor resistance in melanoma.* Sci Signal, 2015. **8**(390): p. ra82.

5

50. Vazquez, F., et al., *PGC1alpha expression defines a subset of human melanoma tumors with increased mitochondrial capacity and resistance to oxidative stress.* Cancer Cell, 2013. **23**(3): p. 287-301.

51. Lade-Keller, J., et al., *E- to N-cadherin switch in melanoma is associated with decreased expression of phosphatase and tensin homolog and cancer progression.* Br J Dermatol, 2013. **169**(3): p. 618-28.

52. Carreira, S., et al., *Mitf regulation of Dia1 controls melanoma proliferation and invasiveness.* Genes Dev, 2006. **20**(24): p. 3426-39.

53. Eichhoff, O.M., et al., *Differential LEF1 and TCF4 expression is involved in melanoma cell phenotype switching.* Pigment Cell Melanoma Res, 2011. **24**(4): p. 631-42.

54. Webster, M.R., C.H. Kugel, 3rd, and A.T. Weeraratna, *The Wnts of change: How Wnts regulate phenotype switching in melanoma.* Biochim Biophys Acta, 2015. **1856**(2): p. 244-51.

55. Sinnberg, T., et al., *A Nexus Consisting of Beta-Catenin and Stat3 Attenuates BRAF Inhibitor Efficacy and Mediates Acquired Resistance to Vemurafenib.* EBioMedicine, 2016. **8**: p. 132-149.

56. Achuthan, S., et al., *Drug-induced senescence generates chemoresistant stemlike cells with low reactive oxygen species.* J Biol Chem, 2011. **286**(43): p. 37813-29.

57. Milanovic, M., et al., *Senescence-associated reprogramming promotes cancer stemness.* Nature, 2018. **553**(7686): p. 96-100.

58. Yang, L., J. Fang, and J. Chen, *Tumor cell senescence response produces aggressive variants.* Cell Death Discov, 2017. **3**: p. 17049.

59. de Keizer, P.L., *The Fountain of Youth by Targeting Senescent Cells?* Trends Mol Med, 2017. **23**(1): p. 6-17.

60. Yamashita, T., et al., *Induction of apoptosis in melanoma cell lines by p53 and its related proteins.* J Invest Dermatol, 2001. **117**(4): p. 914-9.

61. Corazao-Rozas, P., et al., *Mitochondrial oxidative stress is the Achille's heel of melanoma cells resistant to Braf-mutant inhibitor.* Oncotarget, 2013. **4**(11): p. 1986-98.

62. Bauer, D., et al., *Critical role of reactive oxygen species (ROS) for synergistic enhancement of apoptosis by vemurafenib and the potassium channel inhibitor TRAM-34 in melanoma cells.* Cell Death Dis, 2017. **8**(2): p. e2594.

63. Ciccarese, F. and V. Ciminale, *Escaping Death: Mitochondrial Redox Homeostasis in Cancer Cells.* Front Oncol, 2017. **7**: p. 117.

64. Marengo, B., et al., *Redox Homeostasis and Cellular Antioxidant Systems: Crucial Players in Cancer Growth and Therapy.* Oxid Med Cell Longev, 2016. **2016**: p. 6235641.

65. Hornsveld, M., et al., *FOXO transcription factors both suppress and support breast cancer progression.* Cancer Res, 2018.

66. Wang, Y., et al., *MALT1 promotes melanoma progression through JNK/c-Jun signaling.* Oncogenesis, 2017. **6**(7): p. e365.

67. Gururajan, M., et al., *c-Jun N-terminal kinase (JNK) is required for survival and proliferation of B-lymphoma cells.* Blood, 2005. **106**(4): p. 1382-91.

68. Svensson, C., et al., *Pro-survival effects of JNK and p38 MAPK pathways in LPS-induced activation of BV-2 cells.* Biochem Biophys Res Commun, 2011. **406**(3): p. 488-92.

69. Fallahi-Sichani, M., et al., *Systematic analysis of BRAF(V600E) melanomas reveals a role for JNK/c-Jun pathway in adaptive resistance to drug-induced apoptosis.* Mol Syst Biol, 2015. **11**(3): p. 797.

70. Ngoei, K.R., et al., *A novel retro-inverso peptide is a preferential JNK substrate-competitive inhibitor.* Int J Biochem Cell Biol, 2013. **45**(8): p. 1939-50.

71. Suckfuell, M., et al., *Efficacy and safety of AM-111 in the treatment of acute sensorineural hearing loss: a double-blind, randomized, placebo-controlled phase II study.* Otol Neurotol, 2014. **35**(8): p. 1317-26.

72. Liu-Smith, F., R. Dellinger, and F.L. Meyskens, Jr., *Updates of reactive oxygen species in melanoma etiology and progression.* Arch Biochem Biophys, 2014. **563**: p. 51-5.

73. Raj, L., et al., *Selective killing of cancer cells by a small molecule targeting the stress response to ROS.* Nature, 2011. **475**(7355): p. 231-4.

74. Xu-Monette, Z.Y., et al., *PD-1/PD-L1 Blockade: Have We Found the Key to Unleash the Antitumor Immune Response?* Front Immunol, 2017. **8**: p. 1597.

75. Espinosa, E., et al., *Predictive factors of response to immunotherapy-a review from the Spanish Melanoma Group (GEM).* Ann Transl Med, 2017. **5**(19): p. 389.

76. Spranger, S., R. Bao, and T.F. Gajewski, *Melanoma-intrinsic beta-catenin signalling prevents anti-tumour immunity.* Nature, 2015. **523**(7559): p. 231-5.

77. Spranger, S. and T.F. Gajewski, *A new paradigm for tumor immune escape: beta-catenin-driven immune exclusion.* J Immunother Cancer, 2015. **3**: p. 43.

5

# CHAPTER 6

## MicroRNA-30 constitutively sets the p53 threshold by repressing its expression to prevent cellular aging phenotypes

**Marjolein P. Baar[1,3], Glenn de Jong[1], Serena T. Bruens[1], Renata M.C. Brandt[1], Sander Barnhoorn[1], Jan H.J. Hoeijmakers[1,2,4], Peter L.J. de Keizer[1,3], Joris Pothof[1]**

[1]Department of Molecular Genetics, Erasmus Medical Center, Rotterdam.

[2]Princess Máxima Centre for Pediatric Oncology, ONCODE Institute, Heidelberglaan 25, 3584, CS, Utrecht, PO Box 113, 3720 AC Bilthoven, the Netherlands

[3]Center for Molecular Medicine, Department of Biomedical Genetics, University Medical Center Utrecht, Utrecht University

[4]CECAD, Forschungszentrum, Universität zu Köln, Joseph-Stelzmann-Straße 26, 50931 Köln, Germany

## Abstract

Time-dependent accumulation of DNA damage and consequent deterioration of key cellular processes contributes to cellular aging. When DNA damage is irreparable, either apoptosis or senescence can be induced depending on the type of damage, cell type, cell cycle stage, or tissue microenvironment. Interestingly, while pro-apoptotic stimuli increase during aging, a desensitization to DNA damage occurs in multiple organs. Recently, we have described a new age-related cellular phenotype termed 'cell preservation' that is characterized by the induction of a DNA damage dependent miRNA signature during aging that actively represses apoptosis. Thereby, it likely prevents excessive age-related tissue damage. However, it remains unknown how this cell preservation signature is regulated, what the specific miRNA targets are, and what the effect of interference with this signature is *in vivo.* We show here that miR-30 is a typical cell preservation miRNA and that this miRNA is induced in human fibroblasts by transcription-blocking DNA lesions in an ATM-dependent manner. Furthermore, miR-30 inhibition enhanced p53 expression in these fibroblasts and increased apoptosis after UV-radiation in a p53-dependent manner. In addition, miR-30 not only increased UV sensitivity but activated other p53-dependent pathways as well, including DNA repair and senescence induction after ionizing radiation. Lastly, preliminary *in vivo* experiments showed inhibition of miR-30 to induce weight loss in mice and to provoke organ damage. In conclusion, miR-30 prevents both apoptosis and senescence through p53 inhibition and thereby possibly protects from accelerated aging.

## Introduction

Aging is a time-dependent decline in normal physiology and a decreased ability to deal with stress [1]. Many theories exist on what processes contribute to cellular aging. It is either believed to be a programmed process that purposely limits life-span, or a random inevitable process due the loss of selection pressure with age [2, 3]. Overall, the general consensus is that irreparable cellular damage accumulates during aging due to both a great variety of damaging agents and inefficient repair processes. For example, the DNA is continuously damaged by a multitude of stressors, including environmental chemicals, radiation or UV light [4] and endogenous (by-)products of normal metabolism such as free radicals [5]. DNA damage is causally linked to aging since defects in DNA repair genes lead to accelerated aging syndromes e.g. Trichothiodystrophy and Cockayne syndrome [4].

Foremost, a cell attempts to repair cellular damage. However, although DNA repair processes are highly effective, they are not perfect. Therefore, some damage will fail to be repaired and over time irreparable DNA lesions or mutations will accumulate [4]. When cells are too severely damaged, pathways can be activated to prevent the preservation and proliferation of potentially deleterious cells. Specifically, apoptosis permanently removes damaged cells, while senescence induction ensures a permanent cell cycle arrest of damaged or stressed cells [6, 7]. The decision whether apoptosis or senescence is induced after DNA damage is made by the DNA damage response (DDR). The DDR detects DNA lesions and decides on the most appropriate response to this damage under the given circumstances [8]. To accomplish this, the DDR consists of a tightly regulated network of DNA damage detecting proteins, signaling kinases and downstream effector proteins. Damage detection proteins primarily trigger relatively fast responses regulated through post-translational modifications. For example, ataxia telangiectasia mutated kinase (ATM) and ATM and Rad-3-related protein (ATR) are activated after DNA damage and in turn directly or indirectly phosphorylate downstream effectors such as p53 to induce DNA repair, apoptosis or senescence [9].

In addition to post-translational modifications, gene expression changes are required for an efficient DNA damage response [10]. This can be achieved by transcriptional regulation, but also more rapidly through post-transcriptional regulation by microRNAs (miRNAs). MiRNAs are short non-coding RNAs of approximately 20 nucleotides that bind to the 3' untranslated region (3'UTR) of mRNAs, inhibiting their translation and often inducing their degradation [11]. A single miRNA is able to regulate the expression of several mRNAs simultaneously since the mRNA-

6

binding sequence is relatively short and non-canonical binding often occurs [12-14]. Accordingly, microRNAs regulate the expression of a myriad of DDR genes [15].

The age-related accumulation of irreparable DNA damage leads to an increase in apoptosis and an accumulation of senescent cells during aging. These cell fates threaten tissue function and contribute to age-related frailty and disease. For example, an excessive amount of apoptotic cells reduces cell number and leads to a functional decline, leading to age-related organ atrophy, overall frailty or e.g. memory loss [16-18]. Alternatively, senescent cells are apoptosis resistant and accumulate during aging due to an increase in damage as well as a decline in immune clearance [19-21]. Senescent cells are therefore chronically present in aged tissue and thereby reduce the number of cells able to regenerate these tissues. Furthermore, senescent cells secrete growth factors, proteases and pro-inflammatory cytokines that are harmful when chronically expressed [7, 22, 23] and this senescence-associated secretory phenotype (SASP) has been linked to a multitude of age-related pathologies [24-27]. The detrimental effect of senescence during aging has been illustrated by studies that show removal of senescent cells to significantly improve organ function and reduce frailty in aged mice [28, 29]. Additionally, the stem cell regenerative potential decreases with age and therefore damaged cells are less likely to be replaced [30-34]. In conclusion, damaged and cancer-prone cells can be debilitated by the induction of apoptosis or senescence, but conversely aging and age-related diseases are promoted.          Although  the amount of apoptotic cells increases with age in some organs, a considerable number of cell types have shown to be unusually apoptosis resistant with age [35-38]. For example, aged mice exposed to 5Gy ionizing radiation show a reduced activation of p53 and apoptosis in the spleen compared to young mice [36]. In addition, we found that pro-apoptotic proteins are downregulated in aged mouse liver, kidney, heart and lung when averaged over the entire organ (unpublished data, MB, JH, and JP). In these organs a specific subset of DNA damage dependent miRNAs is upregulated that actively repress apoptosis *in vitro*. We hypothesized that this miRNA signature functions as a protection mechanism against apoptosis in aged and damaged cells and we have termed this new cellular aging phenotype 'cell preservation', an active maintenance of viability in the presence of pro-apoptotic signals.

The cell preservation miRNA signature has so far only been studied *in vitro* and several questions remain unanswered. First, it is unknown how the cell preservation miRNA signature is regulated after DNA damage. Secondly, it is clear that the cell preservation response inhibits apoptosis, but not what pathways and targets the miRNAs specifically act on and how this affects other cellular processes. Lastly, it remains unclear whether the cell preservation response is beneficial or detrimental

during organismal aging. On the one hand, these miRNAs potentially postpone apoptosis *in vivo* and thereby preserve tissue integrity during aging. On the other hand, cells that upregulate these microRNAs exhibit altered intracellular signaling due to the presence of persistent DNA damage signals. Here, we aim to answer these questions by investigating miR-30, an individual miRNA of the cell preservation response.

## Methods

### Antibodies

The following antibodies were used: ATM (2873S), PUMA (4976), Bax (2772S) from Cell Signaling, P21$^{cip1}$ (610234) antibody from BD Transduction Laboratories, Il-6 (ab6672), HMGB1 (ab18256) and Histone H3 (ab8580) from Abcam and p53 (sc-126) from Santa Cruz. The secondary antibodies used were: Goat-anti-rabbit conjugated to HRP (P0448) and rabbit-anti-mouse conjugated to HRP (P0161) from Dako and Alexa Fluor donkey anti-rabbit 488 from Invitrogen.

### Cell culture and transfection

IMR90, NIH3T3 and U2OS cells were cultured in Dulbecco's Modified Eagle Medium (DMEM) with 10% FCS and 1% pen/strep. IMR90 cells and mouse derived fibroblasts (MDFs) were kept at 3% O2, while NIH3T3 and U2OS cells were cultured at ambient oxygen. All cells were kept at 37°C and 5% CO2. Cells were seeded in a 6-well plate and transfected the following day. Lipofectamine RNAiMAX (Invitrogen) was used for the transfection of miR30-family power inhibitor (460026, Exiqon) and the control inhibitor (199006-101, Exiqon) as well as siRNAs against DGCR8 (GE healthcare) and KHSRP (Dharmacon). The day after transfection, cells were split into 6 cm dishes and damaged the day after. Where applicable, 10µM ATM (KU-55933, SelleckChem) or 10µM ATR inhibitor (VE-821, SelleckChem) was added 45 minutes before UV radiation. Cells were radiated with 10 J/m2 UV-C using a 254 nm germicidal lamp (Philips) and 10 Gy IR was given by exposing cells to X-rays. Cisplatin (sigma) was added to the medium to a final concentration of 20µM.

### Quantitative real-time PCR

At indicated time points, 6 cm plates were washed with ice-cold PBS and scraped in 1ml TRI reagent (Qiagen) on ice. 200 mL chloroform per 1 ml TRI reagent was added to the samples in a 1.5 ml Eppendorf tube. The samples were shaken for 15 seconds, incubated for 5 minutes at room temperature and then centrifuged at 12000 g for 15 minutes at 4 °C. Subsequently, the upper aqueous layer was transferred to

6

a fresh Eppendorf tube to which 500 mL isopropanol was added. The samples were centrifuged again at 12000g for 15 minutes at 4 °C after 15 seconds of shaking and 10 minutes of incubation at room temperature. After centrifugation, the supernatant was removed and the pellet was washed in 1 ml of 75% ethanol before another centrifugation step at 12000g for 15 minutes at 4 °C. The supernatant was removed again and the pellet was air dried for 15 minutes. The pellet was resuspended in 30 mL RNAse free $H_2O$ and the RNA concentration was measured using the Nanodrop. The miScript II RT Kit (Qiagen) was used to convert total RNA into cDNA according to manufacturer's instruction. Subsequently, the cDNA was diluted 10 times in $H_2O$ and mixed with primers and SYBR Green Master Mix (Bio-Rad) to perform a qPCR. For this reaction, qPCR plates and the CFX96 Touchä Real-Time PCR Detection System were used from Bio-Rad. Relative gene expression was calculated using the DD Cq method.

Primers used in our experiments:
miR-30a: Fwd: gcagtgtaaacatcctcgac, Rev: tccagttttttttttttttttcttcca
miR-30b: Fwd: gcagtgtaaacatcctacactc, Rev:gtccagtttttttttttttttttagc
miR-30c: Fwd: cagtgtaaacatcctacactc, Rev: gtccagtttttttttttttttttagc or tccagttttttttttttttttttcttcca
miR-30d: Fwd: agtgtaaacatccccgact, Rev: tccagttttttttttttttttcttcca
miR-30e: Fwd: cgcagtgtaaacatccttgac, Rev: tccagtttttttttttttttttcttcca
hRPL21: Fwd: ccttgcgtgtggagagagaat, Rev: ggcttctactcgaacaagatcct
hGapdh: Fwd: aaggtgaaggtcggagtcaa, Rev: accatgtagttgaggtcaatg
hTubulin: Fwd: cttcgtctccgccatcag, Rev: ttgccaatctggacacca

**Microarray analysis**

RNA was isolated from organs of 13 and 104 week old C57BL/6J mice that did not show signs of age-related pathology. The LNA-based capture probeset (Exiqon) was spotted on Nexterion E slides using a Virtek Chipwriter Pro. Total RNA was labelled (Cy3 only) using the ULS aRNA labelling kit (Kreatech) before the RNA was hybridized overnight in a Tecan HS4800 pro hybridization station at 60°C. The slides were scanned in a Tecan LS Reloaded scanner and data was extracted using Imagene software. Subsequently, heatmaps were generated using TM4 microarray software suite.

**Immunoblotting**

Cells were washed with ice-cold PBS and scraped on ice in laemni sample buffer at indicated time points. Sample proteins and Precision Plus Protein All Blue Standards (BioRad) were then loaded onto 4-12% Bis-Tris Plus Gels (15 wells,

Invitrogen) and were run at 150V for ~1 hr. Subsequently, proteins were transferred at 4°C to an Immobilon-FL PVDF membrane (Merck Millipore) for 1.15h at 350 mA. Prior to transferring, the membrane was activated with methanol (Sigma-Aldrich). Blocking of the membrane was done for 1h at room temperature using 5% bovine serum albumin (BSA, Sigma-Aldrich) in Tris-buffered saline (TBS, Sigma-Aldrich) before the membrane was incubated overnight at 4°C in TBS containing antibodies against the indicated proteins. The next day, the membrane was washed with TBS containing 0.1% TWEEN20 (Sigma-Aldrich) three times for 15 minutes and incubated with secondary antibodies in TBS for 1h at RT. Subsequently, the membrane was washed again with TBS-TWEEN three times before the chemiluminescent signal of the membrane was measured using the Western Lightning Chemiluminescence plus reagent (PerkinElmer) and imaged using the LAS 4000 Mini system (ImageQuant).

**FACS analysis**

Cells were pulse labeled for 15 minutes with the nucleotide analogue bromodeoxyuridine (BrdU, 5 µM, Sigma-Aldrich) to enable the detection of S-phase cells. Subsequently, the cells were fixed with 100% ethanol (VWR Chemicals) and stored overnight at 4°C. The following day, the cells were re-suspended with 0,05% pepsin (Sigma-Aldrich) in 0,1N HCl (Sigma-Aldrich) for 20 min at RT and washed with PBS containing 0,1% BSA and 0.5% TWEEN (PBS-TB). To isolate nuclei, cell pellets were incubated with 2N HCl for 12 min at 37°C and subsequently neutralized with Borate buffer (pH 8.5) at 4°C (Sigma-Aldrich). The nuclei were then washed with PBS-TB and incubated in the dark for 1h at 4°C with αBrdU FITC-conjugated antibody (BD Pharmingen) in PBS-TB (1:50) to stain for S-phase cells. After another PBS-TB wash, the nuclei were stained with propidium iodine (2 µg/mL, Life Technologies) in PBS with RNAse A (0,25 mg/mL) to distinguish G1 and G2 cells. The next day, the nuclei were analyzed by flow cytometry using the BD LSRFortessa system (BD Biosciences).

**Apoptosis staining**

MDFs were grown on 13mm coverslips in a 24 well plate and transfected 2 days before UV radiation. The coverslips were washed with ice-cold Tris Buffered Saline (TBS) 36 hours after 10J UV radiation and fixed in 4% formalin for 30 minutes on ice. Subsequently, the cells were washed twice with TBS and permeabilized in a fresh solution of 0.1% sodium citrate in 0.1% TX-100 for 2 minutes on ice. DNA fragments were then labeled with 10% TUNEL enzyme in labeling solution (Roche) for 45 minutes at 37°C. After 2 TBS washes, the coverslips were washed briefly in H2O and mounted with soft set mounting medium with DAPI (Vectashield). A LSM700 Zeiss

6

Microscope was used to obtain images and the CellProfiler software was used to quantify the amount of apoptotic cells.

### Immunofluorescence

Cells were split one day after transfection and grown on 13mm coverslips in a 24 well plate. At indicated time points, the coverslips were washed with ice-cold TBS and fixed in 4% formalin for 30 minutes on ice. After fixation, cells were washed twice again and permeabilized with 0.1% TX-100 in TBS for 2 minutes on room temperature. The cells were then washed twice and incubated in TBS containing 50mM glycine for 10 minutes before another wash step and incubation in 5% normal horse serum (NHS) in 0.2% gelatin-TBS solution to reduce background staining. Subsequently, the coverslips were stained overnight at 4°C upside down on 30µl droplets of 0.2% gelatin-TBS containing antibodies against the proteins of interest. The next day, the cells were washed 3 times with 0.2% gelatin-TBS for 15 minutes before an hour incubation on droplets of 0.2% gelatin-TBS containing the secondary antibodies at RT. Subsequently, the coverslips were washed twice more in 0.2% gelatin-TBS, once in TBS and briefly in H2O before being mounted with soft set mounting medium with DAPI (Vectashield). A LSM700 Zeiss Microscope was used to obtain images and FIJI was used to quantify the amount of HMGB1-positive cells or the IL-6 intensity per cell.

### EU and EdU staining

Transfected cells were spilt on 13mm coverslips in a 24 well plate the day before UV-radiation. After UV radiation, cells were treated with either 10µM EdU (Invitrogen) 2 hours before fixation or 1mM EU (Invitrogen) 1 hour before fixation. The cells were fixed in 4% formalin for 20 minutes on ice after being washed with ice-cold Tris Buffered Saline (TBS). The cells were then washed in 3% BSA in PBS and permeabilized using 0.5% TX-100 in PBS for 20 minutes at RT. After permeabilization, the coverslips were washed twice with 3% BSA in TBS and incubated with click-it reaction mix (Invitrogen) for 30 minutes Subsequently, the cells were washed once with 3% BSA in PBS and once with PBS before being incubated in PBS containing 1:1000 Hoechst 33342 for 30 minutes. Subsequently the coverslips were washed and mounted using soft set mounting medium (Vectashield). Images were obtained with a LSM700 Zeiss Microscope and quantified with FIJI.

### 3'UTR luciferase assay

U2OS cells were transfected with control or miR-30 inhibitor and either the psiCHECK2 plasmid or 145-pGL3ctrl-3' UTR plasmid using XtremeGen transfection

reagent (Roche). The 145-pGL3ctrl-3' UTR plasmid was a gift from Michael Kastan (Addgene plasmid # 28175 [39]. All cells were transfected with a Renilla luciferase control reporter (Promega). Two days later, cells were lysed and the luciferase activity was measured by the Dual-Luciferase Reporter Assay kit (Promega) according to manufacturer's protocol.

### Mice

Mouse experiments were performed after approval from the Dutch animal ethics committee. We used male and female C57BL/6J WT and XPD$^{TTD/TTD}$ mice that either received a non-targeting microRNA inhibitor (Exiqon, N=2 per genotype) or miR-30 family inhibitor (Exiqon, N=3 per genotype) designed specifically for *in vivo* use. We started the treatment when these mice were 27-31 week old and treated the mice with 5mg/kg control or in miR-30 inhibitor in PBS by i.v. injection. The mice were treated 3 times with one day in between. We repeated this treatment regime twice with 2 weeks between the last injection and the first of the next round. The mice were sacrificed 1 week after the third treatment round by CO2 exposure.

### Plasma measurements

Blood was collected in a microvette with lithium heparin (Sarstedt) and spun down at 4.6 x g for 10 minutes to separate the plasma. Plasma creatinine concentration was measured using the creatinine assay kit from Sigma. 3µl of the samples was incubated in a 96 well plate in 50µl reaction mix for 3 hours at 37°C. Subsequently, absorbance was measured at 570 nm using GloMax 96 well plate reader (Promega). In order to measure the urea plasma concentration the samples were incubated in 100ul reaction mix of the QuantiChrom Urea assay kit (Gentaur) at room temperature for 15 minutes before the absorbance was measured at 520 nm. AST levels were determined using the AST activity kit (Sigma). Samples were incubated in 100 µl reaction mix at 37°C and the plate was measured at 450nm after 2 minutes for a baseline measurement and after 45 minutes for the final measurement.

## Results

### MiR-30 is part of the cell preservation miRNA signature

To investigate the cell preservation response during aging, we decided to further study individual components of the cell preservation microRNA signature. We set out to examine how individual miRNAs of this signature are upregulated after damage and how they inhibit apoptosis or senescence. In a micro array, miR-30 showed to be upregulated in 4 different organs of aged mice compared to their young counterparts (Figure 1a).

6

137

Furthermore, this microRNA was induced after UV irradiation and in DNA repair deficient *Ercc1*$^{\delta/-}$ mice, revealing a DNA damage dependent upregulation. Together, these results illustrate that miR-30 is representative of the miRNAs of the cell preservation response.
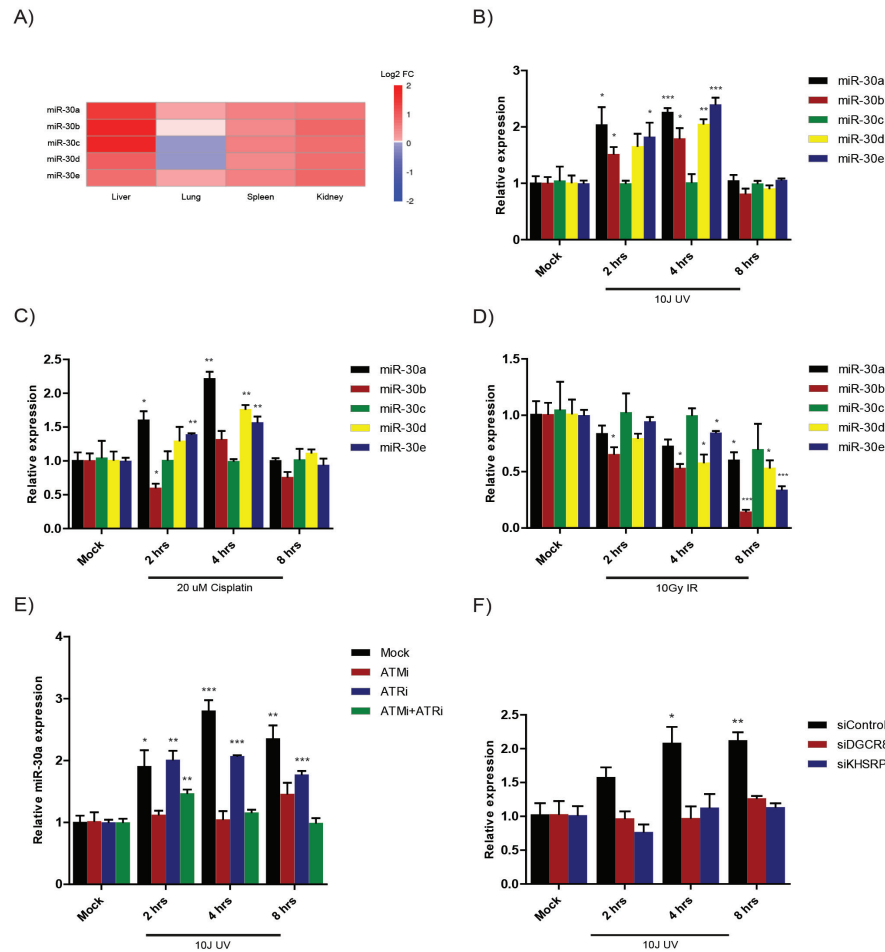


**Figure 1: miR-30 is upregulated after UV radiation in an ATM-dependent manner**
A) A microarray analysis was performed to determine the fold change (log2) of miR-30 expression in aged mouse organs (104 weeks) relative to miR-30 levels in young organs (13 weeks) .B) A qPCR was performed to detect the level of the miR-30 family after UV radiation in human IMR90 fibroblasts. miR-30 values were compared to RPL21, Gapdh and Tubulin mRNA expression through the DD Cq method. C) Cells were treated with Cisplatin and a qPCR was performed as in (B). D) Cells were radiated with ionizing radiation and a qPCR was performed as in (B). E) Cells were incubated in 10μM ATM (KU-55933) or 10μM ATR inhibitor (VE-821) for 45 minutes before UV-radiation and a qPCR was performed as described above. F) DGCR8 and KHSRP were inhibited with siRNAs 2 days before UV-radiation. Subsequently miR-30 levels were determined as before.

To better understand the DNA damage dependent inducibility, we investigated the expression of the distinct miR-30 family members after treatment with various damaging agents, selected to induce distinct DNA lesions. We treated our cells with either UV radiation, which mainly induces helix-distorting lesions, cisplatin, which induces the very cytotoxic interstrand DNA crosslinks as well as the less toxic intrastrand DNA crosslinks or ionizing radiation (IR), which generates mainly single- and very toxic double-strand DNA breaks and a variety of oxidative lesions. For these experiments we used a dose that induces similar levels of apoptosis in IR- or cisplatin-treated cells compared to our previously used UV dose (data not shown). Each miRNA has a seed sequence, which is a sequence of 7-8 nucleotides that binds a complementary sequence in the mRNA. MiRNAs belong to the same family if this seed sequence is identical. Indeed, we observed that all but miR-30c were significantly upregulated after UV, which relates to our micro array data (Figure 1b). Cisplatin-treated cells mainly showed an increase in miR-30a and a slight induction of miR-30d and miR-30e after 4 hours (Figure 1c). Interestingly, we did not observe an increase in any miRNA of this family after IR (Figure 1d). On the contrary, a downregulation was detected. These findings reveal a differential DNA damage response of the miR30 family.

### ATM regulates miR-30 expression after DNA damage

MiRNA expression after damage can be regulated by a variety of DDR proteins and we wondered which factor induces miR-30 expression after UV damage. MiRNA genes might be induced at the level of transcription after damage, however, it is more likely that their expression at least initially is regulated on a post-transcriptional level, since this is faster. ATM and ATR are key signaling kinases after DNA damage and therefore might well be involved in regulating miR-30 expression. Indeed, we did not witness an upregulation of miR-30 after UV damage when ATM was inhibited, showing miR-30 levels to be dependent on ATM (Figure 1E, sup. Figure 1). On the other hand, miR-30 induction after UV damage proved to be ATR independent, although primarily ATR is thought to be involved in the DDR after UV [40].

Post-transcriptional miRNA biogenesis involves the processing of primary miRNAs (pri-miRNAs) into precursor miRNAs (pre-miRNAs) by the Drosha-DCGR8 protein in the nucleus. These pre-miRNAs form a hairpin structure of about 70 nucleotides and can be stored in the nucleus. When miRNAs are needed, pre-miRNAs are transported to the cytoplasm and processed into mature miRNA duplexes by the Dicer-TRBP complex. Interestingly, ATM is known to play a critical role in miRNA maturation through interacting with RNA-binding protein KSRP [41]. Pri- and pre-miRNAs can be bound by this protein to increase their processing efficiency. To

examine the role (if any) of ATM in miR-30 induction, we inhibited both the Drosha-DCGR8 complex and KHSRP with siRNAs. Indeed, miR-30 expression after UV showed to be dependent on these factors, further confirming the dependency on ATM signaling.

### MiR30 inhibits apoptosis through p53

Upon activation ATM induces several downstream pathways involved in DNA damage repair, cell cycle arrest and apoptosis [9, 42]. It is therefore expected that the miRNAs induced through ATM signaling are involved in these processes, possibly through controlling p53 levels. P53 expression after damage oscillates and ATM is has a key role in the negative feedback that is required to prevent premature apoptosis [43, 44]. Therefore, we wondered whether miR-30 inhibits p53 expression after UV. Although miR-30 is not predicted to target p53 mRNA based on the sequence of the 3'UTR of p53, microRNAs are also able to form non-canonical base pairs [12]. We performed a 3'UTR luciferase assay where direct binding of miR-30 to the 3'UTR of p53 reduces luciferase expression. Indeed, we discovered miR-30 to target the 3'UTR of p53 directly (Figure 2a). Furthermore, we showed that p53 expression was induced upon miR-30 inhibition (Figure 2b) and known p53 target genes such as Puma and p21 were induced by miR-30 inhibition as well. Notably, ATM expression was not affected, indicating that ATM itself is not a miR-30 target. Interestingly, the upregulation of p53 and its targets showed to be UV independent in human fibroblasts. It appears that miR-30 expression is relatively high at baseline and prevents p53 induction in undamaged cells. MiR-30 is part of the cell preservation response and represses apoptosis after UV damage. To verify that miR-30 represses apoptosis through p53 inhibition we measured apoptosis in fibroblasts derived from p53$^{-/-}$ mice (Figure 2c). We confirmed that miR-30 inhibition increases apoptosis in mouse fibroblasts after UV. Furthermore, we indeed did not detect an increase in cell death after miR-30 was inhibited in the p53 knockout cells, confirming that the pro-apoptotic effect of miR-30 inhibition is p53 dependent.
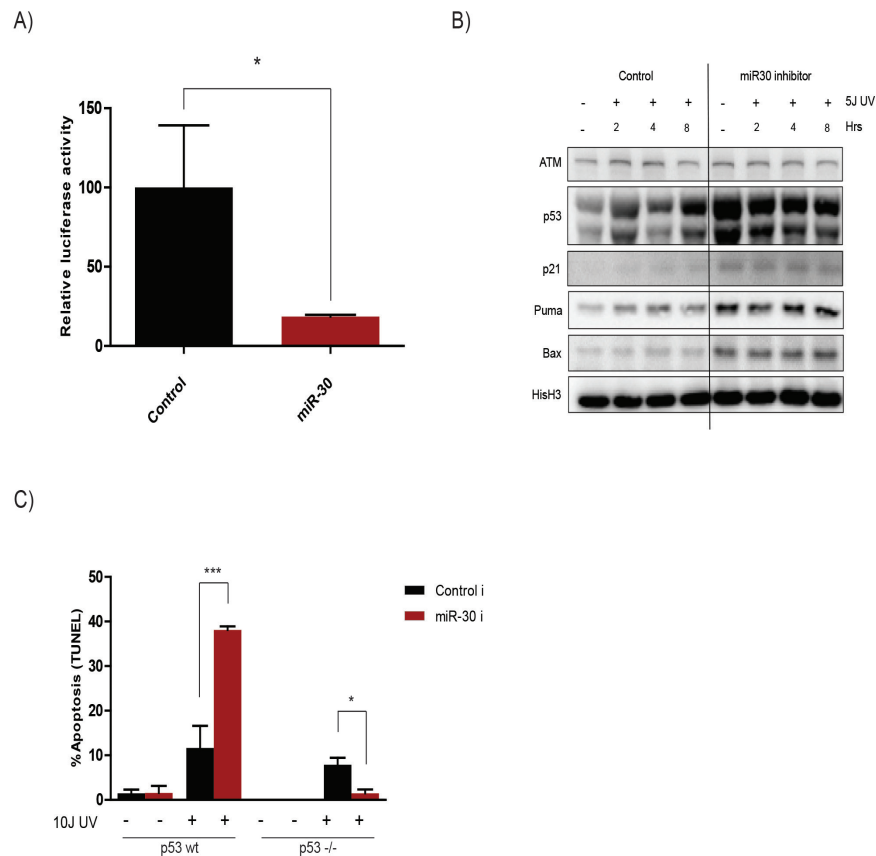
A)



B)



C)



**Figure 2: miR-30 inhibition increases UV sensitivity through p53**
A) U2OS cells were transfected with a control vector or a vector containing the p53 3'UTR, both with a luciferase reporter. In addition, cells were transfected with either a control or miR-30 mimic. The relative luciferase activity was measured using the Dual-Luciferase Reporter Assay kit to determine binding of miR-30 to the p53 3'UTR. B) IMR90 cells were transfected with a control or miR-30 family inhibitor before UV-radiation. Samples were scraped for immunoblot at indicated time points. B) MDFs were obtained from p53 wt and p53^{-/-} mice, transfected with miR-30 inhibitor and radiated with 10J UV. Apoptotic cells were detected 36 hours later through a TUNEL assay and quantified using FIJI.

## MiR-30 influences the senescence phenotype

P53 is not only involved in apoptosis induction after damage, but is able to activate a wide range of cellular processes. For example, it can induce a cell cycle arrest, facilitate DNA damage repair and activate senescence, depending on the cell type, cell history and the stimulus. Therefore, we wondered whether miR-30 has a role in other pathways regulated by p53. To this end, we determined the cell cycle phase of miR-30 inhibited NIH3T3 cells (Figure 3a).
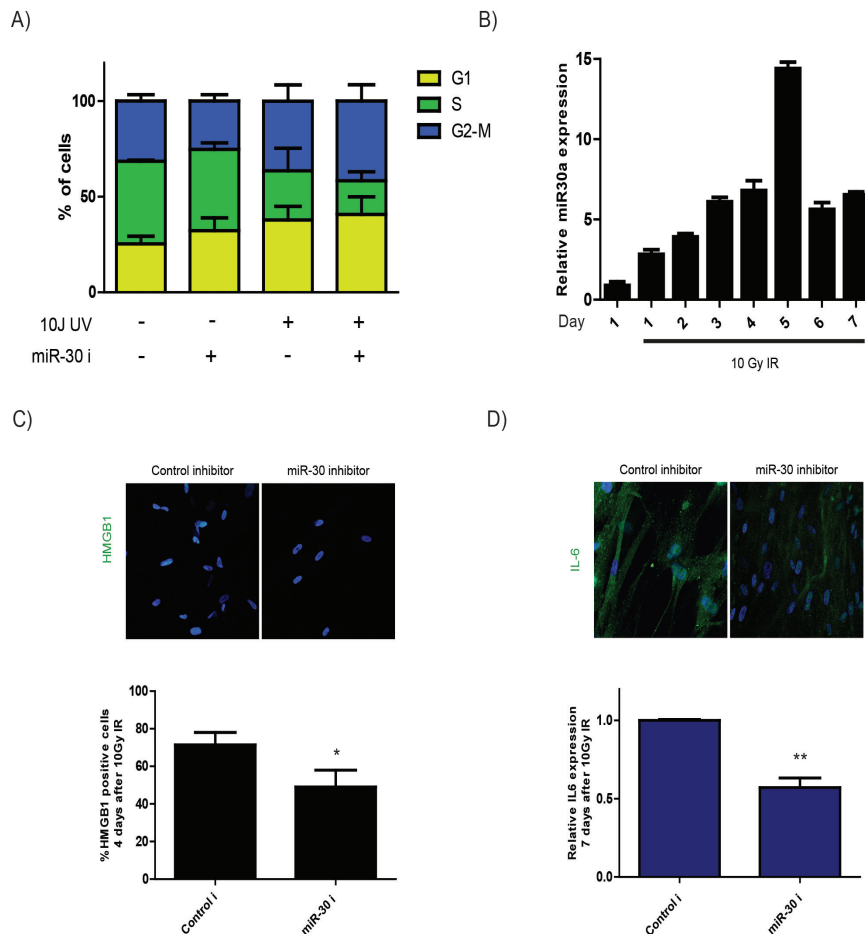
141

**Figure 3: miR-30 inhibition accelerates senescence induction but represses SASP protein IL-6**

A) The cell cycle phase of miR-30 inhibited cells was determined after mock or UV radiation by FACS analysis. B) miR-30a expression in IMR90 cells was measured by qPCR after 10Gy IR on indicated time points. The relative values were determined by subtracting the measured values of RPL21, Gapdh and Tubulin mRNA through the DD Cq method. C) Control and miR-30 inhibited IMR90 cells were exposed to 10Gy IR and fixed 4 days later. HMGB1 positive cells were detected through immunofluorescence and quantified with FIJI. D) IMR90 cells were treated as in (C), but fixed on day 7 to assess IL-6 expression by immunofluorescence. IL-6 expression was quantified with FIJI.

Independent of UV, we observed a slight G1 arrest after miR-30 inhibition and a lower proportion of G2/M cells. However, this both didn't reach the level of significance. The cell preservation response after DNA damage protects cells from

apoptosis, possibly to maintain as much as possible tissue integrity during aging. Besides apoptosis, a persistent presence of senescent cells and the associated secretion phenotype may become a threat to tissue function during aging. To investigate a possible role of miR-30 in senescence *in vitro*, we induced senescence by radiating IMR90 fibroblasts with 10Gy IR. As a consequence, all cells are fully senescent 7 days later. As mentioned earlier, we did not detect an induction of miR-30 in a timeframe of hours after IR. However, miR-30 increased significantly days later (Figure 3b). Therefore, we determined whether miR-30 inhibits senescence induction in these days after radiation. To this end, we inhibited miR-30 in fibroblasts a day before inflicting IR damage and determined senescence induction 4 days after (Figure 3c). HMGB1 is a chromatin-associated protein that is actively released from senescent cells and downregulation of this protein induces senescence [45, 46]. Therefore, HMGB1 loss is a marker for senescence. 4 days after radiation, a proportion of cell showed to have released HMGB1, while other cells still maintained a high level of HMGB1 in the nucleus (Figure 3c). When miR-30 was depleted before irradiation, the proportion of HMGB1-positive cells was lower at day 4, indicating that senescence induction was accelerated in these cells. Furthermore, we studied the effect of miR-30 inhibition in already senescent cells at day 7. Interestingly, miR-30 inhibition blunted the expression of known SASP factor IL-6 in these cells (Figure 3d). Overall, miR-30 inhibits senescence induction and features of senescence when the permanent cell cycle arrest is already in place.

**MiR-30 inhibition facilitates DNA repair**

Inhibition of both apoptosis and senescence has beneficial effects on tissue function during aging. However, cells that upregulate the cell preservation miRNA signature retain persistent damage signaling and thereby likely show a cellular functional decline. We wondered whether cells that actively repress apoptosis possibly increase DNA repair. Therefore, we analyzed the transcription restart after UV damage as a marker for transcription-coupled repair. EU incorporation is a sign of newly synthesized RNA and we mainly observed a small increase in RNA production after miR-30 inhibition (Figure 4a). Furthermore, global genome nucleotide excision repair was examined after UV in miR-30 depleted cells. Here, a slight but significant difference was detected 2 hours after radiation (Figure 4b). MiR-30 inhibition increased EdU incorporation and therefore enhanced DNA repair. Therefore, it appears that miR-30 inhibition causes a p53-dependent induction of DNA repair and therefore the age-related increase in miR-30 conversely does not aid DNA repair. However, additional experiments need to be performed to interpret these preliminary findings.
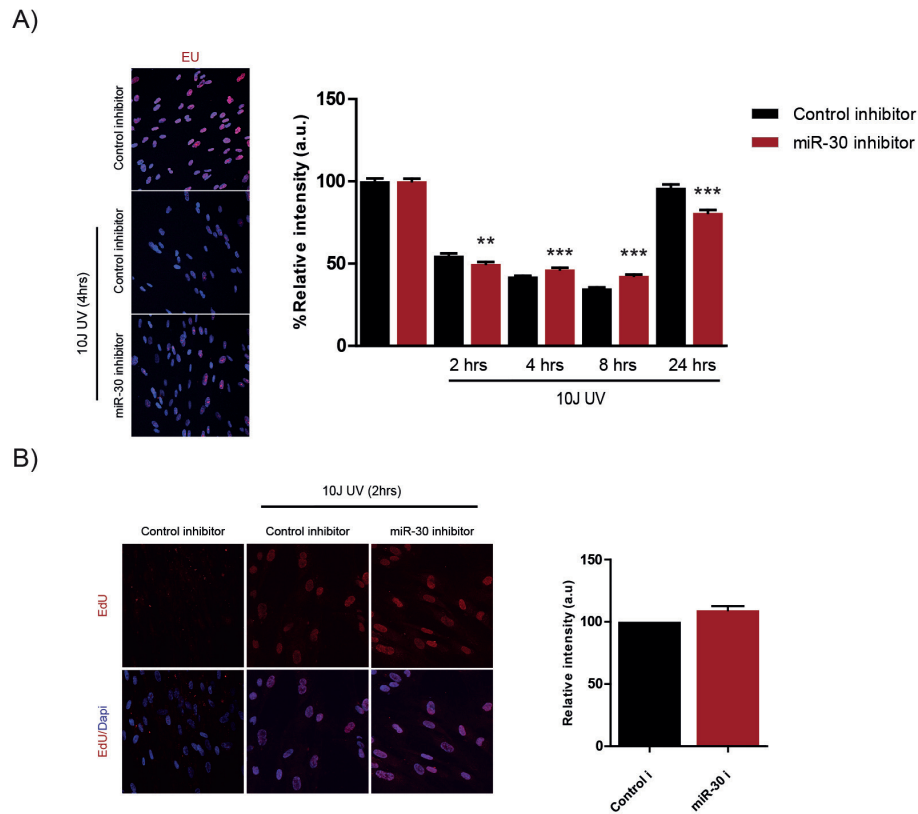
**Figure 4: DNA repair after UV radiation is affected by miR-30 inhibition**
A) MiR-30 was inhibited in IMR90 fibroblasts before UV radiation. EU was added to the medium 1 hour before fixation at indicated time points and EU incorporation was detected using a click reaction between the alkyne containing EU and azide containing dye. The EU intensity was quantified using FIJI. B) IMR90 cells were treated and stained as in (A), but EdU was added to the medium 2 hours before fixation instead of EU.

## MiR-30 inhibition provokes weight loss and affects organ function *in vivo*

Since p53 activity can induce both apoptosis and senescence during aging and it is unknown whether the cell preservation response has an overall beneficial or detrimental effect on tissue function during aging, we aimed to determine whether miR-30 protects tissue integrity during aging. To this end, we treated both wild type and fast aging XPD[ttd/td] mice (TTD) with either a control or miR-30 inhibitor that were specifically designed for *in vivo* use. These TTD mice have a mutation in the *XPD* gene and thereby resemble repair-deficient progeroid Trichothiodystrophy patients [47]. Furthermore, these mice show an accelerated induction of senescence and concomitant age-related disorders [48]. We used miRNA inhibitors containing LNA nucleotides in our experiments, since these nucleotides ensure stability and similar

inhibitors have shown to be tolerated and reliable *in vivo* [49-53]. These previous studies demonstrated a downregulation of the miRNA of interest and a biological effect 1 to 3 weeks after injection. Therefore, we treated our mice three times per week with three weeks intervals. One WT mouse treated with the miR-30 inhibitor endured a myocardial infarction and was therefore left out of further analysis. After two treatment rounds, we witnessed a significant reduction in weight of mice treated with the miR-30 inhibitor (Figure 5a). Surprisingly, this showed to be independent of genotype. To establish whether this weight loss indicated detrimental effects of the miR-30 inhibitor, we measured markers for declined organ function in the plasma. Kidney function can be determined through measuring plasma urea and creatinine levels. These molecules are secreted into urine by healthy kidneys, but when the renal filtration capacity drops during aging or disease, levels in the plasma increase. Mice treated with miR-30 inhibitor showed a higher increase in plasma creatinine levels after treatment than mice treated with the control inhibitor, indicative of a decreased filtering capacity in miR-30 inhibitor treated mice (Figure 5b). Again, the effects of miR-30 inhibitor were not dependent on genotype. Conversely, Urea levels did not show an increase (Figure 5c). A change in muscle mass could influence creatinine levels and it is therefore possible that miR-30 inhibition induces muscle damage. The aspartate aminotransferase (AST) level in blood plasma is a marker of liver function. We did not detect an increase in AST activity in plasma from miR-30 inhibitor treated mice compared to control treated mice (Figure 5d). Therefore, liver toxicity did not appear to be induced by this inhibitor. Overall, it remains unclear whether miR-30 inhibition induces organ damage by promoting apoptosis or senescence and whether miR-30 expression protects tissue integrity.
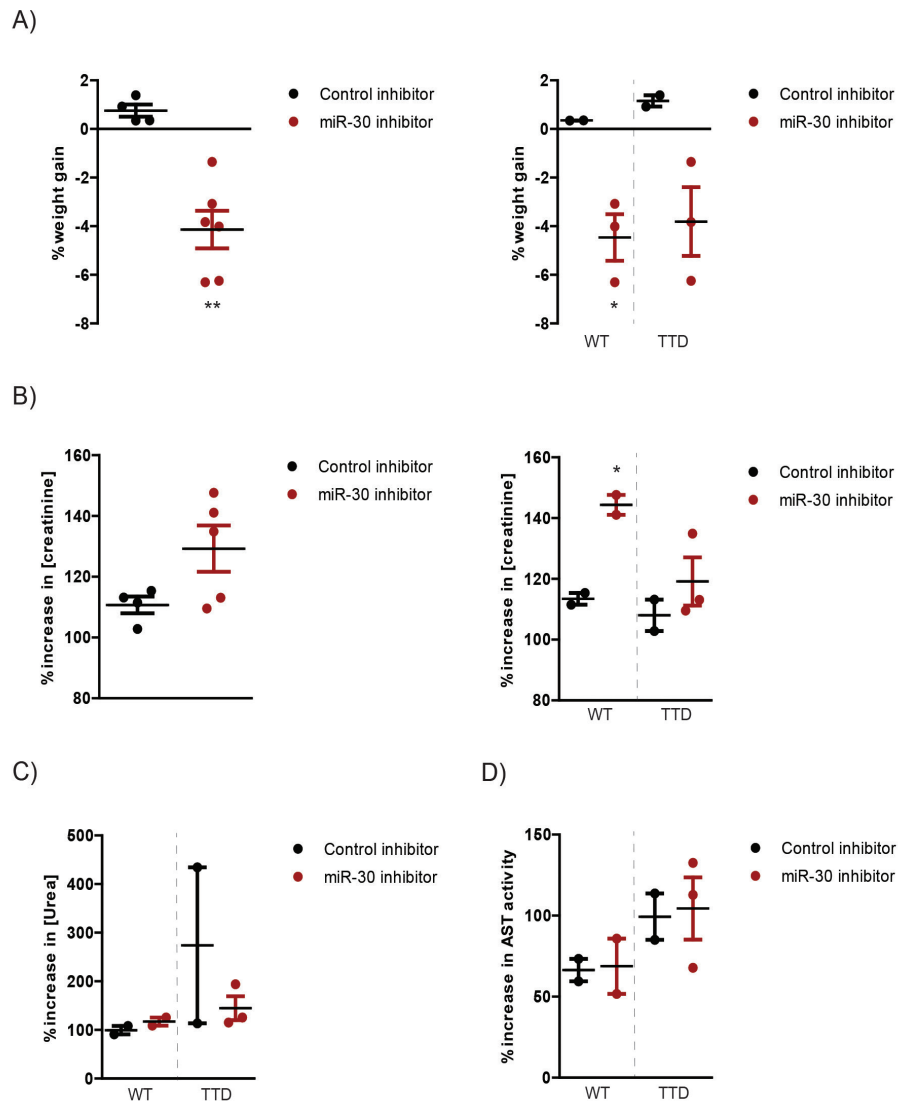
6

A)



B)



C)                                              D)



**Figure 5: miR-30 inhibition induces weight loss and toxicity in mice**
A) 30 week old WT and XPD$^{ttd/ttd}$ (TTD) mice were treated 3 times per week with 5mg/kg miR-30 inhibitor. This treatment regime was repeated twice with 2 weeks between the last injection and the first of the next round. Each data point represents one mouse and all mice are pooled in the left panel, while the data is separated per genotype in the right panel. B) Blood was taken before the 3 treatment rounds and at the time of sacrifice. The change in plasma [Creatinine] was determined by dividing the concentration at the end of the experiment by the baseline value. C) Change in [Urea] was measured as described above. D) Change in AST activity was determined as described.

## Discussion

Cell preservation is a new cellular aging phenotype that is characterized by an active inhibition of apoptosis after DNA damage in the presence of pro-apoptotic signals. During aging, miRNAs of the cell preservation response are upregulated and possibly contribute to an age-related resistance to damage. However, it is unknown what type of damage induces cell preservation miRNAs, how these microRNAs specifically inhibit apoptosis and what the effect of this signature is on tissue integrity during aging.

Here we have shown that one cell preservation miRNA, miR-30, is increased after UV and cisplatin-induced damage but not after IR. Common DNA repair pathways for UV- or cisplatin-damaged DNA are transcription-coupled and global genome nucleotide excision repair (NER) [54-56], whereas cisplatin damage also requires crosslink repair for the removal of interstrand crosslinks. IR, on the other hand, induces many single strand breaks and oxidative lesions which are quickly repaired by base excision repair and a lower number of very toxic double strand breaks that are primarily repaired through homologous recombination or non-homologous end joining and not through NER. Therefore, it appears that miR-30a,b,d and e are induced by the NER pathway. Furthermore, ATR is thought to mainly induce the DDR after UV radiation, but we observe an ATM-dependent miR-30 upregulation after UV. Although ATM is mainly activated by double strand breaks and these occur in limited amounts after UV [48], it is known that ATM can be induced by UV- and cisplatin-DNA damage as well [57-60] and is phosphorylated on a different site after UV than after IR [61]. Furthermore, it was previously shown that transcription-blocking lesions after UV-radiation induce ATM through R-Loop formation, explaining how ATM could induce miR-30 after UV radiation [58].

The cell preservation microRNA signature likely inhibits apoptosis through various targets. We have shown that miR-30 inhibition induces p53 expression and that miR-30 inhibition increases the UV sensitivity of fibroblasts in a p53 dependent manner. Furthermore, miR-30 directly targets the 3'UTR of p53. Together, this indicates that miR30 upregulation after damage inhibits apoptosis through p53. [62]. Besides the mechanism of apoptosis inhibition, it was unclear how modulating cell preservation miRNAs would influence health span. *In vitro* miR30 inhibition resulted in the activation of various p53-dependent pathways and therefore it was expected that *in vivo,* miR-30 inhibition would have significant effects as well. P53 overexpression can both decrease and increase lifespan in mice. For example, mice that over express truncated isoforms of p53 show constitutive p53 activity [63, 64]. These mice have a reduced lifespan and exhibit signs of accelerated aging

6

and an increase in senescence. Although less spontaneous tumors occur, atrophy in several organs is detected and therefore, these mice are less able to deal with stress. Additionally, mice with a knock in of activating p53 phosphorylation site mutations show a constitutive phosphorylation and activation of p53 [65], resulting in an excessive amount of apoptosis. Especially adult stem cells in brain and bone marrow were depleted, which was causative of accelerated aging. On the other hand, mice with p53 loss show tumor development early in life [66], highlighting the importance of the tumor suppressive role of p53. Furthermore, physiological p53 activity protects tissues from damage during aging. Namely, extra copies of the p53 gene has been shown to decrease age-related damage in mice, protect against cancer formation and increase lifespan [67, 68].

It is not yet known whether miR-30 inhibition leads to an increase in p53 that extends lifespan or to detrimental effects. In preliminary experiments we observed a slight increase in repair after miR-30 inhibition and a decrease in pro-inflammatory cytokine Il-6. P53 has a role in global genome nucleotide excision repair (GG-NER) and possibly in transcription-coupled NER (TC-NER), through interacting with proteins such as XPB and XPC or transcription of factors such as DDB2 [69, 70]. Furthermore, p53 expression in senescent cells decreases the expression of SASP proteins such as IL-6 and thereby represses tumor formation and fibrosis [23, 71, 72]. Therefore, miR-30 inhibition and concomitant increase in p53 could have beneficial effects during aging. The weight loss that we witnessed in our mice after miR-30 inhibition could indicate an induction of pro-survival responses. For example, downregulation of the insulin-like growth factor 1 (IGF1) pathway is known to result in a reduced weight and increased lifespan in repair-deficient mice [73, 74]. Conversely, the observed weight loss could be a result of heightened stress level and increased levels of apoptosis. Additionally, miR-30 inhibition increases plasma creatinine levels in mice, indicative of muscle breakdown. Interestingly, it has been shown that miR-30 inhibition decreases muscle cell differentiation and this miRNA is downregulated during muscle injury [75]. Therefore, it remains unclear whether miR-30 inhibition is beneficial or detrimental during aging and more research is required to clarify its effect on senescence and health span.

The miR-30 upregulation that is observed during aging possibly prevents accelerated aging, but promotes survival of damaged cells. We did not study the effect of miR-30 overexpression, but this would certainly be interesting *in vivo*. For example, miR-30 could be overexpressed in accelerated aging models such as the TTD mouse, but also in mice that exhibit an increased level of apoptosis, such as DNA repair deficient $Ercc1^{\delta/-}$ mice [74]. MiR-30 overexpression could delay apoptosis induction in these mice and possibly delay age-related pathology. On the other hand,

cancer is possibly promoted and miR-30 inhibition might trigger a survival response in *Ercc1$^{\delta/-}$* mice that could be beneficial.

Other unanswered questions include the role of miR-30 in cancer. P53 repression in cancer cells ensures apoptosis resistance and promotes metastasis [76]. Thus, this could have implications for miR-30 expression in cancer cells. However, the role of miR30 in cancer remains unclear. It has been shown that miR-30 indeed promotes breast cancer invasiveness [77] and miR-30 inhibition reduced the amount of glioma stem cells able to form a tumor *in vivo* [78]. However, other studies have shown that miR-30 expression inhibits growth, metastasis and chemotherapy resistance in various cancer types, including breast cancer [79-81], hepatocellular carcinoma [82] and non-small cell lung cancer [83]. Therefore, it appears that miR-30 mainly targets other pathways in cancer cells, where p53 is often mutated.

When it is clear whether inhibition or overexpression of miR-30 contributes to health span during aging, both strategies could potentially be employed *in vivo.* Targeting miRNAs has shown to have limited toxicity and as mentioned earlier, miRNA inhibitors containing LNA molecules are stable for weeks *in vivo.* For example, a miR-221 LNA inhibitor was detected for up to 3 weeks in mice with myeloma and showed no toxicity in monkeys [51]. Additionally, a miR-122 inhibitor is tested in a clinical trial against Hepatitis C and is well tolerated [84]. Besides inhibitors, specific miRNA mimics have shown to be well tolerated *in vivo* as well. For example, overexpression of miR-375 through a 2'-O-methyl-modified mimic suppresses hepatocellular carcinoma without reported side effects [85]. Furthermore, miR-16 overexpression is tested in patients with malignant pleural mesothelioma or non-small cell lung cancer, with limited toxicity so far [86]. Thus, miRNA expression modulation is clinically applicable.

Overall, we have shown that miR-30 inhibition induces p53 expression and hereby induces apoptosis and other p53-dependent processes. However, although it appears that miR-30 inhibition induces damage *in vivo,* it remains unknown whether uncontrolled p53 over expression is induced *in vivo* and whether excessive apoptosis occurs. Furthermore, much is still unknown about the cell preservation response during aging and more miRNAs of the cell preservation signature need to be studied *in vivo* in order to fully understand its role. It is expected that the cumulative effect of the cell preservation miRNAs determines whether the cell preservation response is beneficial for tissue homeostasis during aging. Conversely, individual miRNAs might have independent effects during aging, and knowledge about this could reveal which miRNA to target or overexpress to promote health span during aging.
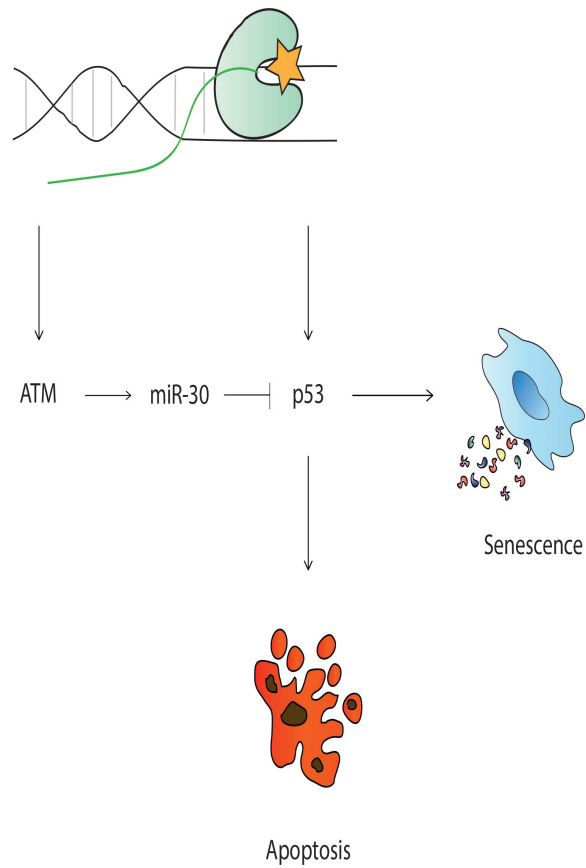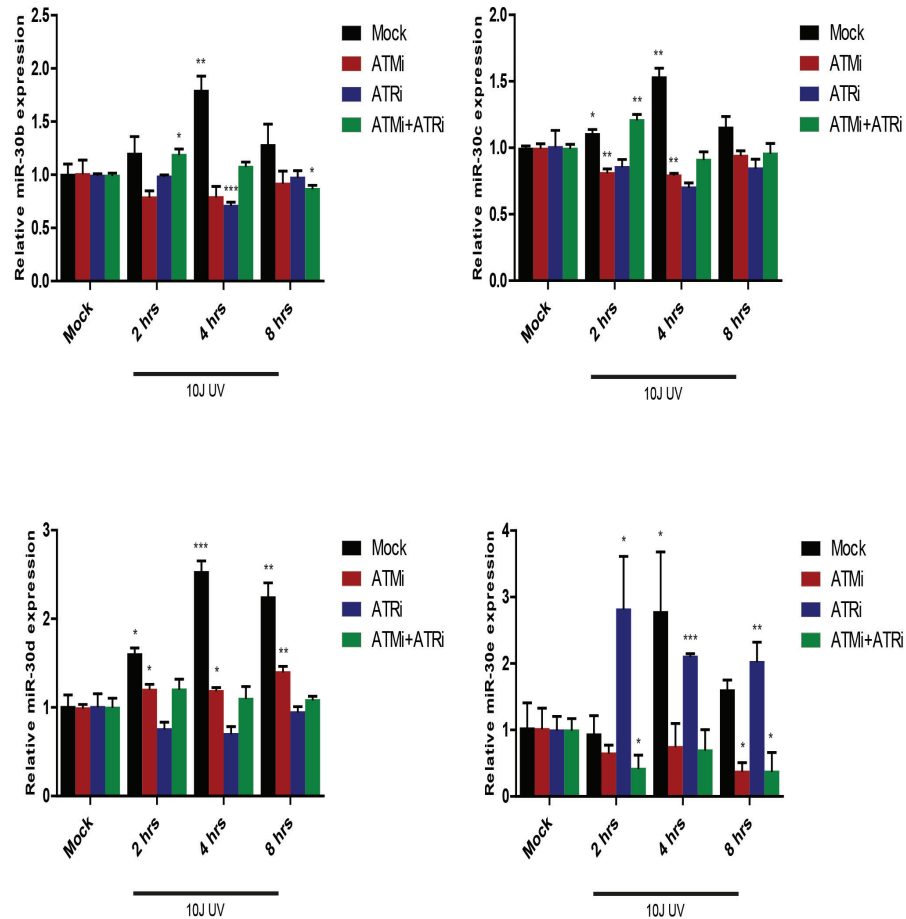
6

**Figure 6: Model of miR-30 upregulation after DNA damage.**
MiR-30 is upregulated by ATM after transcription blocking lesions. In turn, miR-30 blocks p53 expression to inhibit apoptosis. Possibly, miR-30 inhibits both apoptosis and senescence during aging and thereby maintains tissue integrity.

**Supplementary Figure 1: miR-30 upregulation after UV is ATM dependent**
Human IMR90 fibroblasts were treated with 10µM ATM (KU-55933) or 10µM ATR inhibitor (VE-821) 45 minutes before UV-radiation and samples were collected at indicated time points. A qPCR was performed to detect miR-30b,c,d and e, and the obtained values were compared to RPL21, Gapdh and Tubulin mRNA expression through the DD Cq method.

6
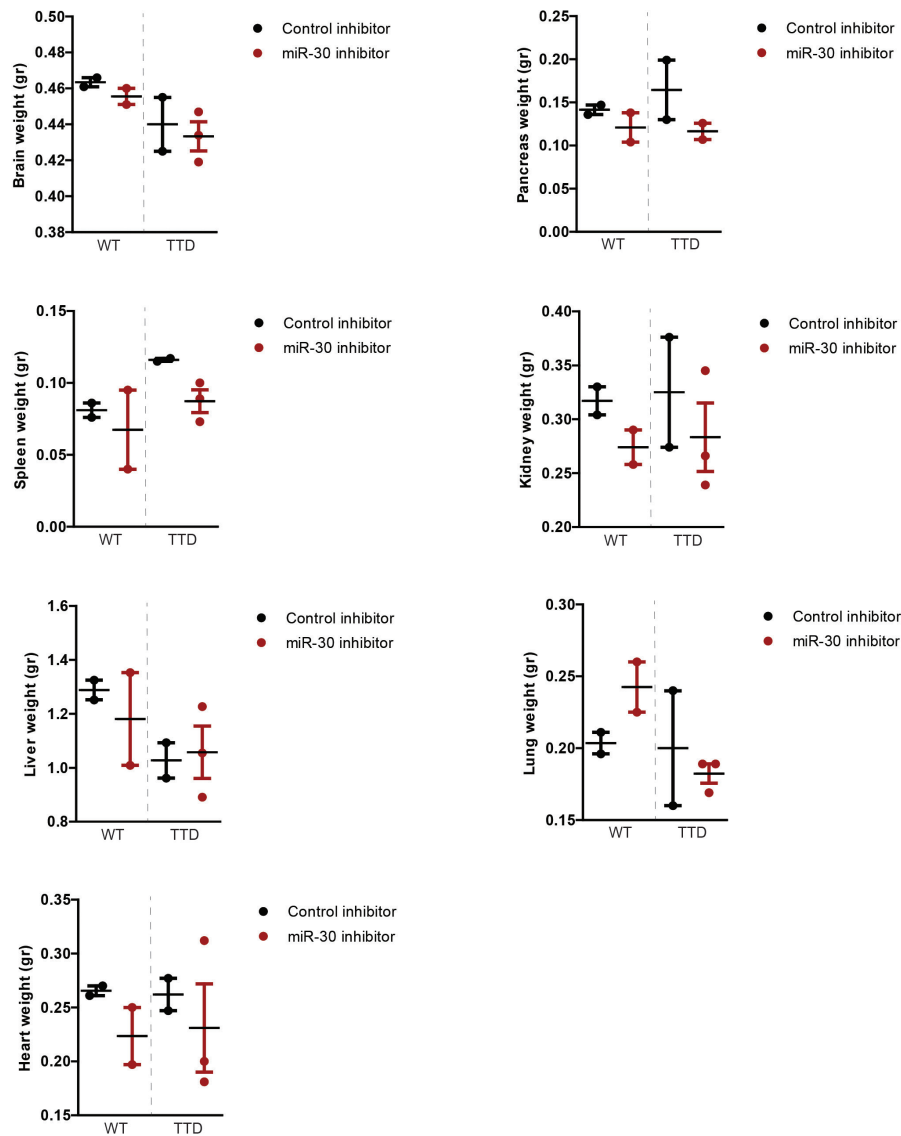
**Supplementary Figure 2: miR-30 inhibition does not significantly alter organ weight in mice.**

30 week old WT and XPD$^{ttd/ttd}$ (TTD) mice were treated with 5mg/kg miR-30 inhibitor 3 times per week. This treatment regime was repeated twice at a 3 week interval. Organ weight was not corrected for total body weight and each data point represents one mouse.

## References

1.    Lopez-Otin, C., et al., *The hallmarks of aging.* Cell, 2013. **153**(6): p. 1194-217.

2.    DiLoreto, R. and C.T. Murphy, *The cell biology of aging.* Mol Biol Cell, 2015. **26**(25): p. 4524-31.

3.    Kowald, A. and T.B. Kirkwood, *Can aging be programmed? A critical literature review.* Aging Cell, 2016.

4.    Hoeijmakers, J.H., *DNA damage, aging, and cancer.* N Engl J Med, 2009. **361**(15): p. 1475-85.

5.    Gates, K.S., *An overview of chemical processes that damage cellular DNA: spontaneous hydrolysis, alkylation, and reactions with radicals.* Chem Res Toxicol, 2009. **22**(11): p. 1747-60.

6.    Shen, J. and J. Tower, *Programmed cell death and apoptosis in aging and life span regulation.* Discov Med, 2009. **8**(43): p. 223-6.

7.    Campisi, J. and F. d'Adda di Fagagna, *Cellular senescence: when bad things happen to good cells.* Nat Rev Mol Cell Biol, 2007. **8**(9): p. 729-40.

8.    Ciccia, A. and S.J. Elledge, *The DNA damage response: making it safe to play with knives.* Mol Cell, 2010. **40**(2): p. 179-204.

9.    Sirbu, B.M. and D. Cortez, *DNA damage response: three levels of DNA repair regulation.* Cold Spring Harb Perspect Biol, 2013. **5**(8): p. a012724.

10.   Liu, Y., Y. Li, and X. Lu, *Regulators in the DNA damage response.* Arch Biochem Biophys, 2016. **594**: p. 18-25.

11.   Bartel, D.P., *MicroRNAs: genomics, biogenesis, mechanism, and function.* Cell, 2004. **116**(2): p. 281-97.

12.   Helwak, A., et al., *Mapping the human miRNA interactome by CLASH reveals frequent noncanonical binding.* Cell, 2013. **153**(3): p. 654-65.

13.   Baek, D., et al., *The impact of microRNAs on protein output.* Nature, 2008. **455**(7209): p. 64-71.

14.   Selbach, M., et al., *Widespread changes in protein synthesis induced by microRNAs.* Nature, 2008. **455**(7209): p. 58-63.

15.   He, M., et al., *MicroRNAs, DNA Damage Response, and Cancer Treatment.* Int J Mol Sci, 2016. **17**(12).

16.   Marzetti, E. and C. Leeuwenburgh, *Skeletal muscle apoptosis, sarcopenia and frailty at old age.* Exp Gerontol, 2006. **41**(12): p. 1234-8.

17.   Kim, S.E., et al., *Treadmill exercise prevents aging-induced failure of memory through an increase in neurogenesis and suppression of apoptosis in rat hippocampus.* Exp Gerontol, 2010. **45**(5): p. 357-65.

6

18. Haughey, N.J., et al., *Disruption of neurogenesis by amyloid beta-peptide, and perturbed neural progenitor cell homeostasis, in models of Alzheimer's disease.* J Neurochem, 2002. **83**(6): p. 1509-24.

19. Dimri, G.P., et al., *A biomarker that identifies senescent human cells in culture and in aging skin in vivo.* Proc Natl Acad Sci U S A, 1995. **92**(20): p. 9363-7.

20. Krishnamurthy, J., et al., *Ink4a/Arf expression is a biomarker of aging.* J Clin Invest, 2004. **114**(9): p. 1299-307.

21. Burd, C.E., et al., *Monitoring tumorigenesis and senescence in vivo with a p16(INK4a)-luciferase model.* Cell, 2013. **152**(1-2): p. 340-51.

22. Coppe, J.P., et al., *The senescence-associated secretory phenotype: the dark side of tumor suppression.* Annu Rev Pathol, 2010. **5**: p. 99-118.

23. Coppe, J.P., et al., *Senescence-associated secretory phenotypes reveal cell-nonautonomous functions of oncogenic RAS and the p53 tumor suppressor.* PLoS Biol, 2008. **6**(12): p. 2853-68.

24. Wang, W.J., G.Y. Cai, and X.M. Chen, *Cellular senescence, senescence-associated secretory phenotype, and chronic kidney disease.* Oncotarget, 2017. **8**(38): p. 64520-64533.

25. Martin, J.A., et al., *Chondrocyte senescence, joint loading and osteoarthritis.* Clin Orthop Relat Res, 2004(427 Suppl): p. S96-103.

26. Zhou, X., et al., *Clonal senescence alters endothelial ICAM-1 function.* Mech Ageing Dev, 2006. **127**(10): p. 779-85.

27. Chilosi, M., et al., *Premature lung aging and cellular senescence in the pathogenesis of idiopathic pulmonary fibrosis and COPD/emphysema.* Transl Res, 2013. **162**(3): p. 156-73.

28. Baker, D.J., et al., *Naturally occurring p16(Ink4a)-positive cells shorten healthy lifespan.* Nature, 2016. **530**(7589): p. 184-9.

29. Baker, D.J., et al., *Clearance of p16Ink4a-positive senescent cells delays ageing-associated disorders.* Nature, 2011. **479**(7372): p. 232-6.

30. Ruzankina, Y., et al., *Deletion of the developmentally essential gene ATR in adult mice leads to age-related phenotypes and stem cell loss.* Cell Stem Cell, 2007. **1**(1): p. 113-26.

31. Paxson, J.A., et al., *Age-dependent decline in mouse lung regeneration with loss of lung fibroblast clonogenicity and increased myofibroblastic differentiation.* PLoS One, 2011. **6**(8): p. e23232.

32. Brack, A.S., H. Bildsoe, and S.M. Hughes, *Evidence that satellite cell decrement contributes to preferential decline in nuclear number from large fibres during murine age-related muscle atrophy.* J Cell Sci, 2005. **118**(Pt 20): p. 4813-21.

33. Renault, V., et al., *Regenerative potential of human skeletal muscle during aging.* Aging Cell, 2002. **1**(2): p. 132-9.

34. Chakkalakal, J.V., et al., *The aged niche disrupts muscle stem cell quiescence.* Nature, 2012. **490**(7420): p. 355-60.

35. Al-Khalaf, H.H. and A. Aboussekhra, *Survivin expression increases during aging and enhances the resistance of aged human fibroblasts to genotoxic stress.* Age (Dordr), 2013. **35**(3): p. 549-62.

36. Feng, Z., et al., *Declining p53 function in the aging process: a possible mechanism for the increased tumor incidence in older populations.* Proc Natl Acad Sci U S A, 2007. **104**(42): p. 16633-8.

37. Suh, Y., et al., *Aging alters the apoptotic response to genotoxic stress.* Nat Med, 2002. **8**(1): p. 3-4.

38. Radziszewska, E., et al., *Effect of aging on UVC-induced apoptosis of rat splenocytes.* Acta Biochim Pol, 2000. **47**(2): p. 339-47.

39. Chen, J. and M.B. Kastan, *5'-3'-UTR interactions regulate p53 mRNA translation and provide a target for modulating p53 induction after DNA damage.* Genes Dev, 2010. **24**(19): p. 2146-56.

40. Yan, S., M. Sorrell, and Z. Berman, *Functional interplay between ATM/ATR-mediated DNA damage response and DNA repair pathways in oxidative stress.* Cell Mol Life Sci, 2014. **71**(20): p. 3951-67.

41. Zhang, X., et al., *The ATM kinase induces microRNA biogenesis in the DNA damage response.* Mol Cell, 2011. **41**(4): p. 371-83.

42. Reinhardt, H.C. and M.B. Yaffe, *Kinases that control the cell cycle in response to DNA damage: Chk1, Chk2, and MK2.* Curr Opin Cell Biol, 2009. **21**(2): p. 245-55.

43. Zhang, X.P., F. Liu, and W. Wang, *Two-phase dynamics of p53 in the DNA damage response.* Proc Natl Acad Sci U S A, 2011. **108**(22): p. 8990-5.

44. Wagner, J., et al., *p53-Mdm2 loop controlled by a balance of its feedback strength and effective dampening using ATM and delayed feedback.* Syst Biol (Stevenage), 2005. **152**(3): p. 109-18.

45. Davalos, A.R., et al., *p53-dependent release of Alarmin HMGB1 is a central mediator of senescent phenotypes.* J Cell Biol, 2013. **201**(4): p. 613-29.

46. Chandrasekaran, K.S., A. Sathyanarayanan, and D. Karunagaran, *Downregulation of HMGB1 by miR-34a is sufficient to suppress proliferation, migration and invasion of human cervical and colorectal cancer cells.* Tumour Biol, 2016. **37**(10): p. 13155-13166.

47. de Boer, J., et al., *A mouse model for the basal transcription/DNA repair syndrome trichothiodystrophy.* Mol Cell, 1998. **1**(7): p. 981-90.

6

48.     Baar, M.P., et al., *Targeted Apoptosis of Senescent Cells Restores Tissue Homeostasis in Response to Chemotoxicity and Aging.* Cell, 2017. **169**(1): p. 132-147 e16.

49.     Hildebrandt-Eriksen, E.S., et al., *A locked nucleic acid oligonucleotide targeting microRNA 122 is well-tolerated in cynomolgus monkeys.* Nucleic Acid Ther, 2012. **22**(3): p. 152-61.

50.     Elmen, J., et al., *Antagonism of microRNA-122 in mice by systemically administered LNA-antimiR leads to up-regulation of a large set of predicted target mRNAs in the liver.* Nucleic Acids Res, 2008. **36**(4): p. 1153-62.

51.     Gallo Cantafio, M.E., et al., *Pharmacokinetics and Pharmacodynamics of a 13-mer LNA-inhibitor-miR-221 in Mice and Non-human Primates.* Mol Ther Nucleic Acids, 2016. **5**(6).

52.     Hinkel, R., et al., *Inhibition of microRNA-92a protects against ischemia/reperfusion injury in a large-animal model.* Circulation, 2013. **128**(10): p. 1066-75.

53.     Boon, R.A., et al., *MicroRNA-34a regulates cardiac ageing and function.* Nature, 2013. **495**(7439): p. 107-10.

54.     Vichi, P., et al., *Cisplatin- and UV-damaged DNA lure the basal transcription factor TFIID/TBP.* EMBO J, 1997. **16**(24): p. 7444-56.

55.     McKay, B.C., C. Becerril, and M. Ljungman, *P53 plays a protective role against UV- and cisplatin-induced apoptosis in transcription-coupled repair proficient fibroblasts.* Oncogene, 2001. **20**(46): p. 6805-8.

56.     Mouw, K.W. and A.D. D'Andrea, *Crosstalk between the nucleotide excision repair and Fanconi anemia/BRCA pathways.* DNA Repair (Amst), 2014. **19**: p. 130-4.

57.     Wakasugi, M., et al., *Nucleotide excision repair-dependent DNA double-strand break formation and ATM signaling activation in mammalian quiescent cells.* J Biol Chem, 2014. **289**(41): p. 28730-7.

58.     Tresini, M., et al., *The core spliceosome as target and effector of non-canonical ATM signalling.* Nature, 2015. **523**(7558): p. 53-8.

59.     Ray, A., et al., *ATR- and ATM-Mediated DNA Damage Response Is Dependent on Excision Repair Assembly during G1 but Not in S Phase of Cell Cycle.* PLoS One, 2016. **11**(7): p. e0159344.

60.     Colton, S.L., et al., *The involvement of ataxia-telangiectasia mutated protein activation in nucleotide excision repair-facilitated cell survival with cisplatin treatment.* J Biol Chem, 2006. **281**(37): p. 27117-25.

61.     Stiff, T., et al., *ATR-dependent phosphorylation and activation of ATM in response to UV treatment or replication fork stalling.* EMBO J, 2006. **25**(24): p. 5775-82.

62. Roca-Alonso, L., et al., *Myocardial MiR-30 downregulation triggered by doxorubicin drives alterations in beta-adrenergic signaling and enhances apoptosis.* Cell Death Dis, 2015. **6**: p. e1754.

63. Maier, B., et al., *Modulation of mammalian life span by the short isoform of p53.* Genes Dev, 2004. **18**(3): p. 306-19.

64. Tyner, S.D., et al., *p53 mutant mice that display early ageing-associated phenotypes.* Nature, 2002. **415**(6867): p. 45-53.

65. Liu, D., et al., *Puma is required for p53-induced depletion of adult stem cells.* Nat Cell Biol, 2010. **12**(10): p. 993-8.

66. Donehower, L.A., et al., *Mice deficient for p53 are developmentally normal but susceptible to spontaneous tumours.* Nature, 1992. **356**(6366): p. 215-21.

67. Matheu, A., et al., *Delayed ageing through damage protection by the Arf/p53 pathway.* Nature, 2007. **448**(7151): p. 375-9.

68. Garcia-Cao, I., et al., *"Super p53" mice exhibit enhanced DNA damage response, are tumor resistant and age normally.* EMBO J, 2002. **21**(22): p. 6225-35.

69. Wang, X.W., et al., *p53 modulation of TFIIH-associated nucleotide excision repair activity.* Nat Genet, 1995. **10**(2): p. 188-95.

70. Hwang, B.J., et al., *Expression of the p48 xeroderma pigmentosum gene is p53-dependent and is involved in global genomic repair.* Proc Natl Acad Sci U S A, 1999. **96**(2): p. 424-8.

71. Lujambio, A., et al., *Non-cell-autonomous tumor suppression by p53.* Cell, 2013. **153**(2): p. 449-60.

72. Pribluda, A., et al., *A senescence-inflammatory switch from cancer-inhibitory to cancer-promoting mechanism.* Cancer Cell, 2013. **24**(2): p. 242-56.

73. Garinis, G.A., et al., *Persistent transcription-blocking DNA lesions trigger somatic growth attenuation associated with longevity.* Nat Cell Biol, 2009. **11**(5): p. 604-15.

74. Vermeij, W.P., et al., *Restricted diet delays accelerated ageing and genomic stress in DNA-repair-deficient mice.* Nature, 2016. **537**(7620): p. 427-431.

75. Guess, M.G., et al., *miR-30 family microRNAs regulate myogenic differentiation and provide negative feedback on the microRNA pathway.* PLoS One, 2015. **10**(2): p. e0118229.

76. Bhatia, S., S.S. Tykodi, and J.A. Thompson, *Treatment of metastatic melanoma: an overview.* Oncology (Williston Park), 2009. **23**(6): p. 488-96.

77. Dobson, J.R., et al., *hsa-mir-30c promotes the invasive phenotype of metastatic breast cancer cells by targeting NOV/CCN3.* Cancer Cell Int, 2014. **14**: p. 73.

78. Che, S., et al., *miR-30 overexpression promotes glioma stem cells by regulating Jak/STAT3 signaling pathway.* Tumour Biol, 2015. **36**(9): p. 6805-11.

6

79. Fang, Y., et al., *Involvement of miR-30c in resistance to doxorubicin by regulating YWHAZ in breast cancer cells.* Braz J Med Biol Res, 2014. **47**(1): p. 60-9.

80. Cheng, C.W., et al., *MicroRNA-30a inhibits cell migration and invasion by downregulating vimentin expression and is a potential prognostic marker in breast cancer.* Breast Cancer Res Treat, 2012. **134**(3): p. 1081-93.

81. Zhang, N., et al., *MicroRNA-30a suppresses breast tumor growth and metastasis by targeting metadherin.* Oncogene, 2014. **33**(24): p. 3119-28.

82. Liu, Z., K. Tu, and Q. Liu, *Effects of microRNA-30a on migration, invasion and prognosis of hepatocellular carcinoma.* FEBS Lett, 2014. **588**(17): p. 3089-97.

83. Zhong, K., et al., *MicroRNA-30b/c inhibits non-small cell lung cancer cell proliferation by targeting Rab18.* BMC Cancer, 2014. **14**: p. 703.

84. Janssen, H.L., et al., *Treatment of HCV infection by targeting microRNA.* N Engl J Med, 2013. **368**(18): p. 1685-94.

85. He, X.X., et al., *MicroRNA-375 targets AEG-1 in hepatocellular carcinoma and suppresses liver cancer cell growth in vitro and in vivo.* Oncogene, 2012. **31**(28): p. 3357-69.

86. Shah, M.Y., et al., *microRNA Therapeutics in Cancer - An Emerging Concept.* EBioMedicine, 2016. **12**: p. 34-42.

6

# CHAPTER 7

## Extracellular vesicles as transporters of the DNA damage response during aging

**Marjolein P. Baar**[1,3], **Thomas Hartjes**[2], **Myrna Aulia**[1], **Peter L.J. de Keizer**[1,3], **Martin E. van Royen**[2], **Jeroen de Vrij**[1], **Jan Hoeimakers**[1,4,5], **Joris Pothof**[1]

[1] Department of Molecular Genetics, Erasmus University Medical Center, Rotterdam.

[2] Department of Pathology, Erasmus University Medical Center, Rotterdam

[3] Center for Molecular Medicine, Department of Biomedical Genetics, University Medical Center Utrecht, Utrecht University

[4] Princess Máxima Centre for Pediatric Oncology, Oncode Institute, Heidelberglaan 25, 3584, CS, Utrecht, PO Box 113, 3720 AC Bilthoven, the Netherlands

[5] CECAD, Forschungszentrum, Universität zu Köln, Joseph-Stelzmann-Straße 26, 50931 Köln, Germany

## Abstract

DNA damage accumulates during aging, ultimately leading to loss of tissue homeostasis and to age-related diseases. The DNA damage response can initiate damage repair or other processes such as apoptosis or senescence. Additionally, cell preservation microRNAs are upregulated after DNA damage that are able to prevent both apoptosis and senescence in order to preserve tissue integrity. Thus, damaged cells show a modified intracellular environment. Importantly, these cells show an altered secretion phenotype as well. Extracellular vesicle (EV) secretion is known to be increased by damaged cells and their content is altered during aging. In addition, EVs contain miRNAs that are able to repress target mRNAs in recipient cells. However, it is largely unknown how exactly vesicle content influences recipient cells during aging. We hypothesize that after damage, cells secrete vesicles that contain cell preservation microRNAs. Here, we show that a DNA damage response is transferred after UV damage to undamaged cells through EVs. Namely, key DNA damage response proteins are activated after cells are treated with EVs from UV irradiated cells. Furthermore, we indeed observe an upregulation of cell preservation microRNAs in these recipient cells. In addition, EVs isolated from aged mouse serum induced a DNA damage response and cell preservation microRNAs in recipient cells as well. Therefore, age-related DNA damage could promote cell preservation systemically in order to prevent loss of tissue homeostasis.

## Introduction

During life, DNA is continuously damaged by a multitude of stressors, including UV light, reactive oxygen species (ROS) and replication errors [1]. The DNA damage response (DDR) ensures genomic integrity by inducing repair pathways or, when the damage cannot be repaired, prevents proliferation of damaged cells through apoptosis or a permanent cell cycle arrest known as senescence. Additionally, damaged cells are known to signal to their surrounding tissue to prevent further damage by inducing immune clearance or to upregulate pro-survival responses to protect from a second injury. For example, senescent cells secrete proteases, growth factors and pro-inflammatory cytokines to the microenvironment [2]. This senescence associated secretory phenotype (SASP) has detrimental effects on tissue homeostasis when chronically expressed, but originally it can function as a signal to the immune system to clear damaged senescent cells [3, 4]. This way, senescence has beneficial effects on tissue restoration [5]. Thus, the SASP functions as a warning that alerts the microenvironment that damage occurred. In another example, UV irradiation induces keratinocytes in the skin to produce cytokines such as TNFα and IL1 that can be involved in suppressing an immune response in order to prevent further damage to the skin [6, 7]. Additionally, inflammatory cytokine secretion from damaged cells can systemically induce pro-survival responses [8]. Thus, intercellular communication after damage is crucial for maintaining tissue integrity.

Another way cells communicate is through the secretion of extracellular vesicles (EVs). EVs are small vesicles released from a cell to their microenvironment. EVs are secreted by all cell types, including cancer cells and are therefore present in the tissue microenvironment and all body fluids. Three subtypes are distinguished, based on origin and size [9]. Exosomes are formed through fusion of multivesicular bodies with the plasma membrane and are the smallest EV subtype (40-100 nm). Microvesicles (50-1000 nm) are a result from outward budding of the plasma membrane and apoptotic bodies are larger vesicles (800-5000 nm) that are formed when cells undergo apoptosis. All these vesicles can contain lipids, proteins, DNA and RNA that can be released in recipient cells to alter intracellular signaling [10]. For example, microRNAs present in EVs can be transferred to other cells and inhibit translation of mRNAs there [11]. Interestingly, it has been shown that damaged or stressed cells release more vesicles and that the vesicle content differs from undamaged cells [12, 13]. Likely, this not a random process. For example, the packaging of microRNAs into extracellular vesicles was shown to be tightly regulated by proteins such as hnRNPA2B1 [14] and p53 can enhance vesicle secretion after

damage [15, 16]. Furthermore, these vesicles can cause significant alterations in neighboring cells. For example, ionizing irradiation causes release of vesicles from glioblastoma cells that cause a migratory phenotype in recipient cells [13]. Thus, EVs likely play a crucial role in the DNA damage response and the effects of damage inflicted reach further than the actual damaged cells. A larger number of cells is affected by this systemic damage response, which can have either detrimental or beneficial consequences.

A systemic damage response may have a significant effect during aging, since irreparable damage accumulates during aging. Constitutive DDR signaling leads to a decline in cellular homeostasis, and to an increase in cellular aging phenotypes such as apoptosis or senescence. Both are crucial in preventing cancer growth, but also contribute to the loss of tissue integrity seen during aging. First, senescent cells accumulate and therefore, SASP proteins are overabundant and negatively influence the microenvironment. Thus, an age-related accumulation of senescent cells ultimately causes a loss of tissue homeostasis and predisposes to age-related diseases. Second, an increase in apoptosis leads to a decline in tissue integrity as well, and can cause diseases such as Alzheimer's disease [17]. However, in multiple organs, a decline in the apoptotic response is observed during aging and pro-apoptotic proteins are often downregulated [18-20]. We have shown that age-related DNA damage accumulation causes the upregulation of a specific subset of microRNAs (unpublished data, MB, JH, JP). These microRNAs actively repress apoptosis in the presence of DNA damage, a process we have termed cell preservation. Overall, the DNA damage response determines whether apoptosis or senescence is induced or if these processes are inhibited to prevent loss of tissue homeostasis.

Since EV secretion was shown to be a result of DDR signaling and an increase in damaged cells is observed during aging, an age-related change in EV signaling is expected. Furthermore, cell preservation microRNAs are increased after damage and during aging. Interestingly, we have found these miRNAs to be upregulated in the serum of centenarians (Y.Suh unpublished data). In addition, all microRNAs of this signature are previously described to be secreted in EVs. For example, miR-30a is released by cardiomyocytes after hypoxia [21] and Let-7 shows an increased expression in circulating EVs after hepatic fibrosis [22]. Here, we aim to determine whether damaged and aged cells release EVs containing cell preservation microRNAs to their microenvironment and examine the influence of these vesicles on undamaged recipient cells. Thus, we aim to establish whether cell preservation microRNAs are induced systemically and influence intercellular communication during aging.

## Materials and methods

### Antibodies

The following antibodies were used from Cell Signaling: p-S1981 ATM (4526), p-S15 p53 (D4S1H, rodent specific), p-S15 p53 (9286), PUMA (4976), p-SQ/TQ (2851). P21$^{cip1}$ (610234) antibody was obtained from BD Transduction Laboratories and the γH2AX antibody (05-636) from Millipore. The secondary antibodies used were: Alexa Fluor donkey anti-rabbit 488 (Invitrogen) and Alexa Fluor donkey anti-mouse 594 (Invitrogen).

### Cell culture

IMR90, NIH3T3 and DU145 cells were cultured in Dulbecco's Modified Eagle Medium (DMEM) culture medium supplemented with 10% FCS and 1% pen/strep. NIH3T3 and DU145 cells were kept at 37°C and 5% CO2 and ambient oxygen, while IMR90 cells were additionally cultured in 3% O2. One day before damaging the cells, the DMEM culture medium was replaced by Advanced Dulbecco's Modified Eagle Medium/Ham's F-12 (DMEM/F-12) (Gibco), supplemented with 1% 1 M HEPES (Lonza), 1% 200 mM Ultraglutamine (Lonza) and 1% pen/strep. All cells were kept in this medium until vesicle isolation. This way, vesicles that are present in fetal calf serum are prevented from influencing the results. 10J/m2 UV-cirradiation was given (254 nm germicidal lamp, Philips). After the cell culture medium was removed and the cells were washed with PBS. Mock irradiated cells were taken from the incubator and washed with PBS as well. 5 Gy IR was given by exposing cells to X-rays.

### EV isolation from cell culture medium

Extracellular vesicles were isolated from cell culture medium 1 day after exposure to either UV or ionizing radiation. The medium was centrifuged at 2000g for 30 minutes at room temperature to exclude cell debris. The supernatant was transferred to new tube and Total Exosome Isolation from Cell Culture Medium reagent was added to the medium in a 1:2 concentration. After overnight incubation at 4°C, the tubes were centrifuged at 10,000 x g for 1 hour at 4°C to isolate the vesicles. The supernatant was removed and the pellet was dissolved in 50ul PBS. The resulting solution contained around 5*10$^{10}$ EVs and was divided over 3 coverslips in a 24 well plate and one well of a 6 well plate containing untreated and undamaged recipient cells.

**EV isolation from serum**

Blood was taken from 8 and 104 old C57BL6J/FVB hybrid mice that were used in other research projects in our lab. These experiments were approved by the Dutch animal ethics committee. The serum was centrifuged at 2000g for 30 minutes. Extracellular vesicles were then isolated by adding Total Exosome Isolation Reagent (from serum; Invitrogen) before 30 minutes incubation at 4°C and centrifugation for 10 minutes at 10000g at room temperature. Subsequently, the supernatant was removed and the pellet resuspended in 30ul PBS. This solution was then added to 2 coverslips in a 24 well plate and 1 well of a 6 well plate.

**Extracellular vesicle quantification**

Isolated vesicles from cell culture medium were quantified using the EVQuant method (unpublished data, TH and MR). In this method, EVs are fluorescently labeled with rhodamine and immobilized in a polyacrylamide gel before being loaded into a microfluidics device. The labeled vesicles can then be detected and quantified. Vesicle diameter was determined using a qNano device (Izon science). This machine uses resistive pulse sensing to detect particle concentration, size and charge.

**Quantitative real-time PCR**

Total RNA was isolated using TRI reagent (Qiagen). Cells were washed twice in ice cold PBS before being scraped in 1ml TRI reagent and transferred to a 1.5 ml Eppendorf tube. 200 mL chloroform per 1 ml TRI reagent was added and the samples were shaken vigorously for 15 seconds before a 5 minute incubation at room temperature. The samples were then centrifuged at 12000 g for 15 minutes at 4 °C after which the upper aqueous layer was transferred to a fresh Eppendorf tube. 500 mL isopropanol was added before 15 seconds of shaking and 10 minutes of incubation at room temperature. Subsequently the samples were centrifuged again at 12000g for 15 minutes at 4 °C. Afterwards, the supernatant was removed and the pellet was washed in 1 ml of 75% ethanol. The samples were then centrifuged for the last time at 12000g for 15 minutes at 4 °C. After removing the supernatant, the pellet was air dried for 15 minutes before resuspension in 30 mL RNAse free $H_2O$. The RNA concentration was measured using the Nanodrop. We used the miScript II RT Kit (Qiagen) to convert 500 ng of total RNA into cDNA according to manufacturer's instruction. The obtained cDNA was 10 times diluted in $H_2O$ before being mixed with SYBR Green Master Mix (Bio-Rad), primers and $H_2O$. qPCR plates and the CFX96 Touchä Real-Time PCR Detection System from Bio-Rad were used to obtain Cq values. Relative gene expression was calculated using the DD Cq method.

Primers used for the described experiments were:

miR-16: cgcagtagcagcacgta cagtttttttttttttttttcgccaa

miR-21: Gcagtagcttatcagactgatg ggtccagttttttttttttttttcaac

miR-22: cagagttcttcagtggcaag ggtccagttttttttttttttttaaagc

miR-26a: gcagttcaagtaatccaggatag ggtccagtttttttttttttttttagc

miR-29a: cgcagtagcaccatctga tccagtttttttttttttttttaaccga

miR-30a: gcagtgtaaacatcctcgac tccagtttttttttttttttttcttcca

miR-30e: cgcagtgtaaacatccttgac tccagttttttttttttttttttcttcca

miR-193: ggtctttgcgggcaag ggtccagtttttttttttttttttcatc

Let-7c: gcagtgaggtagtaggttgt ggtccagttttttttttttttttttaacca

p21: cgaagtcagttccttgtggag catgggttctgacggacat.

mp21: gagcaaagtgtgccgttgtc ggtttggagactgggagagg

mHPRT: tgatagatccattcctatgactgtaga aagacattctttccagttaaagttgag

hRPL21: ccttgcgtgtggagagagaat ggcttctactcgaacaagatcct

**Viability assay**

Cells were cultured in a 96 well plate and 2 days after UV radiation 10ul AQueousOne Solution Cell Proliferation assay (Promega) was added to the wells. Subsequently, the plate was incubated at 37°C for 1 hour. The absorbance was then measured at 490nm in a GloMax 96 well plate reader (Promega).

**Immunofluorescence**

Cells were grown on 13mm coverslips in a 24-well plate to facilitate immunofluorescence stainings. Cells were washed with Tris Buffered Saline (TBS) on ice before fixation by 4% formalin for 30 minutes on ice. After fixation, cells were washed twice in TBS and permeabilized with 0.1% TritonX-100 in TBS for 3 minutes on room temperature. Subsequently, cells were washed twice before quenching with 50mM glycine in TBS for 10 minutes. Cells were then washed again and then incubated for 30 minutes with 5% normal horse serum (NHS) in 0.2% gelatin-TBS solution to reduce background staining. In order to stain our proteins of interest, the coverslips were put upside down on 30µl droplets containing the primary antibody 0.2% gelatin-TBS on parafilm in a humid chamber. Following overnight incubation at 4°C, the cells were washed 3 times in 0.2% gelatin-TBS. subsequently, the cells were incubated in the secondary antibodies for one hour at room temperature. The coverslips were mounted with soft set mounting medium with DAPI (Vectashield), after washing twice in 0.2% gelatin-TBS, once with TBS and once briefly in $H_2O$. Images were obtained using LSM700 Zeiss Microscope and p-p53 and p-ATM positive cells were quantified with FIJI [23].

**Vesicle uptake measurement**

EVs were fluorescently labeled with a PKH26 red fluorescent cell linker kit (Sigma). Isolated vesicles from cell culture medium were dissolved in 400ul PBS and added to 600ul Diluent C containing 4ul PKH26 dye. This solution was incubated for 10 minutes at room temperature before the reaction was stopped by adding 1 ml of 1% BSA in PBS, vortexing and a 5 minute incubation at room temperature. After adding another ml PBS, the mixture was transferred to ultracentrifuge tubes (Beckman, #328874). The vesicles were centrifuged in a Sw60 rotor at 31,200 rpm (=Avg RCF 100,000) for 1hour at 4°C. After removing the supernatant, the pellet was dissolved in 500ul PBS containing 0.01% BSA and transferred to an Eppendorf tube. IMR90 cells were incubated with the labeled EVs for 4 hours before they were fixed to determine vesicle uptake in these cells. After fixation, green fluorescent PKH67 dye in dilutent c was added to the cells to label the cell membrane before the coverslips were mounted and imaged as described. Accordingly, separate cells could be distinguished and the amount of vesicles taken up per cell could be quantified using FIJI.

## Results

In aged and UV-irradiated cells, a specific subset of microRNAs is upregulated. We have previously shown that these microRNAs inhibit apoptosis after damage and therefore termed them the cell preservation miRNAs. Since miRNAs are known to be secreted in EVs and cell preservation miRNAs were found in the serum of centenarians, we wondered if these were transferred to recipient cells as well and whether they are involved in the DNA damage response. Therefore, we radiated cells with 10J UV and isolated vesicles from the cell culture medium 1 day after. We first wanted to confirm that we indeed isolated vesicles from these damaged cells. Furthermore, in this study we were not interested in the effect of apoptotic bodies and therefore we wanted to ensure that we only isolated exosomes and microvesicles. To this end, we measured our isolated vesicles on the qNano machine. This machine is able to detect the size and charge of particles present in a fluid by driving them through a nanopore. This showed that our isolated vesicles were mostly around 60-80 nm (Figure 1a). Since exosomes are thought to be around 40-100 nm, we indeed mainly isolated exosomes. A smaller amount of vesicles was detected that could be microvesicles (100-1000nm) and no vesicles larger than 280nm were isolated, indicating that we did not use apoptotic bodies in our experiments. Additionally, we did not detect a significant difference in vesicle size between vesicles isolated from irradiated and mock-irradiated cells. However, we did confirm that UV-irradiated cells secrete slightly more vesicles per cell (Figure 1b). Overall, these results give an indication that we were indeed able to isolate vesicles and that we did not obtain unwanted vesicles or debris.
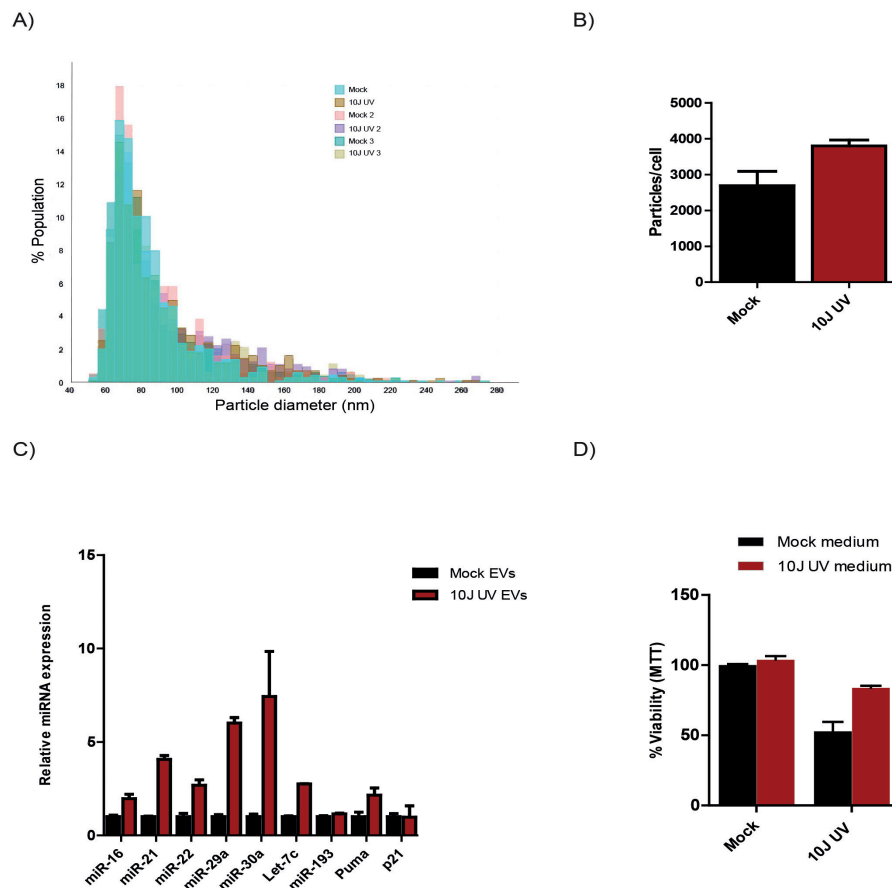
A)



B)



C)



D)



**Figure 1: Extracellular vesicles transfer cell preservation miRNAs after UV irradiation**
A) Isolated extracellular vesicles (EVs) were analyzed on the qNano machine to examine the size of EVs released by mock or UV treated cells (n=3). B) The amount of EVs secreted by mock or UV irradiated cells was quantified using the EVQuant method (n=2). C) Recipient cells were treated with EVs from mock or irradiated cells. In order to determine whether cell preservation microRNAs are activated in cells treated with EVs from UV irradiated cells, a QPCR for these microRNAs was performed (n=3). miR193, p21 and Puma RNA levels were examined as a control. D) Recipient cells were incubated with medium from mock or UV-radiated cells before another dose of UV. Viability was measured 2 days later through a CellTiter 96 AQueous One Solution cell proliferation assay.

Next, we wondered whether vesicles that are released from damaged cells have a different effect on these recipient cells compared to vesicles secreted by healthy cells. Therefore, we added vesicles isolated from the medium of irradiated IMR90 fibroblasts to otherwise untreated or undamaged recipient cells. We compared these results to cells that received vesicles from undamaged cells and to cells that did not receive any vesicles, to exclude the effects of vesicle uptake in general. Interestingly, we indeed observed a subset of cell preservation microRNAs upregulated in recipient

7

169

cells after treatment with EVs from irradiated cells (Figure 1c). As a control we determined the level of miR-193 in recipient cells, a microRNA that we normally do not see upregulated in UV irradiated cells. Indeed, this microRNA was not upregulated either in our recipient cells. Additionally, we observed a slight increase in Puma mRNA expression but no increase in p21 mRNA. On a protein level, we did not detect a difference in Puma or p21 expression between cells treated with vesicles from mock versus irradiated cells, indicating that these cells did not activate known DDR outcomes, such as cell cycle arrest or apoptosis (sup. Figure 1). Furthermore, when we radiated recipient cells that were incubated in cell culture medium from UV-radiated cells, these cells showed to be more UV resistant than cells that received medium from non-radiated cells (Figure 1d).

The cell preservation miRNAs are known to be rapidly induced after 10J UV radiation and return to normal levels within a day. However, we detected a miRNA upregulation one day after recipient cells were treated with the EVs. We therefore wondered whether a more durable DNA damage response was activated in these recipient cells. Therefore, we performed an immunofluorescence staining on the recipient cells for activated ATM (p-ser1981), phosphorylated ATM/ATR targets (p-SQ/TQ sites) and phosphorylated p53 (ser15), in order to determine whether a DNA damage response can be transferred via vesicles. Indeed, we witnessed an increase in ATM signaling after treatment with EVs derived from UV-damaged cells, since both the phosphorylation of ATM and the ATM target proteins increased (Figure 2a). In addition, p53 activation increased, confirming the activation of DDR signaling (Figure 2b). However, we did not observe a clear accumulation of γH2AX foci after treatment with EVs from UV-irradiated cells. (sup. Figure 1). Thus, an ATM-dependent DNA damage response is induced in recipient cells without the presence of the DNA damage that normally activates this protein.

Since extracellular vesicles appeared to transfer a DNA damage response after UV damage, we wondered whether the same occurs after different stressors. Therefore, we isolated vesicles 1 day after irradiating NIH3T3 cells with either UV or ionizing radiation (IR). We confirmed that both p-ATM and p-p53 were increased after treatment with EVs from UV-irradiated cells (Figure 3). Interestingly, we did not witness this effect after treatment with vesicles from cells damaged with IR. In this condition we did observe p-ATM-positive cells, however this did not appear to differ from mock-treated cells. In addition, we did not detect an upregulation of cell preservation microRNAs. Thus, this indicates that the difference between UV and IR damage and the concomitant DNA damage response determines the transfer of cell preservation microRNAs to recipient cells.
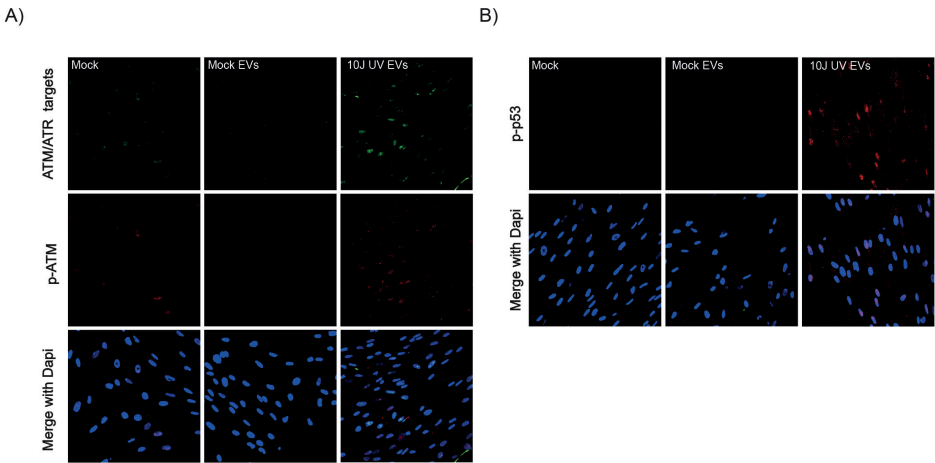
**Figure 2: Extracellular vesicles transfer a DNA damage response to recipient cells after UV irradiation**
A+B) Recipient cells were treated with EVs from mock or irradiated cells or with no EVs (mock). An immunofluorescence staining was performed for phosphorylation of ATM, ATM substrates and p53, in order to determine DDR activation in recipient cells. Representative pictures are shown (n=3).
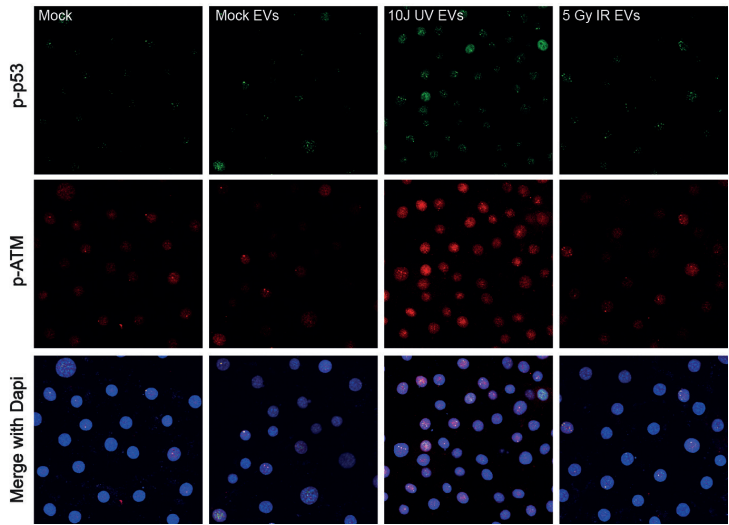


**Figure 3: Extracellular vesicles from IR-treated cells do not activate ATM and p53 in recipient cells**
Recipient cells were either untreated or treated with EVs from mock or UV-radiated cells or with EVs from cells that received IR. Phosphorylation of p53 and ATM was determined by an immunofluorescence staining to examine the DDR (n=3).

Since we were mainly interested in the effect of vesicles from damaged cells on recipient cells during aging, we explored the effects of vesicles from young and aged organisms on recipient cells. For this purpose we isolated EVs from mouse serum, since we have previously shown that our cell preservation microRNAs are abundant in serum from human centenarians (unpublished data, MB, JH, JP). After isolation, we treated mouse NIH3T3 cells with the vesicles in order to exclude possible effects from inter species differences. Interestingly, we observed p53 activation after treatment with EVs obtained from 2 year old week old mice, but not after treatment with EVs from young mice (Figure 4). However, this signal was mainly seen in the cytoplasm. Furthermore, we determined cell preservation microRNA levels in treated cells. Indeed, we did detect a slight upregulation of a subset of microRNAs. However, the effect of EVs from aged mice appeared to be smaller than the effect of the UV-induced vesicles on recipient cells, possibly due to a lower cell preservation microRNA expression or dilution by other factors present in serum. Overall, these results indicate that a DNA damage response is possibly transferred to recipient cells during aging as well.
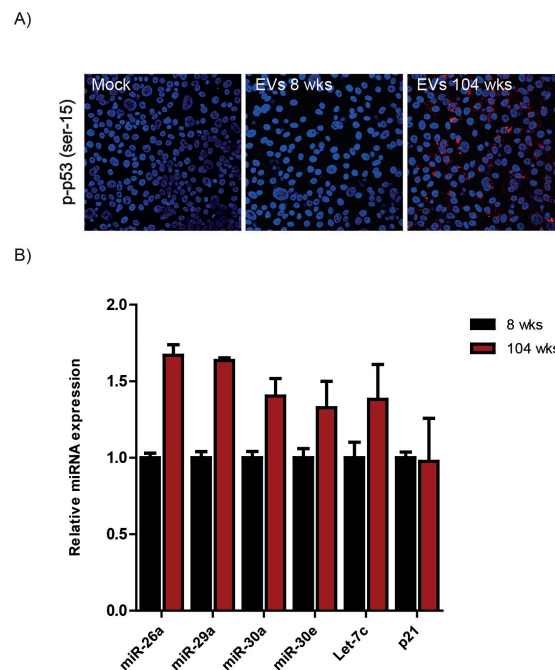


**Figure 4: EVs from aged mouse serum induce a DDR in recipient cells**
A) Recipient cells were either untreated or treated with EVs from young or aged mice. P-p53 was stained to determine DDR activation after vesicle treatment.
B) Cells were treated as in (A). Cell preservation microRNA levels were determined by QPCR (n=3). P21 mRNA level was measured as a control.

## Discussion

Extracellular vesicles are involved in intercellular communication after DNA damage. During aging, this communication could affect tissue function and influence disease progression. However, more research is needed to fully understand the effect of DNA damage-induced EV secretion during aging. In this preliminary study, we showed that extracellular vesicles can transfer a DNA damage response to recipient cells. We isolated EVs from the cell culture medium of UV-irradiated cells and observed an upregulation of p-ATM, p-p53 and cell preservation microRNAs in recipient cells treated with the isolated vesicles.

We measured the vesicle size of our isolated EVs and we observed that we mainly isolated exosomes and microvesicles. However, to further exclude the possibility that we also isolated apoptotic bodies or even cellular debris, we could use electron microscopy or atomic force microscopy to detect these extremely small particles. Although we did not aim to include apoptotic bodies in our study, these vesicles could be involved in signaling as well. For example, apoptotic cancer cells are known to promote survival in neighboring cancer cells [24]. This could be facilitated by apoptotic bodies as well. To distinguish the separate role of exosomes, microvesicles and apoptotic bodies in the DDR, we could isolate these three different EV subtypes. This remains challenging, but isolation based on size and membrane composition might be achievable. The EV subtypes are expected to have a separate function, since they originate from distinct cellular compartments. For example, although both exosomes and microvesicles proved to be taken up by recipient cells, it has been demonstrated that their content differs [25, 26]. Furthermore, microvesicles have shown to be able to deliver plasmid DNA into recipient cells, while exosomes did not [25].

Although recipient cells show upregulation of key DDR proteins and microRNAs, it remains unclear how this response is transferred. It is known that extracellular vesicles often contain high levels of microRNAs and that these microRNAs influence cellular processes when taken up by other cells. Since cell preservation microRNAs are highly expressed after UV, it appears likely they are secreted from these cells in EVs. However, multiple mechanisms could explain our observations. For example, it is possible that the microRNAs are upregulated due to DNA damage in recipient cells. Namely, ionizing radiation showed to induce secretion of EVs that create DNA damage in recipient cells [27], [28] and EVs from IR-treated cells showed γH2AX staining [29]. Furthermore, EVs isolated from the bone marrow of X-Ray irradiated mice induce chromosomal aberrations and a DNA damage response in recipient mice. In these mice, γH2AX foci were detected in splenocytes [30]. Although we do

7

not see an increase in γH2AX, this needs to be further investigated. For example, by additional stainings for DNA damage markers or experiments in DNA repair deficient cells. Furthermore, most cell preservation microRNAs can be induced independently of DNA damage by ATM activation in recipient cells [31]. It is therefore possible that EVs transfer ATM activating factors after UV damage, thereby inducing ATM signaling and microRNA expression in recipient cells. Possible factors could be microRNAs targeting ATM inhibitors, DNA fragments or R-loops that are created at sites of transcription-blocking lesions after UV damage [32][33]. To test these multiple hypotheses, various experiments should be performed. First, total RNA content of EVs can be isolated and sequenced. It is then possible to determine whether cell preservation microRNAs are upregulated in these vesicles after UV damage. Additionally, it can be determined how the DDR is activated in recipient cells by for example ATM inhibition before vesicle treatment, overexpressing RNAseH1 to degrade R-loops and perform total RNA sequencing on recipient cells.

Although EVs secreted after UV irradiation induce a DDR in recipient cells, we do not observe this after IR. This difference could provide information about the mechanism of the DDR transfer. We have previously shown that the cell preservation microRNAs are not upregulated after IR, possibly because mainly transcriptional stress induces these microRNAs. Since UV-radiation induces transcription stress and IR does not, this could explain the absence of cell preservation microRNAs in recipient cells after treatment of IR EVs. Although vesicle loading is tightly regulated and vesicle content might not completely relate to donor cell levels, the content of EVs has shown to somewhat reflect the status of the donor cells [34]. Therefore, when cell preservation microRNAs are highly upregulated in cells after UV and not after IR, this most likely influences the abundancy of these microRNAs in EVs. Furthermore, if the cell preservation microRNAs are upregulated indirectly in recipient cells, an unknown factor is loaded into EVs after UV, but not after IR, to induce a DDR in recipient cells. However, possible factors that are secreted into EVs are currently unknown.

There is no evidence that the release of EVs is increased during aging. However, EV content and characteristics are expected to be altered during aging and in age-related diseases [35]. We observe EVs isolated from aged mouse serum to induce a DDR in recipient cells, indicating that these vesicles indeed differ in content from young counterparts. However, it remains unclear what factor in aged EVs induces this DDR. It has been previously shown that microRNAs are differentially expressed in EVs during aging. For example, specific miRNAs are upregulated in bone marrow derived vesicles with age [36] and differential microRNA expression was found in circulating EVs from patients with cognitive decline compared to healthy individuals

[37]. Besides miRNAs, it has been demonstrated that EVs from aged rat serum contain an increased ROS concentration that could possibly induce a DDR in recipient cells [38]. Furthermore, aged cells are known to release waste products through EVs that in turn influences neighboring cells. For example, Alzheimer's disease associated proteins are secreted in EVs, possibly to alleviate the cell from these toxic proteins [39]. This indicates that EVs could have a protective function during Alzheimer's disease. However, it has been shown that toxic tau proteins are spread through EVs to recipient cells, and that this could contribute to disease pathology [40, 41]. The activation of DDR proteins and microRNAs in recipient cells most likely has a significant biological effect. We previously showed that cell preservation microRNAs actively repress apoptosis when DNA damage occurs. Therefore, we expect that the transfer of these microRNAs via EVs protects recipient cells from consecutive DNA damage. A protective effect of EVs on recipient cells has been described before. For example, cells treated with EVs from heat-shocked cells are more resistant to heat shock themselves [42] and ROS expression in cells induces them to secrete vesicles that enhance ROS resistance in recipient cells [43]. Furthermore, *in vivo* studies show that UV light induces melanocytes to produce EVs that protect melanocytes and keratinocytes against further damage [44], [45]. Thus, a systemic cell preservation response transferred through EVs could influence survival of recipient cells *in vivo.* Possibly, this microRNA upregulation has negative effects as well, since inhibition of apoptosis could facilitate tumorigenesis and chemo- and radiotherapy resistance. For example, EVs promote radiotherapy resistance through transferring microRNAs that repress PTEN in recipient cancer cells [46]. Thus, EVs secreted by damaged or stressed cells could prepare neighboring cells to consecutive damage and thereby protect tissue homeostasis, but also promote cancer therapy resistance. Overall, EVs likely are critical for intercellular communication during aging. Due to the increase in damaged cells during aging, cell preservation microRNA secretion is expected to be induced. Thereby, the tissue microenvironment is altered during aging, influencing tissue integrity and age-related diseases.

7
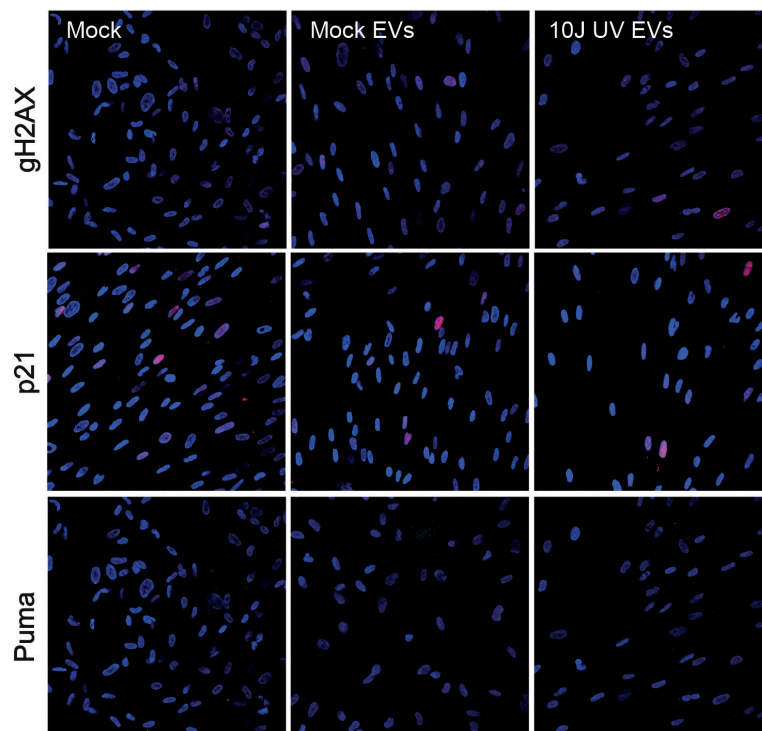
**Supplementary figure 1: EVs from UV-radiated cells do not increase p21 and Puma expression**

EVs from mock or UV-radiated cells were added to recipient cells and an immunofluorescence staining was performed for p21 and Puma. Representative pictures are shown (n=3).

## References

1.  Hoeijmakers, J.H., *DNA damage, aging, and cancer.* N Engl J Med, 2009. **361**(15): p. 1475-85.

2.  Coppe, J.P., et al., *The senescence-associated secretory phenotype: the dark side of tumor suppression.* Annu Rev Pathol, 2010. **5**: p. 99-118.

3.  Kang, T.W., et al., *Senescence surveillance of pre-malignant hepatocytes limits liver cancer development.* Nature, 2011. **479**(7374): p. 547-51.

4.  Hoenicke, L. and L. Zender, *Immune surveillance of senescent cells--biological significance in cancer- and non-cancer pathologies.* Carcinogenesis, 2012. **33**(6): p. 1123-6.

5.  Demaria, M., et al., *An essential role for senescent cells in optimal wound healing through secretion of PDGF-AA.* Dev Cell, 2014. **31**(6): p. 722-33.

6.  Patra, V., S.N. Byrne, and P. Wolf, *The Skin Microbiome: Is It Affected by UV-induced Immune Suppression?* Front Microbiol, 2016. **7**: p. 1235.

7.  Nasti, T.H. and L. Timares, *Inflammasome activation of IL-1 family mediators in response to cutaneous photodamage.* Photochem Photobiol, 2012. **88**(5): p. 1111-25.

8.  Grivennikov, S., et al., *IL-6 and Stat3 are required for survival of intestinal epithelial cells and development of colitis-associated cancer.* Cancer Cell, 2009. **15**(2): p. 103-13.

9.  Crescitelli, R., et al., *Distinct RNA profiles in subpopulations of extracellular vesicles: apoptotic bodies, microvesicles and exosomes.* J Extracell Vesicles, 2013. **2**.

10. Valadi, H., et al., *Exosome-mediated transfer of mRNAs and microRNAs is a novel mechanism of genetic exchange between cells.* Nat Cell Biol, 2007. **9**(6): p. 654-9.

11. Chen, X., et al., *Secreted microRNAs: a new form of intercellular communication.* Trends Cell Biol, 2012. **22**(3): p. 125-32.

12. Jelonek, K., et al., *Ionizing radiation affects protein composition of exosomes secreted in vitro from head and neck squamous cell carcinoma.* Acta Biochim Pol, 2015. **62**(2): p. 265-72.

13. Arscott, W.T., et al., *Ionizing radiation and glioblastoma exosomes: implications in tumor biology and cell migration.* Transl Oncol, 2013. **6**(6): p. 638-48.

14. Villarroya-Beltri, C., et al., *Sumoylated hnRNPA2B1 controls the sorting of miRNAs into exosomes through binding to specific motifs.* Nat Commun, 2013. **4**: p. 2980.

15. Yu, X., S.L. Harris, and A.J. Levine, *The regulation of exosome secretion: a novel function of the p53 protein.* Cancer Res, 2006. **66**(9): p. 4795-801.

16. Lehmann, B.D., et al., *Senescence-associated exosome release from human prostate cancer cells.* Cancer Res, 2008. **68**(19): p. 7864-71.

7

17. Gervais, F.G., et al., *Involvement of caspases in proteolytic cleavage of Alzheimer's amyloid-beta precursor protein and amyloidogenic A beta peptide formation.* Cell, 1999. **97**(3): p. 395-406.

18. Camplejohn, R.S., et al., *Apoptosis, ageing and cancer susceptibility.* Br J Cancer, 2003. **88**(4): p. 487-90.

19. Feng, Z., et al., *Declining p53 function in the aging process: a possible mechanism for the increased tumor incidence in older populations.* Proc Natl Acad Sci U S A, 2007. **104**(42): p. 16633-8.

20. Suh, Y., et al., *Aging alters the apoptotic response to genotoxic stress.* Nat Med, 2002. **8**(1): p. 3-4.

21. Yang, Y., et al., *Exosomal transfer of miR-30a between cardiomyocytes regulates autophagy after hypoxia.* J Mol Med (Berl), 2016. **94**(6): p. 711-24.

22. Matsuura, K., et al., *Circulating let-7 levels in plasma and extracellular vesicles correlate with hepatic fibrosis progression in chronic hepatitis C.* Hepatology, 2016. **64**(3): p. 732-45.

23. Schindelin, J., et al., *Fiji: an open-source platform for biological-image analysis.* Nat Methods, 2012. **9**(7): p. 676-82.

24. Tang, D., et al., *HMGB1 release and redox regulates autophagy and apoptosis in cancer cells.* Oncogene, 2010. **29**(38): p. 5299-310.

25. Kanada, M., et al., *Differential fates of biomolecules delivered to target cells via extracellular vesicles.* Proc Natl Acad Sci U S A, 2015. **112**(12): p. E1433-42.

26. Minciacchi, V.R., M.R. Freeman, and D. Di Vizio, *Extracellular vesicles in cancer: exosomes, microvesicles and the emerging role of large oncosomes.* Semin Cell Dev Biol, 2015. **40**: p. 41-51.

27. Al-Mayah, A., et al., *The non-targeted effects of radiation are perpetuated by exosomes.* Mutat Res, 2015. **772**: p. 38-45.

28. Al-Mayah, A.H., et al., *Possible role of exosomes containing RNA in mediating nontargeted effect of ionizing radiation.* Radiat Res, 2012. **177**(5): p. 539-45.

29. Wang, Z. and P.M. Lieberman, *The crosstalk of telomere dysfunction and inflammation through cell-free TERRA containing exosomes.* RNA Biol, 2016. **13**(8): p. 690-5.

30. Szatmari, T., et al., *Extracellular Vesicles Mediate Radiation-Induced Systemic Bystander Signals in the Bone Marrow and Spleen.* Front Immunol, 2017. **8**: p. 347.

31. Zhang, X., et al., *The ATM kinase induces microRNA biogenesis in the DNA damage response.* Mol Cell, 2011. **41**(4): p. 371-83.

32. Takahashi, A., et al., *Exosomes maintain cellular homeostasis by excreting harmful DNA from cells.* Nat Commun, 2017. **8**: p. 15287.

33. Tresini, M., et al., *The core spliceosome as target and effector of non-canonical ATM signalling.* Nature, 2015. **523**(7558): p. 53-8.

34. Antonyak, M.A. and R.A. Cerione, *Emerging picture of the distinct traits and functions of microvesicles and exosomes.* Proc Natl Acad Sci U S A, 2015. **112**(12): p. 3589-90.

35. Eitan, E., et al., *Age-Related Changes in Plasma Extracellular Vesicle Characteristics and Internalization by Leukocytes.* Sci Rep, 2017. **7**(1): p. 1342.

36. Davis, C., et al., *MicroRNA-183-5p Increases with Age in Bone-Derived Extracellular Vesicles, Suppresses Bone Marrow Stromal (Stem) Cell Proliferation, and Induces Stem Cell Senescence.* Tissue Eng Part A, 2017. **23**(21-22): p. 1231-1240.

37. Rani, A., et al., *miRNA in Circulating Microvesicles as Biomarkers for Age-Related Cognitive Decline.* Front Aging Neurosci, 2017. **9**: p. 323.

38. Bertoldi, K., et al., *Circulating extracellular vesicles in the aging process: impact of aerobic exercise.* Mol Cell Biochem, 2017.

39. Perez-Gonzalez, R., et al., *The exosome secretory pathway transports amyloid precursor protein carboxyl-terminal fragments from the cell into the brain extracellular space.* J Biol Chem, 2012. **287**(51): p. 43108-15.

40. Baker, S., J.C. Polanco, and J. Gotz, *Extracellular Vesicles Containing P301L Mutant Tau Accelerate Pathological Tau Phosphorylation and Oligomer Formation but Do Not Seed Mature Neurofibrillary Tangles in ALZ17 Mice.* J Alzheimers Dis, 2016. **54**(3): p. 1207-1217.

41. Polanco, J.C., et al., *Extracellular Vesicles Isolated from the Brains of rTg4510 Mice Seed Tau Protein Aggregation in a Threshold-dependent Manner.* J Biol Chem, 2016. **291**(24): p. 12445-66.

42. Bewicke-Copley, F., et al., *Extracellular vesicles released following heat stress induce bystander effect in unstressed populations.* J Extracell Vesicles, 2017. **6**(1): p. 1340746.

43. Grindheim, A.K. and A. Vedeler, *Extracellular vesicles released from cells exposed to reactive oxygen species increase annexin A2 expression and survival of target cells exposed to the same conditions.* Commun Integr Biol, 2016. **9**(4): p. e1191715.

44. Waster, P., et al., *Extracellular vesicles are transferred from melanocytes to keratinocytes after UVA irradiation.* Sci Rep, 2016. **6**: p. 27890.

45. Bin, B.H., et al., *Fibronectin-Containing Extracellular Vesicles Protect Melanocytes against Ultraviolet Radiation-Induced Cytotoxicity.* J Invest Dermatol, 2016. **136**(5): p. 957-66.

46. Zheng, Y., et al., *The extracellular vesicles secreted by lung cancer cells in radiation therapy promote endothelial cell angiogenesis by transferring miR-23a.* PeerJ, 2017. **5**: p. e3627.

7

# CHAPTER 8

## Organotypic slice culture of adult mouse liver, kidney and heart

**Marjolein P. Baar[1], Marco Schreijenberg[1], Marina Magin[1], Jan H.J. Hoeijmakers[1,2,3], Peter L.J. de Keizer[1,4], Joris Pothof[1]**

[1] Department of Molecular Genetics, Erasmus Medical Center, Rotterdam.

[2] Princess Máxima Centre for Pediatric Oncology, PO Box 113, 3720 AC Bilthoven, the Netherlands

[3] CECAD Forschungszentrum Raum 5.068, Joseph Stelzmann Strasse 26, 50931 Cologne, Germany

[4] Center for Molecular Medicine, Department of Biomedical Genetics, University Medical Center Utrecht, Utrecht University

## Abstract

Most experiments are performed in cell cultures or in various model organisms. However, it remains challenging to conduct mechanistic experiments in a representative micro-environment, since cell cultures do not show a proper tissue context while generating an appropriate *in vivo* model takes time. Organotypic slice culture is an intermediate technique in which mouse organs are sliced into 200 µm sections and kept for some time in culture. This technique can combine the advantages of both *in vitro* and *in vivo* systems. Molecular mechanistic experiments can be conducted while the natural tissue niche is largely maintained. Since adult tissue is often required for these experiments, we have optimized a protocol to culture adult mouse kidney, liver and heart slices *ex vivo*. We show that it is feasible to culture liver and heart slices for 3 days without loss of viability or tissue integrity. In contrast, kidney slices only remained intact for one day after slicing. This protocol allows for short term experiments in both healthy and diseased tissue from any species and at any age. In conclusion, these adult organotypic slices can be employed in various experiments, since they uphold a proper tissue context *ex vivo*.

## Introduction

Model systems are essential to study biological processes and disease etiology. Additionally, it is imperative to choose the most relevant model system for each research question. Many experiments are performed in 2D cell cultures, since these are often easy to maintain and to manipulate for molecular and cell biological mechanistic studies. There is a great variety of cell lines available from almost all human tissue, both healthy and diseased. Accordingly, many functional experiments can be executed in cells that are relevant for the biological process or disease that is studied. However, these are all dividing cells while a large fraction of an organ consists of a precise organization of different, terminally differentiated, non-dividing and post-mitotic cells. These cells can show pathology and can play an important role in disease progression. Post-mitotic cells can be obtained through differentiation of induced pluripotent stem cells (iPSCs) [1, 2] but in this setting, aging and disease phenotype remain difficult to study. In addition, *in vitro* cell cultures do not resemble the *in vivo* environment of these cells nor the cell or organ history in the animal. Organs consist of a variety of cells that each have a different role in maintaining tissue function and all contribute to the tissue microenvironment. Therefore, there is no relevant micro-environment in 2D cultures. In short, diseases are often multifactorial and the cellular microenvironment is crucial in deciding cell fate during disease.

In contrast to cell cultures, studies in experimental organisms provide the proper tissue context and can provide insight into how cells behave during disease progression, but mechanistic studies in this system are time consuming, technically demanding and expensive. Also, there is a public demand for the reduction of animal experiments. Therefore, there is a growing interest for developing intermediate models that combine the advantages of both *in vitro* and *in vivo* systems. These new systems should in theory resemble the *in vivo* environment more than 2D cell cultures, but should also be easily manipulated.

Organoids are 3D cultures that originate from a single stem cell isolated from an organ of interest [3]. This culture thus can contain all cell types this stem cell can generate. For example, organoids generated from intestinal stem cells contain the crypts and villi that comprise the intestine *in vivo* [4]. Multiple intestinal cell types are seen in these organoids, such as paneth cells, goblet cells, and other epithelial cells [5]. These cells within an organoid are surrounded by their natural tissue niche, and behave like they would *in vivo* through interaction with neighboring cells. Most experiments that are typically performed in 2D cell cultures are now also feasible in 3D organoids. For example, viability assays, mass spectrometry and multiple imaging

8

techniques can be performed [6]. In addition, it has been shown that CRIPR/Cas9 gene editing is possible in organoids [7]. Accordingly, diseases can be modeled in this system such as cancer, cystic fibrosis and polycystic kidney disease [6-8]. Other clear advantages are that these organoids can be multiplied and cultured over a longer time period and that post-mitotic cells are produced in these structures [9]. However, there are also limitations to this technique. For example, although diseases can be modeled in organoids, disease progression takes time and is multi-factorial. Since organoids retain proliferation, ultimately the disease phenotype in organoids will differ from the *in vivo* situation. This is apparent in aging research, for example, where multiple cell-intrinsic processes and systemic and exogenous factors contribute to a decline in cellular function that ultimately leads to age-related diseases [10]. Organoids obtained from aged tissues, however, rejuvenate through proliferation *in vitro* and therefore do not resemble the aged *in vivo* microenvironment. Furthermore, an organoid always originates from one stem cell and although different cells from a tissue are represented, organoids do not contain every cell of the organ of origin. Lastly, it is important to realize that the micro-environment in an organoid is not the same as *in vivo* [11]. For example, an organoid does not contain fibroblasts or immune cells and they do not have a vasculature structure.

For many experiments a proper tissue physiology is needed and therefore, the usage of organotypic tissue slices has gained popularity as well [12]. These slices are obtained by slicing the organ of interest into thin sections that can be kept alive in culture medium. Although tissue slices cannot be cultured indefinitely, tissue structure is maintained and the slices are easily manipulated for molecular and cell biological studies, e.g. through using siRNAs or small molecule inhibitors [13, 14]. In addition, tissue from aged or diseased organs can in theory be utilized for this technique. These slices provide a relevant microenvironment present at the moment of slicing. Often, fetal or neonatal mouse tissues are used since these have shown to be more plastic and therefore survive longer than adult tissue *ex vivo* [15]. However, fetal tissue does not resemble the *in vivo* situation in which diseases develop. For example, age-related diseases do not occur in a fetal or neonatal environment. Therefore, our objective is to develop a simple method to culture slices from various adult mouse organs. We provide an optimized protocol for adult organotypic slice culture and show that these slices can be kept in culture for two or three days depending on the tissue. Throughout these days the tissue remains viable and tissue integrity is maintained.

## Methods

### Animals

Organs from C57BL/6J mice (age 8-26 weeks) were used in the performed experiments. All experiments were approved by the Dutch animal ethics committee.

### Tissue slice preparation and culture

Adult mouse organs were obtained by sacrificing the mice by CO2 exposure. Livers and kidneys were kept on ice in PBS or culture medium before being sliced. Hearts were flushed *in situ* by retrograde perfusion via the thoracic aorta with pre-oxygenized Tyrode's solution (4°C, NaCl 126.7 mM, $NaH_2PO_4$ 0.4 mM, $NaHCO_3$ 22 mM, KCl 5.4 mM, $CaCl_2$ 1.8 mM, $MgCl_2$ 1.1 mM, Glucose 5 mM, pH 7.4) and pre-oxygenized High Potassium ($HK^+$) solution (4°C, NaCl 120 mM, Kcl 20 mM, $CaCl_2$ 2 mM, $MgCl_2$ 1mM, HEPES 10 mM, Glucose 10 mM, 2,3-butanedione monoxime (BDM) 15 mM, pH 7.4) for one minute respectively. A high potassium concentration was used to inhibit electrical activity, while contractile activity was suppressed by BDM. Hearts were submerged in pre-oxygenized $HK^+$ solution and kept on ice before being sliced. The organs were glued to the specimen holder of a vibrating blade microtome (Leica VT1200) using histoacryl superglue (Bison). Hearts were first embedded into 5% low melting agarose in PBS. The vibrating blade microtome was used to generate 200µm slices of these organs. The machine was set to a blade amplitude of 3 mm and a speed of 0.6 mm/s. During slicing the tissue was kept cold by slicing in ice-cold PBS (liver, kidney) or $HK^+$ solution (heart) in a buffer tray surrounded by ice. In order to prevent tissue damage, a small brush was used to prevent the tissue from folding back and touching the blade during slicing and transferring the slice after slicing. Slices were cultured in 6 well plates on a shaker (60RPM) at 5% CO2 and ambient oxygen. Liver and kidney slices were cultured in Dulbecco's Modified Eagle Medium (DMEM) culture medium supplemented with 10% FCS and 1% pen/strep. Heart slices were cultured in DMEM:Ham's F12 2:1, 2% Fetal Calf Serum, Hydrocortisone 0,3 µg/mL, Insulin 4 µg/mL, Transferrin 4 µg/mL, 3,3',5-triiodothyronin 1 ng/mL, Epidermal Growth Factor 8 ng/mL, Cholera toxin 7 ng/mL, Adenine 0.2 mg/mL, Penicillin/Streptavidin).

### Viability assays

To assess tissue slice viability at least 3 slices were used per condition to allow for variability between slices. Before the measurement the slices were transferred to a 96 well plate with fresh DMEM culture medium. Subsequently, 20 ul AQueousOne Solution Cell Proliferation assay (Promega) was added per well and the plate was incubated for 2 hrs at 37˚C. The slices were removed from the wells before the

8

absorbance was measured at 490nm in a GloMax 96 well plate reader (Promega). The absorbance values were normalized to the weight.

## HE and PAS staining

In order to examine tissue integrity and morphology after slicing, the tissue slices were embedded into paraffin. Paraffin sections were deparaffinized and rehydrated in xylene and in decreasing concentrations of ethanol. To determine tissue morphology, the sections were stained with Gills Hematoxylin (Sigma) for 4 minutes and 30s with Eosin-Y solution. For a periodic acid Schiff (PAS) staining, rehydrated kidney sections were immersed in periodic acid solution for 5 minutes before being rinsed and incubated in Schiff's reagent for 15 minutes. Nuclei were again stained with Gills Hematoxylin (Sigma). All slides were dehydrated, mounted with pertex mounting medium and images were acquired using a bright field microscope (Olympus Bx-40).

## Apoptosis staining

Apoptosis was determined with a TUNEL assay. For this assay rehydrated sections were treated with 20ug/ml ProtK solution in PBS for 15 minutes and permeabilized in 0.1% Triton X-100 in 0.1% sodium citrate. Subsequently, the tissue was labeled for 1 hour with 10% TUNEL enzyme in labeling solution (ROCHE) at 37 ˚C. Nuclei were labeled with Hoechst 33342 (ThermoFisher) before the slides were mounted with soft set mounting medium (Vectashield). Images were acquired using a LSM510 confocal microscope (Zeiss) and the percentage of TUNEL-positive cells was analyzed using CellProfiler software v2.3.

## Connexin-43 staining

For the Connexin-43 (CX43) staining, rehydrated heart sections were boiled for 30 minutes in 10 mM sodium citrate buffer (PH6) for antigen unmasking. Endogenous peroxidase activity was quenched by incubating in 3% hydrogen peroxide for 10 minutes. The sections were permeabilized in 0.05% Tween-20 in Tris Buffered Saline (TBS) and blocked for 30 minutes at room temperature (RT) using 1% albumin from bovine serum in 5% normal goat serum dissolved in TBS. Subsequently, the sections were incubated overnight at 4°C with the primary antibody (rabbit polyclonal anti-Cx43; Santa Cruz sc-9059, 1:150) and 1 hour at RT with the secondary antibody (Goat anti-rabbit IgG-biotine; Vector Labs BA-1000, 1:300 dilution). The sections were then incubated with Avidine/Biotinylated Complex (Vector Labs) for 45 minutes at RT before these complexes were stained with 3,3'-Diaminobenzidine (DAB) chromogen (DAKO) for 20 minutes at RT. Nuclei were stained with methyl green for 11 minutes, dehydrated in n-butanol and xylene and mounted using mounting medium (Pertex).

## Results

To make adult tissue amenable to research and experimentation, we aimed to develop methods to culture adult mouse tissue *ex vivo* (Figure 1).
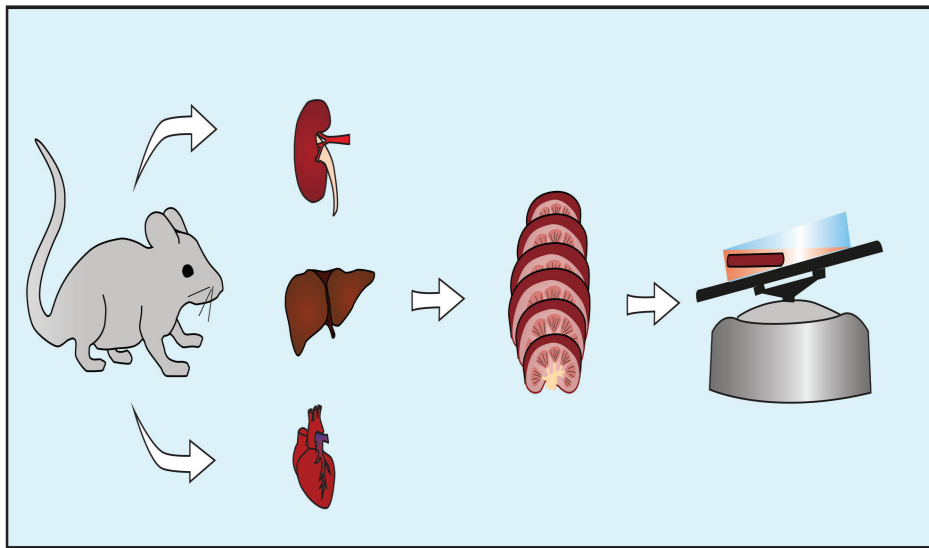


**Figure 1: Schematic overview of the protocol**
Liver, kidney and hearts are isolated from a mouse and sliced into 200um sections using a Leica vibrating blade microtome. The obtained organotypic tissue slices are then cultured in a 6-well plate on a softly rotating shaker.

After testing different devices we found that a vibrating blade microtome is the most suitable for making slices and best preserves tissue morphology after slicing [16]. To optimize our protocol, we isolated multiple organs and made slices that varied in width. Similar to other studies, we observed that the thickness of the slices is essential for cell survival as oxygen and nutrient delivery is more efficient in thinner slices [16-18]. Therefore, we choose to slice 200μm slices for all further experiments, since this was the minimal width we could slice without disrupting tissue structure too much. In addition, we incubated our slices on a slowly rotating shaker to facilitate nutrient and oxygen uptake and tested various media to ensure optimal culture conditions, including DMEM, William's medium E and medium 1 [19]. Surprisingly, we did not observe significant differences in apoptosis in kidney and liver slices after 2 days culture in the separate media types. Since the type of culture medium did not appear to be crucial, we choose to culture these slices in DMEM. Subsequently, we

8

cultured slices from mouse liver, kidney and heart. First, we produced liver slices that we cultured up to 4 days to study the survival of the tissue *ex vivo*. We were able to culture these slices for 3 days without losing normal tissue structure (Figure 2a). Within these 3 days, the tissue appeared to be relatively intact, since nuclei were not lost and the connective tissue seemed normal. However, at day 4 liver tissue integrity was degrading. This loss of tissue structure observed at day 4 corresponded with an increased amount of apoptotic cells (Figure 2b,c). Together, this indicates that these tissue slices are less functional at day 4 compared to the first days after slicing. In contrast, viability was maintained for more than 3 days in these slices (Figure 2d).
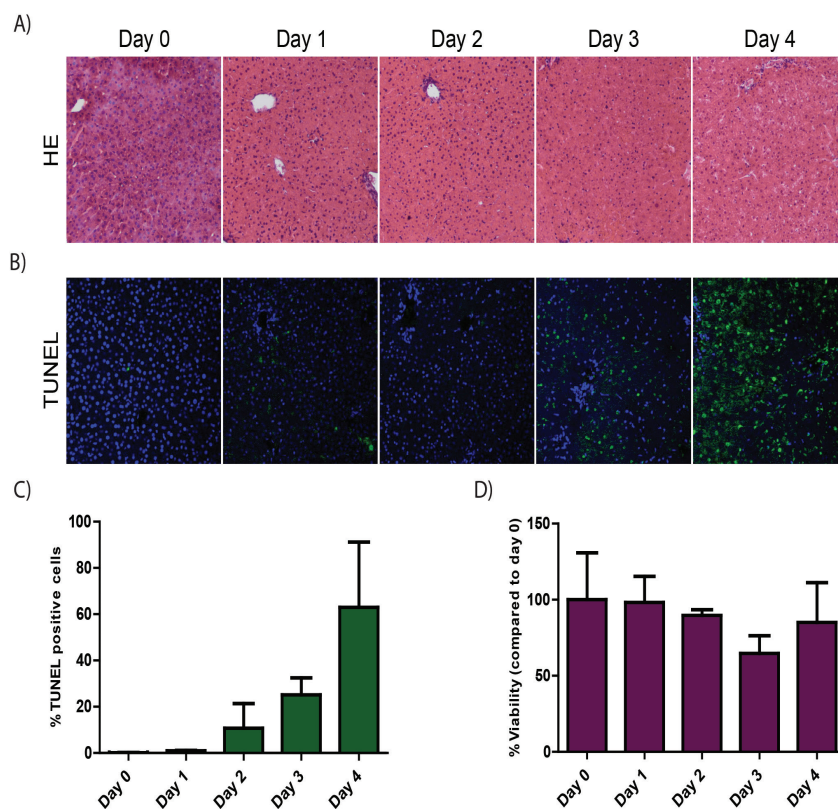


**Figure 2: Tissue structure and viability of organotypic liver slices can be maintained for 3 days ex vivo**
(A) An HE staining was performed on organotypic liver slices fixed on consecutive days to study tissue morphology after slicing. Representative images are shown (n=3). (B) The same slices as in (A) were processed for a TUNEL assay to assess apoptosis. (C) Cell profiler software was used to quantify the percentage of TUNEL-positive cells over time. (D) The viability of liver slices was measured by MTT on different days (n=3).

To determine whether we could obtain similar results with kidney slices, we performed the same assays as for liver. Kidney slices appeared to be viable for 3 days, with a more than 50% drop in viability at day 4 (Figure 3a). However, also in these slices we observed that apoptosis increased earlier than the viability decreased (Figure 3b,c). Already on the first days after slicing we observed a relatively high amount of apoptotic cells, although the percentage of apoptotic cells remained constant up until 2 days. At day 3, however, a clear increase in apoptosis was detected. At day 4 the kidney slices lost most of the nuclei, due to a loss of tissue structure, explaining the drop in percentage of apoptotic cells on this day. In addition, the loss of tissue structure was confirmed by both a PAS and HE staining. These stainings showed that a healthy tissue morphology in kidney slices was only maintained for 1 day in culture. It is clearly seen that the structure deteriorates in later days and that nuclei progressively disappear from the tissue (Figure 3d).Therefore, these kidney slices seem to be more sensitive to slicing injury and less plastic in culture than liver slices.

Similar to liver, normal morphology in heart slices was maintained for at least 3 days (Figure 4a). Most nuclei were still present at day 3 and a normal longitudinal cardiomyocyte organization was observed at this time point. However, after 7 days in culture, tissue structure is clearly disrupted and an increased fraction of nuclei was lost. To further examine tissue structure, we have stained the heart slices for gap junction protein Connexin 43 (Cx43) to determine the level of differentiation in the slices (Figure 4b). Cx43 staining is typically observed microscopically in banded patterns between the cardiomyocytes. Immediately after slicing, the staining indeed showed the characteristic pattern of Cx43 bands between these cells. After 24 hours in culture, the total amount of Cx43 protein appeared to be reduced, but the normal banded distribution remained intact. After 3 days and 7 days in culture, the pattern of Cx43 was similar to the 1 day time point. This data suggest that slicing and culturing of adult mouse heart tissue indeed leads to slight dedifferentiation, but slices still retain characteristics of normal cardiac tissue. In addition, the amount of apoptotic cells in heart slices was not increased on day 3, but was increased significantly on day 7. Together, these results indicate that these slices can be used for experiments until at least day 3 (Figure 4c).

8

A)

B)



C)



D)



E)
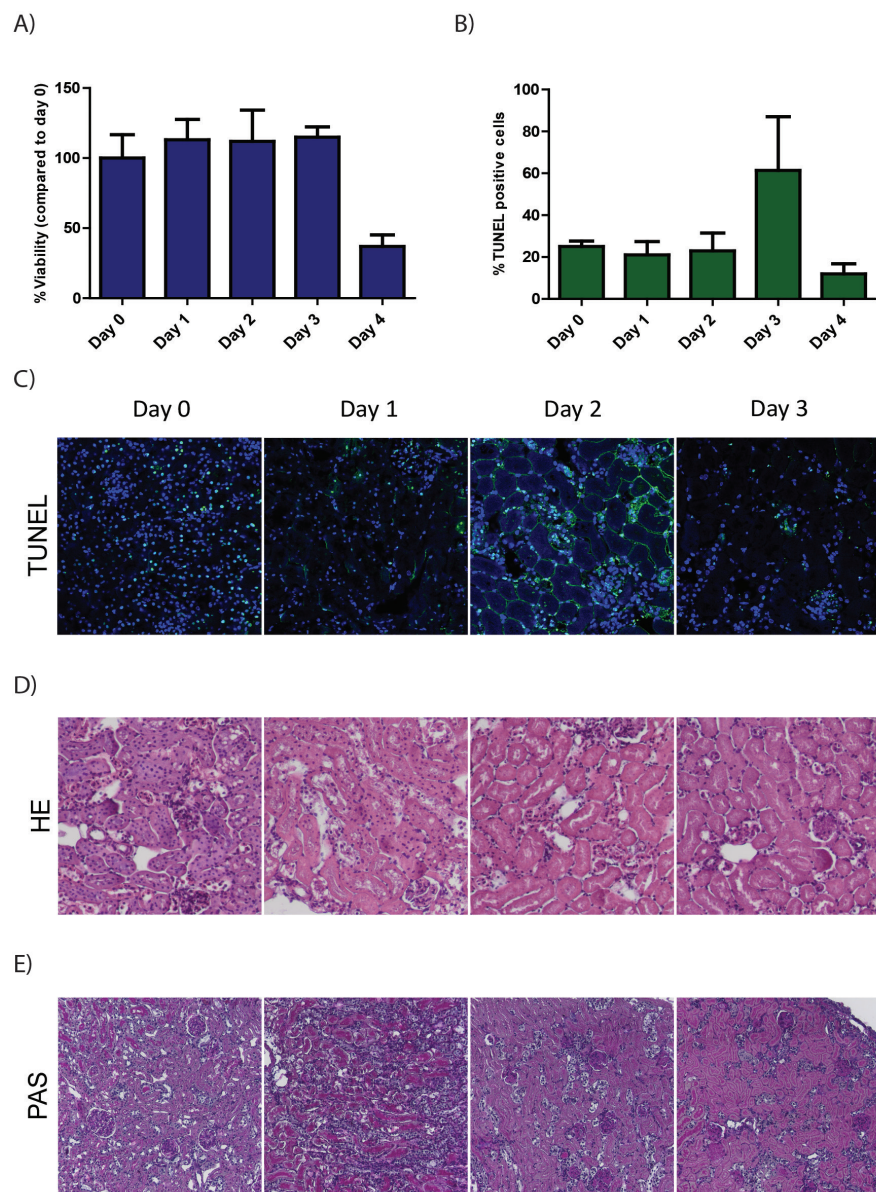


**Figure 3: Organotypic kidney slices lose tissue structure after 1 day in culture**
(A) An MTT assay was performed to determine kidney slice viability over time (n=3). (B) A TUNEL assay was performed to determine the percentage of apoptotic cells in the kidney slices. The results were quantified using the CellProfiler software (n=3). Representative images are shown in (C). (D)Tissue morphology of organotypic kidney slices was examined on consecutive days by an HE staining. Representative images are shown (n=3). (E) The same slices were stained for PAS to further study kidney morphology.

A)



B)



C)



D)



8
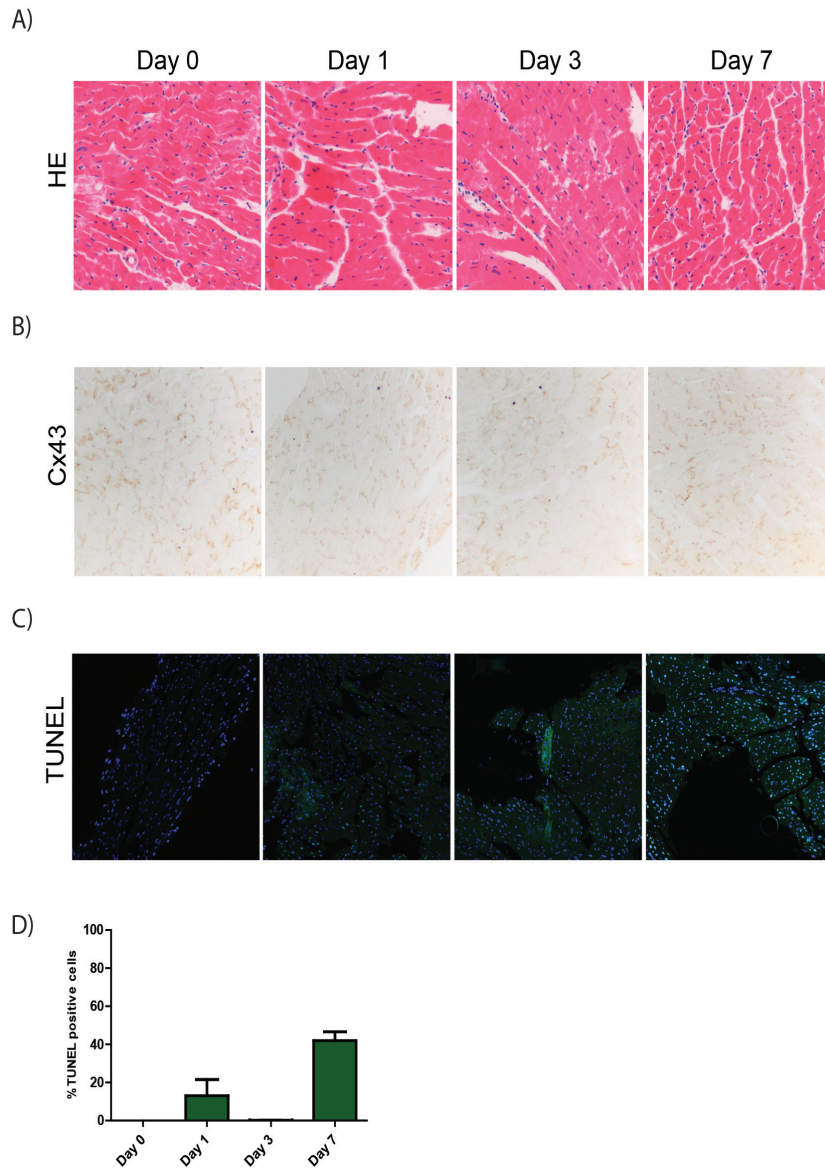
**Figure 4: Organotypic heart slices can be cultured for 3 days without losing tissue integrity**
(A) Heart slices were fixed on consecutive days and stained with HE to examine tissue morphology
(n=3). Representative images are shown. (B) A Cx43 staining was performed on the same slices
to determine whether cardiomyocyte dedifferentiation occurs in organotypic heart slices. (C) The
percentage of apoptotic cells in these heart slices was measured through a TUNEL assay of which
representative images are shown (n=3). (D) The percentage of TUNEL-positive cells was determined
using the CellProfiler software.

## Discussion

Here, we have developed a simple protocol to culture adult slices from mouse liver, kidney and heart to study biological processes in a proper tissue context. We show that liver and heart slices are kept alive for 3 days without loss of tissue integrity, while kidney slices only remain intact for 1 day. Thus, experimental interventions in liver and heart slices should be performed between day 0 and day 3, and kidney slices can be utilized for relatively short experiments. A few days seems short, but adult organotypic slices are known to be very sensitive to slicing injury and cannot regenerate *ex vivo* [15]. For example, others have shown that adult lung tissue is viable in culture for 5 days [20] and thyroid or parotid slices only retain tissue integrity for 48 hours [21, 22]. In contrast, it has previously been shown that it is possible to culture adult mouse hippocampus, whole brain and spinal cord sections for weeks without losing viability [15, 23-25]. However, in some of these studies only viability is measured, while we show that this is not a reliable measurement regarding tissue structure and possibly tissue function. Nevertheless, some studies do show convincingly that brain slices that are kept in culture for a month still have a comparable morphology and function to *in vivo* brains. Hence, it is possible that we did not find the optimal culture conditions for our tissue slices yet. However, it is likely that there are tissue-specific differences in plasticity and the sensitivity to slicing injury. Overall our protocol allows for experiments to be performed in tissue slices over multiple days in a straightforward manner.

Although organotypic slices can only be cultured for a short amount of time, many experiments that are performed *in vitro* seem to be achievable in *ex vivo* tissue slices as well. For example, we show that simple experiments such as viability and apoptosis assays are easily managed in these slices. Furthermore, various experiments in neonatal and adult brain tissue slices show that more elaborate experiments are also feasible. For example, several live imaging techniques are set up [26, 27]. These experiments make use of a transgene present in the model organism or transduce the slices with a viral construct. Additionally, luminescence can be measured in these slices, using a transgene with a luciferase coding region [28]. In order to do mechanistic experiments, it is convenient to use small molecule inhibitors. It has been shown that these inhibitors penetrate tissues sufficiently and therefore have great potential for drug screens [13, 29]. A protocol for culturing adult tissue slices allows for drug testing in a relevant environment. For example, drugs targeting the age-related accumulation of senescent cells can be tested in actually aged tissue [30]. In addition, lentiviral transduction is possible in organotypic tissue slices. So far, this has mainly been used for imaging techniques, but multiple virus strains have shown to successfully transduce tissue slices and it is therefore

probable that RNA interference can be achieved using virus particles as well [31-33]. In contrast, CRISPR/Cas9-mediated gene editing is expected to be challenging. Furthermore, the usage of siRNAs has shown to be less straightforward than in cell cultures, since these oligo's do not readily pass through membranes [34]. However, a siRNA-mediated knock-down is manageable as well, using self-deliverable siRNAs or a gene gun [14, 34]. Accordingly, it is possible to upregulate or downregulate pathways of interest in organotypic tissue slices.

In addition to healthy mouse organs, slices can be obtained and cultured from any species and from healthy or aged and diseased tissue. For example, it has been demonstrated that human *ex vivo* cancer tissue slices can be employed to predict treatment response [35, 36]. Furthermore, human brain slices were shown to be a promising in studying mechanisms underlying Alzheimer's disease [37]. To conclude, organotypic tissue slices can be employed in various research questions and are therefore a valuable tool to study biological processes in an appropriate cellular environment, as well as enable powerful applications for clinical translation.

## Acknowledgements

8

# References

1. Hu, B.Y. and S.C. Zhang, *Differentiation of spinal motor neurons from pluripotent human stem cells.* Nat Protoc, 2009. **4**(9): p. 1295-304.

2. Tsunemoto, R.K., et al., *Forward engineering neuronal diversity using direct reprogramming.* EMBO J, 2015. **34**(11): p. 1445-55.

3. Shamir, E.R. and A.J. Ewald, *Three-dimensional organotypic culture: experimental models of mammalian biology and disease.* Nat Rev Mol Cell Biol, 2014. **15**(10): p. 647-64.

4. Sato, T., et al., *Single Lgr5 stem cells build crypt-villus structures in vitro without a mesenchymal niche.* Nature, 2009. **459**(7244): p. 262-5.

5. Sato, T., et al., *Paneth cells constitute the niche for Lgr5 stem cells in intestinal crypts.* Nature, 2011. **469**(7330): p. 415-8.

6. Dutta, D., I. Heo, and H. Clevers, *Disease Modeling in Stem Cell-Derived 3D Organoid Systems.* Trends Mol Med, 2017. **23**(5): p. 393-410.

7. Driehuis, E. and H. Clevers, *CRISPR/Cas 9 genome editing and its applications in organoids.* Am J Physiol Gastrointest Liver Physiol, 2017. **312**(3): p. G257-G265.

8. Freedman, B.S., et al., *Modelling kidney disease with CRISPR-mutant kidney organoids derived from human pluripotent epiblast spheroids.* Nat Commun, 2015. **6**: p. 8715.

9. Bagley, J.A., et al., *Fused cerebral organoids model interactions between brain regions.* Nat Methods, 2017. **14**(7): p. 743-751.

10. Lopez-Otin, C., et al., *The hallmarks of aging.* Cell, 2013. **153**(6): p. 1194-217.

11. Fatehullah, A., S.H. Tan, and N. Barker, *Organoids as an in vitro model of human development and disease.* Nat Cell Biol, 2016. **18**(3): p. 246-54.

12. Humpel, C., *Organotypic brain slice cultures: A review.* Neuroscience, 2015. **305**: p. 86-98.

13. Sundstrom, L., et al., *Organotypic cultures as tools for functional screening in the CNS.* Drug Discov Today, 2005. **10**(14): p. 993-1000.

14. Arsenault, J., et al., *Regioselective biolistic targeting in organotypic brain slices using a modified gene gun.* J Vis Exp, 2014(92): p. e52148.

15. Tan, G.A., et al., *Organotypic Cultures from the Adult CNS: A Novel Model to Study Demyelination and Remyelination Ex Vivo.* Cell Mol Neurobiol, 2018. **38**(1): p. 317-328.

16. Zimmermann, M., et al., *Improved reproducibility in preparing precision-cut liver tissue slices.* Cytotechnology, 2009. **61**(3): p. 145-52.

17. Mewes, A., H. Franke, and D. Singer, *Organotypic brain slice cultures of adult transgenic P301S mice--a model for tauopathy studies.* PLoS One, 2012. **7**(9): p. e45017.

18. Bingmann, D. and G. Kolde, *PO2-profiles in hippocampal slices of the guinea pig.* Exp Brain Res, 1982. **48**(1): p. 89-96.

19. Garvin, S., et al., *Estradiol increases VEGF in human breast studied by whole-tissue culture.* Cell Tissue Res, 2006. **325**(2): p. 245-51.

20. Gibbs, J.E., et al., *Circadian timing in the lung; a specific role for bronchiolar epithelial cells.* Endocrinology, 2009. **150**(1): p. 268-76.

21. Vickers, A.E., et al., *Thyroid organotypic rat and human cultures used to investigate drug effects on thyroid function, hormone synthesis and release pathways.* Toxicol Appl Pharmacol, 2012. **260**(1): p. 81-8.

22. Warner, J.D., et al., *Visualizing form and function in organotypic slices of the adult mouse parotid gland.* Am J Physiol Gastrointest Liver Physiol, 2008. **295**(3): p. G629-40.

23. Schommer, J., et al., *Method for organotypic tissue culture in the aged animal.* MethodsX, 2017. **4**: p. 166-171.

24. Xiao, L., et al., *Human Dental Pulp Cells Differentiate toward Neuronal Cells and Promote Neuroregeneration in Adult Organotypic Hippocampal Slices In Vitro.* Int J Mol Sci, 2017. **18**(8).

25. Sypecka, J., et al., *The organotypic longitudinal spinal cord slice culture for stem cell study.* Stem Cells Int, 2015. **2015**: p. 471216.

26. Gogolla, N., et al., *Long-term live imaging of neuronal circuits in organotypic hippocampal slice cultures.* Nat Protoc, 2006. **1**(3): p. 1223-6.

27. Dailey, M.E., et al., *Imaging microglia in brain slices and slice cultures.* Cold Spring Harb Protoc, 2013. **2013**(12): p. 1142-8.

28. Chaves, I., et al., *The Potorous CPD photolyase rescues a cryptochrome-deficient mammalian circadian clock.* PLoS One, 2011. **6**(8): p. e23447.

29. Drexler, B., et al., *Organotypic cultures as tools for testing neuroactive drugs - link between in-vitro and in-vivo experiments.* Curr Med Chem, 2010. **17**(36): p. 4538-50.

30. Baar, M.P., et al., *Targeted Apoptosis of Senescent Cells Restores Tissue Homeostasis in Response to Chemotoxicity and Aging.* Cell, 2017. **169**(1): p. 132-147 e16.

31. Ehrengruber, M.U., et al., *Gene transfer into neurons from hippocampal slices: comparison of recombinant Semliki Forest Virus, adenovirus, adeno-associated virus, lentivirus, and measles virus.* Mol Cell Neurosci, 2001. **17**(5): p. 855-71.

8

32. Schatzle, P., L.C. Kapitein, and C.C. Hoogenraad, *Live imaging of microtubule dynamics in organotypic hippocampal slice cultures.* Methods Cell Biol, 2016. **131**: p. 107-26.

33. Kennedy, L.H. and J.E. Rinholm, *Visualization and Live Imaging of Oligodendrocyte Organelles in Organotypic Brain Slices Using Adeno-associated Virus and Confocal Microscopy.* J Vis Exp, 2017(128).

34. Ruigrok, M.J.R., et al., *siRNA-Mediated RNA Interference in Precision-Cut Tissue Slices Prepared from Mouse Lung and Kidney.* AAPS J, 2017. **19**(6): p. 1855-1863.

35. Naipal, K.A., et al., *Tumor slice culture system to assess drug response of primary breast cancer.* BMC Cancer, 2016. **16**: p. 78.

36. Meijer, T.G., et al., *Functional ex vivo assay reveals homologous recombination deficiency in breast cancer beyond BRCA gene defects.* Clin Cancer Res, 2018.

37. Mendes, N.D., et al., *Free-floating adult human brain-derived slice cultures as a model to study the neuronal impact of Alzheimer's disease-associated Abeta oligomers.* J Neurosci Methods, 2018. **307**: p. 203-209.

8

# CHAPTER 9

**General discussion**

An age-dependent accumulation of cellular damage leads to both an increase in senescent cells as well as an increased number of cells undergoing apoptosis over time. Both processes have both distinct beneficial as well as detrimental effects on tissue integrity. While apoptosis ensures permanent removal of damaged cells, senescent cells maintain their function within a tissue, except when their function is to divide. However, detrimental consequences prevail during aging. A disproportional increase in apoptosis severely damages tissue structure, while senescent cells exhibit a secretion phenotype that reduces tissue function. Cell fate after damage is dependent on multiple factors, including the cell type, the type of damage and previous exposure to damage. *In vivo*, some tissues show accumulation of senescent cells, while others exhibit an increase in apoptotic cells during aging. Furthermore, certain cell types have shown to be increasingly resistant to apoptosis. It is largely unclear, however, what factors ultimately decide whether either apoptosis or senescence is induced. Furthermore, determining unique characteristics in senescent cells that prevent apoptosis is key in the development of anti-senescence drugs. Lastly, it is unknown how apoptosis resistance after damage is regulated during aging and whether this is ultimately beneficial for tissue homeostasis. We aimed to answer these questions in order to identify promising leads for the development of anti-aging therapies.

**FOXO4 determines whether damaged cells undergo apoptosis or senescence**

Senescent cells are extremely apoptosis resistant [1, 2]. However, in **chapter 2** we show that senescent cells upregulate pro-apoptotic proteins, but that the interaction between FOXO4 and p53 in damage foci prevents p53 from actually inducing apoptosis. When this interaction is broken or when FOXO4 is inhibited, senescent cells readily undergo apoptosis. Furthermore, FOXO4 inhibition prior to a senescence inducing stimulus leads to the induction of apoptosis instead of senescence. Thus, FOXO4 is crucial in deciding cell fate after damage.

While an excessive amount of cells undergoing apoptosis is expected to negatively affect tissue integrity during aging, clearance of senescent cells in aged animals does not lead to a detrimental amount of cell loss [3, 4]. On the contrary, these mice were rejuvenated. However, preventing senescence induction instead of removing these cells when they are already present in a tissue, is not necessarily beneficial. FOXO4 knock out mice show a decreased organ function after acute damage (unpublished data), emphasizing that acutely inducing high levels of apoptosis is detrimental for tissue integrity. The difference between preventing senescence by FOXO4 inhibition and clearing senescent cells when they are already established could be explained by the role of FOXO proteins in tissue regeneration [5].

P53 is key in determining cell fate after damage, since it can activate DNA repair, apoptosis or senescence, depending on the cell type, dose and type of damage [6]. Adjusting p53 signaling alters cell fate. For example, mutating p53 at R172 in MEFs prevents p53-induced apoptosis through BCL-2. Thus, senescence is induced after UV-radiation instead of apoptosis [7]. Furthermore, p53 induces senescence through cell cycle inhibitor p21$^{Cip1}$ and knockdown of this protein results in apoptosis instead of senescence in development [8, 9]. Besides senescence induction, we showed that p53 inhibition is crucial in maintaining senescent cell viability as well. It has been argued before that apoptosis resistance in senescence is p53 dependent, since these cells are resistant to p53 dependent apoptosis stimuli, unless p53 is ectopically expressed [10]. Furthermore, we observed a drop in p21 after FOXO4 inhibition and p21$^{Cip1}$ is a known pro-survival factor in cancer cells [11-13] indicating that p21 inhibition would induce apoptosis in senescent cell as well. Indeed, p21 knockdown kills senescent cells that exhibit persistent damage signaling [14], emphasizing the crucial role of p53 signaling in maintaining senescent cell viability.

We demonstrated that a miRNA signature inhibits apoptosis after DNA damage as well. This cell preservation miRNA signature is upregulated in aged tissues, in tissues of DNA damage repair deficient Ercc1$^{\delta/-}$ mice and after UV-radiation. In **chapter 6** we examined miR-30, a representative cell preservation miRNA. We showed that miR-30 inhibits p53 expression by binding to the p53 3'UTR. MiR30 inhibition enhanced p53 expression and thereby increased apoptosis induction after DNA damage. Thus, this miRNA determines whether apoptosis is induced after damage. However, unlike FOXO4 and p53, miR-30 likely does not induce senescence. Although miR-30 has been reported to induce a growth arrest in HeLa cells [15], another study shows miR-30 to inhibit oncogene-induced senescence and to thereby promote tumor growth in the skin [16]. We studied senescence induction in fibroblasts after ionizing radiation in the presence of a miR-30 inhibitor and indeed observed a slight increase in senescence compared to irradiated cells where miR-30 was not inhibited, indicating that miR-30 has the potential to inhibit both apoptosis and senescence. In addition, however, it is possible that miR-30 inhibition is toxic to senescent cells, since p53 upregulation could tip the balance to apoptosis in these cells.

**Loss of tissue integrity can be counteracted by senescent cell clearance**

Senescent cells accumulate during aging due to an increase in cellular damage and a decrease in clearance of these cells by the immune system. This increase in senescence levels is harmful, since senescent cells secrete SASP proteins that negatively influence the microenvironment through, for example, promoting

9

inflammation, matrix degradation or inhibiting tissue regeneration. Genetic removal of senescent cells proved to rejuvenate old mice and to extend life span. Therefore, we aimed to develop a therapeutic applicable compound that specifically induces apoptosis in senescent cells. **Chapter 2** describes the development of FOXO4-DRI, a D-retro-inverso peptide that breaks the interaction of FOXO4 and p53 in senescent cells and thereby induces apoptosis. The experiments using FOXO4-DRI demonstrate that senescent cells can be targeted therapeutically *in vivo* without obvious adverse effects. Indeed, we observed an overall increase in fitness and an improved kidney function in aged mice. These results demonstrate that features of aging are reversible and that thereby healthspan can be extended during aging.

The development of cell-penetrating peptides (CPPs), such as FOXO4-DRI, provides innumerable possibilities. CPPs are in theory able to target any protein domain, in contrast to small kinase inhibitors that are usually restricted to the active site of an enzyme or allosteric pockets [17]. This enables the inhibition of protein interactions without interfering with other functions of the proteins of interest. D-retro-inverso peptides proved to be effective in constraining specific protein interactions *in vitro* and *in vivo*. For example, the Tat-Beclin 1 peptide inhibits the interaction between Beclin and an autophagy inhibitor, resulting in autophagy induction [18]. Furthermore, D-JNK is a CPP that prevents JNK from binding its substrates and thereby prevents their phosphorylation [19]. This peptide proved to inhibit neuronal apoptosis *in vivo* [20] and is now tested in clinical trials against hearing loss [21]. Thus, CPPs have the potential to be applied in clinical translation.

Although senescent cell clearance through FOXO4-DRI treatment improved healthspan in aged mice, several questions remain. For example, it remains unclear how heterogeneous the senescence phenotype is *in vivo* and which senescent cells are targeted by FOXO4-DRI. Furthermore, it is unknown how senescence clearance restores tissue function and whether negative side effects of senescent cell removal over an extended period of time are to be expected.

The senescence phenotype is heterogeneous and dynamic [22]. It is therefore expected that a multitude of senescence subtypes exist *in vivo*. It is imperative to determine which of these subtypes contribute to disease progression, in order to avoid targeting senescent cells that are not deleterious and to identify unique treatment targets. Thus, potential side effects are minimized. Multiple factors contribute to heterogeneity in the senescent phenotype, including the senescence inducing stimulus, the cell type and prior exposure to exogenous agents [22]. In our research we have focused on IR-induced senescence. However, senescence can be activated independent of actual DNA damage as well. For example, telomere dysfunction leads to senescence induction though activation of the DDR.

Furthermore, a decline in mitochondrial function leads to a reduction in cellular NAD+ levels which can stimulate AMPK and p53 to induce senescence [23]. In addition, sustained oncogene activation can induce senescence through excessive ROS production and subsequent activation of cell cycle inhibitors [24, 25]. Both telomere shortening and oncogene signaling induce senescent cells that secrete a high level of inflammatory proteins such as IL1-α and IL-6 [26, 27]. Furthermore, persistent DNA damage foci are mainly localized in telomeres [28] and FOXO4 is involved in senescence induction due to oncogene signaling [29]. These characteristics are known to prerequisites for FOXO4-DRI function and therefore, FOXO4-DRI possibly targets these subset of senescent cells. In contrast, mitochondrial dysfunction leads to senescent cells that do not increase IL-1 signaling [23] and are therefore not a target for FOXO4-DRI. Besides the senescence-inducing stimulus, distinct cell types are expected to exhibit dissimilar senescence features. For example, the composition of the SASP varies per cell type [30] and transcriptome analyses demonstrated that transcriptome signatures vary greatly between senescent cells of separate cell lineages [22]. Overall, it remains unknown which of the myriad of senescent cell subtypes will be sensitive to FOXO4-DRI, and other compounds may be designed to target insensitive cells that are deleterious.

It is known that senescence has a major role in a multitude of age-related diseases. We have shown that FOXO4-DRI specifically targets senescent cells that exhibit FOXO4 foci and express high levels of inflammatory factors. The inflammatory arm of the SASP is implicated in multiple age-related pathologies and these will potentially benefit from FOXO4-DRI treatment. As described in **chapter 3**, pro-inflammatory proteins are key in the development of age-related musculoskeletal disorders. For example, IL-6 is causally linked to age-related muscle wasting [31, 32], and both IL-1 and IL-6 secretion induce cartilage degeneration [33, 34]. Furthermore, senescent osteocytes secrete IL-1 and MMP3 in aged bones and thereby promote bone degradation [35]. Since senescent cells expressing high levels of interleukins seem especially sensitive to FOXO4-DRI, this would suggest FOXO4-DRI to be effective in these pathologies. On the other hand, in other age-related disorders the loss of proliferative capacity contributes more to disease progression than SASP expression. For example, the loss of regenerative potential of senescent β cells in the pancreas contributes to type 2 diabetes [36], and CD8+ T-cell senescence decreases T-cell responses during aging, resulting in an increased risk of infections [37]. It is not known whether senescent cells that contribute to these pathologies express FOXO4 foci or inflammatory proteins and thus whether FOXO4-DRI could benefit here.

9

It is not fully understood how a tissue is regenerated after senescent cells are cleared. An apparent explanation is a boost in stem cell regenerative potential. Stem number decreases in some tissues with age due to stem cell apoptosis, senescence or differentiation [38], while in others the stem cells might be locked in a pluripotent state and not be able to produce daughter cells that differentiate and restore the tissue. It is hypothesized that these stem cells are repressed from regenerating tissue structure when senescent cells and concomitant SASP proteins are chronically present and overabundant [39]. In contrast, tissue regeneration may not only be due to stem cell activation. For example, in the kidney tubular cells have a great regenerative potential themselves [40, 41]. These cells are able to proliferate after damage to replace apoptotic cells. When senescent cells accumulate in these structures, tubular cells lose proliferative capacity and release SASP factors that might prevent non-senescent cells from proliferating as well. Furthermore, even tissues with a low regenerative capacity such as cartilage are rejuvenated after senescent cell removal [42, 43]. Insight into how senescent cell clearance induces tissue regeneration could aid the development of anti-senescence drugs and minimize adverse effects.

It remains to be seen what the long-term side effects of targeting senescence will be *in vivo*. For example, clearing senescent cells and inducing tissue regeneration by stem cell activation on a regular basis could ultimately reduce stem cell function or stimulate cancer growth. Furthermore, pancreatic β cells express p16$^{INK4A}$ and are considered to be senescent, but are functional and have shown to increase insulin production [44]. Clearing these cells may therefore have adverse effects on glucose metabolism. However, mice where senescent cells were removed periodically in a genetic fashion did not present obvious side effects on tissue function. This indicates that adverse effects of senescent cell clearance will mainly arise from side effects of anti-senescence drugs.

**Cell preservation is a DNA damage-induced cell fate that restrains apoptosis**
The loss of irreplaceable cells through apoptosis has a negative effect on tissue integrity during aging. Some organs exhibit an increase in apoptotic cells during aging, such as the brain, heart and thymus [45-47], while other aged cells show an increased apoptotic resistance after DNA damage, such as the liver, spleen and skin [48-51]. We have previously termed this resistance 'cell preservation' and we have shown that cell preservation miRNAs are able to repress apoptosis in the presence of DNA damage, but it is unknown how the individual miRNAs are regulated, what targets the miRNAs specifically act on and how cell preservation influences aging and age-related diseases. To study the role of this signature during aging, we studied miR-30 as a representative cell preservation miRNA. MiR-30 inhibition not only increased apoptosis after UV damage

in a p53-dependent manner, it also increased senescence induction and enhanced DNA repair in fibroblasts. Furthermore, p53 levels were increased independently of DNA damage. Together this suggest miR-30 to set a threshold for p53 expression and that miR-30 inhibition results in a constitutive increase in p53 levels. This would have major implications for miR-30 function *in vivo.* To study the role of miR30 during aging, we inhibited miR-30 in DNA repair deficient XPD$^{TTD/TTD}$ mice that show features of aging already at 26 weeks. We observed weight loss in all mice that received the miR-30 inhibitor and an increase in plasma creatine concentration. These preliminary results do not clarify whether miR-30 inhibition has detrimental or beneficial effects on healthspan during aging. Since various p53 activated pathways appear to be affected by miR-30 inhibition *in vitro*, it is expected that miR-30 inhibition has significant effects *in vivo* during aging. On the one hand, an increase in apoptosis could severely damage tissue integrity. The weight loss of mice treated with miR-30 inhibitor is possibly caused by negative effects of miR-30 inhibition, such as induction of apoptosis or senescence, resulting in loss of tissue homeostasis. On the other hand, miR-30 inhibition enhanced DNA repair *in vitro* and reduced IL-6 expression by senescent cells. Therefore, the observed weight loss could result from activated pro-survival responses, also observed after dietary restriction [52, 53].

P53 has a crucial role in tumor suppression and aging. Distinct mouse models where p53 expression is altered show dissimilar effects on life span and cancer, and results from these studies could give insight into possible effects of *in vivo* miR-30 inhibition. On the on hand, p53 knock out mice develop cancer relatively early in life [54, 55]. This is unsurprising, since p53 is a crucial tumor suppressor. Conversely, p53 overexpression inhibits tumor formation but accelerates aging. For example, mice that overexpress truncated p53 isoforms that ensure constitutive p53 expression show accelerated aging, an increase in senescence and a shortened lifespan [56, 57]. Furthermore, constitutive p53 activation through mutations in the T21D and S23D phosphorylation sites induces stem cell depletion in the mouse brain and bone marrow, resulting in a shortened life span [58]. Therefore, both p53 downregulation and upregulation ultimately decrease life span. This illustrates that p53 expression during aging is a delicate balance, where either cancer or aging is promoted when this balance is disrupted. Interestingly, increasing p53 activity physiologically by introducing extra gene copies does prevent tissue damage and cancer formation, resulting in an increased life span [59, 60]. MiR-30 inhibition increases p53 expression independent of DNA damage and activates multiple p53-dependent pathways *in vitro*, indicating that p53 is constitutively upregulated. Thus, miR-30 inhibition possibly negatively influences healthspan during aging, as seen in other mouse models where p53 is constitutively activated. This also implies that

9

administering miR-30 would increase cancer incidence. However, the described mouse models do not give insight into the effect of temporary p53 activation or inhibition later in life. For example, p53 deletion proved to protect kidney tubular cells from apoptosis after ischemia reperfusion injury and prevented kidney fibrosis [61]. Inhibition of p53 and apoptosis may protect aged organs from injury during acute stress and therefore prevent the loss of cells that are more difficult to replace in old organisms than in young organisms. Further research is required to elucidate the effect of adjusting miR-30 levels *in vivo.*

The expression of miR-30 and other cell preservation miRNAs is likely to be a balance where either premature induction of apoptosis after damage is prevented to protect tissue integrity, but on the other hand a prolonged desensitization to damage could ultimately protect cancer prone cells from dying. Not all cells are likely to form cancer cells during aging and there is a difference in cancer incidence between distinct tissues [62, 63]. For example, tumors in the heart or originating from neurons are rare, while colon and breast cancer are very common. Cell types that are unlikely to become cancerous may be more prone to apoptosis during aging and these cells could benefit from an upregulation of cell preservation miRNAs when it would be achievable to deliver these miRNAs specifically to these cells. Additional experiments should be performed to determine the role of cell preservation *in vivo* and whether overexpression or inhibition of individual components may improve health span during aging. These experiments may include the use of mouse models where DNA damage-induced apoptosis is enhanced, such as the Ercc1$^{\delta-}$ mouse model.

With the limited information at hand, the definition of cell preservation response overlaps somewhat with cellular senescence. We defined cell preservation as the maintenance of viability in the presence of DNA damage induced pro-apoptotic signals. It is known that senescent cells are highly apoptotic resistant. Furthermore, we have shown that senescent cells upregulate pro-apoptotic signaling pathways that are actively repressed by the p53-FOXO4 interaction. In theory, this could be described as cell preservation. However, cells with heightened expression of cell preservation miRNAs maintain proliferation and cell preservation miRNAs are not increased in senescence (unpublished data, MB, JH, JP). Furthermore, these miRNAs may even inhibit senescence, although further research is required to confirm this. Conversely, the senescence phenotype is highly heterogeneous and volatile. The only common marker between all senescent cells is the permanent cell cycle arrest. However, post-mitotic cells, such as neurons and podocytes, are permanently arrested in growth. These cells are only characterized as being senescent, when they express additional senescence markers such as p16$^{ink4a}$ or

known SASP proteins [64]. Therefore, is appears that age-related cell fates such as senescence and cell preservation cannot be described as a one well defined cellular state.

**Extracellular vesicles transfer a DNA damage response during aging**

Persistent DNA damage significantly alters intracellular signaling resulting in protection against further insults. Furthermore, damaged cells communicate with their environment as well. For example, senescent cells exhibit persistent DNA damage foci and secrete inflammatory factors to attract immune cells and promote tissue repair [65-67]. Furthermore, UV-radiation promotes keratinocytes to produce cytokines that suppress the immune system and prevent skin damage [68, 69]. Thus, intercellular communication after DNA damage may have a beneficial effect on tissue homeostasis.

During aging the amount of damaged cells increases, and since these cells exhibit an altered secretion phenotype the systemic milieu is altered. For example, the accumulation of senescent cells results in the chronic presence of SASP molecules, such as proteases or pro-inflammatory cytokines, which contributes to systemic inflammation. In addition, damaged cells are known to increase vesicle secretion. Extracellular vesicles (EVs) contain RNA, lipids and proteins from the donor cell and are able to alter signaling in neighboring cells after releasing their content [70]. Although it remains unclear whether EV secretion increases with age, vesicle content has proven to be altered [71]. In **chapter 7** we have demonstrated that vesicles from aged mice induce a differential effect on recipient cells compared to vesicles from young mice. These aged EVs induced a response similar to a UV damage induced DDR and upregulated cell preservation miRNAs. This indicates that the vesicle content was indeed altered during aging.

To further study EV secretion during aging and the effect of EVs from aged organisms on recipient cells, additional experiments should be performed. For example, the DDR in recipient cells should be further characterized to assess whether these cells are truly more apoptosis resistant or simply more damaged. We hypothesized that recipient cells treated with vesicles derived from UV-radiated cells do not exhibit an increase in DNA damage, but only an increase of downstream DDR components such as the cell preservation miRNAs. Since this miRNA signature is ATM dependent, ATM activators, such as R-loops or miRNAs, could be transferred to recipient cells [72, 73]. The content of EVs from aged individuals can be studied through, for example, RNA sequencing or proteomics techniques to determine whether cell preservation miRNAs or other factors that could induce this signature are present in aged vesicles.

9

An altered EV secretion during aging has various implications for tissue homeostasis. On one hand EV secretion may harm the micro-environment. For example, EVs are secreted by aged cells to protect themselves from cellular waste. It has been demonstrated that an intracellular protein accumulation during age-related neurodegenerative diseases induces an increased secretion of these toxic proteins in vesicles [74, 75], reducing viability in recipient cells [76]. Furthermore, senescent cells exhibit an increased vesicle secretion [72] and these vesicles proved to contain harmful DNA fragments [72, 77]. Furthermore, EVs secreted by senescent cells were shown to promote cancer growth [78]. On the other hand, vesicles secretion has proven to have beneficial effects on recipient cells. We showed EVs from UV-radiated cells and from aged mice to upregulate pro-survival miRNAs in recipient cells, indicating that these cells are possibly resistant to subsequent damage. Furthermore, EVs from UV-radiated melanocytes are able to protect recipient cells from damage through upregulation of fibronectin [79, 80]. In addition, resistance to heath shock can be promoted by treating cells with EVs from cells previously exposed to a heath shock [81] and ROS resistance can be established by exposing cells to EVs from cells exhibiting high levels of ROS [82]. *In vivo*, EVs have shown to have beneficial effects after damage as well. For example, EVs derived from mesenchymal stem cells are known to regenerate diseased tissue in mammals, including kidneys after ischemia reperfusion injury [83], damaged lung [84] and neuronal cells after a stroke [85]. Overall, EVs from cells with persistent DNA damage could induce systemic pro-survival cues, beneficial for tissue integrity during aging.

**Anti-senescence drugs improve cancer treatment**

The cancer incidence increases with age due to mutation accumulation. These mutations may facilitate growth and apoptosis resistance and thereby promote carcinogenesis [86, 87]. Furthermore, an aged tissue microenvironment benefits tumor growth as well. For example, systemic inflammation can induce genomic instability and stimulates growth [88, 89]. Senescent cells are implicated in both cancer formation and progression. Although senescence prevents damaged or stressed cells from undergoing malignant transformation, cells can circumvent senescence through additional mutations in proteins required for the cell cycle arrest, such as p16$^{ink4a}$ and PTEN, and grow out into a tumor [90]. Furthermore, senescence promotes tumor growth in the microenvironment through the SASP. Pro-inflammatory interleukins such as IL-6 and IL-8 stimulate proliferation of premalignant cells [91], as well as angiogenesis and metastasis formation in a later stage [92, 93].

Senescence not only promotes tumorigenesis, it contributes to therapy resistance as well. We have shown in **chapter 5** that therapy-resistant malignant melanoma

cells exhibit features of senescence after treatment with MAPK pathway inhibitors, while still proliferating. The mutated BRAF inhibitor Vemurafenib induced expression of FOXO4, p21 and known SASP protein IL-6. Interestingly, both suppression of pro-inflammatory interleukins as well as FOXO4 inhibition sensitized these cells to treatment. Thus, resistant melanoma cells upregulate senescence markers to resist apoptosis after chemotherapy. Furthermore, FOXO4-DRI treatment proved to be synthetically lethal in combination with BRAF inhibition in both treatment-resistant melanoma cell lines and human metastatic melanoma tissue slices. In senescent cells, FOXO4-DRI induces apoptosis through breaking the interaction between FOXO4 and p53, and subsequent translocation of p53 from the nucleus to the cytoplasm. P53 is not often mutated in melanoma cells [94] and therefore, FOXO4-DRI could be applicable in many of these tumors. Although it remains unclear whether FOXO4-DRI induces apoptosis in melanoma cells through the same mechanism, the parallel with senescent cells proves that targeting senescence markers in melanoma cells is a promising treatment strategy.

We have studied senescence features in melanoma cells, but other cancers are expected to resist treatment through upregulating senescence markers as well. For example, cell cycle inhibitor p21$^{Cip1}$ was shown to promote colon carcinoma cell survival after DNA-damaging therapies [12, 95] and senescence-associated heterochromatin foci (SAHF) aid in resisting cell death in oncogene-expressing cells [96]. Furthermore, SASP proteins such as IL-1α can be upregulated in breast cancer cells after chemotherapy to repress apoptosis [97, 98]. In addition, DNA-damaging therapies, such as radiation therapy, induce persistent DNA damage foci and are expected to induce FOXO4 foci as well. Since multiple malignant tumors have shown to express senescence markers after chemotherapy, FOXO4-DRI may be a promising adjuvant therapy for these cancers as well. However, cancer cells should express FOXO4 foci in order for FOXO4-DRI to have an effect, as well as partly intact p53. Further research is required to establish other biomarkers that predict FOXO4-DRI effectivity.

The senescence features expressed in cancer cells are possibly part of a stem-like state. It is known that cancer cells can adopt this state when exposed to chemotherapy, in order to resist stress and inhibit their apoptotic response to chemotherapy [99-102]. Markers expressed by stem-like cancer cells can be linked to markers of senescence. For example, senescence-escaped lung cancer cells still express senescence-associated markers and show an increased tumor initiation potential *in vivo* [103]. Furthermore, both breast cancer and b-cell lymphoma cells that have escaped senescence show high expression of stemness markers such as β-catenin, CD133 and Oct-4 and an increase in anti-oxidants [104, 105]. In addition,

9

it has been shown that chemotherapy–induced senescent lymphoma cells express stem cell markers [105]. When these cells escaped senescence, their growth rate was significantly enhanced and they exhibited a higher tumorigenic potential than cells that were not previously senescent [105]. Thus, targeting senescence properties in cancer cells potentially decreases stemness and thereby enhances treatment sensitivity.

Not only do senescence features in cancer cells promote therapy resistance, but senescence also contributes to therapy resistance through secretion of SASP factors to the tumor-microenvironment. Multiple proteins secreted by senescent cells have been implicated in treatment resistance. For example, Il-6 and Il-8 are upregulated in therapy-resistant breast cancer cells and have shown to be involved in resistance to a multitude of anti-cancer drugs [106]. Chemo- and radiotherapy induce senescence in the tumor microenvironment and thereby increase the presence of these deleterious proteins, promoting resistance to a consecutive treatment round. Importantly, it was shown that genetic removal of senescent cells significantly reduces chemotherapy resistance in mice implanted with breast cancer cells [107]. Therefore, therapeutically targeting senescent cells could significantly improve the outcome of cancer therapy. We have shown in **chapter 2** that FOXO4-DRI treatment effectively cleared doxorubicin-induced senescence and could therefore reduce resistance to this drug. Thus, FOXO4-DRI potentially targets both cancer cells and a hostile microenvironment, resulting in improved cancer treatment. This drug will therefore be further studied in *in vivo* cancer models.

Senescence is not the only age-related process that contributes to cancer development. Among others, the gradual upregulation of cell preservation miRNAs over time could be partly responsible for the age-related increase in cancer. This miRNA signature represses apoptosis during aging and could therefore in theory contribute to cancer formation in (pre-) malignant cells or promote treatment resistance. MiR-30 represses p53 expression and thereby promotes apoptosis resistance after damage. Therefore, miR-30 possibly has a role in cancer progression and chemotherapy resistance. Indeed, miR-30 has been shown to inhibit oncogene induced senescence by targeting both p53 and p16 in pre-malignant cells [16]. Furthermore, miR-30 expression has proven to aid breast cancer progression [108] and to promote stemness in glioma cells [109]. However, this miRNA has also been described to inhibit cancer growth and metastasis formation in several cancer types [110-114] and even enhanced doxorubicin sensitivity in breast cancer cells [110]. It therefore appears that miR-30 has a higher affinity for other targets in these cells, possibly because p53 is often mutated in cancer. Overall, the cell preservation signature likely has a role in cancer progression, since many of its

individual components have been implicated in cancer growth, metastasis and therapy resistance.

**Anti-aging therapies**

Results obtained in **chapter 2** prove that aging is reversible through senescent cell clearance and that this greatly improves healthspan. FOXO4-DRI is not the only compound that targets senescent cells *in vivo.* Indeed, other drugs have shown to reduce senescence during aging as well [115, 116]. These are mainly compounds that are previously used in the clinic to treat other indications. One of these is BCL-2 inhibitor Navitoclax, an anti-cancer drug that induces apoptosis by inhibiting BCL-2 [117, 118]. BCL-2 is thought to maintain viability in senescent cells as well, and BCL inhibition indeed targets senescence *in vivo* [107, 115, 119] and showed to rejuvenate aged hematopoietic stem cells [115]. It remains unknown what the long term effects of senescent cell removal will be and it is probable that anti-senescence drugs need to be administered periodically in order to obtain a prolonged effect. Therefore, the change of side effects will overall be higher. For example, Navitoclax is known to cause diarrhea and neutropenia preventing long term treatment during aging [120]. Furthermore, side effects of FOXO4-DRI are currently unknown, but the selectivity of the current version for senescent cells over non-senescent cells seems too small to be applicable in humans yet and needs to be optimized before being tested in clinical trials.

Anti-senescence therapies counteract the negative effects of senescence on tissue function during aging. Besides senescence, an increase in apoptosis negatively affects tissue integrity as well. Possibly, apoptosis can be prevented by upregulating miRNAs of the cell preservation response. Both overexpression and inhibition of miRNAs is achievable *in vivo.* MiRNA mimics are modified with 2'-O-methyl groups for stability and do not show major adverse effects in patients [121, 122]. Furthermore, miRNA inhibitors consisting of LNA molecules are stable in plasma for weeks and are well tolerated [123, 124]. Furthermore, other anti-apoptotic drugs are investigated for their use in neurodegenerative diseases, such as JNK, NMDA and GSK-3 inhibitors [125].

Opposing apoptosis or senescence is not the only tactic to extend healthspan during aging. Other strategies include the use of mesenchymal stem cell derived EVs. These vesicles induce regeneration of several tissues and could therefore benefit aged patients. Furthermore, EVs could be employed for targeted delivery of anti-aging compounds, since they protect their content from degradation, are stable in the circulation over an extended time period [126] and can cross the blood brain barrier. In addition, heterochronic parabiosis between a young and an aged mouse

9

showed that systemic factors present in young blood can rejuvenate aged muscle stem cells [127] and improved cardiac function in old mice [128]. Furthermore, brain function and synaptic plasticity were improved in aged mice after exposure to young blood [129] and mice treated with young serum showed an improved neurogenesis [130]. Together, this inspired clinical trials in which Alzheimer's patients are treated with plasma from young volunteers (NCT02803554, NCT02256306).

Besides young circulating factors, stem cell rejuvenation could enhance tissue integrity during aging. Terminally differentiated cells can be reprogrammed into pluripotent stem cells through expression of Yamanaka factors [131]. Interestingly, this reprogramming induces rejuvenation in these cells as well. For example, reprogramming of senescent fibroblasts showed that telomere length and gene expression resembled that of stem cells. When these reprogrammed cells were differentiated again, they were rejuvenated and did not show senescence properties anymore [132]. Furthermore, reprogramming improved mitochondrial function and reduced ROS levels in cells from centenarians [132]. Lastly, reprogrammed cells from Hutchinson-Gilford progeria patients do not show progerin and other features related to the syndrome [133]. *In vivo* induction of Yamanaka factors frequently leads to teratoma formation [134]. However, it has been shown that short-term expression through cyclic induction of these factors does not cause tumor formation, but increases life span in fast aging mice [135]. Furthermore, expression of the Yamanaka factors reduces senescence and markers for DNA damage, such as 53BP1 and γH2Ax, *in vitro* and improved age-related changes in multiple organs in mice. Thus, the rejuvenating effects of reprogramming shows potential for the treatment of age-related diseases.

Overall, multiple anti-aging strategies show great promise, but the risks and benefits should be studied carefully before being applied. Additionally, a combination of several of such strategies will likely be necessary to truly rejuvenate elderly people.

**Conclusion**

We aimed to unravel the mechanisms and functions of age-related DNA damage responses with the ultimate goal to provide leads for potential strategies that prolong healthspan during aging. We have developed a FOXO4-DRI peptide that potently and selectively kills senescent cells, improving tissue homeostasis in fast aging $Xpd^{TTD/TTD}$ and naturally aged mice. FOXO4-DRI targets senescent cells that exhibit FOXO4 foci and a high secretion of inflammatory proteins. Therefore, it is potentially beneficial for a multitude of age-related pathologies where senescence is known to be causal for disease progression. Furthermore, inflammatory SASP factors stimulate cancer growth, stemness and migration. FOXO4-DRI treatment could therefore reduce

cancer progression. We have shown that this peptide can target cancer cells that exhibit senescence features, indicating that FOXO4-DRI has the potential to target the tumor micro-environment as well as the tumor itself. Thus, anti-senescence drugs could greatly benefit both tissue integrity during aging and cancer treatment. Besides senescence, we highlighted a micro-RNA signature that is upregulated during aging and inhibits DNA damage-dependent apoptosis *in vitro.* Furthermore, we showed that this signature is transferred to neighboring cells via extracellular vesicles. The miRNA targets and *in vivo* role were unknown and therefore we studied miR-30, a representative miRNA. MiR-30 inhibition proved to constitutively upregulate p53 expression, increasing apoptosis after UV-damage. This has potential detrimental effects during aging, since mouse models where p53 levels are increased show accelerated aging. Increasing cell preservation miRNAs may prevent apoptosis induction in cell types that are prone to cell death during aging. However, there is a risk for stimulating cancer growth as well. Therefore, further experiments are required to determine whether adjusting levels of these miRNAs and thereby affecting apoptosis induction during aging could benefit healthspan. Overall this thesis illustrates how apoptosis and senescence underlie organismal aging and provides starting points for the development of potential therapeutic treatment for age-related pathology.

9

# References

1.  Sasaki, M., et al., *Senescent cells are resistant to death despite low Bcl-2 level.* Mech Ageing Dev, 2001. **122**(15): p. 1695-706.

2.  Yeo, E.J., et al., *Reduction of UV-induced cell death in the human senescent fibroblasts.* Mol Cells, 2000. **10**(4): p. 415-22.

3.  Baker, D.J., et al., *Clearance of p16Ink4a-positive senescent cells delays ageing-associated disorders.* Nature, 2011. **479**(7372): p. 232-6.

4.  Baker, D.J., et al., *Naturally occurring p16(Ink4a)-positive cells shorten healthy lifespan.* Nature, 2016. **530**(7589): p. 184-9.

5.  Miyamoto, K., et al., *Foxo3a is essential for maintenance of the hematopoietic stem cell pool.* Cell Stem Cell, 2007. **1**(1): p. 101-12.

6.  Liu, Y. and M. Kulesz-Martin, *p53 protein at the hub of cellular DNA damage response pathways through sequence-specific and non-sequence-specific DNA binding.* Carcinogenesis, 2001. **22**(6): p. 851-60.

7.  Tavana, O., et al., *Absence of p53-dependent apoptosis leads to UV radiation hypersensitivity, enhanced immunosuppression and cellular senescence.* Cell Cycle, 2010. **9**(16): p. 3328-36.

8.  Munoz-Espin, D., et al., *Programmed cell senescence during mammalian embryonic development.* Cell, 2013. **155**(5): p. 1104-18.

9.  Storer, M., et al., *Senescence is a developmental mechanism that contributes to embryonic growth and patterning.* Cell, 2013. **155**(5): p. 1119-30.

10. Childs, B.G., et al., *Senescence and apoptosis: dueling or complementary cell fates?* EMBO Rep, 2014. **15**(11): p. 1139-53.

11. Gartel, A.L., *Is p21 an oncogene?* Mol Cancer Ther, 2006. **5**(6): p. 1385-6.

12. Gorospe, M., et al., *p21(Waf1/Cip1) protects against p53-mediated apoptosis of human melanoma cells.* Oncogene, 1997. **14**(8): p. 929-35.

13. Weiss, R.H., *p21Waf1/Cip1 as a therapeutic target in breast and other cancers.* Cancer Cell, 2003. **4**(6): p. 425-9.

14. Yosef, R., et al., *p21 maintains senescent cell viability under persistent DNA damage response by restraining JNK and caspase signaling.* EMBO J, 2017. **36**(15): p. 2280-2295.

15. Martinez, I., et al., *miR-29 and miR-30 regulate B-Myb expression during cellular senescence.* Proc Natl Acad Sci U S A, 2011. **108**(2): p. 522-7.

16. Su, W., et al., *miR-30 disrupts senescence and promotes cancer by targeting both p16(INK4A) and DNA damage pathways.* Oncogene, 2018. **37**(42): p. 5618-5632.

17. Wu, P., M.H. Clausen, and T.E. Nielsen, *Allosteric small-molecule kinase inhibitors.* Pharmacol Ther, 2015. **156**: p. 59-68.

18. Shoji-Kawata, S., et al., *Identification of a candidate therapeutic autophagy-inducing peptide.* Nature, 2013. **494**(7436): p. 201-6.

19. Barr, R.K., T.S. Kendrick, and M.A. Bogoyevitch, *Identification of the critical features of a small peptide inhibitor of JNK activity.* J Biol Chem, 2002. **277**(13): p. 10987-97.

20. Zhao, Y., et al., *The JNK inhibitor D-JNKI-1 blocks apoptotic JNK signaling in brain mitochondria.* Mol Cell Neurosci, 2012. **49**(3): p. 300-10.

21. Eshraghi, A.A., et al., *Preclinical and clinical otoprotective applications of cell-penetrating peptide D-JNKI-1 (AM-111).* Hear Res, 2018. **368**: p. 86-91.

22. Hernandez-Segura, A., et al., *Unmasking Transcriptional Heterogeneity in Senescent Cells.* Curr Biol, 2017. **27**(17): p. 2652-2660 e4.

23. Wiley, C.D., et al., *Mitochondrial Dysfunction Induces Senescence with a Distinct Secretory Phenotype.* Cell Metab, 2016. **23**(2): p. 303-14.

24. Ogrunc, M., et al., *Oncogene-induced reactive oxygen species fuel hyperproliferation and DNA damage response activation.* Cell Death Differ, 2014. **21**(6): p. 998-1012.

25. Di Micco, R., et al., *Oncogene-induced senescence is a DNA damage response triggered by DNA hyper-replication.* Nature, 2006. **444**(7119): p. 638-42.

26. Orjalo, A.V., et al., *Cell surface-bound IL-1alpha is an upstream regulator of the senescence-associated IL-6/IL-8 cytokine network.* Proc Natl Acad Sci U S A, 2009. **106**(40): p. 17031-6.

27. Kuilman, T., et al., *Oncogene-induced senescence relayed by an interleukin-dependent inflammatory network.* Cell, 2008. **133**(6): p. 1019-31.

28. Fumagalli, M., et al., *Telomeric DNA damage is irreparable and causes persistent DNA-damage-response activation.* Nat Cell Biol, 2012. **14**(4): p. 355-65.

29. de Keizer, P.L., et al., *Activation of forkhead box O transcription factors by oncogenic BRAF promotes p21cip1-dependent senescence.* Cancer Res, 2010. **70**(21): p. 8526-36.

30. Coppe, J.P., et al., *Senescence-associated secretory phenotypes reveal cell-nonautonomous functions of oncogenic RAS and the p53 tumor suppressor.* PLoS Biol, 2008. **6**(12): p. 2853-68.

31. Tsujinaka, T., et al., *Interleukin 6 receptor antibody inhibits muscle atrophy and modulates proteolytic systems in interleukin 6 transgenic mice.* J Clin Invest, 1996. **97**(1): p. 244-9.

32. Belizario, J.E., et al., *Skeletal muscle wasting and renewal: a pivotal role of myokine IL-6.* Springerplus, 2016. **5**: p. 619.

33. Portal-Nunez, S., et al., *Oxidative stress, autophagy, epigenetic changes and regulation by miRNAs as potential therapeutic targets in osteoarthritis.* Biochem Pharmacol, 2016. **108**: p. 1-10.

34. Livshits, G., et al., *Interleukin-6 is a significant predictor of radiographic knee osteoarthritis: The Chingford Study.* Arthritis Rheum, 2009. **60**(7): p. 2037-45.

9

35.   Piemontese, M., et al., *Old age causes de novo intracortical bone remodeling and porosity in mice.* JCI Insight, 2017. **2**(17).

36.   Krishnamurthy, J., et al., *p16INK4a induces an age-dependent decline in islet regenerative potential.* Nature, 2006. **443**(7110): p. 453-7.

37.   Quinn, K.M., et al., *Age-Related Decline in Primary CD8(+) T Cell Responses Is Associated with the Development of Senescence in Virtual Memory CD8(+) T Cells.* Cell Rep, 2018. **23**(12): p. 3512-3524.

38.   Ahmed, A.S., et al., *Effect of aging on stem cells.* World J Exp Med, 2017. **7**(1): p. 1-10.

39.   de Keizer, P.L., *The Fountain of Youth by Targeting Senescent Cells?* Trends Mol Med, 2017. **23**(1): p. 6-17.

40.   Humphreys, B.D., *Kidney injury, stem cells and regeneration.* Curr Opin Nephrol Hypertens, 2014. **23**(1): p. 25-31.

41.   van Willigenburg, H., P.L.J. de Keizer, and R.W.F. de Bruin, *Cellular senescence as a therapeutic target to improve renal transplantation outcome.* Pharmacol Res, 2018. **130**: p. 322-330.

42.   Candela, M.E., et al., *Resident mesenchymal progenitors of articular cartilage.* Matrix Biol, 2014. **39**: p. 44-9.

43.   Jeon, O.H., et al., *Local clearance of senescent cells attenuates the development of post-traumatic osteoarthritis and creates a pro-regenerative environment.* Nat Med, 2017. **23**(6): p. 775-781.

44.   Helman, A., et al., *p16(Ink4a)-induced senescence of pancreatic beta cells enhances insulin secretion.* Nat Med, 2016. **22**(4): p. 412-20.

45.   Giannaris, E.L. and D.L. Rosene, *A stereological study of the numbers of neurons and glia in the primary visual cortex across the lifespan of male and female rhesus monkeys.* J Comp Neurol, 2012. **520**(15): p. 3492-508.

46.   Kubli, D.A., et al., *Parkin protein deficiency exacerbates cardiac injury and reduces survival following myocardial infarction.* J Biol Chem, 2013. **288**(2): p. 915-26.

47.   Sainz, R.M., et al., *Apoptosis in primary lymphoid organs with aging.* Microsc Res Tech, 2003. **62**(6): p. 524-39.

48.   Feng, Z., et al., *Declining p53 function in the aging process: a possible mechanism for the increased tumor incidence in older populations.* Proc Natl Acad Sci U S A, 2007. **104**(42): p. 16633-8.

49.   Suh, Y., et al., *Aging alters the apoptotic response to genotoxic stress.* Nat Med, 2002. **8**(1): p. 3-4.

50.   Polyak, K., et al., *Less death in the dying.* Cell Death Differ, 1997. **4**(3): p. 242-6.

51.   Camplejohn, R.S., et al., *Apoptosis, ageing and cancer susceptibility.* Br J Cancer, 2003. **88**(4): p. 487-90.

52. Garinis, G.A., et al., *Persistent transcription-blocking DNA lesions trigger somatic growth attenuation associated with longevity.* Nat Cell Biol, 2009. **11**(5): p. 604-15.

53. Vermeij, W.P., et al., *Restricted diet delays accelerated ageing and genomic stress in DNA-repair-deficient mice.* Nature, 2016. **537**(7620): p. 427-431.

54. Sah, V.P., et al., *A subset of p53-deficient embryos exhibit exencephaly.* Nat Genet, 1995. **10**(2): p. 175-80.

55. Donehower, L.A., et al., *Mice deficient for p53 are developmentally normal but susceptible to spontaneous tumours.* Nature, 1992. **356**(6366): p. 215-21.

56. Maier, B., et al., *Modulation of mammalian life span by the short isoform of p53.* Genes Dev, 2004. **18**(3): p. 306-19.

57. Tyner, S.D., et al., *p53 mutant mice that display early ageing-associated phenotypes.* Nature, 2002. **415**(6867): p. 45-53.

58. Liu, D., et al., *Puma is required for p53-induced depletion of adult stem cells.* Nat Cell Biol, 2010. **12**(10): p. 993-8.

59. Matheu, A., et al., *Delayed ageing through damage protection by the Arf/p53 pathway.* Nature, 2007. **448**(7151): p. 375-9.

60. Garcia-Cao, I., et al., *"Super p53" mice exhibit enhanced DNA damage response, are tumor resistant and age normally.* EMBO J, 2002. **21**(22): p. 6225-35.

61. Ying, Y., et al., *Targeted deletion of p53 in the proximal tubule prevents ischemic renal injury.* J Am Soc Nephrol, 2014. **25**(12): p. 2707-16.

62. Thomas, F., et al., *Evolutionary Ecology of Organs: A Missing Link in Cancer Development?* Trends Cancer, 2016. **2**(8): p. 409-415.

63. Rozhok, A.I. and J. DeGregori, *The evolution of lifespan and age-dependent cancer risk.* Trends Cancer, 2016. **2**(10): p. 552-560.

64. Sapieha, P. and F.A. Mallette, *Cellular Senescence in Postmitotic Cells: Beyond Growth Arrest.* Trends Cell Biol, 2018. **28**(8): p. 595-607.

65. Kang, T.W., et al., *Senescence surveillance of pre-malignant hepatocytes limits liver cancer development.* Nature, 2011. **479**(7374): p. 547-51.

66. Hoenicke, L. and L. Zender, *Immune surveillance of senescent cells--biological significance in cancer- and non-cancer pathologies.* Carcinogenesis, 2012. **33**(6): p. 1123-6.

67. Demaria, M., et al., *An essential role for senescent cells in optimal wound healing through secretion of PDGF-AA.* Dev Cell, 2014. **31**(6): p. 722-33.

68. Patra, V., S.N. Byrne, and P. Wolf, *The Skin Microbiome: Is It Affected by UV-induced Immune Suppression?* Front Microbiol, 2016. **7**: p. 1235.

69. Nasti, T.H. and L. Timares, *Inflammasome activation of IL-1 family mediators in response to cutaneous photodamage.* Photochem Photobiol, 2012. **88**(5): p. 1111-25.

9

70. Valadi, H., et al., *Exosome-mediated transfer of mRNAs and microRNAs is a novel mechanism of genetic exchange between cells.* Nat Cell Biol, 2007. **9**(6): p. 654-9.

71. Eitan, E., et al., *Age-Related Changes in Plasma Extracellular Vesicle Characteristics and Internalization by Leukocytes.* Sci Rep, 2017. **7**(1): p. 1342.

72. Takahashi, A., et al., *Exosomes maintain cellular homeostasis by excreting harmful DNA from cells.* Nat Commun, 2017. **8**: p. 15287.

73. Tresini, M., et al., *The core spliceosome as target and effector of non-canonical ATM signalling.* Nature, 2015. **523**(7558): p. 53-8.

74. Shi, M., et al., *Plasma exosomal alpha-synuclein is likely CNS-derived and increased in Parkinson's disease.* Acta Neuropathol, 2014. **128**(5): p. 639-650.

75. Fevrier, B., et al., *Cells release prions in association with exosomes.* Proc Natl Acad Sci U S A, 2004. **101**(26): p. 9683-8.

76. Emmanouilidou, E., et al., *Cell-produced alpha-synuclein is secreted in a calcium-dependent manner by exosomes and impacts neuronal survival.* J Neurosci, 2010. **30**(20): p. 6838-51.

77. Ivanov, A., et al., *Lysosome-mediated processing of chromatin in senescence.* J Cell Biol, 2013. **202**(1): p. 129-43.

78. Takasugi, M., et al., *Small extracellular vesicles secreted from senescent cells promote cancer cell proliferation through EphA2.* Nat Commun, 2017. **8**: p. 15729.

79. Bin, B.H., et al., *Fibronectin-Containing Extracellular Vesicles Protect Melanocytes against Ultraviolet Radiation-Induced Cytotoxicity.* J Invest Dermatol, 2016. **136**(5): p. 957-966.

80. Waster, P., et al., *Extracellular vesicles are transferred from melanocytes to keratinocytes after UVA irradiation.* Sci Rep, 2016. **6**: p. 27890.

81. Bewicke-Copley, F., et al., *Extracellular vesicles released following heat stress induce bystander effect in unstressed populations.* J Extracell Vesicles, 2017. **6**(1): p. 1340746.

82. Grindheim, A.K. and A. Vedeler, *Extracellular vesicles released from cells exposed to reactive oxygen species increase annexin A2 expression and survival of target cells exposed to the same conditions.* Commun Integr Biol, 2016. **9**(4): p. e1191715.

83. Gatti, S., et al., *Microvesicles derived from human adult mesenchymal stem cells protect against ischaemia-reperfusion-induced acute and chronic kidney injury.* Nephrol Dial Transplant, 2011. **26**(5): p. 1474-83.

84. Chen, J., C. Li, and L. Chen, *The Role of Microvesicles Derived from Mesenchymal Stem Cells in Lung Diseases.* Biomed Res Int, 2015. **2015**: p. 985814.

85. Xin, H., et al., *Systemic administration of exosomes released from mesenchymal stromal cells promote functional recovery and neurovascular plasticity after stroke in rats.* J Cereb Blood Flow Metab, 2013. **33**(11): p. 1711-5.

86.  Risques, R.A. and S.R. Kennedy, *Aging and the rise of somatic cancer-associated mutations in normal tissues.* PLoS Genet, 2018. **14**(1): p. e1007108.

87.  Armitage, P., *Multistage models of carcinogenesis.* Environ Health Perspect, 1985. **63**: p. 195-201.

88.  Vakkila, J. and M.T. Lotze, *Inflammation and necrosis promote tumour growth.* Nat Rev Immunol, 2004. **4**(8): p. 641-8.

89.  Lin, R., et al., *Chronic inflammation-associated genomic instability paves the way for human esophageal carcinogenesis.* Oncotarget, 2016. **7**(17): p. 24564-71.

90.  Liu, W. and N.E. Sharpless, *Senescence-escape in melanoma.* Pigment Cell Melanoma Res, 2012. **25**(4): p. 408-9.

91.  Krtolica, A., et al., *Senescent fibroblasts promote epithelial cell growth and tumorigenesis: a link between cancer and aging.* Proc Natl Acad Sci U S A, 2001. **98**(21): p. 12072-7.

92.  Wei, L.H., et al., *Interleukin-6 promotes cervical tumor growth by VEGF-dependent angiogenesis via a STAT3 pathway.* Oncogene, 2003. **22**(10): p. 1517-27.

93.  Oh, K., et al., *A mutual activation loop between breast cancer cells and myeloid-derived suppressor cells facilitates spontaneous metastasis through IL-6 trans-signaling in a murine model.* Breast Cancer Res, 2013. **15**(5): p. R79.

94.  Yamashita, T., et al., *Induction of apoptosis in melanoma cell lines by p53 and its related proteins.* J Invest Dermatol, 2001. **117**(4): p. 914-9.

95.  Bunz, F., et al., *Requirement for p53 and p21 to sustain G2 arrest after DNA damage.* Science, 1998. **282**(5393): p. 1497-501.

96.  Di Micco, R., et al., *Interplay between oncogene-induced DNA damage response and heterochromatin in senescence and cancer.* Nat Cell Biol, 2011. **13**(3): p. 292-302.

97.  Jain, A., S. Kaczanowska, and E. Davila, *IL-1 Receptor-Associated Kinase Signaling and Its Role in Inflammation, Cancer Progression, and Therapy Resistance.* Front Immunol, 2014. **5**: p. 553.

98.  Stender, J.D., et al., *Structural and Molecular Mechanisms of Cytokine-Mediated Endocrine Resistance in Human Breast Cancer Cells.* Mol Cell, 2017. **65**(6): p. 1122-1135 e5.

99.  Hoek, K.S. and C.R. Goding, *Cancer stem cells versus phenotype-switching in melanoma.* Pigment Cell Melanoma Res, 2010. **23**(6): p. 746-59.

100.  Sharma, S.V., et al., *A chromatin-mediated reversible drug-tolerant state in cancer cell subpopulations.* Cell, 2010. **141**(1): p. 69-80.

101.  Ramsdale, R., et al., *The transcription cofactor c-JUN mediates phenotype switching and BRAF inhibitor resistance in melanoma.* Sci Signal, 2015. **8**(390): p. ra82.

9

102. Vazquez, F., et al., *PGC1alpha expression defines a subset of human melanoma tumors with increased mitochondrial capacity and resistance to oxidative stress.* Cancer Cell, 2013. **23**(3): p. 287-301.

103. Yang, L., J. Fang, and J. Chen, *Tumor cell senescence response produces aggressive variants.* Cell Death Discov, 2017. **3**: p. 17049.

104. Achuthan, S., et al., *Drug-induced senescence generates chemoresistant stemlike cells with low reactive oxygen species.* J Biol Chem, 2011. **286**(43): p. 37813-29.

105. Milanovic, M., et al., *Senescence-associated reprogramming promotes cancer stemness.* Nature, 2018. **553**(7686): p. 96-100.

106. Jones, V.S., et al., *Cytokines in cancer drug resistance: Cues to new therapeutic strategies.* Biochim Biophys Acta, 2016. **1865**(2): p. 255-65.

107. Demaria, M., et al., *Cellular Senescence Promotes Adverse Effects of Chemotherapy and Cancer Relapse.* Cancer Discov, 2017. **7**(2): p. 165-176.

108. Dobson, J.R., et al., *hsa-mir-30c promotes the invasive phenotype of metastatic breast cancer cells by targeting NOV/CCN3.* Cancer Cell Int, 2014. **14**: p. 73.

109. Che, S., et al., *miR-30 overexpression promotes glioma stem cells by regulating Jak/STAT3 signaling pathway.* Tumour Biol, 2015. **36**(9): p. 6805-11.

110. Fang, Y., et al., *Involvement of miR-30c in resistance to doxorubicin by regulating YWHAZ in breast cancer cells.* Braz J Med Biol Res, 2014. **47**(1): p. 60-9.

111. Cheng, C.W., et al., *MicroRNA-30a inhibits cell migration and invasion by downregulating vimentin expression and is a potential prognostic marker in breast cancer.* Breast Cancer Res Treat, 2012. **134**(3): p. 1081-93.

112. Zhang, N., et al., *MicroRNA-30a suppresses breast tumor growth and metastasis by targeting metadherin.* Oncogene, 2014. **33**(24): p. 3119-28.

113. Liu, Z., K. Tu, and Q. Liu, *Effects of microRNA-30a on migration, invasion and prognosis of hepatocellular carcinoma.* FEBS Lett, 2014. **588**(17): p. 3089-97.

114. Zhong, K., et al., *MicroRNA-30b/c inhibits non-small cell lung cancer cell proliferation by targeting Rab18.* BMC Cancer, 2014. **14**: p. 703.

115. Chang, J., et al., *Clearance of senescent cells by ABT263 rejuvenates aged hematopoietic stem cells in mice.* Nat Med, 2016. **22**(1): p. 78-83.

116. Baar, M.P., et al., *Targeted Apoptosis of Senescent Cells Restores Tissue Homeostasis in Response to Chemotoxicity and Aging.* Cell, 2017. **169**(1): p. 132-147 e16.

117. Chen, J., et al., *The Bcl-2/Bcl-X(L)/Bcl-w inhibitor, navitoclax, enhances the activity of chemotherapeutic agents in vitro and in vivo.* Mol Cancer Ther, 2011. **10**(12): p. 2340-9.

118. Kang, M.H. and C.P. Reynolds, *Bcl-2 inhibitors: targeting mitochondrial apoptotic pathways in cancer therapy.* Clin Cancer Res, 2009. **15**(4): p. 1126-32.

119. Yosef, R., et al., *Directed elimination of senescent cells by inhibition of BCL-W and BCL-XL.* Nat Commun, 2016. **7**: p. 11190.

120. Tolcher, A.W., et al., *Safety, efficacy, and pharmacokinetics of navitoclax (ABT-263) in combination with irinotecan: results of an open-label, phase 1 study.* Cancer Chemother Pharmacol, 2015. **76**(5): p. 1041-9.

121. He, X.X., et al., *MicroRNA-375 targets AEG-1 in hepatocellular carcinoma and suppresses liver cancer cell growth in vitro and in vivo.* Oncogene, 2012. **31**(28): p. 3357-69.

122. Shah, M.Y., et al., *microRNA Therapeutics in Cancer - An Emerging Concept.* EBioMedicine, 2016. **12**: p. 34-42.

123. Gallo Cantafio, M.E., et al., *Pharmacokinetics and Pharmacodynamics of a 13-mer LNA-inhibitor-miR-221 in Mice and Non-human Primates.* Mol Ther Nucleic Acids, 2016. **5**(6).

124. Janssen, H.L., et al., *Treatment of HCV infection by targeting microRNA.* N Engl J Med, 2013. **368**(18): p. 1685-94.

125. Sureda, F.X., et al., *Antiapoptotic drugs: a therapautic strategy for the prevention of neurodegenerative diseases.* Curr Pharm Des, 2011. **17**(3): p. 230-45.

126. Chulpanova, D.S., et al., *Therapeutic Prospects of Extracellular Vesicles in Cancer Treatment.* Front Immunol, 2018. **9**: p. 1534.

127. Conboy, I.M., et al., *Rejuvenation of aged progenitor cells by exposure to a young systemic environment.* Nature, 2005. **433**(7027): p. 760-4.

128. Loffredo, F.S., et al., *Growth differentiation factor 11 is a circulating factor that reverses age-related cardiac hypertrophy.* Cell, 2013. **153**(4): p. 828-39.

129. Villeda, S.A., et al., *Young blood reverses age-related impairments in cognitive function and synaptic plasticity in mice.* Nat Med, 2014. **20**(6): p. 659-63.

130. Katsimpardi, L., et al., *Vascular and neurogenic rejuvenation of the aging mouse brain by young systemic factors.* Science, 2014. **344**(6184): p. 630-4.

131. Takahashi, K. and S. Yamanaka, *Induction of pluripotent stem cells from mouse embryonic and adult fibroblast cultures by defined factors.* Cell, 2006. **126**(4): p. 663-76.

132. Lapasset, L., et al., *Rejuvenating senescent and centenarian human cells by reprogramming through the pluripotent state.* Genes Dev, 2011. **25**(21): p. 2248-53.

133. Liu, G.H., et al., *Recapitulation of premature ageing with iPSCs from Hutchinson-Gilford progeria syndrome.* Nature, 2011. **472**(7342): p. 221-5.

134. Abad, M., et al., *Reprogramming in vivo produces teratomas and iPS cells with totipotency features.* Nature, 2013. **502**(7471): p. 340-5.

135. Ocampo, A., et al., *In Vivo Amelioration of Age-Associated Hallmarks by Partial Reprogramming.* Cell, 2016. **167**(7): p. 1719-1733 e12.

9

# APPENDIX

**English summary**

**Nederlandse samenvatting**

**Curriculum Vitae**

**PhD portfolio**

**Dankwoord**

## English summary

Aging is a progressive loss of normal physiology, ultimately resulting in age-related pathology. One of the main drivers of aging is an accumulation of irreparable damage to the genome. This damage results in both an increase in cells undergoing apoptosis and an accumulation of senescent cells. These two processes have beneficial effects on tissue integrity in young organisms, since both restrain damaged cells and can induce tissue repair. However, detrimental consequences of apoptosis and senescence prevail during aging. An excessive amount of cells undergoing apoptosis damages tissue structure, resulting in age-related pathologies such as heart failure and Alzheimer's disease. Conversely, senescent cells are extremely resistant to apoptosis and secrete factors that negatively influence the microenvironment through, for example, promoting inflammation, matrix degradation and inhibiting tissue regeneration. Cell fate after damage is dependent on multiple factors, such as the damage or cell type, but it is largely unclear how damaged cells decide to undergo either apoptosis or senescence. We aimed to unravel the mechanisms and functions of age-related DNA damage responses to ultimately provide starting points for potential treatment of age-related pathology.

Since senescent cells have a detrimental effect on their tissue microenvironment during aging, we aimed to develop a therapeutically applicable compound to eliminate these cells. In **Chapter 2** we show that FOXO4 binds to p53 in senescent cells to prevent cell death. We developed a cell penetrating peptide that perturbs this interaction and thereby specifically induces apoptosis in senescent cells. Furthermore, this peptide (FOXO4-DRI) proved to reduce the amount of senescent cells *in vivo* in Doxorubicin treated mice, fast aging Xpd$^{TTD/TTD}$ and naturally aged mice. In all models, tissue homeostasis was restored after FOXO4-DRI treatment and overall fitness was markedly improved. These results demonstrate that senescent cells can be targeted therapeutically and that thereby healthspan can be extended during aging. In **chapter 3 and 4**, we discuss the possibilities of FOXO4-DRI and anti-senescence therapy in general. For example, elderly suffering from frailty and age-related pathologies such as osteoarthritis and osteoporosis are likely to benefit from anti-senescence drugs. Besides aging, senescence is implicated in cancer formation and progression. Although damaged cells are prevented from undergoing malignant transformation through senescence induction, these cells can circumvent senescence through additional mutations. Furthermore, senescent cells can promote tumorigenesis in neighboring cells through their secretion phenotype. In **chapter 5** we demonstrate that malignant melanoma cells can exhibit senescence features as well. Although these cells are not necessarily arrested in growth, these features protect cells from apoptosis when treated with chemotherapy. Again, FOXO4 proved to be crucial for the inhibition of apoptosis and FOXO4-DRI greatly enhanced chemosensitivity in treatment-resistant cells.

In various organs an excessive amount of cells undergoing apoptosis is observed during aging, ultimately resulting in a decline of tissue function. However, in distinct tissues (such as liver, spleen and skin) the number of apoptotic cells does not increase and pro-apoptotic proteins are even downregulated during aging. Furthermore, cells derived from these tissues exhibit a reduced DNA damage and apoptotic response after damage exposure. Thus, aged cells appear to inhibit apoptosis and thereby prevent further tissue damage. We have previously identified a microRNA signature as the regulator of this response. However, it is unknown how this signature is regulated, what the specific miRNA targets are, and whether interference with this signature is beneficial *in vivo*. To answer these questions, we studied a representative miRNA of this signature, miR-30, in **chapter 6**. We indeed found miR-30 to be upregulated in various aged tissues and this miRNA proved to target p53 mRNA directly to inhibit apoptosis after DNA damage. Furthermore, miR-30 inhibition slightly enhanced senescence induction and DNA repair in fibroblasts. P53 levels were increased after miR-30 inhibition independently of DNA damage, suggesting miR-30 to set a p53 threshold. To study the effect of miR-30 inhibition *in vivo*, we treated XPD$^{TTD/TTD}$ mice with miR-30 inhibitors in a preliminary study. We observed weight loss and an increase in plasma creatinine concentration in all mice that received the miR-30 inhibitor, irrespective of genotype. However, whether miR-30 inhibition promotes aging remains unclear.

DNA damage signaling is known to result in an altered secretion phenotype. For example, secretion of extracellular vesicles (EVs) is increased and the content of these vesicles altered. Since miRNAs are abundant in vesicles and we have previously discovered our DNA damage-induced miRNA signature to be present in serum of centenarians, we wondered whether these miRNAs are indeed secreted after damage and whether they are transferred to neighboring cells. In **Chapter 7** we show that EVs derived from both UV-radiated cells and serum from aged mice induced the expression of these miRNAs in recipient cells. Therefore, it appears that the DNA damage-induced miRNA response is indeed transferred to neighboring cells through extracellular vesicles (EVs). These results imply that age-related DNA damage induces systemic pro-survival cues.

Lastly, in **chapter 8** we describe the optimization of a protocol to culture adult organotypic liver, kidney and heart slices *ex vivo*. This technique allows for molecular mechanistic experiments while maintaining a natural tissue niche. Thus, we can study age-related responses such as apoptosis and senescence within a relevant environment and after anti-aging interventions.

In this thesis we have identified DNA damage-dependent mechanisms that regulate apoptosis and senescence induction during aging. Furthermore, we have developed a peptide that selectively kills senescent cells *in vivo*. Thus, we have discovered leads for potential strategies that prolong healthspan during aging.

A

## Nederlandse samenvatting

We ontkomen er niet aan, ouder worden we allemaal. Vaak gaat dit gepaard met een scala aan lichamelijke klachten, zoals verlies aan motoriek, vermindering van zicht of gehoor en vergeetachtigheid. Ook neemt het risico op verschillende ziektes toe, waaronder osteoartritis, de ziekte van Alzheimer en kanker. Het verschilt per individu welke aandoeningen zich ontwikkelen en ouderen kunnen aan verschillende ziektes tegelijk lijden. Nu worden deze ziektes apart behandeld en dat betekent dat veel ouderen verschillende medicijnen slikken met uiteenlopende bijwerkingen. Ook kunnen er vaak alleen symptomen worden bestreden in plaats van de oorzaak. Omdat veroudering aan de basis ligt van al deze aandoeningen is het belangrijk de onderliggende oorzaak van veroudering te begrijpen, zodat we een stap dichterbij zijn in het behandelen van verouderingsaandoeningen met uiteindelijk het doel om de kwaliteit van leven zoveel mogelijk te verbeteren tijdens het verouderingsproces.

Een van de belangrijkste onderliggende oorzaken van veroudering is het ophopen van schade aan het DNA. Er wordt geschat dat een cel elke dag wel 10.000 DNA beschadigingen oploopt. Deze schade kan gelukkig vaak goed hersteld worden door verschillende DNA-reparatie processen. Echter, ondanks de efficiëntie van deze processen, zijn ze niet perfect. Sommige schades kunnen niet gerepareerd worden en de DNA-reparatiesystemen verouderen waarschijnlijk ook. Dit betekent dat het DNA minder goed hersteld kan worden met als gevolg dat DNA schade zich langzaam ophoopt. Deze permanente schade zorgt ervoor dat cellen minder goed of anders functioneren dan voorheen. Zo kunnen ze bijvoorbeeld minder goed delen of andere stoffen uitscheiden dan onbeschadigde cellen. Daarnaast treden er DNA mutaties op die juist de celdeling kunnen bevorderen en op deze manier kanker kunnen veroorzaken. Als er teveel DNA schade plaatsvindt of als er mutaties zijn ontstaan die kankergroei bevorderen, kan een cel actief besluiten om dood te gaan (apoptose) of om de celdeling permanent stil leggen (senescence).

Zowel apoptose als senescence kunnen een positief gevolg hebben voor de gezondheid van een orgaan. Beiden dragen er bijvoorbeeld aan bij dat het weefsel wordt hersteld na acute schade en dat beschadigde cellen niet kunnen uitgroeien tot een tumor. Echter, tijdens veroudering vindt er steeds meer apoptose plaats en is er een ophoping van senescente cellen. Als er teveel cellen dood gaan, vermindert de werking van een orgaan. Een verlies aan neuronen kan bijvoorbeeld leiden tot de ziekte van Parkinson. Verder veroorzaakt een teveel aan senescente cellen een vermindering van het aantal cellen dat kan delen, waardoor een weefsel zich minder goed herstelt na schade. Ook scheiden deze cellen een grote hoeveelheid groeifactoren en ontstekingseiwitten uit naar hun omgeving. Dit heeft als gevolg dat

omliggend weefsel langzaam beschadigd raakt. Het is aangetoond dat senescence een belangrijke rol speelt bij een aanzienlijk aantal ouderdomsaandoeningen zoals diabetes, osteoartritis en atherosclerose. Het doel van dit proefschrift is om apoptose en senescence te bestuderen als onderliggende oorzaken van veroudering. Door te bepalen wat ervoor zorgt dat een van de twee processen wordt geactiveerd na DNA schade en wat het effect is van het remmen van beide, hopen we aanknopingspunten te ontdekken voor mogelijke anti-verouderingstherapieën.

In **Hoofdstuk 2** onderzochten we een manier om senescente cellen gericht te kunnen verwijderen uit een oud lichaam, omdat we weten dat deze cellen de gezondheid tijdens veroudering negatief beïnvloeden. We ontdekten dat in senescente cellen twee eiwitten aan elkaar binden, in tegenstelling tot gezonde cellen waar dat niet gebeurt. Deze eiwitten heten FOXO4 en p53. P53 staat bekend als eiwit dat celdood veroorzaakt als cellen gestrest of beschadigd zijn en we hebben aangetoond dat senescente cellen inderdaad dood gaan als de binding tussen FOXO4 en p53 wordt verbroken. In senescente cellen werkt FOXO4 dus als een soort handrem die celdood verhindert. Als gevolg van deze ontdekking hebben we een peptide ontwikkeld dat deze binding kan verbreken, genaamd FOXO4-DRI. Met deze stof kunnen we gericht senescente cellen verwijderen en we hebben aangetoond dat dit de gezondheid van oude muizen sterk verbetert. In **hoofdstuk 3 en 4** bespreken we hoe anti-senescence therapie in de toekomst mogelijk ingezet zou kunnen worden bij de behandeling van meerdere ouderdomskwalen en ziektes zoals spierverlies, osteoartritis en osteoporose.

Ook kanker is één van de ouderdomsziektes waarin senescence een rol speelt. Het is aangetoond dat kankercellen kunnen ontstaan als senescente cellen in een uiterst geval toch weer gaan delen. Verder kunnen de stoffen die senescente cellen uitscheiden, zoals ontstekingseiwitten en groeifactoren, kankergroei bevorderen in nabijgelegen cellen. Ook kunnen deze factoren bijdragen aan ongevoeligheid voor chemotherapie. In **hoofdstuk 5** hebben we aangetoond dat chemotherapie ervoor zorgt dat melanoomcellen eigenschappen van senescente cellen krijgen en daardoor ongevoeliger worden voor therapie. Zo bezitten deze kankercellen een grote hoeveelheid FOXO4 en wordt celdood hierdoor geremd, net als in senescente cellen. We hebben deze cellen met FOXO4-DRI behandeld en aangetoond dat melanoomcellen hierdoor gevoeliger worden voor chemotherapie.

Naast senescence heeft ook apoptose negatieve invloed op veroudering. We hebben eerder ontdekt dat een verouderde cel een natuurlijk beschermingsmechanisme heeft om vroegtijdige apoptose te voorkomen. Oude of beschadigde cellen hebben namelijk een verhoogde hoeveelheid van een aantal microRNA's die celdood kunnen remmen. MicroRNA's zijn kleine RNA moleculen

A

227

die de productie van specifieke eiwitten kunnen remmen door aan hun mRNA te binden. Het remmen van celdood in de aanwezigheid van DNA schade hebben we celpreservatie genoemd. Celpreservatie voorkomt in theorie dat er te veel cellen dood gaan tijdens veroudering en een weefsel dus nog zijn functie kan uitoefenen. Het is echter onbekend hoe deze microRNA's precies apoptose remmen en of ze in een verouderd lichaam inderdaad de gezondheid van een orgaan beschermen. In **hoofdstuk 6** laten we zien dat één van deze microRNA's, miR-30, inderdaad verhoogd is tijdens veroudering en dat het celdood kan remmen door de hoeveelheid p53 in een cel te verminderen. De rol van miR-30 tijdens veroudering is nog grotendeels onbekend en zal daarom nog verder onderzocht moeten worden. Mogelijk remt dit microRNA apoptose tijdens veroudering, waardoor er minder weefselschade optreedt, maar misschien wordt hierdoor ook kankergroei bevorderd.

Het is bekend dat beschadigde cellen andere eiwitten en nucleotiden uitscheiden dan gezonde cellen, bijvoorbeeld om er voor te zorgen dat deze cellen opgeruimd worden. Senescente cellen scheiden bijvoorbeeld een relatief grote hoeveelheid ontstekingseiwitten uit naar hun omgeving en kunnen daardoor immuuncellen aantrekken. Verder scheiden cellen met schade aan het DNA een grote hoeveelheid kleine blaasjes uit die extracellular vesicles (EVs) worden genoemd. Beschadigde cellen scheiden meer van deze blaasjes uit dan normale cellen en de inhoud verschilt zeer waarschijnlijk. Wij onderzochten **in hoofdstuk 7** of de eerder beschreven microRNA's ook in deze blaasjes worden uitgescheiden na DNA schade en of ze op die manier worden doorgegeven aan naburige cellen. We vonden de microRNA's inderdaad in cellen die we behandeld hadden met vesicles van beschadigde cellen en in cellen die vesicles ontvingen uit serum van oude muizen. Omdat we eerder hebben aangetoond dat deze microRNA's celdood kunnen remmen, impliceren deze resultaten dat beschadigde cellen naburige cellen tegen apoptose kunnen beschermen door vesicles uit te scheiden. Als laatste hebben we in **Hoofdstuk 8** een protocol geoptimaliseerd om plakjes weefsel te kunnen kweken. Zo kunnen we verouderingsprocessen zoals apoptose en senescence bestuderen in hun natuurlijke omgeving, zonder levende muizen te gebruiken.

Dit proefschrift beschrijft studies naar processen die aan de basis van veroudering liggen. We hebben mechanismen ontdekt die bepalen of apoptose of senescence geactiveerd wordt na DNA schade. Ook hebben we een therapeutisch toepasbaar peptide ontwikkeld die senescent cellen gericht verwijdert uit een oud organisme. Hierdoor hebben we nieuwe aanknopingspunten voor mogelijke therapieën die de gezondheid tijdens veroudering verbeteren.

A

## Curriculum Vitae

**Name:** Marjolein Petronella Baar
**Date of birth:** 18 November 1989
**Place of birth:** Hilversum
**Nationality:** Dutch

**Work experience and education:**

| | |
|---|---|
| 2018 – Present | **Senior Scientist** |
| | Cleara Biotech |
| 2013 – 2018 | **PhD student** |
| | Department of Molecular Genetics, Erasmus Medical Centre Rotterdam, The Netherlands |
| 2011 – 2013 | **Master Molecular Life Sciences** |
| | Radboud University, Nijmegen, The Netherlands |
| | Research internship, Department of Molecular Genetics, Erasmus Medical Centre, Rotterdam, The Netherlands. |
| | Research internship, Department of Pathology, Radboud University, Nijmegen, The Netherlands |
| 2008 – 2011 | **Bachelor Molecular Life Sciences** |
| | Radboud University, Nijmegen, The Netherlands |
| | Research internship, Department of Molecular Developmental Biology, Nijmegen Center for Molecular Life Sciences (NCMLS), Nijmegen, the Netherlands |
| 2002 – 2008 | **VWO-Gymnasium** |
| | Comenius College, Hilversum |

**Publications**

<u>M.P. Baar</u>, R.M.C. Brandt, D.A. Putavet, J.D.D. Klein, K.W.J. Derks, B.R.M. Bourgeois, S. Stryeck, Y. Rijksen, H. van Willigenburg, D.A. Feijtel, I. van der Pluijm, J. Essers, W.A. van Cappellen, W.F. van IJcken, A.B. Houtsmuller, J. Pothof, R.W.F. de Bruin, T. Madl, J.H.J. Hoeijmakers, J. Campisi, P.L.J. de Keizer. *Targeted Apoptosis of Senescent Cells Restores Tissue Homeostasis in Response to Chemotoxicity and Aging.* Cell, 169 (2017)

<u>M.P. Baar</u>, E. Perdiguero, P. Muñoz-Cánoves, P.L.J. de Keizer. *Musculoskeletal senescence: a moving target ready to be eliminated.* Curr Opin Pharmacol, 147-155 (2018)*.*

<u>M.P. Baar</u>, H. van Willigenburg, P.L.J. de Keizer. *Maintenance and repair of an aging life cycle* Oncotarget, 1–2 (2017).

F. Kruiswijk, S.C. Hasenfuss, R. Sivapatham, <u>M.P. Baar</u>, D. Putavet, K.A. Naipal, N.J. van den Broek, W. Kruit, P.J. van der Spek, D.C. van Gent, A.B. Brenkman, J. Campisi, B.M. Burgering, J.H. Hoeijmakers, P.L. de Keizer. *Targeted inhibition of metastatic melanoma through interference with Pin1-FOXM1 signaling.* Oncogene, 17 (2016).

A.C. van Engen-van Grunsven, <u>M.P. Baar</u>, R. Pfundt, J. Rijntjes, H.V. Küsters-Vandevelde, A.L. Delbecq, J.E. Keunen, J.B. Klevering, P. Wesseling, W.A. Blokx, P.J. Groenen. *Whole-genome copy-number analysis identifies new leads for chromosomal aberrations involved in the oncogenesis and metastatic behavior of uveal melanomas.* Melanoma Res, 3 (2015).

A

# PhD Portfolio

**Name:** Marjolein P. Baar
**Department:** Molecular Genetics
**PhD period:** 2013-2018
**Promotor:** Prof. Dr. Jan H.J. Hoeijmakers
**Co-promotor:** Dr. Joris Pothof, Dr. Peter L.J. de Keizer

| Courses | Year |
| --- | --- |
| Functional Imaging and Super Resolution | 2013 |
| Safely working in the laboratory | 2013 |
| Cell and Developmental Biology | 2014 |
| Genetics | 2014 |
| Biochemistry and Biophysics | 2014 |
| Laboratory animal science | 2015 |

| Workshops and conferences | Presentation | Year |
| --- | --- | --- |
| CGC meeting (Amsterdam) | | 2013-2017 |
| CGC meeting (Utrecht) | | 2014-2017 |
| MGC symposium (Rotterdam/Leiden) | | 2014, 2016 |
| MGC PhD workshop (Munster, Germany) | | 2014 |
| MGC PhD workshop (Maastricht) | Poster presentation | 2015 |
| Cell Senescence: from Physiology to Pathology (Santiago de Compostela, Spain) | Poster presentation | 2015 |
| KWF Cancer Biology meeting (Lunteren) | | 2015, 2016 |
| Radiotherapy Research Day (Rotterdam) | Oral presentation | 2015, 2016 |
| MGC PhD workshop (Dortmund, Germany) | Oral presentation | 2016 |
| Molecular Biology of Ageing Meeting (Groningen) | Poster presentation | 2015, 2017 |
| AACR Annual Meeting (New Orleans, USA) | Poster presentation | 2016 |
| EACR - FEBS Advanced Lecture Course (Spetses, Greece) | Poster and Oral presentation | 2017 |
| MGC symposium (Rotterdam) | Oral presentation | 2017 |
| International symposium on geriatrics and gerontology (Aichi, Japan) | Oral presentation | 2018 |
| Departmental meeting, Laboratory of Cell Cycle Regulation (Kyoto University, Japan) | Oral presentation | 2018 |
| Nederlandse Nefrologiedagen (Veldhoven) | Oral presentation | 2018 |

| Teaching | Workload | Year |
|---|---|---|
| Master student (Regenerative Medicine, Utrecht University) | 7 months | 2015 |
| Master student (Life Science and Technology, Leiden University) | 12 months | 2016-2017 |
| Master student (Molecular Medicine, Erasmus MC) | 6 months | 2017 |
| Shared supervision of several master and HLO students | | 2013-2017 |
| Bachelor student (BRiP minor, Erasmus MC) | 1 month | 2017 |
| BSc Nanobiology werkcolleges | 10 hours | 2014-2016 |
| 6 VWO Profielwerkstuk students | 1 week | 2017 |

A

## Dankwoord

My PhD years were unforgettable due to the many research opportunities and due to all the people that supported me during this time. Thanks for all the scientific discussions and fun conversations in the cell culture or at the coffee table, and for the interest you showed in my research.

Jan, je had sinds ons allereerste gesprek vertrouwen in mij en het was fijn dat ik altijd bij je naar binnen kon lopen voor advies. Heel erg bedankt voor alle hulp, vooral met het nakijken van mijn proefschrift. Joris, bedankt voor de leuke besprekingen en filosofische discussies. Ik was vaak optimistisch na een brainstorm sessie bij het koffieapparaat. Peter, ik ben je heel erg dankbaar voor alle kansen die je me hebt gegeven. Je hebt me altijd uitgedaagd om alles uit mijn onderzoek te halen en je hebt me alles geleerd wat ik nodig had om mijn PhD af te ronden.

Diana and Hester, I am very happy that you are my paranymphs and that you will support me during my defence, as you have supported me during the last years. Diana, we have worked together during my entire PhD. Not only have we experienced a lot together at work, we have also done many fun activities outside of the lab. I love that you always know about events or new restaurants to try. Thanks for all the ice cream/whiskey/punk festivals and trips to Christmas markets. I am very happy that we still work together in Utrecht. Hester, vanaf het moment dat je stage kwam lopen konden we het goed met elkaar vinden. Bedankt voor alle goede gesprekken over werk en alle andere dingen in het leven, en voor alle kleine creatieve projectjes die we samen hebben gedaan. Ik ben ook heel blij met de voorkant van mijn proefschrift die jij hebt geschilderd.

Kyra, we zijn al vriendinnen vanaf de eerste week dat we samen stage liepen in Rotterdam. Ik voelde me gelijk thuis in een nieuwe stad doordat we er veel samen op uit gingen. De jaren daarna hebben we heel veel leuke dingen samen meegemaakt, zoals reisjes naar Bali en Japan. Bedankt voor alle gezelligheid, maar vooral ook dat je onvoorwaardelijk voor me klaar staat en naar me luistert. Sander en Renata, toen ik in het Erasmus begon voelde ik me gelijk helemaal op mijn plek, wat voor het grootste deel aan jullie te danken is. Sander, voor iemand die soms het eind van zijn verhaal niet meer weet, zeg je toch altijd de juiste dingen. Meestal zijn dit (meesterlijke) grapjes, maar vaak ook goed advies. Renata, bedankt dat je altijd naar me luistert en aan mijn kant staat. Dat betekent veel voor me. Shirley, allereerst moet duidelijk zijn dat ik wel heel goed pannenkoeken kan bakken. Naast je net-iets-te-eerlijke analyses over mijn onhandige acties ben ik je heel dankbaar voor je steun en natuurlijk de gezellige uitjes/ontbijtjes.

Serena, we hebben heel wat kopjes koffie en taartjes samen gedeeld. Het was heel erg fijn om met iemand te kunnen kletsen die in hetzelfde schuitje zat en aangezien je een jaar op mij voorliep, kon ik bij jou altijd terecht voor advies.

Mariangela, bedankt dat ik altijd bij je terecht kan voor een praatje of een knuffel. We hebben veel leuke uitstapjes gemaakt en er staan nog heel wat plannen op dat to-do lijstje, dus je bent nog niet van me af. Imke, we hebben veel gemeen, van studieachtergrond tot gevoel van humor. Bedankt voor alle gezelligheid! Akos, thanks for all the fun conversations we had over the years and for your support in challenging times. Hope the kids are doing well. Ines, bedankt voor alle gezellige lunches en je goede praktische tips. Chiara, Aida and Rana, thanks for all the fun we had at our favorite hangout spots such as Hamburg or Worm. I especially enjoyed our cooking sessions together, where you did all the cooking (even when Rana was cooking meat balls at 7 in the morning). Jiang, I am very sorry for teaching you a bad sense of humor. Thanks for accepting this and for all the fun conversations in our office. Astrid en Joris, ik heb jammer genoeg niet heel lang met jullie samengewerkt, maar het waren gezellige maanden door jullie en dat maakte het extra moeilijk om weg te gaan. Sylvia, Yvette en Yvonne, bedankt voor alle gezelligheid in het lab. Ook fijn dat jullie me af en toe (terecht) uitlachte als ik weer eens een puntje naast de prullenbak schoot. Yvonne, heel erg bedankt voor je hulp bij het senescence project. Het was vooral heel fijn dat al die paraffine coupes al klaar lagen voordat ik er over na kon denken. Nicole, voor mijn gevoel hebben we veel te kort samen gewerkt. Ik mis je rare dansjes op de gang! Jeroen, Sabine, Tomas en Martin, heel erg bedankt voor jullie hulp en enthousiasme voor mijn vesicle experimenten. Ik hoop hier in de toekomst zeker nog verder mee te gaan. Many thanks to all the students that worked with me on my projects or in our group: Marina, Glenn, Myrna, Anne, Danny, David, Dian, Felicity, Julian, Meneka, Katelijne and Shirley. You are all hard working, motivated and fun people.

Thanks to all my new colleagues at Cleara and the UMC for the warm welcome. You are very enthusiastic and intelligent people and I look forward to the research and fun events we will do in the coming years. Anne's colleagues, thanks for letting me write in your department (especially Eveline), it gave me the quiet writing place that I needed at the time! Thanks for all the drinks/dinners/game nights as well.

Ik wil ook heel graag mijn vrienden en familie bedanken. Jullie houden van me zoals ik ben, inclusief mijn rare humor en neiging om valse liedjes te zingen. Tom, Samantha en Luc, bedankt voor alle semi-maandelijkse uitjes, wat vind ik het fijn dat we elkaar nog zo vaak zien. Sam, je bent als een zus voor me en ik vind het heel fijn dat we nu samen in Utrecht werken. Tom, bedankt voor de goede gesprekken die we altijd hebben en je flauwe grappen. Die mis ik nu je in Zweden woont! Luc, ik vind het heel leuk dat je helemaal je rol als leraar gevonden hebt, het past bij je. Matthijs, je hebt wat te verduren gehad tijdens onze uitstapjes terwijl wij het over cellen/bacteriën/muizen/studenten hadden en toch leek je dit niet erg te vinden.

A

Heel erg bedankt voor je oprechte interesse. Saskia, Carien, Marleen en Rebecca, we zijn na de middelbare school allemaal iets anders gaan studeren, maar onze vriendschap is alleen maar hechter geworden. Bedankt voor alle etentjes, uitstapjes en spelletjesavonden! Eveline, ik vind het fijn dat we nog steeds vriendinnen zijn en dat je ook van sushi houdt. Petra (tantemam), bedankt voor alle hardlooprondjes en kopjes koffie waar we over van alles en nog wat praten. Je hebt me erg geholpen hiermee!

Anne, ik weet niet hoe ik zonder jou dit proefschrift had afgekregen. Je hebt me gesteund door naar me te luisteren en hoofdstukken door te lezen, maar ook door af en toe te zeggen dat ik me onnodig druk maakte. Je begrijpt me altijd en je weet altijd hoe ik me voel, dat is voor mij onmisbaar en tegelijkertijd heel bijzonder. Bram, bedankt voor al je interesse in mijn onderzoek (zelfs knappe broertjes worden ooit oud) en vooral je goede schrijf tips! Ik hoop toch ooit wat van je zelfvertrouwen/bluf over te kunnen nemen. Pap en mam, ik ben heel erg dankbaar voor alles wat jullie voor me doen. Jullie staan altijd voor me klaar, zonder er over na te denken. Jullie luisteren naar me als ik weer eens over werk praat, geven me de beste adviezen, helpen me altijd met verhuizen en maken precies de goede grapjes. Bedankt voor dit alles en nog een ontelbaar andere dingen.

A